Texturization of dairy protein systems with whey protein isolate aggregates

Anna Kharlamova

UNIVERSITE BRETAGNE LOIRE

Le Mans Université

Thèse de Doctorat

Anna KHARLAMOVA

Mémoire présenté en vue de l'obtention du
grade de Docteur de Le Mans Université
sous le sceau de l'Université Bretagne Loire

École doctorale: 3M - Matière, Molécules et Matériaux

Discipline: Chimie
Spécialité: Chimie moléculaire et macromoléculaire
Unité de recherche: ***IMMM UMR CNRS 6283 – Equipe PCI***

Soutenue le 15 novembre 2017
Thèse N°:

Texturer des matrices laitières avec des agrégats de protéines laitières.

Texturization of dairy protein systems with whey protein isolate aggregates.

JURY

Rapporteurs :	**M Gérard CUVELIER,** Professeur, AgroParisTech **M Christophe SCHMITT**, Docteur, Nestlé Research Center, Lausanne
Examinateurs :	**Mme Marie-Hélène FAMELART,** Chargé de recherche, INRA, Agrocampus Ouest, Rennes **M Benoît GOLDSCHMIDT**, Responsable de recherche, Fromageries BEL, Vendôme **M Stéphane PEZENNEC,** Chargé de recherche, INRA Agrocampus Ouest, Rennes
Directeur de Thèse :	**M Taco NICOLAI,** Docteur, Le Mans Université
Co-directeur de Thèse :	**M Christophe CHASSENIEUX,** Professeur, Le Mans Université

Acknowledgements

I would like to thank Dr. Taco Nicolai and Pr. Christophe Chassenieux for giving me an opportunity to work on this project. Thank you for all your hard work and the enormous effort that you put into your students! I would also like to thank Taco and his wife Siobhan for their hospitality and kindness. Christophe, I am very grateful for your invaluable help with all administrative procedures and in problematic situations!

I wish to thank the State of France, in particular the governments of the regions Pay de la Loire and Brittany, for the financial support of the project. Dr. Joële Léonil, Morgane Raison and Stéphan Rouverand from PROFIL are thanked for the coordination of the project and cooperation with the industrial partners.

Dr. Marie-Hélène Famelart and Dr. Anne Pitkowski are thanked for the yearly assessment of the project progress.

I would like to express my deep gratitude to Dr. Bach Nguyen, who taught me all the technical details concerning the work in the PCI laboratory. Bach, thank you for your enormous help, friendship, kindness, optimism and your great sense of humour!

I would like to thank the personnel of the PCI laboratory for all the great help with the measurements, especially to Olivier Colombani for his help with titration experiments, to Lazhar Benyahia for the help with rheological measurements, to Frédérick Niepceron for his help with CLSM analysis and to Boris Jacquette for the help with SDS-page analysis and chromatography. I thank Cyrille Dechancé for constant technical support.

All the former and current students working in PCI, thank you for your help and cooperation! I especially thank Juliana, Frederico and Alberto for their friendship!

I also thank warmly my friends in Russia Ksenia Bayurova, Ekaterina Kuznetsova (Durakova) and Evgenia Trubnikova (Kopylova), for I can always rely on you.

I would also like to thank Juliana Semenova and Mark Spicoluk from Boho Beautiful for their amazing yoga classes that helped me dealing with the stress of working on the thesis.

I express my sincere gratitude to Alexey Navalny, a Russian political activist and opposition leader, for his outstanding work in fighting the corrupt and antidemocratic regime of Vladimir Putin and for an example of leadership and personal bravery.

Table of contents

List of abbreviations

CAC – critical association concentration

CCP – colloidal calcium phosphate

CLSM – confocal laser scanning microscopy

CMP – caseinomacropeptide

DLS – dynamic light scattering

GDL – glucono-delta-lactone

MC – micellar casein

MCP –micellar calcium phosphate

MUF – milk ultrafiltrate

NaCas – sodium caseinate

NPCS – native phosphocaseinate powder suspension

NPCP – native phosphocaseinate powder

NPN – non-protein nitrogen

SANS – small-angle neutron scattering

SAXS – small-angle X-ray scattering

SC – sodium caseinate

SMUF – simulated milk ultrafiltrate

UF – ultrafiltrate

WP – whey protein

WPC – whey protein concentrate

WPI – whey protein isolate

General introduction.

Bovine milk contains proteins that can be divided into two categories: caseins and whey proteins. The two types of proteins have very different morphologies and functionality. They are routinely separated from milk during different technological operations. Globular proteins are found in the milk serum as small dense molecules with a compact structure. They are amongst the most extensively studied food proteins known for their excellent functional properties. In particular, their solutions can form gels when heated – a process known as heat-induced gelation. Gelation may be considered as the final stage of denaturation and aggregation of globular proteins. The aggregation results in formation of gels above a critical gel concentration, but at lower concentrations suspensions of stable aggregates are formed. Aggregates of different morphologies formed by globular milk proteins have been described in the literature. The morphology depends on the conditions of preparation. At low pH fibrillar aggregates are produced. Around the isoionic point (pH = 4.2-6.0) spherical dense aggregates known as microgels are formed with radii 100 nm to 1 μm that strongly scatter light and have a milk-like appearance in suspensions. At higher pH transparent solutions of smaller elongated aggregates called “strands” are formed at concentrations below 40 g/L that at higher protein concentrations further aggregate into self-similar (fractal) aggregates. The size of different aggregates depends on the conditions of preparation. The aggregates of whey proteins have been studied in detail in the literature. They present interest for applications in food products as they can be used for modifications of textural characteristics of foods – for gelation and as viscosifiers. In particular, they form gels at ambient temperatures after addition of salt or decrease of the pH.

The objective of presented work was to study properties of whey protein aggregates as texturizing ingredients, in particular their capacity to form viscous solutions or gels in mixtures with other milk proteins and in presence of common dairy ingredients such as calcium. The properties of aggregates of globular proteins were studied in mixtures with micellar casein. The obtained results might be useful for applications of the aggregates as efficient “clean label” texturizing ingredients.

This thesis is conducted as part and with the financial support of the PROFIL project (PROtéines Fonctionnalisées pour l’Industrie Laitière) organized by the governments of two regions of France – Brittany and Pays de la Loire, where a largest part of the country’s dairy industry is concentrated. The global objective of PROFIL is to support research of the functional properties of dairy proteins in order to promote innovation and new product development in the dairy industry of the region. The research projects are organized in four directions (“axes”): study of the antifungal, emulsifying and textural properties of dairy proteins and their application for encapsulation of valuable food ingredients. This thesis is conducted to investigate the textural properties of dairy proteins. PROFIL is organized by the Bba Association that includes 10 main dairy manufacturers of the region (Sodiaal, Lactalis, Savencia Fromage & Dairy, CF&R, Bel, Laïta, Laiterie de Montaigu, Sill, Eurial and Coopérative d’Isigny). The scientific coordination of the project is conducted by Agrocampus Ouest of INRA in Rennes, the scientific coordinator is Dr. Joëlle Léonil.

The thesis consists of the following chapters:

Chapter 1 gives a general overview of the milk composition, its protein fractions, functional properties of the proteins and formation of gels in different dairy systems.

Chapter 2 describes the materials and methods.

In chapters 3-7 published articles (3-5) and articles prepared for publication (6-7) are presented.

In **Chapter 3** the flow properties of water solutions of fractal aggregates and microgels are described ("Structure and flow of dense suspensions of protein fractal aggregates in comparison with microgels").

Chapter 4 gives the comparison of the proton binding properties of fractal aggregates and microgels ("The effect of aggregation into fractals or microgels on the charge density and the isoionic point of globular proteins").

Chapter 5 reports on the investigation of Ca^{2+}-induced cold gelation of fractal aggregates. The results are compared with gelation of microgels ("Calcium-induced gelation of whey protein aggregates: kinetics, structure and rheological properties").

Chapter 6 describes the results of the investigation of acid-induced cold gelation of fractal aggregates. The comparison with the Ca^{2+}-induced gelation is made ("Acid-induced cold gelation of whey protein aggregates: kinetics, gel structure and rheological properties").

In **Chapter 7** heat-induced gelation of suspensions of casein micelles in water with fractal aggregates is investigated. The comparison with mixtures of micelles with microgels is made ("Heat-induced gelation of mixtures of casein micelles with whey protein aggregates").

Chapter 1. Bibliography.

1. Milk composition: overview.

Bovine milk is a complex liquid produced by mammals in order to satisfy the nutritional needs of infant mammals. It consists of an aqueous phase containing globular proteins, sugars, salts and minerals along with fat droplets and colloidal protein particles formed by caseins. Cow's milk contains on average 4.5 % of fat, 2.9 % protein, 4.1 % lactose and 0.8 % ash (O'Mahony and Fox, 2013).

The average normal concentration of proteins in milk is 35-40 g/L (Marchal et al., 1995). Proteins represent 95 % of the nitrogen content of milk. The remaining non-protein nitrogen (NPN, 5 %) is presented by urea, creatine, uric and orotic acids, peptides, ammonia etc. (Walstra, 1999). Approximately 80 % of the milk nitrogen is presented by caseins and 20 % by whey proteins and NPN (Tremblay et al., 2003). The proteins of milk are presented by two fractions: the globular proteins (α-lactalbumin, β-lactoglobulin, immunoglobulins and bovine serum albumin (BSA)) and caseins in the form of casein micelles. β-Lactoglobulin represents ~50 % of whey proteins and 12 % of the total protein in bovine milk, α-lactalbumin – ~20 % of the whey protein (3.5 % of total milk protein) (O'Mahony and Fox, 2013).

2. Casein micelles.

2.1 The casein micelle: overview.

The caseins of milk are organized in complex particles called casein micelles that are described in the literature as "amorphous aggregates", "functional protein aggregates" (Holt et al., 2013), "complex macromolecular assemblies" (Bouchoux et al., 2010), "complex aggregates of the proteins and mineral calcium phosphate" (Horne, 2009), "dynamic association colloids" (De Kruif, 2014) or "complex association colloids" (Dalgleish, 2011) and even as a "packaging system" (Lucey and Horne, 2009). The dry matter of bovine casein micelles is ~94 % protein and ~6 % mineral (De Kruif et al., 2012; Horne, 2006).

The micelles are usually characterized as very polydisperse particles (Broyard and Gaucheron, 2015) with the size varying from 50 to 500 nm and the molecular weight ranging from 10^6 to $>10^9$ Da (Fox, 2003). However, de Kruif et al. (2012) noted that the polydispersity of the micelles probably comes from the measurements conducted on pooled milk. They performed SANS experiments on the milk obtained from the same cow and found that the micelles are "quite monodisperse and extremely constant in time".

The caseins represent the largest protein content in most milks. In bovine milk they make up 80 % of the total protein content and consist mainly of α_{s1}-, α_{s2}-, β- and κ- caseins with weight fractions of 40, 10, 35 and 15 % (w/w), respectively (Dalgleish, 2011). They belong to the group of phosphoproteins and can be divided into calcium-sensitive and calcium-insensitive members (Horne, 2006). In bovine milk, α_{s1}-, α_{s2}- and β- caseins are calcium-sensitive, and κ-casein is calcium-insensitive. Calcium-sensitive caseins are highly phosphorylated and can be precipitated in the presence of ionic calcium, with α_{s2}-casein being the most sensitive of the three, while β-casein is the least sensitive (Horne, 2009). According to Lucey and Horne (2009), "phosphorylation is a

posttranslational modification of the caseins and it occurs at the serine groups, or rarely threonine, following a recognized template sequence Ser-X-Y, where X is any amino acid and Y = Glu, Ser-P or Asp. Due to the placing of the serine residues along the molecular sequences of α_{s1}-, α_{s2}- and β-caseins, most of the phosphorylated residues are found in clusters." The sensitivity of caseins to calcium increases with the increase of the phosphoserine content.

κ-Casein is characterized by glycosylation resulting in its C-terminal part (the so-called caseinomacropeptide, CMP) being hydrophilic (Broyard and Gaucheron, 2015), which confers this protein its stabilization properties. It is generally accepted that κ-casein is found on the surface of the micelle, forming a so-called "hairy layer" allowing the protection of calcium-sensitive caseins and stabilization of the micelles by steric stabilization (Fox, 2003; Horne, 2006). The surface location of κ-casein is supported by the inverse dependence between the κ-casein content and the micelle size (Dalgleish et al., 1989).

The minerals of milk play a crucial role in the stabilization of the casein micelles. For instance, extensive dialysis of the micelles against water at neutral pH leads to the dissociation of micelles (Aoki et al., 1988; Lucey and Horne, 2009).

The concentration of the mineral fraction of milk is about 8-9 g/L (Gaucheron, 2005) and it contains mainly calcium, magnesium, sodium and potassium as cations and inorganic phosphate, citrate and chloride as anions. The mineral fraction of milk was reviewed by Lucey and Horne (2009) and Gaucheron (2005). The minerals in milk are found in the dynamic equilibrium between the ionic (dissolved) and colloidal (undissolved) fractions and in strong interaction with the proteins. For instance, about two-thirds of the total calcium, half of magnesium and half of inorganic phosphate in milk are present in the micelles (Lucey and Horne, 2009; Mekmene et al., 2010). The equilibrium depends greatly on pH, temperature and concentration of the medium.

The estimated concentration of calcium in milk is 32 mM, of which 22 mM are in the micelles and 10 mM are diffusible. Of this diffusible calcium, only 2 mM are in the free ionic state Ca^{2+} and the rest is found in complexes with citrate, phosphate, caseins or whey proteins (Philippe et al., 2003).

The calcium and phosphate within the micelle form small species that are called colloidal calcium phosphate (CCP), micellar calcium phosphate (MCP) or calcium phosphate nanoclusters (Horne, 2009). The micellar calcium phosphate consists of the colloidal inorganic phosphate (P_i) connected directly to caseins through their phosphoserine residues. These residues make up the organic phosphate of the micelle (P_o) (Gaucheron, 2005).

The synthesis and assembly of the caseins into the casein micelle occurs in the Golgi apparatus of the mammary gland (Horne, 2006). The structure of the casein micelle results from the evolutionary development to ensure three biological functions: prevention of the formation of dysfunctional deposits of calcium phosphate in the mammary gland, suppression of amyloid fibril formation and, lastly, delivery of the necessary nutrients to the neonate for the bone and tissue formation (Holt et al., 2013). The formation of fibrils is considered a common property of unfolded proteins due to the presence of short sequences called steric zippers, which are present abundantly in nearly all caseins (Donald, 2008; Holt and Carver, 2012). Therefore, the casein micelles represent "an open, hydrated, dynamic, and amorphous structure that competes effectively with pathways forming amyloid fibrils" (Holt et al., 2013).

2.2 The structure of casein micelles.

Although it is known that the micelles essentially consist of highly phosphorylated caseins interacting with calcium phosphate and are stabilized by κ-casein layer found on their surface, their exact internal organization and the mechanism of assembly in the cell remain a subject of investigation. Several models of the casein micelle organization have been proposed over decades of research. The models are regularly reviewed: Ingham et al. (2016), De Kruif (2014), Holt et al. (2013), De Kruif et al. (2012), Dalgleish (2011), Fox and Brodkorb (2008), Horne (2006), Horne (2002). The historical evolution of the casein micelle models is reviewed by McMahon & Oommen (2013).

Below are the three models of the casein micelle organization proposed in the literature.

(1). The submicelle model (proposed by Slattery and Evard, with further modification by Schmidt).

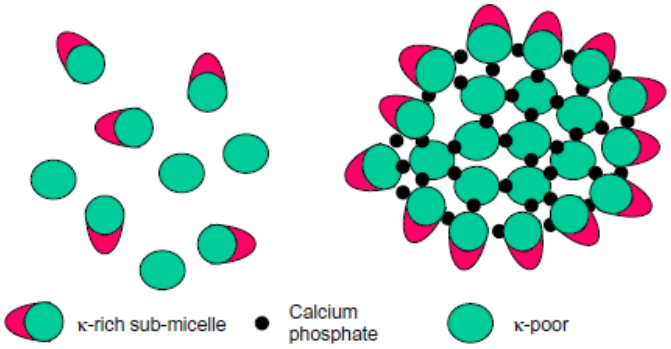

Figure 1. The schematic representation of the submicelle model of the caseine micelle (from Horne (2006)).

The submicelle model was based on the studies of sodium caseinate solutions that were reported to form small aggregates (Waugh et al., 1970). This observation produced the hypothesis that casein micelles can be composed of protein sub-units stabilized by calcium phosphate (Walstra, 1990).

Slattery and Evard (1973) suggested formation of two types of protein aggregates (or sub-micelles): κ-rich and κ-poor. The κ-rich sub-micelles are suggested to be situated on the surface of the micelles, while the κ-poor sub-micelles are hidden inside the micelle. Schmidt elaborated this model by proposing that the internal sub-micelles are connected by colloidal calcium phosphate.

The model is now considered obsolete. One of its major drawbacks is that the mechanism driving the segregations of κ-casein rich and poor sub-micelles has never been proposed, as well as the precise location of the calcium phosphate was not established clearly.

(2). The nanocluster model of Holt (De Kruif and Holt, 2003).

The nanocluster model of the casein micelle is based on the studies by Holt and coworkers (1998) who demonstrated that calcium phosphate particles in supersaturated solutions are surrounded by proteins and prevented from precipitation in mixtures with β-casein. It is suggested that the nanoclusters are formed in the secretory vesicle as a result of the increasing concentration of calcium and phosphates. The nanoclusters are then surrounded and stabilized by α_s- and β-

caseins, which leads to the separation with κ-casein that plays a size-limiting role and stabilizes the final structure of the micelle.

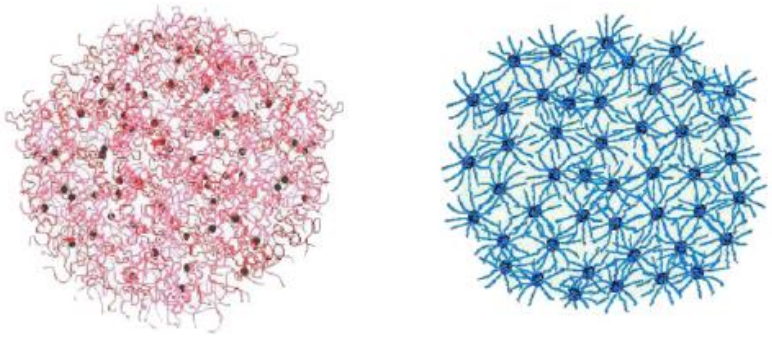

Figure 2. "Collection of artist's impressions of the casein micelle particle" based on the model proposed by Holt (from de Kruif et al. (2012)).

(3). The dual-binding model (Horne, 1998).

In the dual-binding model the casein micelle assembly and growth are driven by a polymerization process of casein molecules through, firstly, the clustering of hydrophobic regions of the caseins and, secondly, connection of the phosphopeptides to the calcium phosphate nanoclusters (Lucey and Horne, 2009).

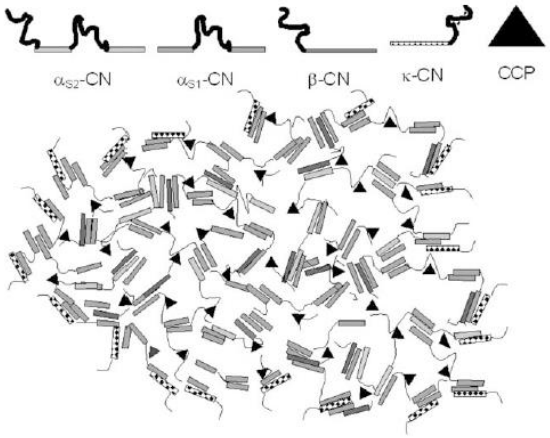

Figure 3. The dual-binding model for the casein micelle. CN is casein and CCP is the colloidal calcium phosphate (from Horne (1998)).

The current discussion concerning the structure of the casein micelles concentrates on the interpretation of the data obtained from numerous scattering experiments conducted on casein micelles (SAXS- and SANS-measurements). The features observed on the scattering data are attributed to the scattering (i) by the casein micelle itself, (ii) by the "incompressible regions" 20 nm in diameter, (iii) the scattering by the CCP particles and, lastly, (iv) the scattering by denser regions of proteins (Ingham et al., 2016). The SAXS measurements conducted on the micelles compressed under osmotic stress demonstrated that there are parts of the casein micelle that collapse under high osmotic pressure, while other parts resist deformation (Bouchoux et al., 2010), implying that there are highly-hydrated channels found inside the micelles, that are probably responsible for the high amount of associated water within the micelles (4 g of water per 1 g of protein) and for the transport of casein molecules and ions during chemical and physical modifications of casein micelles.

2.3 Physico-chemical modifications of casein micelles.

2.3.1 Influence of temperature, heat treatment.

The casein micelles in milk are generally considered thermally stable. They sustain heat treatment even at 95 °C for a few minutes. However, higher temperatures cause irreversible changes in the salt equilibrium and lead to the destruction of the micellar structure (Broyard and Gaucheron, 2015; Gaucheron, 2005).

The solubility of calcium phosphates depends on the temperature. It decreases with increasing temperature, which can be approximately described by the following process (Lucey and Horne, 2009):

$$3Ca^{2+} + 2HPO_4^{2-} \rightarrow Ca_3(PO_4)_2\downarrow + 2H^+.$$

As a result, with increasing temperature a slight increase of pH is observed (McMahon and Oommen, 2013). The heat-induced calcium phosphate appears to associate with the CCP of casein micelles. The decrease of calcium phosphate solubility is manifested by the undesirable formation of deposits rich in calcium phosphate in heat exchangers during ultra-high-temperature pasteurization of milk.

The decrease of the temperature, on the other hand, increases the calcium phosphate solubility and its release into the aqueous phase of milk (Broyard and Gaucheron, 2015; Gaucheron, 2005).

The decrease of the temperature of milk is reported to result in dissociation of β-casein from the micelle and increase of its concentration in the soluble phase. It is reported that up to 50 % of total β-casein can diffuse into the soluble phase at lower temperatures (Fox and Brodkorb, 2008). The amount of water associated with casein micelles also decreases during cooling of milk (Broyard and Gaucheron, 2015).

These changes in casein micelles occurring at temperatures below 95 °C are considered reversible.

During heating of milk at temperatures above 70 °C irreversible interactions of whey proteins with caseins take place (Donato and Guyomarc'h, 2009).

2.3.2 Decrease of the pH.

The native pH of milk is around 6.7. Decrease of the pH below this value leads to gradual solubilization of the colloidal calcium phosphate within the micelles (Dalgleish et al., 1989). In the range between 7.0 and 6.0 the solubilization of casein molecules from the micelles decreases, especially in pure water, due to the reduction of repulsive forces (Famelart et al., 1996). Then between pH 6.0 and 5.8 dissociation of the caseins (including κ-casein) from the micelles increases. The maximum dissociation of β-casein is reported at pH 5.6 (Broyard and Gaucheron, 2015). Famelart et al. (1996) reported the presence of a peak of the concentration of non-micellar caseins in 25 g/L native phosphocaseinate suspensions at 20 °C at pH 5.4-5.5. The maximum was observed for

different media (water, 0.1 M NaCl and milk ultrafiltrate), with the fraction of non-micellar caseins determined by HPLC of 7 %, 30 % and 12 % in water, NaCl and UF, respectively. The dissociation of caseins from micelles increases strongly with decreasing temperature. The peak of solubility generally shifts to lower pH values with decreasing temperature. Dalgleish and Law (1988) reported the peaks of total casein solubility in skimmed milk at pH 5.1, 5.4 and 5.5 at 4 °C, 20 °C and 30 °C, corresponding to dissociation of more than half, one third and less than one tenth fractions of total casein, respectively. There are significant differences in dissociation behavior of individual caseins, with β-casein dissociating in highest quantities and α_{s2}-casein – in smallest (Dalgleish and Law, 1988).

Below pH 5.6 the extent of solubilization of CCP "increases markedly" (Lucey et al., 1996; Lucey and Horne, 2009). Between pH 5.5 and 5.0 the casein dissociation decreases and proteins aggregate and attach back to the micelles, especially strongly in the presence of NaCl (Famelart et al., 1996; Ingham et al., 2016). By pH 5.2 (Broyard and Gaucheron, 2015; Gaucheron, 2005) or 5.1 (Ingham et al., 2016) or 5.0 (Lucey and Horne, 2009) all the CCP in micelles is solubilized. Lucey and Horne (2009) note that "the pH at which CCP is completely solubilized presumably varies with the conditions (rate and temperature) of acidification". Ingham et al. (2016) found for SAXS data for cow skim milk after addition of GDL powder at 37 °C that when the pH reached 5.15 the high-q feature became broader and disappeared at pH 4.85, which they attributed to "the disruption of the dense protein regions, linked to the release of caseins into the serum phase and redistribution of phosphoproteins following the solubilization of calcium". Further decrease of pH to 4.7 (Ingham et al., 2016) or 4.6 (Broyard and Gaucheron, 2015) results in an acid-induced gelation of caseins due to charge neutralization. Below the pH of minimal solvation (the isoelectric pH 4.4-4.6) caseins are positively charged (Famelart et al., 1996). At pH 3.5, calcium is completely solubilized (present in the solution only in the ionic form Ca^{2+}) (Gaucheron, 2005; Le Graet and Brulé, 1993).

Lucey et al. (1996) demonstrated that decrease of the pH to 4.6 causes an irreversible solubilization of the CCP of the micelles. The micellar structure is not restored back even after an immediate neutralization of the system after the initial decrease of the pH. The solubilization of CCP with the decrease of pH down to 5.2 does not, however, result in the loss of the micellar structure. Marchin et al. (2007) reported that the micelles remained intact at pH 5.2, while cryo-transmission electron microscope images indicated that CCP had dissolved.

Famelart et al. (1996) reported on the change of the diffusible calcium concentration as function of pH for 25 g/L suspensions of native phosphocaseinate powder in water, 0.1 M NaCl and milk utrafiltrate (MUF) (Figure 4).

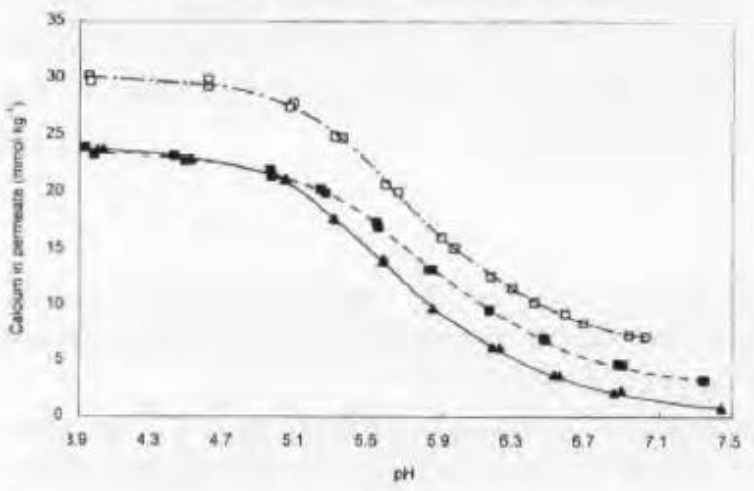

Figure 4. Solubilization with the decrease of the pH at 20 °C of calcium in 25 g/L suspensions of native phosphocaseinate in water (▲), 0.1 M NaCl (■) and milk ultrafiltrate (□). Concentrations of calcium in permeates obtained by ultrafiltration on Centriflo CF25 are presented. The pH values were obtained after 15 h after the addition of GDL at 20 °C. Two replicates for each medium are presented (from Famelart et al. (1996)).

Gonzalez-Jordan et al. (2015) used magic angle spinning (MAS) ^{31}P NMR in order to study the mobility of organic and inorganic phosphorus in micellar casein solutions as a function of pH between pH 4 and pH 8 to trace the dissolution of the CCP. They found a sharp increase of mobile phosphate fraction below pH 5.5 that reached 75 % at pH 4.8 for both organic and inorganic phosphorus. The authors found precipitation of a significant fraction of the proteins in casein micelles solutions below pH 5.0 at 100 g/L by visual observations. Microscopic casein flocks appeared on confocal microscopy images starting at pH 5.2. It was found that the decrease of the pH and dissolution of the CCP renders the phosphorylated serines mobile, but there was no correlation between the mobility of the phosphates and the solubility of the caseins.

2.3.3 Addition of calcium chelatants.

The addition of chelatants (chemicals having high affinity for calcium such as EDTA, citrate or polyphosphates) causes a decrease of the calcium activity in the serum phase and therefore leads to the solubilization of micellar calcium phosphate. Consequently, suspensions of micellar casein become less turbid and less white (Broyard and Gaucheron, 2015). According to Udabage et al. (2000), the addition of 5 mmol and 10 mmol of EDTA per kg of reconstituted skimmed milk caused the removal of 5 % and 30 % of the micellar casein, repectively. Addition of small amounts of chelatants, similarly to the slight decrease of the pH, does not lead to a significant change of the micellar structure.

Thomar and Nicolai (2015) studied the effect of adding different amounts of sodium caseinate to water suspensions of micellar casein at pH 6.7. The mixtures were centrifuged 16 h after preparation and the supernatant was analyzed. With increasing sodium caseinate concentration the weight fraction of non-sedimentable proteins increased. At a weight fraction of NaCas above 0.8 almost all casein remained in the supernatant. Therefore, all casein micelles were dissociated by the

presence of NaCas in large excess, which is explained by a high affinity of sodium caseinate for calcium that causes fast solubilization of the CCP. The authors concluded that “the capacity of phosphate groups to dissociate casein micelles is only weakly larger in polyphosphate than in sodium caseinate”.

The nature of the chelating agent is reported to influence the rheological properties of the protein mixtures obtained as a result of the CCP removal. For instance, the removal of CCP by addition of polyphosphates induces the aggregation and gelation of the caseinate particles at C > 30 g/L, especially fast at high temperatures, which is not observed in sodium caseinate mixtures obtained by acid precipitation (Panouillé et al., 2004, 2005; Pitkowski et al., 2007).

2.3.4 Addition of NaCl.

The addition of NaCl to milk and suspensions of micelles causes the interaction of the added sodium with the calcium and protons bound to phosphoseryl residues of casein molecules (Famelart et al., 1996). As a result, pH slightly decreases, while soluble calcium concentration is reported to increase (Famelart et al., 1996, 1999; Le Graet and Brulé, 1993). For example, it has been shown that “addition of 0.1 mol/L NaCl in milk at pH 6.7 leads to about 0.75-1.00 mM/kg diffusible calcium increase (11 % increase)” (Famelart et al., 1996). Addition of NaCl to a suspension of micelles in water is reported to cause solubilization of phosphorus, while NaCl addition into milk leads to solubilization of calcium only (Famelart et al., 1996, 1999). At the same time, the hydration of micelles also increases (Broyard and Gaucheron, 2015). The addition of salt also leads to the shielding of the negative charges of casein micelles. It influences the technological properties of the micelles, the most important one being the delay of the rennet gelation in the presence of NaCl (Famelart et al., 1999).

2.3.5 Addition of di- and three-valent ions.

The influence of minerals on the casein micelles has been studied on different systems. Different salts of di- and three-valent cations, such as calcium chloride, might be added to milk during its technological treatment (for example in cheesemaking), but also in order to increase its nutritional value.

Philippe, Le Graet and Gaucheron (2005) studied addition of different cations (Fe, Cu, Ca, Zn and Mg) to casein micelle suspensions in milk ultrafiltrate. They noted the important role of ultrafiltrate molecules (citrate, inorganic phosphate) on the mechanism of cation association with casein micelles, which is affected by the affinity of the added cation for citrate and inorganic phosphate.

The addition of calcium to skimmed milk results in a pH decrease. For instance, the addition of 13.5 mM/kg of $CaCl_2$ leads to the pH change from 6.75 to 6.30 (Philippe et al., 2003). After pH readjustment back to 6.75 it is reported that 80 % of the added calcium is bound to casein micelles. The displacement of inorganic phosphate was also observed (a 67 % decrease of free inorganic phosphate after addition of 13.5 mM/kg of $CaCl_2$ and pH regulation and 52 % decrease without pH

regulation). Addition of 13.5 mM/kg of $CaCl_2$ also causes a 70 % decrease in α_{s1}- and β-casein content in supernatant after ultracentrifugation. These changes result in the modification of the structure of casein micelles with decreased zeta potential, hydration and heat stability, leading to the acceleration of rennet coagulation (Broyard and Gaucheron, 2015). The studies of skim milk enriched in calcium suggest that addition of calcium salts does not result in formation of calcium bridges between micelles (Philippe et al., 2003).

2.3.6 The influence of the aqueous phase on gelation of casein micelles.

A considerable number of scientific publications describe the physico-chemical changes of casein micelles occurring during production of dairy products, such as yoghurt or cheese. Absolute majority of these publications study the behavior of micelles in their natural environment, i.e. in milk or in MUF. However, the technological processes of dairy manufacturing often require standardization of the raw materials that is achieved by fractionation of the ingredients found in milk. The examples of products obtained from milk include the sodium and calcium caseinate powders, different isolates of whey proteins and so on. The product called native phosphocaseinate powder (NPCP) is produced by membrane microfiltration of milk, followed by spray drying of the diafiltration retentate, which results in a powder enriched in micellar casein (Broyard and Gaucheron, 2015; Famelart et al., 1996). It has been reported that NPCP demonstrates reduced rennet clotting time and increased gel development kinetics (Famelart et al., 1996). The use of this product, however, involves reconstitution of the micelles in the medium that is different from the natural environment of micelles found in milk. The micelles might be simply redistributed in water or in a solution with mineral composition that is different from the aqueous phase of milk. On the other hand, as milk represents a complex fluid with several components found in the dynamic equilibrium, the micelles redistributed in water serve as an easier model system that can allow the understanding of their behavior in more complex environments (Broyard and Gaucheron, 2015).

Below we discuss the few studies investigating the behavior of the micelles extracted from milk and placed in a different environment.

Famelart et al. (1996) compared the acidification by GDL of suspensions of native phosphocaseinate powder (NPCS) in water, 0.1 M NaCl solution and in milk ultrafiltrate (UF). Diffusible calcium and phosphorus contents were higher for NPCS in NaCl than in water (2.862 mmol/kg in water versus 5.525 mmol/kg in NaCl at concentration 25 g/L and pH 6.7). The diffusible minerals content of NPCS in UF was slightly lower than the diffusible mineral content on NPCS in water plus the minerals of UF, suggesting that some soluble material of UF becomes an insoluble part of the micelles. More CCP dissolves with addition of NaCl to water suspensions of NPCP than to milk: 2.7 mmol/kg of solubilized calcium in NPCS versus 0.75-1 mmol/kg of solubilized calcium in milk with 0.1 M of NaCl. Moreover, the addition of salt to water suspensions of NPCP caused also an increase of soluble phosphorus (0.758 mmol/kg), which had not been observed when salt was added to milk. The solubilization of the CCP with addition of salt is caused, firstly, by the absence of calcium phosphate in the aqueous phase and, secondly, by the decrease of free calcium activity coefficient with addition of NaCl. It was found that “total mineral solubilization obtained with the pH reduction was observed at higher pH values for NPCS in NaCl”. The suspension medium influenced the pH of the onset of protein gelation: around 5.2 for micelles in water and lower pH (around 4.8) for micelles

in NaCl and in UF. The firmness of the acid gels measured with a constant speed cone penetrometer at pH 4.4 and 20 °C was approximately 240 Pa for micelles in water, and 40-50 Pa in NaCl and UF. The addition of salt lowers the net positive charge of casein molecules, increasing the interactions and therefore leads to the coarser gel structure.

Auty et al. (2005) studied GDL-induced gelation of micellar casein (50 g/L) dispersed in water and in lactose-free simulated milk ultrafiltrate (SMUF) containing 40, 70, 100 and 200 % of the salts normally present in milk. They found that the pH at which gelation started decreased from ~6.0 to ~4.8 with increasing ionic strength of the medium. The gels prepared at low ionic concentrations (≤ 40 % SMUF) had a coarse microstructure with large pores, while at higher SMUF concentrations the gels were more homogeneous with smaller pores. Strong syneresis occurred in the micellar casein sample dispersed in water causing difficulty measuring the elastic modulus. The authors note that "while casein micelles dissociate significantly in solutions of low ionic concentrations, this is generally due to extensive dilution and significant dissociation does not occur at the protein concentration used in this study (5 %, w/v)". They found that in the sample containing 50 g/L micelles dispersed in water only 1.03 mM, or ~3 % of total micellar calcium was solubilized. Similarly, very little micellar calcium or casein solubilized in the sample dispersed in 100 % SMUF. Similarly to Famelart et al. (1996), in the sample containing micellar casein in 200 % SMUF "~20 % of the calcium from the dispersant became non-ultrafilterable and thus became associated with the micellar component".

Thomar and Nicolai (2015) studied the stability of water suspensions of native phosphocaseinate powder (NPCP) at concentrations between 0.4 to 40 g/L at pH 6.7 by measuring the turbidity and found that the stability of the suspensions depends dramatically on the concentration of micelles. The micelles dissociated quickly at low concentrations (0.4-2 g/L) and their dissociation was completed within 16 hours, while at 40 g/L the turbidity decreased by only 6 % in 16 hours. At higher concentrations of micelles the further solubilization of the CCP is inhibited by the presence of minerals that are initially released from the micelles.

Thomar and Nicolai (2016) studied heat-induced gelation of suspensions of casein micelles in water in the concentration range between 25 g/L and 160 g/L and in the pH range 5.2 - 6.7. The micelles flocculated at pH ≤ 5.2. It was found that when the temperature was increased above a critical value T_C the casein micelle suspensions gelled. T_C increased with increasing pH and decreasing protein concentration. At 160 g/L T_C increased much stronger with increasing pH in the range 5.8 - 6.5 (from 30 °C to 90 °C) than in the range 5.4 - 5.8. A steep increase of T_C below 55 g/L was found. At 25 g/L the critical temperatures were even higher, the micelles could not support their own weight and precipitated.

Remarkably, little influence of the heating time on T_C was found: if the temperature was 5 °C higher than T_C, gelation happened almost immediately; 5 °C below T_C did not lead to gelation overnight. By contrast, the stiffness of the gels dropped dramatically in a narrow temperature range around T_C, while heating at higher temperatures had no effect on gel stiffness.

In the same work, the effect of the protein concentration in the range between 40 g/L and 160 g/L on the stiffness of the gels at pH 5.6, 6.0 and 6.2 after heating was studied. Micelles precipitated at C < 40 g/L. The gel stiffness increased steeply with increasing protein concentration in the concentration range between 40 and 60 g/L. At higher C the increase was weaker. Remarkably,

no effect of pH on the gel stiffness was found in the studied range. T_C varied little for concentrations above 100 g/L and increased quite steeply below 100 g/L at all studied pH values.

The results were compared with those obtained for sodium caseinate heated at 160 g/L at pH 5.4, 5.6, 6.0 and 6.7. Gel formation with sodium caseinate requires more time and gives much weaker gels, which demonstrated the importance of the micellar structure for the properties of the gels.

More recently, Balakrishnan et al. (2017) demonstrated the critical importance of free calcium on thermal gelation of aqueous suspensions of micelles. It has been shown that addition of $CaCl_2$ leads to a steep decrease of T_C. The effect of calcium cannot be explained by simple reduction of electrostatic interactions as addition of NaCl has been shown to increase T_C. Addition of EDTA also strongly increased critical gelation temperature. It was suggested that aggregation of micelles happens through formation of calcium bridges between micelles.

3. Globular proteins of milk.

3.1 Globular proteins: general overview. Aggregation and gelation.

Unlike casein, globular proteins, such as hemoglobin, egg ovalbumin or β-conglycinin of soy, have well-defined secondary and tertiary (and sometimes quaternary) structures and are usually found in aqueous solutions in a compactly packed form. The proteins in milk whey – α-lactalbumin (α-lac), β-lactoglobulin (β-lg), bovine serum albumin (BSA) and immunoglobulins – are all globular proteins.

When solutions of globular proteins are heated, their compact structure unfolds exposing active groups of amino acids, for example, free thiol groups, to the surface (Donald, 2008; Nicolai et al., 2011; Phan-Xuan et al., 2011). Consequently, the proteins irreversibly aggregate forming aggregates of different morphology and size, depending on the heating conditions, such as pH and ionic strength of the solution and protein concentration. Under certain conditions, the aggregation of globular proteins might result in a formation of a gel (Baussay et al., 2004). The gelation conditions and the gel properties depend strongly on the protein concentration, type of salt and the pH (Ako et al., 2010).

The aggregation and gelation of globular proteins have been studied comprehensively. β-Lg has been studied particularly in great detail due to its relative simplicity and importance for the food industry (Ako et al., 2010; Durand et al., 2002). The results of β-lg studies are closely related to the heat-induced aggregation of proteins found in whey protein isolate (WPI), which is a by-product of cheese manufacturing, and contains a mixture of globular proteins mentioned above (Mahmoudi et al., 2007).

β-Lactoglobulin is a globular protein that represents more than 50 % of the bovine whey proteins (Walstra and Jenness, 1984) with the molar mass of about 18 kg/mol and molecule radius of about 2 nm (Pessen et al., 1988). Seven genetic variants of the protein that differ in the amino acid composition in the primary structure have been described with variants A and B being the most

common in cow's milk (Pessen et al., 1988). Different variants have been demonstrated to have the same aggregation rate and aggregate structure upon heating (Le Bon et al., 2002).

In aqueous solutions β-lg is present in dynamic equilibrium between its monomer and dimer forms. The monomer form is favored at strong electrostatic repulsion conditions. The equilibrium shifts towards the monomeric configuration with decreasing ionic strength, increasing temperature (Aymard et al., 1996), and at low protein concentrations (Baussay et al., 2004). At pH 7 β-lg molecules are mostly found in solutions in the dimer form (Baussay et al., 2004; Gimel et al., 1994).

The aggregation of globular proteins is preceded by protein denaturation (or unfolding) (Verheul et al., 1998). The depletion rate of native proteins during heating depends on the temperature, concentration, pH and ionic strength. The dependence of the depletion rate on different parameters has a very complex character, as reviewed by Nicolai, Britten and Schmitt (2011), because the rates of denaturation and aggregation are influenced differently with changing conditions.

At pH 7 the denaturation and aggregation of β-lg starts at a considerable rate at temperatures above 50 °C (Le Bon et al., 1999). The aggregation rate depends strongly on the heating temperature with high activation energy: the values between 250 and 400 kJ/mol have been reported in the literature (Baussay et al., 2004). The temperature affects only the aggregation rate (Durand et al., 2002), but not the structure of aggregates (Bon et al., 1999; Le Bon et al., 1999).

For the process of aggregation and gelation, there are two important values of protein concentration: the critical association concentration (CAC) and the critical gelation concentration (C_g). The protein aggregation does not start at protein concentrations below CAC and only oligomers and denatured monomers are formed (Baussay et al., 2004; Mehalebi et al., 2008). At concentrations above CAC the aggregation of protein occurs. First, primary aggregates are formed that might further aggregate into larger aggregates. If protein concentration reaches C_g one observes formation of a gel. At concentrations between CAC and C_g a suspension of soluble protein aggregates is produced (Ako et al., 2010). The exact values of CAC and C_g depend strongly on the pH and the ionic strength and the type of protein. The addition of salt and decrease of pH down to the isoelectric point (pI) reduce the repulsive interactions between protein molecules and consequently the values of CAC and C_g decrease (Ako et al., 2010; Baussay et al., 2004).

The electrostatic interactions also determine the structure and appearance of gels formed above C_g. Turbid gels with dense and strongly branched networks are formed at high ionic strengths and pH closer to pI (Baussay et al., 2004; Pouzot et al., 2004; Vreeker et al., 1992). On the other hand, the gels formed under strong electrostatic repulsion are transparent with well-ordered fibrillar structure (Pouzot et al., 2004).

3.2 Characteristics of aggregates formed by β-lactoglobulin and WPI.

The structure of the globular protein aggregates has been studied in most detail for β-lg, but similar observations have been done for solutions of WPI, which contains β-lg in large majority. The morphology of the aggregates depends strongly on the pH and the ionic strength.

At pH 1.5 - 2.5 rigid linear aggregates are formed; at pH > 6 curved strands are formed at low concentration and fractal aggregates of these strands at higher concentrations. Between pH 4 and 6 homogeneous spherical aggregates called microgels are formed that flocculate and precipitate between pH 4.5 and 5.7, but are stable just above or just below this range (Nicolai et al., 2011; Nicolai, 2016; Schmitt et al., 2007).

In the context of this thesis only fractals aggregates formed at pH 7.0 and microgels formed close to pH 6 were used.

3.2.1 Aggregates formed at pH 2 (fibrils).

At pH 2 β-lg molecules have a strong positive charge of +20 per monomer (Phillips et al., 1994) and aggregate forming linear aggregates (Durand et al., 2002) sometimes called amyloid fibrils (Donald, 2008). The diameter of the fibrils is equivalent to the one of a monomer (2-4 nm) (Nicolai et al., 2011). At low ionic strength the aggregates are very rigid. At high ionic strength the aggregates are flexible with fractal dimension 2 (Durand et al., 2002). Aymard et al. (1999) studied the β-lg aggregates formed at pH 2 and different ionic strengths and found a strong decrease of the persistence length with increasing ionic strength suggesting the increase of fibril flexibility with increasing ionic strength.

The monomer depletion is much slower at pH 2 than at pH 7 (Baussay et al., 2004) and the aggregation mechanism at pH 2 differs from the two-step mechanism observed at pH 7 (Aymard et al., 1999).

3.2.2 Microgels.

In a narrow regions of pH around pH 4.6 and pH 5.9 whey proteins at concentrations up to 50 g/L and low ionic strength form dense spherical particles with a diameter between 100 nm and 1 µm called microgels. It was shown that microgels formed close to pH 6 are self-stabilized by spontaneous increase of pH during their formation (Nicolai, 2016; Phan-Xuan et al., 2011).

3.2.3 Fractal aggregates.

At pH 7 whey proteins form elongated aggregates consisting of about 100 monomers with a length of about 50 nm and a diameter of about 10 nm (Mahmoudi et al., 2007). With increasing protein concentration these primary aggregates further associate forming fractals or self-similar aggregates. The size and the molar mass of the aggregates increases exponentially with increasing protein concentration above about 50 g/L and diverges close to C_g (Nicolai et al., 2011; Pouzot et al., 2004). The aggregates may be diluted in water without change of their structure (Ako et al., 2010; Nicolai et al., 2011).

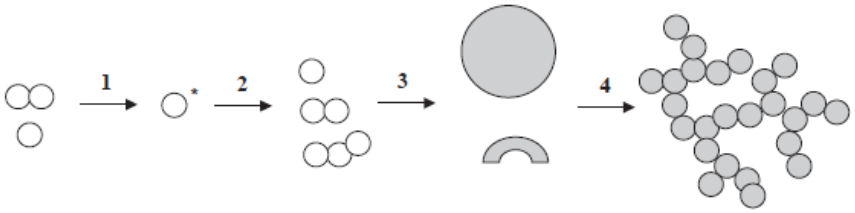

Figure 5. Schematic representation of the heat-induced aggregation of β-lg at pH > 5.7. Step 1 – dissociation and denaturation; step 2 – formation of denatured monomers and small oligomers; step 3 – formation of primary aggregates; step 4 – at C > CAC primary aggregates further associate into self-similar (fractal aggregates) (from Nicolai, Britten and Schmidt (2011)).

Gimel, Durand and Nicolai (1994) studied the structure of soluble aggregates of β-lg formed at pH 7 and found that they have a self-similar structure with a fractal dimension $d_f = 2$.

Baussay et al. (2004) conducted a systematic study of β-lg aggregates formed at pH 7 and different protein concentrations and ionic strength up to 0.4 M NaCl. At low protein concentrations and salt concentrations up to 20 mM only a weak effect on the aggregate molar mass was observed because in these conditions only small oligomers are formed. The value of C_g decreased dramatically with addition of salt: from 100 g/L in pure water to 1 g/L at 0.4 M NaCl.

Interestingly, Baussay et al. (2004) found the same structure factor $d_f = 2$ for aggregates formed at all salt concentrations.

For fractal objects:

$$M_w = aR_{gz}^{d_f}, \quad (1)$$

where M_w and R_{gz} – the weight average molar mass and the z-average radius of gyration found with light scattering;

a – the prefactor depending on the local structure of the aggregates;

d_f – the fractal dimension.

As the fractal dimension d_f was found to be the same for aggregates formed at all salt concentrations, their large length scale structure does not depend on the amount of added salt, while on short length scale the packaging is denser with increasing salt concentration (Baussay et al., 2004). At high ionic strength the aggregates appear to be more branched and therefore less flexible (Baussay et al., 2004; Pouzot et al., 2005).

4. Cold gelation: overview. Ca^{2+}-induced cold gelation.

Cold gelation of globular proteins involves two steps. First, a solution of native protein is heated to cause denaturation of protein molecules and formation of a suspension of soluble aggregates stabilized by electrostatic repulsions. Subsequently, salt is added or the pH is decreased in

order to reduce the repulsion between protein aggregates, which leads to gelation. Although the second step does not necessitate elevated temperatures, gelation happens faster when temperature is increased (Barbut and Drake, 1997; B. Hongsprabhas and Barbut, 1997a).

Cold gelation has been reported for β-lactoglobulin (β-lg) (Ako et al., 2010), BSA (Chinchalikar et al., 2014; Kundu et al., 2014; Navarra et al., 2009), egg ovalbumin (Alting et al., 2004; Doi, 1993), whey protein isolate (WPI) (Barbut and Foegeding, 1993; Bryant and McClements, 2000; Glibowski et al., 2006; B. Hongsprabhas and Barbut, 1997a; P. Hongsprabhas and Barbut, 1997; Kuhn et al., 2010; Wu et al., 2005), soy protein isolate (Lu et al., 2010; Maltais et al., 2005; Murekatete et al., 2014).

The most remarkable feature of cold-set gels is their optical properties: they give clearer and more transparent gels compared to heat-set gels at the same composition (Ako et al., 2010; Barbut and Foegeding, 1993; Doi, 1993; McClements and Keogh, 1995). Formation of a gel at ambient temperatures is a valuable property for a number of applications in food manufacturing (to avoid degradation of vitamins, for example). Cold-set gels are also reported to demonstrate higher water-holding capacity.

The process of cold gelation was first introduced in the literature in the 1990s (Barbut and Foegeding, 1993), when the mechanism of aggregation of globular proteins was yet to be understood. The early publications described experiments involving preparation of gels by the cold-set method and their characterization. The experiments involved varying one of the parameters either during the first step of gel preparation (protein concentration during preheating, the preheating temperature or the time of preheating at a constant temperature) or during the second step (salt and the preheated protein concentrations; temperature and time of gel setting after mixing; gel preparation method through either direct addition of salt or by dialysis through a membrane). A few earlier papers compared the properties of cold-set gels with those of heat-set gels with the same salt and protein composition (Barbut and Foegeding, 1993).

The results of the earlier studies usually demonstrated that longer preheating at the same temperature (B. Hongsprabhas and Barbut, 1997a), preheating at higher temperature (Hongsprabhas and Barbut, 1996) and at higher protein concentration (Alting et al., 2004; B. Hongsprabhas and Barbut, 1997b; Ju and Kilara, 1998a) lead to formation of stronger gels. Vardhanabhuti et al. (2001) studied mixtures of native and aggregated WPI with addition of salts (NaCl and $CaCl_2$), which is essentially similar to the studies of the effect of preheating time.

Concerning the second step of cold gelation, it was found that the increase of preheated protein concentration influences strongly the gel strength. Hongspabhas, Barbut and Marangoni (1999) found a strong increase of the Young's modulus for gels with calcium with the increase of the protein concentration from 60 to 100 g/L. A power-law relationship of the modulus on protein concentration was reported. A few studies investigated the influence of the calcium concentration added to preheated protein (B. Hongsprabhas and Barbut, 1997b; Hongsprabhas and Barbut, 1996; Marangoni et al., 2000). Some of them found a strong increase of the gel hardness with increasing calcium concentration (B. Hongsprabhas and Barbut, 1997a). Most studies, however, found that the mechanical and textural properties of gels as well as the water-holding capacity and other parameters first increase with increasing calcium concentration up to a particular value. However, the following addition of calcium either does not increase the gel strength or even leads to its decrease. Barbut (1995) reported no significant change in textural and mechanical properties of 100

g/L WPI gels prepared by dialysis of the preheated protein against calcium chloride solution in the concentration range between 180 mM (which corresponds to the molar ratio between calcium and whey protein R = 31.5) and 360 mM (R = 63). Barbut (1997) reported a leveling off of the penetration force for 100 g/L gels at 80 mM calcium (R = 14) and of the fracture break force at 60 mM calcium (R = 11). Hongsprabhas and Barbut (1997b) found a maximum of the Young's modulus at the calcium concentration of 30 mM for gels prepared by a 16 hour dialysis at room temperature of preheated WPI at protein concentrations between 60 g/L (R = 9) and 100 g/L (R = 5). Bryant and McClements (2000) found that for cold-set 90 g/L WPI gels prepared by dialysis against 0-15 mM $CaCl_2$ solutions for 48 hours at ambient temperatures, the Young's modulus did not change at calcium concentration above 10 mM (R between 2 and 3). Chinchalikar et al. (2014) studied cold gelation of bovine serum albumin (BSA) at various $CaCl_2$ concentrations using small-angle neutron scattering (SANS). A 50 g/L solution of BSA was preheated at pH 7 and 50 ^{o}C for 2 hours. $CaCl_2$ was added at concentrations 0, 20, 40 and 60 mM (considering the BSA molar mass of 66500 g/mol R = 0; 27; 53; 80) at 30 ^{o}C prior the measurements. However, Hongsprabhas et al. (1999) correctly suggested that the differences of the structure and rheological properties observed in gels prepared at different calcium concentrations might be attributed to the differences in the rate of aggregation.

Hongsprabhas and Barbut (1997) studied the effect of temperature during the second step of cold gelation. They dialyzed preheated WPI solutions (100 g/L) against calcium chloride at 1 ^{o}C, 11 ^{o}C and 24 ^{o}C until gels were obtained. They attributed the differences in mechanical and structural properties of the gels to the change of the aggregation rate, and also to the change of the types of interactions involved in the network formation.

The general drawback of these earlier (and more recent) studies was the lack of the analysis of the composition of the preheated protein solution. Typically, the solution of native protein was diluted to the required concentration (varying from 10 to 100 g/L) at neutral pH and heated in the temperature range between 70 and 90 ^{o}C for 30 (sometimes 15 or even 10) minutes. It was later convincingly shown by size-exclusion chromatography in the study of Ju and Kilara (1998a) that the rate of conversion of native protein into aggregates might reach 97 % at the protein concentration of 90 g/L after 30 min heating at 80 ^{o}C. However, the same heating protocol leads to denaturation of 90 % of native proteins into aggregates at 70 g/L, 56 % at 50 g/L and only 34 % at 30 g/L. Marangoni et al. (2000) obtained similar results in their study. It was also demonstrated that heating even concentrated protein solutions (80 g/L) at high temperature (80 ^{o}C) but for short periods of time (10 minutes) leads to significant amounts of protein left in the native state (Ju and Kilara, 1998a). Therefore, in most of the early studies various mixtures of native protein with protein aggregates were investigated. The information on the size of the aggregates is also absent in most of the earlier studies.

Furthermore, in many of the initial studies gels were prepared by adding calcium to the preheated whey protein by dialysis through a membrane to ensure a slow change of the salt concentration in the gelling system (Barbut, 1995; Barbut and Foegeding, 1993). Apparently, it was considered that by the time the bag was taken out of the calcium solution, the equilibrium of the calcium concentration was reached. In reality, most probably there was a calcium concentration gradient to at least some extent in the gels prepared by this method.

Although calcium is commonly added at a fixed total concentration, Ju and Kilara (Ju and Kilara, 1998b) pointed out that it is the ratio between calcium ions and protein molecules that influences the gelation due to the specific binding of calcium to protein molecules (Zittle et al., 1957). In publications on calcium-induced cold gelation the ratios of calcium added to a preheated protein solution sometimes went to values as high as 63 (Barbut, 1995). Kuhn et al. (2010) who prepared protein aggregates by heating a 100 g/L WPI solution at 90 ^{o}C for 30 minutes and dialyzed the dilutions (50, 60, 70, 80 and 90 g/L) against 150 mM NaCl or $CaCl_2$ for 48 hours at 10 ^{o}C found an increase in the stress at rupture and elasticity modulus values with increasing WPI concentration. Although the total calcium concentration was kept constant in this study, the calcium to protein molar ratio changed from 53 at 50 g/L to 29 at 90 g/L protein concentration, therefore, two parameters were changed contrariwise at the same time, which might have resulted in erroneous interpretation of the results.

It may be also noted that the charge density of protein solutions playing a prominent role in protein aggregation (see Chapter 4) sometimes was not kept constant in studies in which researchers kept constant the pH of systems.

Finally, few of the earlier studies addressed the kinetics of gelation and simply compared the values reached after the established period of time. The evolution of the system with time and temperature was rarely investigated consistently. The mechanical properties of the gels were mostly investigated by the compression or fracture tests (the distance to fracture and the fracture force) and the studies reflect mostly the non-linear properties of the investigated systems.

Ju and Kilara (1998c) conducted a more systematic study. Instead of preparing aggregates by heating protein solutions at different concentrations, they prepared aggregates by heating a 90 g/L WPI solution at pH 7.0 at 80 ^{O}C for 30 minutes and this stock solution was used to prepare 80 g/L mixtures with different amounts of salts. They verified with size exclusion HPLC that at these heating conditions the rate of WPI denaturation was 98 %. The gels with calcium were prepared by adding salt solution (5 to 60 mM, corresponding to R = 1 to 13) directly to the aggregate solution and keeping the mixtures at 45 ^{O}C for 4 hours. They found that the hardness of gels increased steeply up to 20 mM of $CaCl_2$ (R = 4.4), and then leveled off.

The same stock solution was also used to check the influence of the protein concentration, but again the authors kept the total calcium concentration constant rather than the calcium to protein ratio. They prepared gels with protein concentration 10 to 80 g/L keeping the salt concentration constant (20 mM for $CaCl_2$ (R = 35-4.4 correspondingly) and 200 mM for NaCl) and found a steep increase of the gel hardness with increasing protein concentration and suggested a power law increase for $CaCl_2$ and exponential increase for NaCl.

Some studies compared heat-set and cold-set gels with the same composition. It was reported that two methods of gel preparation yielded gels with different structure and mechanical properties. Barbut and Foegeding (1993) reported a fine structure of cold-set gels in comparison with “a particulate microstructure composed of bead-like particles attached to each other” in heat-set gels. They also reported lower penetration force values for cold-set gels than for heat-set gels.

A few publications reported the effect of the type of salt added to the preheated protein on the gel properties. Barbut and Drake (1997) found that the amount of NaCl required to initiate cold

gelation of preheated 100 g/L WPI solution at ambient temperature overnight by dialysis was 10-fold higher compared to $CaCl_2$. Calcium is not only more effective at screening electrostatic interactions but it also cross links negatively charged carboxylic acid groups (Bryant and McClements, 2000). Ju and Kilara (1998c) found for gels with 80 g/L protein (preheated at 90 g/L) formed after 4 hours at 45 ^oC that maximum gel hardness defined by a penetration method was reached at 20 mM $CaCl_2$ and 200 mM NaCl. The following increase of salt concentration did not lead to any change of the gel hardness in case of $CaCl_2$, but led to its decrease in the case of NaCl. Marangoni et al. (2000) found that "the overall rate of aggregation in the presence of $CaCl_2$ was greater than in the presence of NaCl, possibly due to the crosslinking effect of Ca^{2+}". Remondetto, Paquin and Subirade (2002) prepared iron-induced (Fe^{2+}) gels from preheated β-lg. The β-lg aggregates were prepared by heating a 95 g/L β-lg solution at pH 7.0 for 30 minutes at 80 ^oC. The gels were prepared by varying preheated protein concentration (60 – 90 g/L) and iron concentration (10 – 40 mM of $FeSO_4$) in the pH range between 7.0 and 9.0. The gels were prepared by keeping protein-salt mixtures at 24 ^oC for 4 hours. It was found that mechanical, optical and structural characteristics of the gels are similar to those obtained in studies with Ca^{2+}-induced cold gels suggesting a similar mechanism of protein network formation. It was found that, similarly to the gels with calcium, the 60 g/L gel prepared with preheated β-lg had a higher value of elastic modulus at 10 mM of Fe^{2+} (R = 3) than at 30 mM (Remondetto and Subirade, 2003). Chinchalikar et al. (2014) conducted SANS experiments on systems with 50 g/L preheated BSA and three ions with different valency (NaCl, $CaCl_2$ and $FeCl_3$) keeping the ionic strength constant (in contrast to the molar ratio or the same total amount). They found closer packing of gel with increasing valency of the ion, resulting in the lesser amount of salt required to achieve gelation. The gelation kinetics was not investigated in the study.

The development of analytical methods such as light scattering allowed a deeper understanding of the aggregation and gelation processes. Navarra et al. (2009) formed protein aggregates by heating 1 mM (66 g/L) solutions of BSA at pH 7.0 and 58 ^oC for 2 hours and defined their size (about 20 nm) by dynamic light scattering. The suspension of protein aggregates demonstrated properties of a weak gel at 20 ^oC. The 66 g/L (1 mM) suspension of BSA aggregates was mixed with $CuCl_2$ and $ZnCl_2$ solutions at room temperature to get the final salt concentration ranging from 1 mM to 30 mM. The evolution of the elastic modulus of the mixtures was followed on the rheometer for 2 hours at 58 ^oC. For both salts, the gel was not formed at salt concentration of 1 mM/mL (R = 1). A gel was formed, however at 5 mM (R = 5). The maximum value of the elastic modulus was obtained at 10 mM (R = 10), followed by progressively lower values of G' at R = 15, 20 and 30, which was explained by a transition from a fine-stranded gel to a particulate gel or, simpler, by syneresis. The maximum values of G' obtained at R = 10 were about 2×10^5 Pa for $CuCl_2$ and between 3 and 4×10^5 Pa for $ZnCl_2$. The higher value for zinc was explained by the presence of "more sites available for Zn^{2+} rather than for Cu^{2+} bridges on the protein surface". Kundu et al. (2014) who studied the influence of Na^+, Ca^{2+}, Cu^{2+} and Fe^{3+} on cold gelation of preheated BSA and found that gelation in the presence of Ca^{2+} is less strong than in the presence of Cu^{2+} ions suggested that "the higher ionic radius of Ca^{2+} produces less charge density which reduces the fractal dimension and hence the gelation".

Wu, Xie and Morbidelli (2005) conducted a small-angle light scattering kinetics study of calcium-induced cold gelation of WPI aggregates under dilute diffusion-limited cluster aggregation (DLSA) conditions. They formed aggregates by heating a 100 g/L WPI solution at 90 ^oC for 30 minutes. The size of the formed aggregates was 32.5 nm. The protein aggregation was studied in diluted

solutions with protein concentration C = 0.007 and 0.02 g/L and $CaCl_2$ concentration 0.1 mol/L as a function of time (not clear at which temperature). They found that at first the aggregation kinetics is described by a power law and the cluster growth follows the mass fractal scaling with the fractal dimension d_f = 1.85. Then the growth of the radius of gyration accelerates indicating the percolation process leading to gelation. The results of the study were found to be in a good agreement with DLSA simulations.

In a more recent publication, Wu et al. (2012) carried out a thorough investigation of $CaCl_2$-induced aggregation and gelation of bovine serum albumin "pre-aggregates" with light-scattering techniques. They heated a BSA solution at C = 30 g/L at 90 ^oC and pH 7.0 for 90 min, which resulted in formation of protein aggregates of a "filamentous structure with an average length of about 150 nm and a diameter of about 8 nm" (as seen with transmission electron microscopy and atomic force microscopy), radius of gyration of 50.3 nm and hydrodynamic radius of 27.7 nm. They studied the evolution of the second virial coefficient A_2 (related to the interaction potential between particles) as a function of $CaCl_2$ concentration in the range [0; 0.2] mol/L in mixtures with pre-heated BSA (C = [0.05; 0.5] g/L) at room temperature. They found that A_2 steeply decreases to reach a minimum value with the addition of salt up to 0.015 mol/L indicating screening of the electrostatic repulsion leading to aggregation. The following addition of salt, however, leads to the increase of the A_2 value meaning the re-stabilization of the system, resulting from the counterion binding and originating from there short-range repulsive hydration interactions. The study of the evolution of the scattered intensity curves with time for a mixture of BSA aggregates (2 g/L) with calcium chloride (0.01 mol/L) revealed two time intervals: first, the reaction-limited cluster aggregation (RLCA) regime (formation of micro-size clusters) with a fractal dimension D_f = 2.1 followed by the micro-size clusters connecting to form macro-structures (gels). The second interval results in the formation of a gel.

Another comprehensive study of cold gelation using light scattering techniques was conducted by Ako, Nicolai and Durand (2010). It was concluded that there is no qualitative difference between the structure of cold-set and heat set gels apart from the local structure of the aggregates, which is denser for the heat-set gels. This minor difference, however, leads to phase separation and transition from so-called fine-stranded to particulate gel structure at significantly lower salt concentrations in heat-set gels compared to the gels produced by cold gelation, reported in many studies (Kuhn et al., 2010). Another conclusion was that gels produced with $CaCl_2$ and NaCl also did not have qualitatively different structure, and higher valency of the ion leads simply to its higher efficiency at lower concentrations. The study of the cold gelation kinetics conducted on β-lg aggregates with R_g = 65 nm at C = 50 g/L and 0.3 M NaCl yielded the value of the activation energy E_a = 70 kJ/mol. It was found that increasing salt concentration accelerates the aggregation kinetics following a power law relationship. Concentration of the aggregates was also reported to speed up the gelation process strongly, even though the quantitative dependence is difficult to suggest. It is the first proper investigation of the influence of the size of the aggregates on cold gelation. It was found that increase of the aggregate size from 19 nm to 260 nm accelerates the gelation process only slightly, and has no influence on the gel structure.

In an earlier publication Mleko (1999) also attempted to study the influence of the aggregates size on the gelation process. The aggregates were prepared by heating 3-10 % solutions of whey protein containing 0.1 M NaCl at pH 8.0 "until just prior to the gel point (24-56 min) determined by flow". The pH of 8.0 was chosen because higher pH favors formation of disulfide

bonds. Prepared protein aggregate suspensions were diluted to 3 %, pH was adjusted to 7.0 and the mixtures were heated again. It was concluded that larger aggregates formed at higher protein concentrations lead to higher storage modulus, hardness and optical density of the gels. Although it was correctly concluded that the conditions of the experiment lead to formation of aggregates of different sizes, the size of the aggregates was not determined and also the rate of conversion of native WPI to aggregates was not investigated. The main drawback of the study was that the gelation of the aggregates at 80 °C in the second step was followed only for 30 minutes and the conclusion regarding the gel properties was drawn without taking into consideration the kinetics of the process. The effect of salt addition and change of the charge density were not decoupled in this study.

A few reports have been published on other types of aggregates prepared at different conditions and therefore having different morphology and properties. Clare et al. (2007) investigated properties of a modified whey protein concentrate (WPC) powder prepared by acidification of a WPC solution to pH 3.35, followed by extended heat treatment, destruction of the obtained gel and its spray drying. Hudson, Daubert and Foegeding (2000) defined the size of the protein particles obtained through this method of 25.3 μm. The addition of calcium to the solutions of the powder increased their viscosity. The measurement of the elastic modulus of the solution containing 56 g/L of modified protein at pH 3.5 with addition of calcium (100 mM) at 4 ^{o}C revealed its constant increase over a period of 14 hours. The heating of the same mixture to 80 ^{o}C resulted in a strong syneresis, which is not surprising considering that the molar ratio between calcium ions and protein in this mixture reached the value of R = 31. Mudgal, Daubert and Foegeding (2009, 2011) produced fibrillar aggregates from β-lg at pH 3.35 and reported their gelling properties. Donato, Kolodziejcyk, and Rouvet (2011) reported on acid-induced cold gelation of mixtures of microgels with fractal aggregates. The gels with higher ratio of microgels were much weaker than gels prepared from fractals.

In conclusion, the recent light scattering studies helped to understand the mechanism of cold gelation and structure of the cold-set gel, as well as heat-set gels. A deeper understanding of the connection of microscopic and macroscopic parameters of the gels would however be useful.

5. Acid-induced cold gelation.

Much fewer publications have appeared on acid-induced cold gelation of globular proteins. The gelation in all the studies is induced by addition of GDL.

In the study mentioned above Ju and Kilara (1998c) compared properties of gels produced from WPI aggregates by addition of two salts ($CaCl_2$ and NaCl) and acidulant (GDL). The aggregates were prepared by heating a 9 % protein solution at pH 7.0 and 80 °C for 30 min. The degree of denaturation of the protein determined by HPLC was 98 %. Cold gelation of the aggregates was induced by dilution to 8 % of protein concentration and addition of 0.2-2.0 % w/v of GDL powder, which resulted in pH decrease to 5.7-3.5. The mixtures were kept at 45 °C for 4 hours and then at 5 °C overnight. The mixture with 0.2 % of GDL (pH 5.8) did not gel in these conditions, while the mixture with 0.4 % GDL (pH 5.3) formed a “semi-clear (translucent)” gel. Addition of more GDL resulted in the formation of “white opaque” gels. The maximum gel hardness, determined by a penetration with a cylinder probe, was reported for the gel at pH 4.7 (0.8 % GDL). “Increasing or

decreasing GDL concentration from 0.8 % decreased gel hardness". The gels produced with GDL were "notably harder" than gels produced by addition of 10-40 mM of $CaCl_2$ (R = 2-8). In the second experiment the same aggregates were diluted to different protein concentrations in the range 1-8 % and the same amount of GDL (0.8 % w/v) was added to all solutions. In other words, both protein concentration and charge density of proteins were changed at the same time. A power-law relationship between gel hardness and WPI concentration was found (the gelation protocol was the same as in the first experiment). "GDL-induced gels were notably harder" than the gels formed by addition of 20 mM of calcium (R = 35-4.4 for 1-8 % protein solutions correspondingly).

In the following publication Ju and Kilara (1998a) heated WPI solutions in the concentration range 1-9 % at 80 °C for 30 min. A series of gels was prepared by diluting 4-9 % heated protein suspensions to 3 % and addition of 0.6 % w/v GDL (to reach pH 5.0). The mixtures were incubated at 37 °C for 1 hour and then left in the fridge overnight. A linear increase of the gel hardness with increasing protein concentration during preheating was found. The size of the aggregates determined by light scattering varied only slightly with increasing concentration: from 21 nm at 3 % to 61 nm at 9 %. The fraction of denatured protein, on the other hand, varied strongly with protein concentration during heating: from 34 % at 3 % protein to 97 % at 9 %. The 90 % conversion was achieved in the heating conditions of the experiment only at 7 % protein. Therefore, the observed effect on the gel strength is determined mostly by the fraction of denatured protein rather than the size of the aggregates. The effect of the heating time on 8 % WPI solution at 80 °C was studied (5-30 minutes). The gels formed with 0.6 % GDL from protein prepared this way demonstrated rapid increase of the gel hardness with the increase of preheating time between 5 and 12 minutes, followed by a limited increase for longer preheating times, due to denaturation of a big fraction of proteins after 12 minutes. The 0.6 % GDL gels were harder than the gels formed with 20 mM $CaCl_2$ (R = 4.4).

Alting et al. (2000) studied the mechanism of acid-induced network formation in 20 g/L suspensions of WPI aggregates by blocking the reactive thiol groups on the aggregate surface. The aggregates were prepared by heating a 9 % w/w WPI solution for 2 hours at 68.5 °C, which caused conversion of > 95 % of native protein. The aggregates were then treated with thiol-blocking agents. The gels were formed by adding 0.15 % w/w of GDL resulting in the decrease of pH from 7.2 to ~5 in the course of 24 hours at ambient temperature. The gelation kinetics in the first 8 hours of acidification, followed by the turbidity measurements, was the same for both aggregates with blocked thiol groups and non-treated aggregates. The microstructure of the gels was also the same for aggregates of two types. However, the hardness of the gels formed with blocked aggregates determined by penetration method after 24 hours of gelation was "5-10-fold" less than for non-treated aggregates. The authors suggested that the initial formation of the network by non-covalent interactions is followed by a slower formation of disulfide bonds that reinforce the network. Interestingly, it is reported that it was still possible to form gels at protein concentrations as low as 5 g/L.

In the following publication Alting et al. (2003a) studied the influence of the aggregates size on the properties of acid-set gels. The aggregates of different sizes were prepared by heating WPI solutions at concentrations 3, 4.5, 6, 7.5 and 9 % (w/w). Longer heating times were applied at lower protein concentrations to ensure the conversion rate of at least 95 %. The gels were prepared by adding 0.14 % w/w of GDL to 2 % w/w suspension of aggregates of different sizes to decrease pH

from 7.2 to 5 after 24 hours at ambient temperature. DLS was applied in order to determine the aggregate size, but the measurements were conducted just at one angle (90 degrees) yielding the hydrodynamic diameter increase from 51 to 67 nm with increasing protein concentration. The stiffness of the gels defined by the penetration test increased with increasing size of the aggregates starting from the aggregates prepared at 6 %. However, it was demonstrated that aggregates of different sizes treated with thiol-blocking agent all produced much weaker gels. In other words, the effect of the aggregate size on the gel hardness was much less significant in comparison with the influence of disulfide bonds forming between thiol groups. The importance of disulfide bonds forming between thiol groups was also demonstrated by Rabiey and Britten (2009) who prepared acidified gels from aggregates prepared by heating solutions of whey proteins with different α-lac/β-lg ratios. The monomer of β-lg contains one free cysteine that becomes available for interactions after denaturation, while α-lac molecule has no free cysteine. It has been shown that aggregates formed by heating solutions with higher ratio of α-lac yielded weaker gels compared to aggregates formed with β-lg.

Alting et al. (2003b) also studied the influence of the aggregate concentration on the mechanical properties of acid-induced WPI gels. The aggregates were prepared by heating a 9 % WPI solution. The gels were formed in the protein concentration range between 0.5 and 9 % by adding different amounts of GDL in order to reach the final value of pH 5 after 24 hours at ambient temperature. The permeability of the gels decreased, while the elastic modulus G' (plateau values) increased with increasing protein concentration, both following the power law dependency on the protein concentration. The plateau values of G' increased from $\sim 10^2$ Pa to more than 10^4 Pa with the increase of the protein concentration from 1 % to 6 %. The structure of the gels observed with CLSM varied strongly with protein concentration: "the protein network structure […] appeared coarser, having larger pores at lower protein concentrations", until "at the highest concentrations (> 6 %) the structures become too small to be fully resolved by the microscope".

Donato et al. (2011) studied acid-induced gelation of mixtures of 270 nm microgels with 100 nm fractal aggregates acidified by addition of 1 %wt GDL at 40 °C. The fractal aggregates were prepared by heating 8 %wt solution at pH 7.6 (z-average hydrodynamic diameter 82 nm) and 4 %wt solution at pH 7.0 (z-average hydrodynamic diameter 106 nm) for 1 h at 85 °C. The rate of conversion of native WPI was at least 96 %. Total protein concentration for mixtures was fixed at 4 and 8 %wt. The ratio between microgels and fractal aggregates was varied. Acidification to pH below pH 4.3 led to formation of non self-supporting gels or decrease of the gel strength. For pure microgels the minimum concentration required to form a self-supporting gel was 6 %. Below this concentration the gels precipitated. They found that for gels prepared with fractals (strands) only, CLSM images were homogeneous at the scale of observation. For mixtures of fractals with microgels formation of a protein network was observed with a denser network structure compared to gels formed with pure microgels. Similar structures were observed by scanning electron microscopy for gels formed by microgels with decrease of the concentration from 8 to 4 %, while for gels formed by pure fractals a coarser and more inhomogeneous gel structure was observed at 4 % than at 8 %. From rheological measurements it appeared that the pH of gelation decreased with increasing fraction of microgels in mixtures (from pH 6.1 to pH 5.5 at 8 % and from pH 6 to pH 5.34 at 4 %). "The gel strength decreased as WPM fraction increased and when pH decreased close to pH 4.3-4.5, G' decreased suggesting a

partial collapse of the gel structure". At 4 % pure fractal aggregates the final value of G' obtained was 500 Pa. At 8 % G' of approximately 5000 Pa was obtained.

The influence of aggregate morphology on acidified gels was studied by Britten and Giroux (2001), who produced aggregates from WPI (80 g/L) at three pH values (6.5, 7.5 and 8.5) with different $CaCl_2$ content (0, 2 and 4 mM). The size of the aggregates, analyzed with a Zetasizer, increased with increasing calcium concentration at pH 6.5 and decreased with addition of calcium at pH 8.5. The hydrodynamic radius of aggregates varied from 20 to 60 nm. At pH 6.5 with 4 mM calcium, microgels were formed characterized by "milky appearance". Gelation was induced by addition of GDL to decrease the pH to 4.6 after 16 hours at 5 °C. It was found that at pH 6.5 the aggregates formed with calcium (that were at least partially microgels) produced weaker gels (from measurements of G') than aggregates prepared without calcium (fractal aggregates), in agreement with observations by Donato et al. (2011). Interestingly, at pH 7.5 addition of calcium did not influence properties of gels, while at pH 8.5 addition of calcium resulted in weaker gels. Measurements of gel firmness (by compression) yielded similar results. Gels with highest firmness were formed from aggregates prepared at pH 7.5 independently of calcium content, the lowest – prepared at pH 6.5 with 4 mM calcium. It was suggested that aggregate shape affects crosslinking during acidification.

Cavallieri et al. (2007) studied properties of acidic cold-set gels of WPI at different pH values. The gels were produced with 7 %wt of preheated protein with GDL added at different quantities to reach different pH values in the range between 5.2 and 3.9 after 48 hours at 10 °C. Gels with maximum values for stress at rupture and elasticity modulus were obtained at pH 5.2, at the pI of β-lg. The gels with lowest stress at rupture and elasticity modulus were formed at pH 4.2. The water holding capacity also decreased with decreasing pH between 5.2 and 4.2. The results were attributed to β-lg solubilization away from the pI. Cavallieri and da Cunha (2008) studied the influence of acidification rate on properties of 7 % cold-set gels acidified with GDL. They found that stress at rupture and elasticity modulus were the same for gels formed in the pH range between 4.7 and 5.1 but much weaker gels were obtained at pH 4.2. It was found that the highest acidification rate promoted formation of weaker gels. It was suggested that the rheological properties were not affected by the acidification rate during network formation but depended on it during bond strengthening and rearrangement.

6. Gelation of milk protein mixtures.

Here we briefly review the milk protein systems that have been mainly studied in the literature to make a distinction with the systems studied for this thesis.

6.1 Gelation in skim milk (simulated skim milk).

Gelation of dairy proteins is quite extensively investigated in skim milk. The micelles are relatively heat-stable in milk, but during heating above 70 °C they bind denatured whey proteins (β-lg, most importantly) which leads to gelation at higher pH values during acidification, stiffer gels and less syneresis (Donato and Guyomarc'h, 2009; Lucey, 2002; Lucey and Singh, 1997).

6.2 Mixtures of sodium caseinate with native whey proteins.

The presence of caseins influences thermal aggregation of whey proteins. It has been demonstrated that κ-casein forms covalent bonds with whey proteins which results in mixed aggregates of smaller size (Guyomarc'h et al., 2009). On the other hand, α-, β-caseins and sodium caseinate do not coaggregate with native whey proteins, but nevertheless inhibit growth of the WPI aggregates presumably through non-covalent interaction with denatured whey proteins (Guyomarc'h et al., 2009; Kehoe and Foegeding, 2011, 2014; Morgan et al., 2005).

However, sodium caseinate has been shown to favour thermal gelation of WPI at higher SC concentrations. Nguyen et al. (2016b) studied gelation of mixtures of native WPI with sodium caseinate at different protein concentrations and mixture compositions in the pH range between 5.8 and 6.6 without salt and with 0.1 NaCl. It was concluded that SC and whey protein did not coaggregate, but SC still inhibited growth of microgels. However, at higher concentrations sodium caseinate reduced the WPI concentration required to form a gel. It was suggested that "SC and WPI aggregates do not mix well so that the local density of WPI is increased, which would favor aggregation". Addition of 0.1 M NaCl further reduced the critical WPI concentration needed to form gels and rendered gels more heterogeneous. In the following study, Nguyen et al. (2016a) investigated heat-induced gelation of native whey proteins in presence of sodium caseinate and calcium at pH 6.6. In 34 g/L mixtures of WPI with addition of 5-20 mM of Ca, gels were formed at low (around 10 g/L) and high (> 65 g/L) concentrations of sodium caseinate, but not at intermediate concentrations. Supposedly, at low concentrations SC competes with WPI for calcium, which quenches formation of microgels and promotes formation and gelation of WPI strands at high SC concentrations.

6.3 Casein micelles with native whey proteins.

As discussed above, thermal gelation of water suspensions of casein micelles has been studied by Thomar and Nicolai (2016). Gelation of aqueous solutions of micelles in presence of native whey proteins has been investigated by Nguyen et al. (2017) at pH between 5.8 and 6.6. The protein network was formed fast during heating and then reinforced by denaturing whey protein. At some conditions, when denaturation of whey protein was slow, a peculiar two-step gelation was observed during rheological measurements. The microstructure of gels was mostly determined by the network that was rapidly formed by micelles. Interestingly, it was found that addition of NaCl increases the critical gelation temperature of micelles.

More recently, Silva et al. (2017) studied gelation of mixtures of micellar casein with three types of globular proteins – native WPI, pea and soy protein isolates. It was shown that addition of globular proteins increased the critical gelation temperature of micelles. It has been shown that addition of globular proteins leads to a decrease of the free calcium in the mixture. It was suggested that gelation of micelles occurs through formation of calcium bridges between micelles. Therefore the decrease of the free calcium concentration bound by globular proteins leads to the increase of the T_C. Addition of globular proteins is similar to addition of calcium chelatants.

6.4 Casein micelles with whey protein aggregates.

Gelation of mixtures of casein micelles with WPI aggregates has been studied by Schorsch et al. (2001), Guyomarc'h (2003), Vastbinder et al. (2004), and more recently Andoyo et al. (2014). Generally, the same approach has been applied. WPI aggregates were prepared separately by heating solutions of WPI and then adding prepared aggregates to suspensions of micelles in milk ultrafiltrate or simulated milk ultrafiltrate. Gelation of the mixtures was induced by addition of GDL. Results were compared with properties of gels produced conventionally by heating mixtures of micelles with native WPI followed by acidification. It has been observed that addition of preheated whey protein to micelles results in the start of gelation at higher pH values. Gels produced in this manner were characterized by increased values of G', higher water holding capacity and more homogeneous structures.

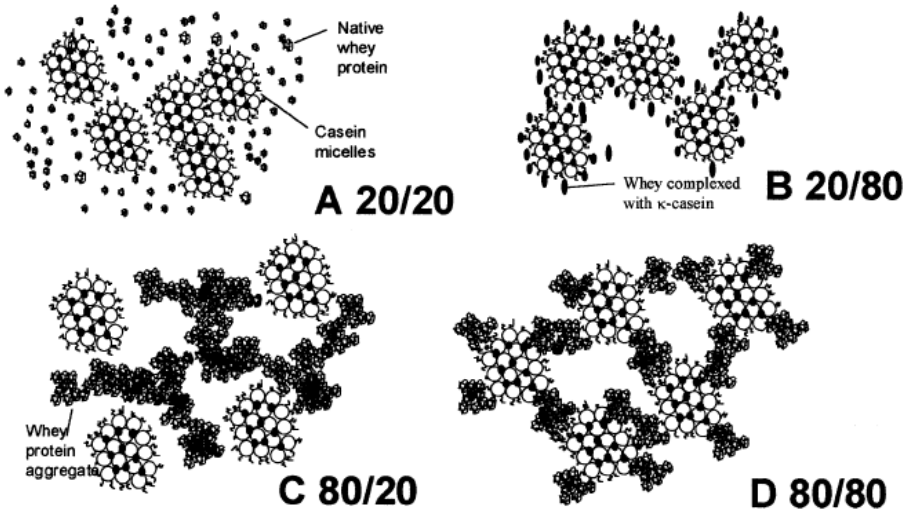

Figure 6. Schematic representation of casein/whey protein acid gels. (A) casein/native whey protein in mixtures heated below 60 °C; (B) casein/native whey protein after heating at temperatures above 60 °C; (C) casein/preheated whey protein mixtures at low temperatures; (D) casein/preheated whey protein mixtures after heating (from Schorsch et al. (2001)).

Schorsch et al. (2001) dispersed casein micelles and whey protein powder separately in simulated milk ultrafiltrate (SMUF). One part of the 20 g/L whey protein solution was heated (30 min at 80 °C). Prepared native and preheated whey protein were mixed with micelles, the mixtures were heated for 30 min at different temperatures (at 20, 60, 80 or 90 °C), cooled, mixed with GDL and left for gelation at 20 °C. The final pH was 4.7. The mixtures with preheated whey protein started to gel when pH decreased to 5.3-6.0 compared to pH 4.7-5.1 for mixtures with native WP. The gels with preheated WP were much more prone to syneresis than the gels with native WP. Four different types of gel network were suggested depending on the preparation (Fig. 6). 1) In mixtures of MC with native WP preheated before acidification at < 60 °C micelles form a network and native whey protein stays as "inactive" filler. 2) When preheating is at > 60 °C, denatured whey protein aggregates with κ-casein on the surface of micelles which strengthens the gel. 3) When WP aggregates are mixed with micelles at room temperature, they are "unable to covalently attach to the κ-casein of the micelles". With decreasing pH to ≤ 6.0, cold gelation of WP aggregates leads to formation of a WP network with clusters of micelles included in it. As a result, weak particulate gels are formed. 4) When mixtures of WP aggregates with micelles are heated before acidification, formation of disulphide links between

aggregates is reduced and aggregates interact with κ-casein on the surface of casein micelle, which results in a hybrid gel.

Vasbinder et al. (2004) studied acid-induced gelation of four systems: 1) unheated whey protein-free reconstituted skim milk with native WP at pH 6.7 (System 1); 2) heated System 1, which led to 70 % of the WP being associated to the micelles and 30 % forming WP aggregates; 3) heated System 1 but at pH 6.55, which resulted in 100 % of WP being associated to the micelles; 4) reconstituted skim milk mixed with preheated WP. The gelation was induced by incubation with GDL at 32 °C for 24 hours, with final pH 4.6. Interestingly, by capillary electrophoresis analysis no interaction between micelles and aggregates was found. Gelation of the three systems with denatured whey protein started at approximately the same pH 5.5, while for the system with native WP gelation started at pH < 5.0. It was concluded that "the start of gelation was induced by the whey protein aggregates around pH 5.5, but that the casein micelles were already so sticky at this pH that they became entrapped in the gelation process as well". For all systems gelation appeared as a one-phase gelation process. The highest gel hardness and heterogeneity of the structure were found for the system with preheated whey protein. The importance of the disulfide bridges for the gel hardness was demonstrated. It was shown by CLSM that both micelles and WP participate in formation of the network.

References

Ako, K., Nicolai, T., Durand, D., 2010. Salt-induced gelation of globular protein aggregates: structure and kinetics. Biomacromolecules 11, 864–871.

Alting, A.C., Hamer, R.J., de Kruif, C.G., Paques, M., Visschers, R.W., 2003a. Number of thiol groups rather than the size of the aggregates determines the hardness of cold set whey protein gels. Food Hydrocoll. 17, 469–479.

Alting, A.C., Hamer, R.J., de Kruif, C.G., Visschers, R.W., 2003b. Cold-set globular protein gels: interactions, structure and rheology as a function of protein concentration. J. Agric. Food Chem. 51, 3150–3156.

Alting, A.C., Hamer, R.J., de Kruif, C.G., Visschers, R.W., 2000. Formation of disulfide bonds in acid-induced gels of preheated whey protein isolate. J. Agric. Food Chem. 48, 5001–5007.

Alting, A.C., Weijers, M., de Hoog, E.H., van de Pijpekamp, A.M., Cohen Stuart, M.A., Hamer, R.J., de Kruif, C.G., Visschers, R.W., 2004. Acid-induced cold gelation of globular proteins: effects of protein aggregate characteristics and disulfide bonding on rheological properties. J. Agric. Food Chem. 52, 623–631.

Alvarez, E.M., Risso, P.H., Canales, M.A.M., Pires, M.S., Gatti, C.A., 2008. Hydrodynamic properties–structure relationship for sodium caseinates in presence of calcium. Colloids Surf. Physicochem. Eng. Asp. 327, 51–56.

Andoyo, R., Guyomarc'h, F., Cauty, C., Famelart, M.-H., 2014. Model mixtures evidence the respective roles of whey protein particles and casein micelles during acid gelation. Food Hydrocoll. 37, 203–212.

Aoki, T., Yamada, N., Kako, Y., Imamura, T., 1988. Dissociation during dialysis of casein aggregates cross-linked by colloidal calcium phosphate in bovine casein micelles. J. Dairy Res. 55, 189–195.

Auty, M.A.E., O'Kennedy, B.T., Allan-Wojtas, P., Mulvihill, D.M., 2005. The application of microscopy and rheology to study the effect of milk salt concentration on the structure of acidified micellar casein systems. Food Hydrocoll. 19, 101–109.

Aymard, P., Durand, D., Nicolai, T., 1996. The effect of temperature and ionic strength on the dimerisation of β-lactoglobulin. Int. J. Biol. Macromol. 19, 213–221.

Aymard, P., Nicolai, T., Durand, D., Clark, A., 1999. Static and dynamic scattering of β-lactoglobulin aggregates formed after heat-induced denaturation at pH 2. Macromolecules 32, 2542–2552.

Balakrishnan, G., Silva, J.V.C., Nicolai, T., Chassenieux, C., 2017. Effect of calcium ions on thermal gelation of aqueous micellar casein suspensions. Submitted for publication.

Barbut, S., 1997. Relationships between optical and textural properties of cold-set whey protein gels. LWT-Food Sci. Technol. 30, 590–593.

Barbut, S., 1995. Effects of calcium level on the structure of pre-heated whey protein isolate gels. LWT-Food Sci. Technol. 28, 598–603.

Barbut, S., Drake, D., 1997. Effect of reheating on sodium-induced cold gelation of whey proteins. Food Res. Int. 30, 153–157.

Barbut, S., Foegeding, E.A., 1993. Ca2+-induced gelation of pre-heated whey protein isolate. J. Food Sci. 58, 867–871.

Baussay, K., Le Bon, C., Nicolai, T., Durand, D., Busnel, J.-P., 2004. Influence of the ionic strength on the heat-induced aggregation of the globular protein β-lactoglobulin at pH 7. Int. J. Biol. Macromol. 34, 21–28.

Berne, B.J., Pecora, R., 2000. Dynamic Light Scattering: With Applications to Chemistry, Biology, and Physics. Courier Corporation.

Bon, C., Nicolai, T., Durand, D., 1999. Growth and structure of aggregates of heat-denatured β-Lactoglobulin. Int. J. Food Sci. Technol. 34, 451–465.

Bouchoux, A., Gesan-Guiziou, G., Pérez, J., Cabane, B., 2010. How to squeeze a sponge: casein micelles under osmotic stress, a SAXS study. Biophys. J. 99, 3754–3762.

Braga, A.L.M., Menossi, M., Cunha, R.L., 2006. The effect of the glucono-δ-lactone/caseinate ratio on sodium caseinate gelation. Int. Dairy J. 16, 389–398.

Britten, M., Giroux, H.J., 2001. Acid-induced gelation of whey protein polymers: effects of pH and calcium concentration during polymerization. Food Hydrocoll. 15, 609–617.

Brown, W., 1993. Dynamic light scattering: the method and some applications. Oxford University Press, USA.

Broyard, C., Gaucheron, F., 2015. Modifications of structures and functions of caseins: a scientific and technological challenge. Dairy Sci. Technol. 95, 831–862.

Bryant, C.M., McClements, D.J., 2000. Influence of NaCl and CaCl2 on Cold-Set Gelation of Heat-denatured Whey Protein. J. Food Sci. 65, 801–804.

Cavallieri, A.L.F., Costa-Netto, A.P., Menossi, M., Da Cunha, R.L., 2007. Whey protein interactions in acidic cold-set gels at different pH values. Le Lait 87, 535–554.

Cavallieri, A.L.F., Da Cunha, R.L., 2008. The effects of acidification rate, pH and ageing time on the acidic cold set gelation of whey proteins. Food Hydrocoll. 22, 439–448.

Chinchalikar, A.J., Kumar, S., Aswal, V.K., Kohlbrecher, J., Wagh, A.G., 2014. SANS study of understanding mechanism of cold gelation of globular proteins, in: AIP Conference Proceedings. AIP, pp. 186–188.

Clare, D.A., Lillard, S.J., Ramsey, S.R., Amato, P.M., Daubert, C.R., 2007. Calcium effects on the functionality of a modified whey protein ingredient. J. Agric. Food Chem. 55, 10932–10940.

Dalgleish, D.G., 2011. On the structural models of bovine casein micelles—review and possible improvements. Soft Matter 7, 2265–2272.

Dalgleish, D.G., Horne, D.S., Law, A.J.R., 1989. Size-related differences in bovine casein micelles. Biochim. Biophys. Acta BBA-Gen. Subj. 991, 383–387.

Dalgleish, D.G., Law, A.J., 1988. pH-induced dissociation of bovine casein micelles. I. Analysis of liberated caseins. J. Dairy Res. 55, 529–538.

Dalgleish, D.G., Parker, T.G., 1980. Binding of calcium ions to bovine α sl-casein and precipitability of the protein–calcium ion complexes. J. Dairy Res. 47, 113–122.

De Kruif, C.G., 2014. The structure of casein micelles: a review of small-angle scattering data. J. Appl. Crystallogr. 47, 1479–1489.

De Kruif, C.G., Holt, C., 2003. Casein micelle structure, functions and interactions, in: Advanced Dairy Chemistry—1 Proteins. Springer, pp. 233–276.

De Kruif, C.G., Huppertz, T., Urban, V.S., Petukhov, A.V., 2012. Casein micelles and their internal structure. Adv. Colloid Interface Sci. 171, 36–52.

Doi, E., 1993. Gels and gelling of globular proteins. Trends Food Sci. Technol. 4, 1–5.

Donald, A.M., 2008. Aggregation in β-lactoglobulin. Soft Matter 4, 1147–1150.

Donato, L., Guyomarc'h, F., 2009. Formation and properties of the whey protein/κ-casein complexes in heated skim milk – A review. Dairy Sci. Technol. 89, 3–29.

Donato, L., Kolodziejcyk, E., Rouvet, M., 2011. Mixtures of whey protein microgels and soluble aggregates as building blocks to control rheology and structure of acid induced cold-set gels. Food Hydrocoll., Food Colloids 2010: On the Road from Interfaces to Consumers 25, 734–742.

Durand, D., Gimel, J.C., Nicolai, T., 2002. Aggregation, gelation and phase separation of heat denatured globular proteins. Phys. Stat. Mech. Its Appl. 304, 253–265.

Famelart, M.H., Le Graet, Y., Raulot, K., 1999. Casein micelle dispersions into water, NaCl and CaCl 2: physicochemical characteristics of micelles and rennet coagulation. Int. Dairy J. 9, 293–297.

Famelart, M.H., Lepesant, F., Gaucheron, F., Le Graet, Y., Schuck, P., 1996. pH-Induced physicochemical modifications of native phosphocaseinate suspensions: Influence of aqueous phase. Le lait 76, 445–460.

Fox, P.F., 2003. Milk proteins: general and historical aspects, in: Advanced Dairy Chemistry—1 Proteins. Springer, pp. 1–48.

Fox, P.F., Brodkorb, A., 2008. The casein micelle: Historical aspects, current concepts and significance. Int. Dairy J. 18, 677–684.

Gaucheron, F., 2005. The minerals of milk. Reprod. Nutr. Dev. 45, 473–483.

Gimel, J.C., Durand, D., Nicolai, T., 1994. Structure and distribution of aggregates formed after heat-induced denaturation of globular proteins. Macromolecules 27, 583–589.

Glibowski, P., Mleko, S., Wesolowska-Trojanowska, M., 2006. Gelation of single heated vs. double heated whey protein isolate. Int. Dairy J. 16, 1113–1118.

Gonzalez-Jordan, A., Thomar, P., Nicolai, T., Dittmer, J., 2015. The effect of pH on the structure and phosphate mobility of casein micelles in aqueous solution. Food Hydrocoll. 51, 88–94.

Guyomarc'h, F., Nono, M., Nicolai, T., Durand, D., 2009. Heat-induced aggregation of whey proteins in the presence of κ-casein or sodium caseinate. Food Hydrocoll., Food Colloids: Creating Structure, Delivering Functionality 23, 1103–1110.

Guyomarc'h, F., Queguiner, C., Law, A.J.R., Horne, D.S., Dalgleish, D.G., 2003. Role of the Soluble and Micelle-Bound Heat-Induced Protein Aggregates on Network Formation in Acid Skim Milk Gels. J. Agric. Food Chem. 51, 7743–7750.

HadjSadok, A., Pitkowski, A., Nicolai, T., Benyahia, L., Moulai-Mostefa, N., 2008. Characterisation of sodium caseinate as a function of ionic strength, pH and temperature using static and dynamic light scattering. Food Hydrocoll. 22, 1460–1466.

Holt, C., Carver, J.A., 2012. Darwinian transformation of a 'scarcely nutritious fluid'into milk. J. Evol. Biol. 25, 1253–1263.

Holt, C., Carver, J.A., Ecroyd, H., Thorn, D.C., 2013. Invited review: Caseins and the casein micelle: their biological functions, structures, and behavior in foods. J. Dairy Sci. 96, 6127–6146.

Holt, C., Timmins, P.A., Errington, N., Leaver, J., 1998. A core-shell model of calcium phosphate nanoclusters stabilized by β-casein phosphopeptides, derived from sedimentation equilibrium and small-angle X-ray and neutron-scattering measurements. FEBS J. 252, 73–78.

Hongsprabhas, B., Barbut, S., 1997a. Ca 2+-induced cold gelation of whey protein isolate: effect of two-stage gelation. Food Res. Int. 30, 523–527.

Hongsprabhas, B., Barbut, S., 1997b. Protein and Salt Effects on Ca2+-Induced Cold Gelation of Whey Protein Isolate. J. Food Sci. 62, 382–385.

Hongsprabhas, P., Barbut, S., 1997. Structure-forming processes in Ca 2+-induced whey protein isolate cold gelation. Int. Dairy J. 7, 827–834.

Hongsprabhas, P., Barbut, S., 1997. Effect of gelation temperature on Ca2+-induced gelation of whey protein isolate. LWT-Food Sci. Technol. 30, 45–49.

Hongsprabhas, P., Barbut, S., 1996. Ca2+-induced gelation of whey protein isolate: effects of pre-heating. Food Res. Int. 29, 135–139.

Hongsprabhas, P., Barbut, S., Marangoni, A.G., 1999. The structure of cold-set whey protein isolate gels prepared with Ca++. LWT-Food Sci. Technol. 32, 196–202.

Horne, D.S., 2009. Casein micelle structure and stability. Milk Proteins Expr. Food 133–162.

Horne, D.S., 2006. Casein micelle structure: models and muddles. Curr. Opin. Colloid Interface Sci. 11, 148–153.

Horne, D.S., 2002. Casein structure, self-assembly and gelation. Curr. Opin. Colloid Interface Sci. 7, 456–461.

Horne, D.S., 1998. Casein interactions: casting light on the black boxes, the structure in dairy products. Int. Dairy J. 8, 171–177.

Hudson, H.M., Daubert, C.R., Foegeding, E.A., 2000. Rheological and physical properties of derivitized whey protein isolate powders. J. Agric. Food Chem. 48, 3112–3119.

Ingham, B., Smialowska, A., Erlangga, G.D., Matia-Merino, L., Kirby, N.M., Wang, C., Haverkamp, R.G., Carr, A.J., 2016. Revisiting the interpretation of casein micelle SAXS data. Soft Matter 12, 6937–6953.

Ju, Z.Y., Kilara, A., 1998a. Effects of preheating on properties of aggregates and of cold-set gels of whey protein isolate. J. Agric. Food Chem. 46, 3604–3608.

Ju, Z.Y., Kilara, A., 1998b. Aggregation induced by calcium chloride and subsequent thermal gelation of whey protein isolate. J. Dairy Sci. 81, 925–931.

Ju, Z.Y., Kilara, A., 1998c. Textural Properties of Cold-set Gels Induced from Heat-denatured Whey Protein Isolates. J. Food Sci. 63, 288–292.

Kehoe, J.J., Foegeding, E.A., 2014. The characteristics of heat-induced aggregates formed by mixtures of β-lactoglobulin and β-casein. Food Hydrocoll. 39, 264–271.

Kehoe, J.J., Foegeding, E.A., 2011. Interaction between β-Casein and Whey Proteins As a Function of pH and Salt Concentration. J. Agric. Food Chem. 59, 349–355.

Kharlamova, A., Inthavong, W., Nicolai, T., Chassenieux, C., 2016. The effect of aggregation into fractals or microgels on the charge density and the isoionic point of globular proteins. Food Hydrocoll. 60, 470–475.

Kuhn, K.R., Cavallieri, Â.L.F., Da Cunha, R.L., 2010. Cold-set whey protein gels induced by calcium or sodium salt addition. Int. J. Food Sci. Technol. 45, 348–357.

Kundu, S., Chinchalikar, A.J., Das, K., Aswal, V.K., Kohlbrecher, J., 2014. Mono-, di-and tri-valent ion induced protein gelation: Small-angle neutron scattering study. Chem. Phys. Lett. 593, 140–144.

Le Bon, C., Durand, D., Nicolai, T., 2002. Influence of genetic variation on the aggregation of heat-denatured β-lactoglobulin. Int. Dairy J. 12, 671–678.

Le Bon, C., Nicolai, T., Durand, D., 1999. Kinetics of aggregation and gelation of globular proteins after heat-induced denaturation. Macromolecules 32, 6120–6127.

Le Graet, Y., Brulé, G., 1993. Les équilibres minéraux du lait: influence du pH et de la force ionique. Le Lait 73, 51–60.

Lu, X., Lu, Z., Yin, L., Cheng, Y., Li, L., 2010. Effect of preheating temperature and calcium ions on the properties of cold-set soybean protein gel. Food Res. Int. 43, 1673–1683.

Lucey, J.A., 2002. Formation and Physical Properties of Milk Protein Gels. J. Dairy Sci. 85, 281–294.

Lucey, J.A., Gorry, C., O'Kennedy, B., Kalab, M., Tan-Kinita, R., Fox, P.F., 1996. Effect of acidification and neutralization of milk on some physico-chemical properties of casein micelles. Int. Dairy J. 6, 257–272.

Lucey, J.A., Horne, D.S., 2009. Milk salts: technological significance, in: Advanced Dairy Chemistry. Springer, pp. 351–389.

Lucey, J.A., Singh, H., 1997. Formation and physical properties of acid milk gels: a review. Food Res. Int. 30, 529–542.

Lucey, J.A., Van Vliet, T., Grolle, K., Geurts, T., Walstra, P., 1997. Properties of acid casein gels made by acidification with glucono-δ-lactone. 2. Syneresis, permeability and microstructural properties. Int. Dairy J. 7, 389–397.

Mahmoudi, N., Mehalebi, S., Nicolai, T., Durand, D., Riaublanc, A., 2007. Light-scattering study of the structure of aggregates and gels formed by heat-denatured whey protein isolate and β-lactoglobulin at neutral pH. J. Agric. Food Chem. 55, 3104–3111.

Maltais, A., Remondetto, G.E., Gonzalez, R., Subirade, M., 2005. Formation of soy protein isolate cold-set gels: protein and salt effects. J. Food Sci. 70.

Marangoni, A.G., Barbut, S., McGauley, S.E., Marcone, M., Narine, S.S., 2000. On the structure of particulate gels—the case of salt-induced cold gelation of heat-denatured whey protein isolate. Food Hydrocoll. 14, 61–74.

Marchal, E., Haïssat, S., Montagne, P., Cuilliere, M.L., Bene, M.C., Faure, G., Humbert, G., Linden, G., 1995. Microparticle-enhanced nephelometric immunoassay of plasminogen in bovine milk. Food Agric. Immunol. 7, 323–331.

Marchin, S., Putaux, J.-L., Pignon, F., Léonil, J., 2007. Effects of the environmental factors on the casein micelle structure studied by cryo transmission electron microscopy and small-angle x-ray scattering/ultrasmall-angle x-ray scattering. J. Chem. Phys. 126, 01B617.

McClements, D.J., Keogh, M.K., 1995. Physical properties of cold-setting gels formed from heat-denatured whey protein isolate. J. Sci. Food Agric. 69, 7–14.

McMahon, D.J., Oommen, B.S., 2013. Casein micelle structure, functions, and interactions, in: Advanced Dairy Chemistry. Springer, pp. 185–209.

Mehalebi, S., Nicolai, T., Durand, D., 2008. Light scattering study of heat-denatured globular protein aggregates. Int. J. Biol. Macromol. 43, 129–135.

Mekmene, O., Le Graët, Y., Gaucheron, F., 2010. Theoretical model for calculating ionic equilibria in milk as a function of pH: comparison to experiment. J. Agric. Food Chem. 58, 4440–4447.

Mleko, S., 1999. Effect of protein concentration on whey protein gels obtained by a two-stage heating process. Eur. Food Res. Technol. 209, 389–392.

Moreels, E., De Ceuninck, W., Finsy, R., 1987. Measurements of the Rayleigh ratio of some pure liquids at several laser light wavelengths. J. Chem. Phys. 86, 618–623.

Morgan, P.E., Treweek, T.M., Lindner, R.A., Price, W.E., Carver, J.A., 2005. Casein Proteins as Molecular Chaperones. J. Agric. Food Chem. 53, 2670–2683.

Mudgal, P., Daubert, C.R., Foegeding, E.A., 2011. Effects of protein concentration and CaCl 2 on cold-set thickening mechanism of β-lactoglobulin at low pH. Int. Dairy J. 21, 319–326.

Mudgal, P., Daubert, C.R., Foegeding, E.A., 2009. Cold-set thickening mechanism of β-lactoglobulin at low pH: concentration effects. Food Hydrocoll. 23, 1762–1770.

Murekatete, N., Hua, Y., Chamba, M.V.M., Djakpo, O., Zhang, C., 2014. Gelation Behavior and Rheological Properties of Salt-or Acid-Induced Soy Proteins Soft Tofu-Type Gels. J. Texture Stud. 45, 62–73.

Navarra, G., Giacomazza, D., Leone, M., Librizzi, F., Militello, V., San Biagio, P.L., 2009. Thermal aggregation and ion-induced cold-gelation of bovine serum albumin. Eur. Biophys. J. 38, 437–446.

Nguyen, B.T., Balakrishnan, G., Jacquette, B., Nicolai, T., Chassenieux, C., Schmitt, C., Bovetto, L., 2016a. Inhibition and promotion of heat-induced gelation of whey proteins in the presence of calcium by addition of sodium caseinate. Biomacromolecules 17, 3800–3807.

Nguyen, B.T., Chassenieux, C., Nicolai, T., Schmitt, C., 2017. Effect of the pH and NaCl on the microstructure and rheology of mixtures of whey protein isolate and casein micelles upon heating. Food Hydrocoll. 70, 114–122.

Nguyen, B.T., Nicolai, T., Chassenieux, C., Schmitt, C., Bovetto, L., 2016b. Heat-induced gelation of mixtures of whey protein isolate and sodium caseinate between pH 5.8 and pH 6.6. Food Hydrocoll. 61, 433–441.

Nicolai, T., 2016. Formation and functionality of self-assembled whey protein microgels. Colloids Surf. B Biointerfaces 137, 32–38.

Nicolai, T., Britten, M., Schmitt, C., 2011. β-Lactoglobulin and WPI aggregates: Formation, structure and applications. Food Hydrocoll., 25 years of Advances in Food Hydrocolloid Research 25, 1945–1962.

Nicolai, T., Gimel, J.C., Johnsen, R., 1996. Analysis of relaxation functions characterized by a broad monomodal relaxation time distribution. J. Phys. II 6, 697–711.

O'Kennedy, B.T., Mounsey, J.S., Murphy, F., Duggan, E., Kelly, P.M., 2006. Factors affecting the acid gelation of sodium caseinate. Int. Dairy J. 16, 1132–1141.

O'mahony, J.A., Fox, P.F., 2013. Milk proteins: Introduction and historical aspects, in: Advanced Dairy Chemistry. Springer, pp. 43–85.

Panouillé, M., Durand, D., Nicolai, T., Larquet, E., Boisset, N., 2005. Aggregation and gelation of micellar casein particles. J. Colloid Interface Sci. 287, 85–93.

Panouillé, M., Nicolai, T., Durand, D., 2004. Heat induced aggregation and gelation of casein submicelles. Int. Dairy J. 14, 297–303.

Parker, T.G., Dalgleish, D.G., 1981. Binding of calcium ions to bovine β-casein. J. Dairy Res. 48, 71–76.

Pessen, H., Kumosinski, T.F., Farrell, H.M., 1988. Investigation of differences in the tertiary structures of food proteins by small-angle X-ray scattering. J. Ind. Microbiol. Biotechnol. 3, 89–103.

Phan-Xuan, T., Durand, D., Nicolai, T., Donato, L., Schmitt, C., Bovetto, L., 2011. On the Crucial Importance of the pH for the Formation and Self-Stabilization of Protein Microgels and Strands. Langmuir 27, 15092–15101.

Philippe, M., Gaucheron, F., Le Graet, Y., Michel, F., Garem, A., 2003. Physicochemical characterization of calcium-supplemented skim milk. Le lait 83, 45–59.

Philippe, M., Le Graët, Y., Gaucheron, F., 2005. The effects of different cations on the physicochemical characteristics of casein micelles. Food Chem. 90, 673–683.

Phillips, L.G., Whitehead, D.M., Kinsella, J., 1994. Structural and chemical properties of β-lactoglobulin. Struct.-Funct. Prop. Food Proteins 75–106.

Pitkowski, A., Durand, D., Nicolai, T., 2008. Structure and dynamical mechanical properties of suspensions of sodium caseinate. J. Colloid Interface Sci. 326, 96–102.

Pitkowski, A., Nicolai, T., Durand, D., 2009. Stability of caseinate solutions in the presence of calcium. Food Hydrocoll. 23, 1164–1168.

Pitkowski, A., Nicolai, T., Durand, D., 2007. Dynamical mechanical characterization of gelling micellar casein particles. J. Rheol. 51, 971–986.

Pouzot, M., Durand, D., Nicolai, T., 2004. Influence of the ionic strength on the structure of heat-set globular protein gels at pH 7. β-Lactoglobulin. Macromolecules 37, 8703–8708.

Pouzot, M., Nicolai, T., Visschers, R.W., Weijers, M., 2005. X-ray and light scattering study of the structure of large protein aggregates at neutral pH. Food Hydrocoll. 19, 231–238.

Rabiey, L., Britten, M., 2009. Effect of protein composition on the rheological properties of acid-induced whey protein gels. Food Hydrocoll. 23, 973–979.

Remondetto, G.E., Paquin, P., Subirade, M., 2002. Cold Gelation of β-lactoglobulin in the Presence of Iron. J. Food Sci. 67, 586–595.

Remondetto, G.E., Subirade, M., 2003. Molecular mechanisms of Fe2+-induced β-lactoglobulin cold gelation. Biopolymers 69, 461–469.

Schmitt, C., Bovay, C., Rouvet, M., Shojaei-Rami, S., Kolodziejczyk, E., 2007. Whey protein soluble aggregates from heating with NaCl: physicochemical, interfacial, and foaming properties. Langmuir 23, 4155–4166.

Schorsch, C., Wilkins, D.K., Jones, M.G., Norton, I.T., 2001. Gelation of casein-whey mixtures: effects of heating whey proteins alone or in the presence of casein micelles. J. Dairy Res. 68, 471–481.

Silva, J.V.C., Jacquette, B., Balakrishnan, G., Schmitt, C., Chassenieux, C., Nicolai, T., 2017. Heat-induced gelation of micellar casein systems as affected by globular protein addition. Submitted for publication.

Slattery, C.W., Evard, R., 1973. A model for the formation and structure of casein micelles from subunits of variable composition. Biochim. Biophys. Acta BBA-Protein Struct. 317, 529–538.

Thomar, P., Durand, D., Benyahia, L., Nicolai, T., 2012. Slow dynamics and structure in jammed milk protein suspensions. Faraday Discuss. 158, 325–339.

Thomar, P., Nicolai, T., 2016. Heat-induced gelation of casein micelles in aqueous suspensions at different pH. Colloids Surf. B Biointerfaces 146, 801–807.

Thomar, P., Nicolai, T., 2015. Dissociation of native casein micelles induced by sodium caseinate. Food Hydrocoll. 49, 224–231.

Thomar, P., Nicolai, T., Benyahia, L., Durand, D., 2013. Comparative study of the rheology and the structure of sodium and calcium caseinate solutions. Int. Dairy J. 31, 100–106.

Tremblay, L., Laporte, M.F., Léonil, J., Dupont, D., Paquin, P., 2003. Quantitation of Proteins in Milk and Milk Products, in: Advanced Dairy Chemistry—1 Proteins. Springer, Boston, MA, pp. 49–138.

Udabage, P., McKinnon, I.R., Augustin, M.-A., 2000. Mineral and casein equilibria in milk: effects of added salts and calcium-chelating agents. J. Dairy Res. 67, 361–370.

Vardhanabhuti, B., Foegeding, E.A., McGuffey, M.K., Daubert, C.R., Swaisgood, H.E., 2001. Gelation properties of dispersions containing polymerized and native whey protein isolate. Food Hydrocoll. 15, 165–175.

Vasbinder, A.J., van de Velde, F., de Kruif, C.G., 2004. Gelation of Casein-Whey Protein Mixtures. J. Dairy Sci. 87, 1167–1176.

Verheul, M., Roefs, S.P., de Kruif, K.G., 1998. Kinetics of heat-induced aggregation of β-lactoglobulin. J. Agric. Food Chem. 46, 896–903.

Vreeker, R., Hoekstra, L.L., Den Boer, D.C., Agterof, W.G.M., 1992. Fractal aggregation of whey proteins. Food Hydrocoll. 6, 423–435.

Walstra, P., 1999. Dairy Technology: Principles of Milk Properties and Processes. CRC Press.

Walstra, P., 1990. On the stability of casein micelles1. J. Dairy Sci. 73, 1965–1979.

Walstra, P., Jenness, R., 1984. Dairy chemistry & physics. John Wiley & Sons.

Waugh, D.F., Creamer, L.K., Slattery, C.W., Dresdner, G.W., 1970. Core polymers of casein micelles. Biochemistry (Mosc.) 9, 786–795.

Wu, H., Arosio, P., Podolskaya, O.G., Wei, D., Morbidelli, M., 2012. Stability and gelation behavior of bovine serum albumin pre-aggregates in the presence of calcium chloride. Phys. Chem. Chem. Phys. 14, 4906–4916.

Wu, H., Xie, J., Morbidelli, M., 2005. Kinetics of cold-set diffusion-limited aggregations of denatured whey protein isolate colloids. Biomacromolecules 6, 3189–3197.

Zittle, C.A., DellaMonica, E.S., Rudd, R.K., Custer, J.H., 1957. The binding of calcium ions by β-lactoglobulin both before and after aggregation by heating in the presence of calcium ions. J. Am. Chem. Soc. 79, 4661–4666.

Chapter 2. Materials and Methods.

1. Materials

1.1 Whey protein isolate powder

The WPI powder was purchased from Lactalis (Laval, France). It contained 89.3 wt% protein, 6 wt% moisture, < 0.4 wt% lactose and 2.0 wt% ash, including 0.25 wt% calcium. The protein composition was determined by size exclusion chromatography. The proteins consisted of 70 % β-lg and 20 % of α-lac, the remaining being other whey proteins and caseins.

1.2 β-lactoglobulin powder

The β-lg powder (Biopure, lot JE 001-8-415) was purchased from Davisco Foods International, Inc. (Le Sueur, MN, USA) and contained approximately equal quantities of variants A and B.

1.3 Micellar casein (MC) powder

The micellar casein powder (Promilk 852B, batch 13610656) was purchased from Cremo SA (Fribourg, Switzerland) and contained 82 wt% protein, of which 92 % caseins and 8 % whey proteins as determined by RP-HPLC analysis done at the Nestlé research center (Fig. 1). The powder contained (in g/100 g wet powder): 2.6 Ca, 0.10 Mg, 0.07 Na, 0.29 K, 1.6 P and 0.05 Cl.

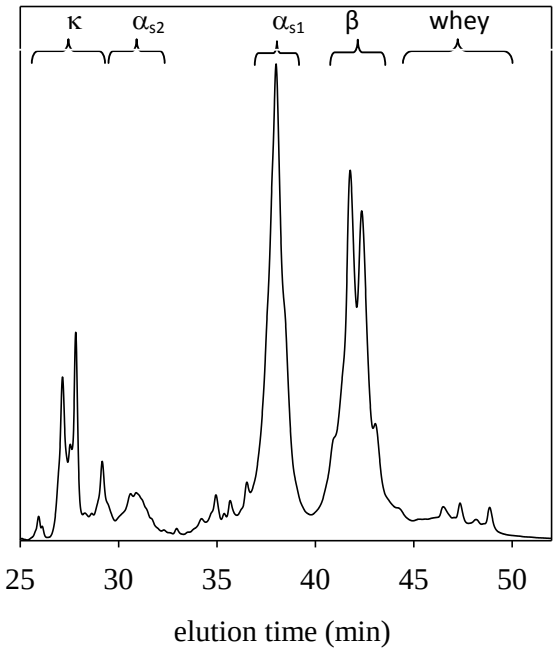

Figure 1. RP-HPLC chromatograms of the micellar casein powder.

1.4 Preparation of fractal aggregates and microgels from WPI powder

The WPI powder was mixed with Milli-Q water, stirred for 4-6 hours and kept overnight in the fridge. The MIlli-Q water contained 200 ppm of sodium azide as an antimicrobial preservative unless the solution was prepared for titration experiments. Sodium azide was not added to solutions prepared for titration experiments as it behaves as a weak acid and binds protons. The solution was filtered through 0.45 µm and 0.2 µm syringe filters (Acrodisc®). The obtained WPI stock solution of

13.5 – 13.7 wt% had a pH of ≈ 6.25. For preparation of WPI aggregates, the pH was adjusted to 7.0 for the concentrated solution by addition of 1 M standard solution of NaOH (Fisher Scientific UK), which corresponds to addition of 2.2 OH^- ions per protein molecule (considering the weight-average molar mass of WPI of 1.75×10^4 g/mol). The protein concentration of the stock solution with adjusted pH was determined on four dilutions to concentrations below 1 g/L by UV absorption at 280 nm using the extinction coefficient ε = 1.046 L g^{-1} cm^{-1} (Mahmoudi et al., 2007). The measurements were conducted using a UV-visible spectrometer Varian Cary-50 Bio (Les Ulis, France).

The concentration was determined using the Beer-Lambert equation:

$$C = \frac{A}{\varepsilon \times l} , \quad (1)$$

where *A* is the absorbanse of the solution at 280 nm, ε and *l* – the path length of the quartz cuvette (*l* = 1 cm).

Fractal aggregates with different hydrodynamic radii R_h were prepared by dilution of the stock solution to different concentrations: R_h = 32-35 nm at C = 62 g/L, R_h= 77-80 nm at C = 80 g/L, R_h = 170-210 nm at C = 91 g/L, and R_h > 500 nm at C = 93 g/L. We stress that the charge density was the same for aggregates of all sizes. Diluted WPI solutions were heated in hermetically closed glass bottles for 24 hours at 80 °C to ensure denaturation of all native protein and kept in a refrigerator. The size of the aggregates was determined by dynamic light scattering.

The microgels were prepared by diluting the filtered WPI solution to 40 g/L and adjusting its pH from ≈ 6.4 to pH values in the range between 5.8-6.1 by addition of 1 M standard HCl solution (Fisher Scientific UK). Prepared solutions were heated in hermetically closed glass bottles for 24 hours at 80 °C. The adjustment of the pH to 5.7 resulted in precipitation of obtained microgels. At pH 5.8 microgels also precipitated with time but at much slower rate. The pH of the solutions increased after heating (see Phan-Xuan, 2011). The rate of conversion of native protein to microgels was calculated by centrifuging solutions of microgels for 1 h at 50000 g rotor speed (Allegra 64R centrifuge, Beckman Coulter, USA). The same results were obtained after centrifugation for 2 h. The microgels precipitated at these conditions, while the fractal aggregates (a small fraction of which also forms at these conditions) stayed in the supernatant. The conversion rate was deduced from the protein content of the supernatant determined by UV absorption at 280 nm as the percentage of protein converted to microgels (in wt%).

The characteristics of the microgels typically prepared for the experiments at different pH values (or different protein charge densities) are collected in Table 1. The change of the protein charge density was calculated as the number of protons H^+ added per protein. The net protein charge density was calculated considering the charge density of proteins in the initial stock solution (before pH adjustment, i. e. the charge density of proteins in the powder) α = –6.7, determined by potentiometric titration measurements (see Chapter 4). The size of the microgels was determined by dynamic light scattering.

Table 1. Characteristics of microgels prepared at different pH (charge density).

No	pH			change of charge density Δα	net protein charge density α before heating	conversion rate, %
	before heating	after heating	microgel size R_h, nm			
1	5.7	Precipitate		1.8	–6.7 + 1.8 = –4.9	---
2	5.8	6.11	370	1.5	–6.7 + 1.5 = –5.2	89
3	5.9	6.22	225	1.2	–6.7 + 1.2 = –5.5	88.8
4	6.0	6.31	160	0.7	–6.7 + 0.7 = –6.0	87.5
5	6.1	6.41	140	0.4	–6.7 + 0.4 = –6.3	84.5

1.5 Preparation of suspensions of micellar casein

Micellar casein suspensions were prepared by mixing the powder with MIlli-Q water containing 200 ppm of sodium azide. The container with the mixture was placed in a glass trough with water and heated on a magnetic agitator at 50 °C at constant agitation with a large magnetic bar for 16 hours. A suspension of micelles prepared by heating had the same values of turbidity as the MC passed through a high pressure homogenizer. The values of turbidity at λ = 700 nm for MC suspensions prepared by different methods as function of MC concentration are shown in Fig. 2.

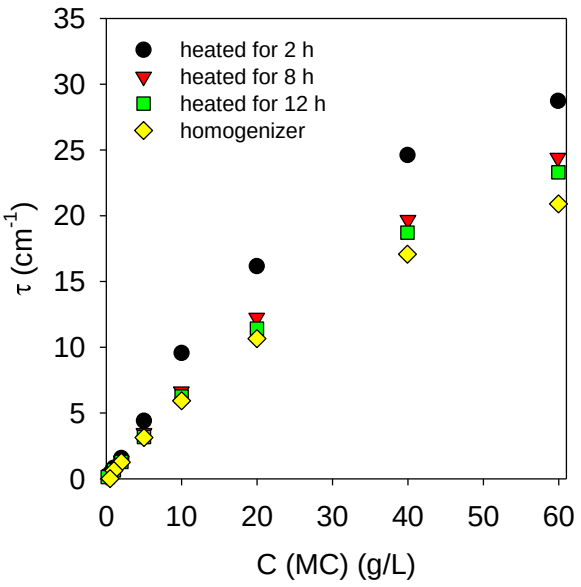

Figure 2. Turbidity of solutions of micelles at λ = 700 nm prepared by stirring at 50 °C for different times indicated in the figure and by high pressure homogenization as function of the concentration at natural pH (pH increases with dilution, pH ≈ 7.0 at 60 g/L).

2. Methods

2.1 Potentiometric titration

Potentimetric titration measurements were conducted with an automatic titrator (TIM 856, Radiometer Analytical) equipped with a combined pH electrode and a thermoprobe. The titrator allowed addition of a titrant at a speed as low as 0.01 mL/min. The electrode was calibrated by a three-point calibration in the pH range between 4 and 10. Protein solutions were titrated with different titrants: standard solutions of NaOH and HCl (Fisher Scientific UK) and $CaCl_2$ and NaCl solutions, prepared by dilution from powder purchased from Sigma. The concentration of the titrants was chosen depending on the protein concentration of the titrated solution. The measurements were performed at room temperature (20 – 25 °C).

2.2 Light scattering

The size of the aggregates was determined by dynamic and static light scattering measurements that were performed on a commercial apparatus (ALV-CGS3, ALV-Langen) using He-Ne laser with wavelength λ = 632 nm at 20 °C. The measurements were conducted on aggregate solutions diluted to below 1 g/L (0.01 g/L for microgels) at angles of observation between 13° and 140°. The relative scattering intensity (I_r), related to the weight average molar mass (M_W) and the structure factor ($S(q)$) of the particles, is calculated as the intensity minus the solvent scattering divided by the scattering intensity of toluene (Brown, 1993):

$$\frac{\mathrm{I_r}}{\mathrm{KC}} = \mathrm{M_w S(q)}, \tag{2}$$

where K is an optical constant defined as

$$\mathrm{K} = \frac{4\pi^2 \mathrm{n_s^2}}{\lambda^4 \mathrm{N_A}} \left(\frac{\partial \mathrm{n}}{\partial \mathrm{C}}\right)^2 \left(\frac{\mathrm{n_{tol}}}{\mathrm{n_s}}\right)^2 \frac{1}{\mathrm{R_{tol}}}, \tag{3}$$

where N_A is Avogadro's number; $(\partial \mathrm{n}/\partial \mathrm{C})$ is the refractive index increment; R_{tol} – the Rayleigh constant of toluene at 20 °C. We used $(\partial \mathrm{n}/\partial \mathrm{C})$ = 0.189 mL/g, R_{tol} = 1.35 × 10^{-5} cm^{-1} (Moreels et al., 1987).

The structure factor describes the dependence of I_r on the scattering wave vector (q). The z-average radius of gyration (R_g) was obtained from the initial dependence of the structure factor:

$$\mathrm{S(q)} = (1 + \mathrm{q^2} \cdot \mathrm{R_g^2}/3)^{-1}. \tag{4}$$

The relationship between the measured normalized intensity autocorrelation function (g2(t)) and the normalized electric field correlation function ($g_1(t)$) (Berne and Pecora, 2000):

$$g_2(t) = 1 + g_1(t)^2 \,. \tag{5}$$

The analysis of $g_1(t)$ was performed in terms of a distribution of relaxation times ($A(\log\tau)$) using the so-called generalized exponential (GEX) distribution (Nicolai et al., 1996):

$$g_1(t) = \int \mathrm{A(log\tau) exp(-t/\tau) dlog\tau} \tag{6}$$

with

$$A(\tau) = k\tau^{p}\exp[-(\tau/\tau^{*})^{s}]. \quad (7)$$

Relationship between the relaxation time (τ) and the diffusion coefficient (D) in dilute solutions when q→0:

$$\tau = (q^2 \times D)^{-1}. \quad (8)$$

The relationship between the diffusion coefficient and the hydrodynamic radius is:

$$D = \frac{kT}{6\pi\eta R_h}, \quad (9)$$

where η is the viscosity, *k* is the Bolzmann's constant, *T* is the absolute temperature.

The relaxation time distribution was represented as a distribution of the hydrodynamic radii ($A(\log R_h)$) and the z-average hydrodynamic radius was calculated from the average diffusion coefficient.

2.3 Rheological measurements

Most rheological measurements were performed using two stress-imposed rheometers AR2000 and ARG2 (TA Instruments, USA) using a cone-plate geometry (d = 40 mm) with a Peltier system for temperature control. The samples were covered with mineral oil to prevent evaporation of water. The measurements were conducted in the linear response regime except when indicated. Some flow measurements were performed using a stress-imposed rheometer MCR 301 (Anton Paar, Germany) with a couette geometry.

2.4 Confocal laser scanning microscopy

The structure of the systems was studied using a Leica TCS-SP2 confocal laser scanning microscope (Leica Microsystems Heidelberg, Germany) with two water immersion objectives: HC × PL APO 63 × NA = 1.2 and HC × PL APO 20 × NA = 0.7. The proteins were labeled with 5 ppm of rhodamine B. The solutions were hermetically sealed in cavity slides and heated on a lab rack placed in a water bath.

2.5 Calcium activity measurements

Calcium activity measurements were performed using ELIT solid state ion selective electrode (Nico2000 Ltd.) complemented with a conventional reference electrode. The calibration curve was obtained by measuring a series of standard solutions in the range 10^{-4} – 10^{-1} M prepared by consecutive dilution of a 0.1 M $CaCl_2$ solution prepared from powder purchased from Sigma. The standards were measured three times. Studied solutions of proteins were measured by immersing the electrodes into the solution. A stable measurement of the potential (in mV) was typically obtained after 5 minutes. The measurements were conducted at 20 °C.

References

Berne, B.J., Pecora, R., 2000. Dynamic Light Scattering: With Applications to Chemistry, Biology, and Physics. Courier Corporation.

Brown, W., 1993. Dynamic light scattering: the method and some applications. Oxford University Press, USA.

Mahmoudi, N., Mehalebi, S., Nicolai, T., Durand, D., Riaublanc, A., 2007. Light-scattering study of the structure of aggregates and gels formed by heat-denatured whey protein isolate and β-lactoglobulin at neutral pH. J. Agric. Food Chem. 55, 3104–3111.

Moreels, E., De Ceuninck, W., Finsy, R., 1987. Measurements of the Rayleigh ratio of some pure liquids at several laser light wavelengths. J. Chem. Phys. 86, 618–623.

Nicolai, T., Gimel, J.C., Johnsen, R., 1996. Analysis of relaxation functions characterized by a broad monomodal relaxation time distribution. J. Phys. II 6, 697–711.

Phan-Xuan, T., Durand, D., Nicolai, T., Donato, L., Schmitt, C., Bovetto, L., 2011. On the Crucial Importance of the pH for the Formation and Self-Stabilization of Protein Microgels and Strands. Langmuir 27, 15092–15101.

Chapter 3. Structure and flow of dense suspensions of protein fractal aggregates in comparison with microgels.

Published as

Inthavong, W., Kharlamova, A., Chassenieux, C., Nicolai, T., 2016. Soft Matter 12, 2785–2793.

Abstract

Solutions of the globular whey protein β-lactoglobulin (β-lg) were heated at different protein concentrations leading to the formation of polydisperse fractal aggregates with different average sizes. The structure of the solutions was analyzed with light scattering as a function of the protein concentration. The osmotic compressibility and the dynamic correlation length decreased with increasing concentration and became independent of the aggregate size in dense suspensions. Results obtained for different aggregate sizes could be superimposed after normalizing the concentration with the overlap concentration. Dense suspensions of fractal protein aggregates are strongly interpenetrated and can be visualized as an ensemble of fractal 'blobs'. The viscosity of heated β-lg solutions increased extremely sharply above 80 g/L and diverged at 98 g/L, mainly due to the sharply increasing aggregate size. At a fixed aggregate size, the viscosity increased initially exponentially with increasing concentration and then diverged. The increase was stronger when the aggregates were larger, but the dependence of the viscosity on the aggregate size was weaker than that of the osmotic compressibility and the dynamic correlation length. The concentration dependence of the viscosity of solutions of fractal β-lg aggregates is much stronger than that of homogeneous β-lg microgels. The behavior of fractal aggregates formed by whey protein isolate was similar.

1. Introduction

Globular proteins may be considered as dense nanoparticles that are stabilized in aqueous solutions by electrostatic repulsion. Heating aqueous protein solutions renders the rigid structure of the globular proteins mobile which allows formation of bonds between the proteins and can cause irreversible aggregation. Aggregation leads to the formation of a percolating network above a critical gel concentration (C_g), but at lower concentrations stable suspensions of finite size aggregates are obtained (Mezzenga and Fischer, 2013; Nicolai et al., 2011). The size of the aggregates increases with increasing protein concentration and diverges at C_g. The local structure of the aggregates and the value of C_g depend on the type of protein, the pH and the added salt. However, for a number of different globular proteins it has been shown that the large scale structure of the aggregates is self-similar (Donato et al., 2005; Gimel et al., 1994; Hagiwara et al., 1996; Mahmoudi et al., 2007; Micali et al., 2006; Vreeker et al., 1992; Weijers et al., 2002). Self-similar aggregates are characterized by

their fractal dimension (d_f) which relates the molar mass (M) to the radius (R): $M \propto R^{df}$. The value of d_f was found to increase weakly from 1.7 when electrostatic interaction is strong to 2.0 when it is weak, but it does not depend on the type of protein.

Fractal protein aggregates have been studied extensively in dilute solutions, but as far as we are aware no systematic investigation has been done on the flow properties of dense suspensions of such aggregates. More in general, while dense suspensions of homogeneous spherical particles have been investigated in much detail (Genovese, 2012; Quemada and Berli, 2002; Sciortino and Tartaglia, 2005; Vlassopoulos and Cloitre, 2014), dense suspensions of fractal aggregates have received relatively little attention (Aubry et al., 1998; Collins, 1996; Kovalchuk et al., 2010; Tsenoglou, 1990). An important difference between homogeneous particles and fractal aggregates is that the density of the former does not depend on their size, but for the latter it decreases with increasing size. Considering that the aggregates are spherical we may define their density as $\rho = 3M/(4\pi N_a R^3)$, with N_a Avogadro's number so that $\rho \propto R^{df-3}$. It has therefore been suggested that the viscosity of dense fractal aggregates can be understood in the same way as for homogeneous particles, by treating them as particles with a lower density. However, since fractal aggregates have an open structure, they are to a certain extent interpenetrable. This is especially important for fractal globular protein aggregates, which are very polydisperse, and are strongly interpenetrated in dense suspensions. In addition, it has been shown that fractal protein aggregates have some degree of flexibility (Baussay et al., 2004). Recently, it was demonstrated that interpenetration and flexibility of the fractal aggregates have important effects on the viscosity in dense suspensions (Nzé et al., 2015).

Here we present an investigation of the structure and the viscosity as a function of concentration for aqueous suspensions of fractal globular protein aggregates with different sizes. We will compare the viscosity of fractal aggregates with that of microgels formed by the same proteins (Nicolai, 2016), which enables a direct assessment of the effect of the structure of protein particles. The globular protein used in this investigation was β-lactoglobulin (β-lg), which is the main component of whey. Stable suspensions of aggregates with different average sizes were formed by heating aqueous β-lg solutions at different protein concentrations at pH 7.0 until steady state was reached. It has already been reported elsewhere that at these conditions β-lg forms initially small curved strands with a hydrodynamic radius $R_h \approx 15$ nm. At higher protein concentrations these strands randomly associate into self-similar aggregates with $d_f = 1.7$. In order to render our findings more relevant for applications we have compared the results obtained for aggregates formed by pure β-lg with those formed by a commercial whey protein isolate.

2. Materials and Methods

2.1 Materials

The β-lactoglobulin (Biopure, lot JE 001-8-415) used in this study was purchased from Davisco Foods International, Inc. (Le Sueur, MN, USA) and consisted of approximately equal quantities of variants A and B. Whey protein isolate (WPI) powder was purchased from Lactalis (Laval, France), which contained 95 % protein on dry weight basis of which 70 % β-lg and 20 % α-lactalbumin. The molar masses of β-lactoglobulin and α-lactalbumin are 18 kg/mol and 14 kg/mol, respectively

(Boland et al., 2014). The powders were dissolved in Milli-Q water to which 200 ppm NaN_3 was added to prevent bacterial growth. The pH of the solution was adjusted to 7 by adding small amounts of NaOH 0.1 M. For light scattering, dilute solutions were filtered through 0.2 μm pore size Anotop filters. The protein concentration was determined by UV absorption at 278 nm using extinction coefficient 0.96 L g^{-1} cm^{-1} and 1.05 L g^{-1} cm^{-1} for β-lg and WPI, respectively. Protein solutions were concentrated using ultrafiltration utilizing the KrosFlo Research II/i/Tangential Flow Filtration (TFF) System (Spectrum Europa B.V.).

2.2 Light scattering

Light scattering measurements were carried out using an ALV-CGS3 multibit, multitau, a full digital correlator in combination with a laser emitting vertically polarized light at λ = 632 nm (ALV-Langen). The temperature was controlled using a thermo-stat bath to within ±0.1 °C. The relative excess scattering intensity (I_r) was determined as the total intensity minus the solvent scattering divided by the scattering of toluene at 20 °C. I_r is related to the osmotic compressibility $((d\pi/dC)^{-1})$ and the z-average structure factor (S(q)) (Brown, 1996; Higgins and Benoît, 1994):

$$I_r = K.C.RT.(d\pi/dC)^{-1}S(q), \quad (1)$$

with R being the gas constant, T the absolute temperature and q the scattering wave vector.

$$K = \frac{4\pi^2 n^2}{\lambda^4 N_a}.\left(\frac{dn}{dC}\right)^2.\left(\frac{n_s}{n}\right)^2.\frac{1}{R_s}, \quad (2)$$

where (dn/dC) is the refractive index increment, and R_s is the Rayleigh ratio of toluene. $(n_s/n)^2$ corrects for the difference in scattering volume of the solution with refractive index n and toluene with refractive index n_s. *S(q)* describes the dependence of I_r on the scattering wave vector: $q = (4\pi n/\lambda).\sin(\theta/2)$, with θ being the angle of observation. We used dn/dC = 0.189 cm^3/g and $R_s = 1.35 \times 10^{-5}$ cm^{-1}. In dilute solutions and in the limit of $q \rightarrow 0$, I_r/KC is equal to the weight average molar mass (M_w). At finite concentrations we measure an apparent molar mass (M_a) that is proportional to the osmotic compressibility: $M_a = RT/(d\pi/dC)$. The initial concentration dependence of M_a can be expressed in terms of a virial expansion:

$$M_a = M_w/(1 + 2A_2M_wC + \ldots). \quad (3)$$

The initial q-dependence of the structure factor extrapolated to $C \rightarrow 0$ can be used to obtain the z-average radius of gyration (R_g):

$$S(q) = (1 + q^2.R_g^2/3)^{-1}. \quad (4)$$

At higher concentrations, when interactions cannot be neglected, the initial q-dependence of the structure factor can be expressed in terms of the static correlation length (ξ_s):

$$S(q) = (1 + q^2.\xi_s^2)^{-1}. \quad (5)$$

The normalized intensity autocorrelation ($g_2(t)$) that is measured with dynamic light scattering (DLS) is related to the normalized electric field correlation function, $g_1(t)$: $g_2(t) = 1 + g_1(t)^2$ (Berne and Pecora, 2000). $g_1(t)$ was analyzed in terms of a distribution of relaxation times using the REPES routine (Brown, 1993):

$$g_1(t) = \int A(log\tau)\exp(-t/\tau)d\log\tau\,. \tag{6}$$

In all cases monomodal distributions were observed and the correlograms could be well described using the following analytical expression for $A(\log\tau)$:

$$A(\log\tau) = k\tau^p \exp[-(\tau/\tau^*)^s]. \tag{7}$$

In binary solutions the relaxation of the intensity fluctuations is caused by the cooperative diffusion of the solute and the cooperative diffusion coefficient can be calculated from the average relaxation rate: $D_c = (q^2.\tau)^{-1}$. The dynamic correlation length (ξ_d) can be calculated from D_c at $q \to 0$:

$$D_c = \frac{kT}{6\pi\eta\xi_d}\,, \tag{8}$$

with η being the viscosity, k being Boltzmann's constant, and T being the absolute temperature. When interactions can be neglected, i.e. at low concentrations, ξ_d is equal to the z-average hydrodynamic radius. We note that the z-average values of R_h and R_g determined by light scattering give strong weight to the larger particles in the distribution and even more so for R_g than for R_h.

2.3 Rheology

The viscosity was measured as a function of the shear rate using a rheometer (AR2000, TA Instruments) with a cone and plate or a couette geometry. After loading the samples were pre-sheared at 100 s^{-1} during 1 min. The viscosity was determined during subsequent shear ramps with increasing and decreasing shear rates. The results obtained with increasing and decreasing shear rates were found to be the same. Measurements done using the cone and plate geometry showed an upturn at low shear rates, which was due to the formation of a weak elastic surface layer of proteins. Sharma et al. (2011) showed that this effect can be much reduced by using a couette geometry. Therefore for one series of samples we have used both geometries and found that indeed the artificial increase was no longer observed. Nevertheless, the same results can be obtained with both geometries after superposition of the data at different concentrations, see Fig. 1 (for cone and plate geometry), Fig. 2 (for couette geometry) and Fig. 3 (comparison). As a much larger quantity of solution is needed for the couette geometry, we have used for the other series of measurements the cone and plate geometry.

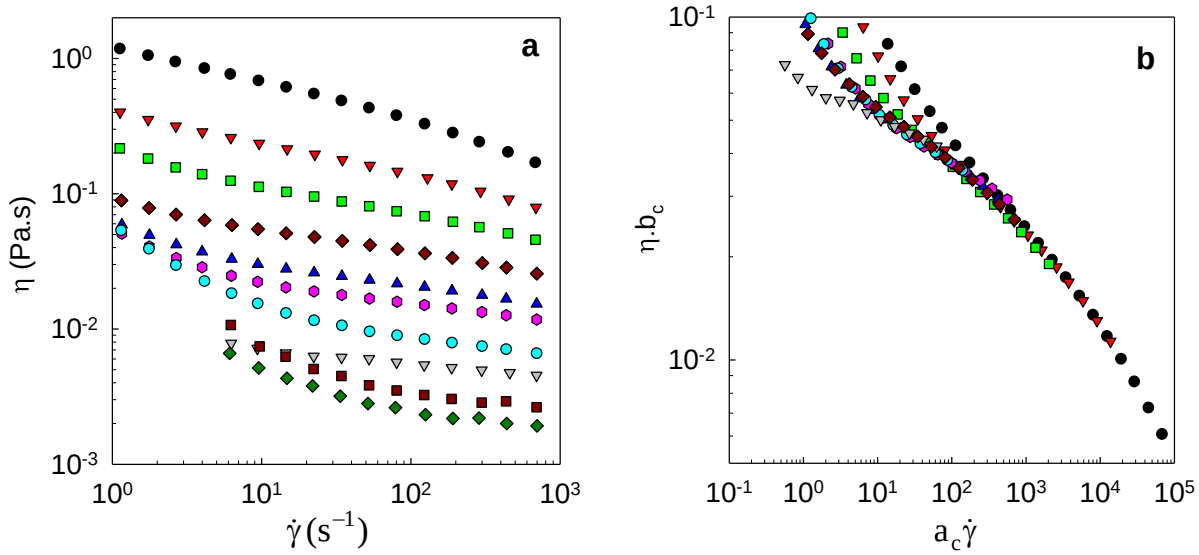

Figure 1. Shear rate dependence of the viscosity of heated β-lg solutions at different concentrations between 10 g/L and 96 g/L measured with a cone and plate geometry (a). Fig. 1b shows the same data after superposition by horizontal and vertical shifts to the reference curve at 68 °C.

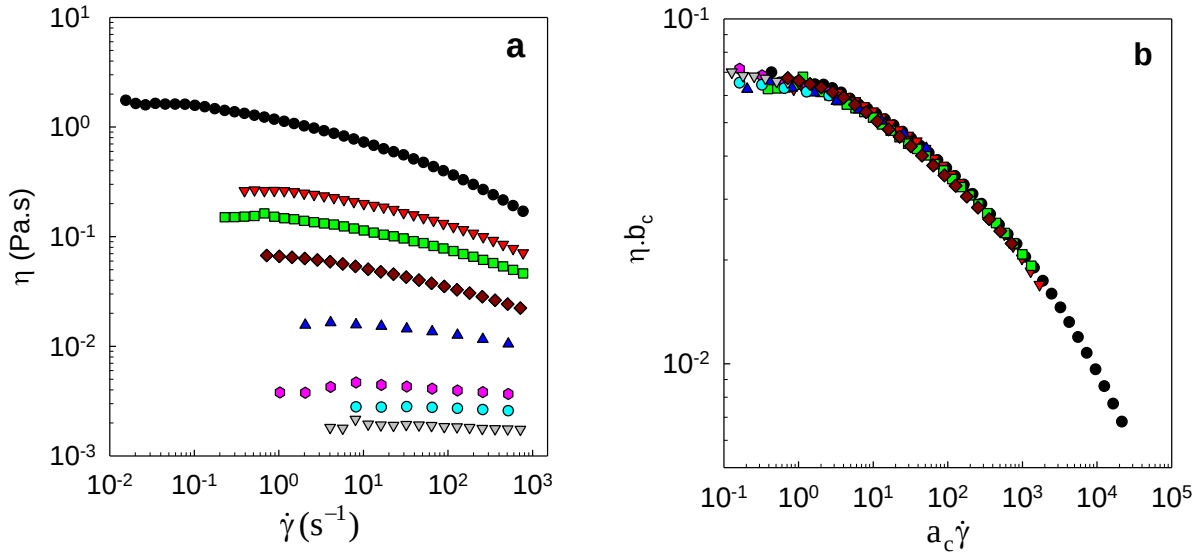

Figure 2. Shear rate dependence of the viscosity of heated β-lg solutions at different concentrations between 10 g/L and 96 g/L measured with a couette geometry (a). Fig. 2b shows the same data after superposition by horizontal and vertical shifts to the reference curve at 70°C.

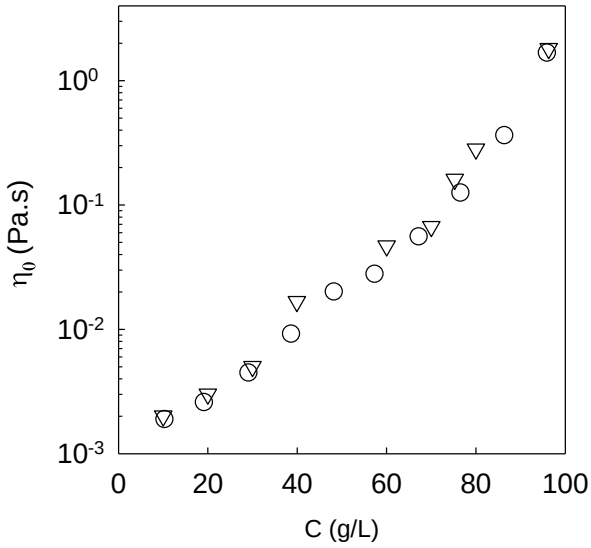

Figure 3. Comparison of the viscosity extrapolated to zero shear rate obtained from the cone and plate geometry (circles) and the couette geometry (triangles).

3. Results

3.1. Characterization of the aggregates

Fractal aggregates of β-lg with different sizes were prepared by heating at 80 °C the aqueous solutions with different protein concentrations at pH 7.0 until steady state was reached. At steady state all proteins are denatured and for C > 40 g/L more than 90 % of the proteins form aggregates (Baussay et al., 2004). The remaining proteins are present in the form of monomers, dimers and trimers. As was mentioned in the Introduction, detailed investigations of the fractal structure of aggregates formed by heating β-lg or WPI in aqueous solution have already been reported elsewhere (Baussay et al., 2004; Gimel et al., 1994; Mahmoudi et al., 2007). Characterization of the aggregates used for the present investigation by light scattering showed that their structure was the same as that reported in the literature.

The weight average molar mass (M_w) of the aggregates was determined using light scattering as described in the Materials and Methods section. The dependence of M_w on the concentration at which the aggregates were formed is shown in Fig. 4a. At low concentrations relatively monodisperse strands were formed, but for C > 40 g/L, random aggregation of these strands led to an increase of M_w with increasing concentration. The molar mass diverged at a critical gel concentration C_g = 98 g/L. The z-average radius of gyration (R_g) and the z-average hydrodynamic radius (R_h) increased with increasing M_w following a power law, which is expected for fractal aggregates, see Fig. 4b. The dependence of both R_h and R_g on M_w is compatible with d_f = 1.7, but R_h is systematically smaller than R_g by a factor of about 0.7, in agreement with findings reported earlier (Baussay et al., 2004). The principal reason for this difference is the polydispersity of the aggregates, R_g is derived from the z-average of R_g^2 and R_h from the z-average of R_h^{-1}. Therefore R_g is more sensitive to larger aggregates.

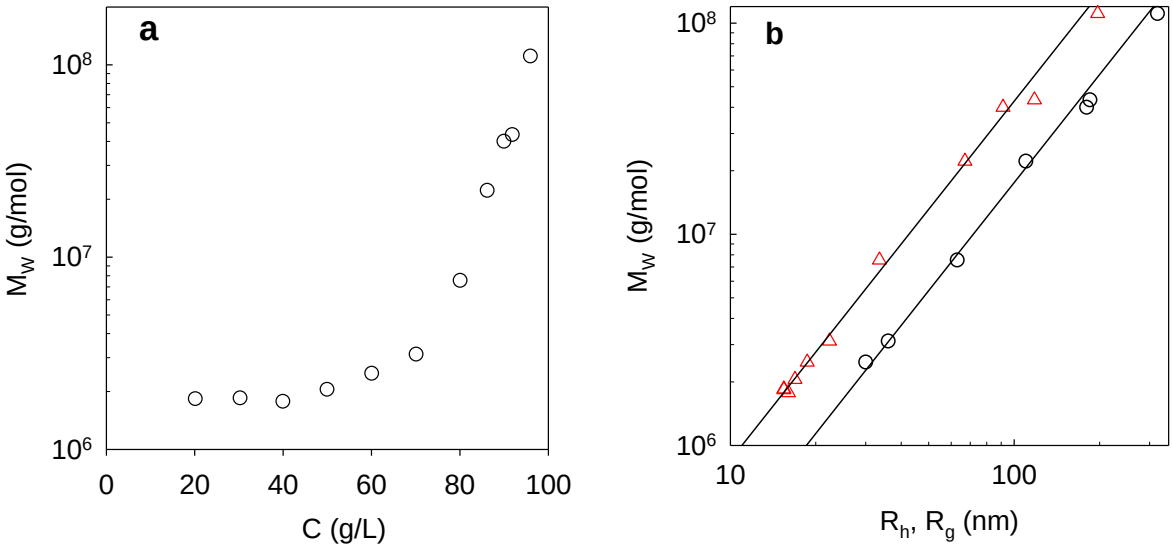

Figure 4. a). Molar mass of β-lg aggregates formed in heated aqueous solutions as a function of the protein concentration. b) Dependence of the molar mass of β-lg aggregates on the radius of gyration (circles) or the hydrodynamic radius (triangles).

3.2. Structure of the aggregate solutions

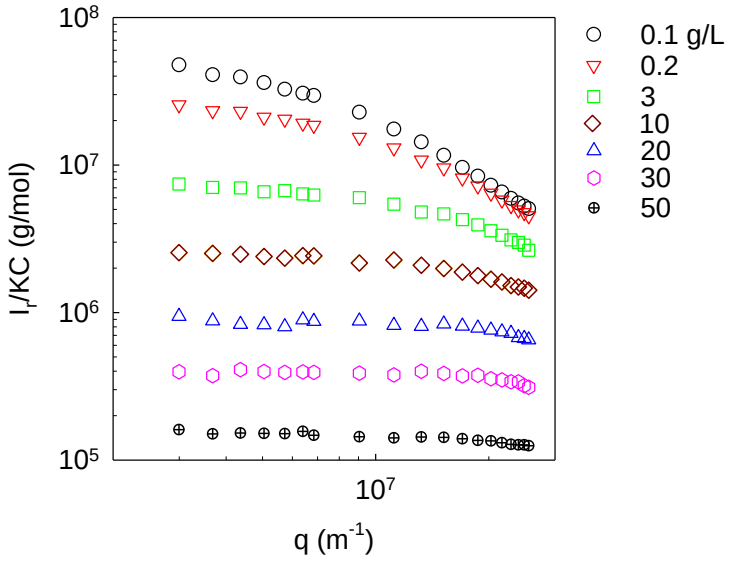

Figure 5. Dependence of Ir/KC on q for aggregates formed by heating at C = 96 g/L and subsequently diluted to different concentrations as indicated in the figure.

All solutions of fractal aggregates were optically clear and their structure was studied with light scattering over a range of concentrations. Fig. 5 shows I_r/KC for large aggregates that were formed by heating at C = 96 g/L and that were subsequently progressively diluted. At high protein concentrations the structure factor was independent of q in the range covered by light scattering, implying that the correlation length of the concentrated solutions was less than 15nm. It was shown elsewhere (Pouzot et al., 2005) using small angle X-ray scattering experiments that the structure

factor of concentrated aggregate solutions shows a peak implying a certain degree of order in the distribution of the proteins. The osmotic compressibility and the correlation length of the concentration fluctuations increased with decreasing concentration causing an increase of I_r/KC and a stronger q-dependence.

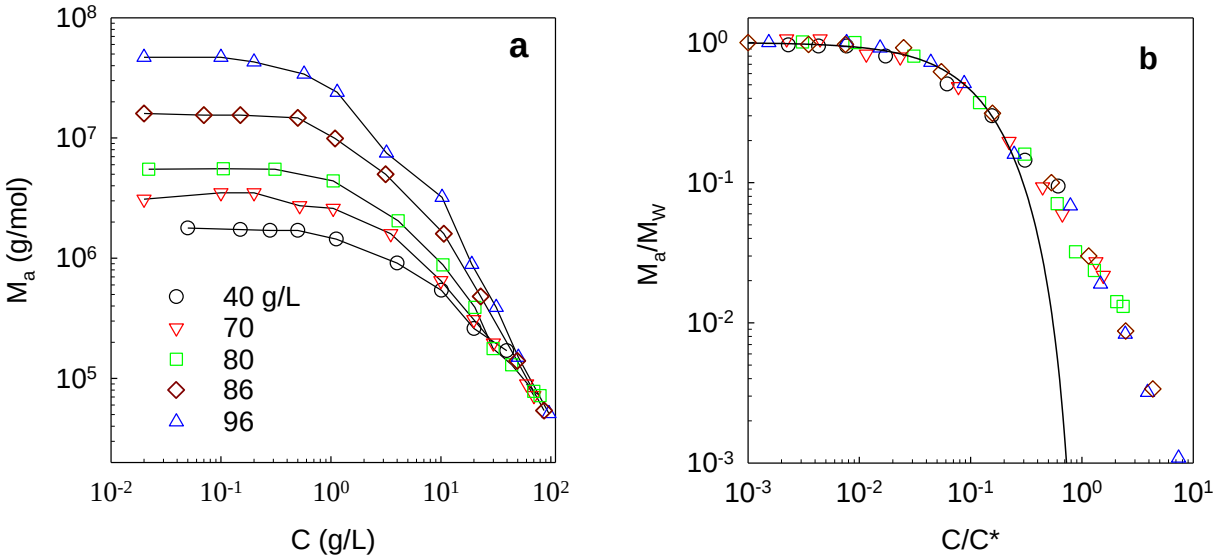

Figure 6. Concentration dependence of M_a for aggregates formed by heating at different protein concentrations indicated in the figure (a). The same data are plotted in Fig. 6b after normalizing M_a with M_w and C with C*. The solid line in Fig. 6b represents eq. 9.

Fig. 6a shows the concentration dependence of the apparent molar mass ($M_a = I_r/KC_{(q\to 0)}$) for protein aggregates with different sizes obtained by heating at different concentrations. As was mentioned above, M_a is proportional to the osmotic compressibility and is equal to M_w if interactions are negligible, i.e. at low concentrations. In all cases the osmotic compressibility decreased with increasing concentration, due to electrostatic and excluded volume interactions between the aggregates and at the highest concentrations M_a became independent of the aggregate size. The latter implies that in dense suspensions the aggregates are strongly interpenetrated and that the osmotic compressibility is determined by interaction between the elementary units of the aggregates.

For non-interacting hard spheres, M_a/M_w can be well described by the following equation (Carnahan and Starling, 1969):

$$\frac{M_a}{M_w} = \frac{(1-\phi)^4}{1+4\phi+4\phi^2-4\phi^3+\phi^4}, \qquad (9)$$

where ϕ is the volume fraction of the particles. For solutions of polydisperse soft particles such as the protein aggregates, the initial concentration dependence of M_a/M_w can still be described by eq. 9 if for ϕ we use an effective volume fraction: $\phi_e = C/C^*$, where C^* is the concentration at which the effective volume fraction of the particles is unity and is related to the second virial coefficient: $C^* = A_2/(4M_w)$. When expressed in units of volume, the second virial coefficient is 4 times the effective

volume of the particles. Fig. 6b shows that eq. 9 describes the results in this representation up to $C/C^* \approx 0.2$. At higher protein concentrations, M_a decreased less steeply than for equivalent hard spheres, because the aggregates are polydisperse and can interpenetrate. As expected, the values of C^* decreased with increasing aggregate size, see Fig. 7.

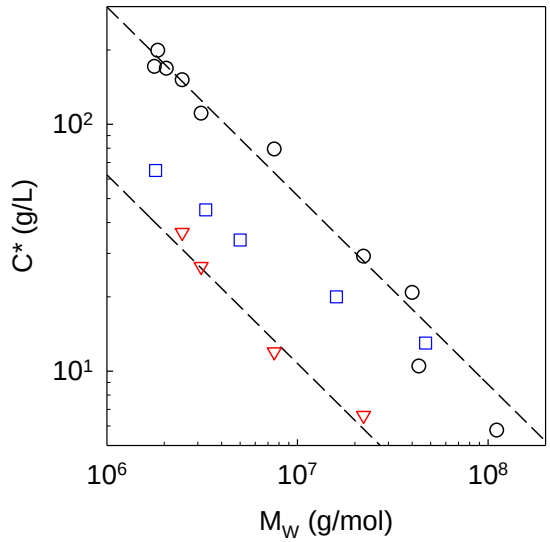

Figure 7. Dependence of C* on the molar mass for fractal β-lg aggregates. The data obtained from fits of the initial concentration dependence of M_a to eq. 9 are indicated by squares, whereas the circles and the triangles indicate the values calculated using eq. 10 with R_h and R_g, respectively. The dashed lines indicate the power law dependence corresponding to the one shown in Fig. 4b.

For spherical particles C^* can also be calculated from their molar mass and their radius:

$$C^* = 3M_w/(4\pi R^3 N_a). \qquad (10)$$

For monodisperse non-interacting hard spheres the two methods give the same value, but for polydisperse or interacting particles they will be different. For the polydisperse protein aggregates studied here, the values calculated using eq. 10 are smaller if one uses R_g for the radius than if one uses R_h, see Fig. 7. The values of C^* obtained from the comparison of the concentration dependence of M_a with eq. 9 were intermediate between those calculated using eq. 10 with $R = R_h$ or $R = R_g$. However, the molar mass dependence was weaker, which is a consequence of the increasing polydispersity with increasing M_w.

As can be seen in Fig. 5, the interpenetration of the aggregates caused a decrease of the correlation length with increasing concentration. At higher concentrations, the static correlation length became too small to be determined with light scattering, but the dynamic correlation length (ξ_d) obtained from dynamic light scattering could be determined over the whole concentration range. Examples of correlograms and the corresponding relaxation time distributions are shown in Fig. 8. As was discussed in Baussay et al. (2004), in dilute solutions the q-dependence of the diffusion coefficient increases with increasing aggregate size, because the fractal aggregates are semi-flexible. With increasing concentration the q-dependence of D_c decreased, because the correlation length of the concentration fluctuations decreased, see Fig. 9. ξ_d obtained from the cooperative diffusion coefficient extrapolated to zero-q, see eq. 8, decreased with increasing concentration down to values

approaching the radius of monomeric β-lg that is about 2nm. Fig. 10 shows that ξ_d has the same power law dependence on M_a as R_h on M_w independent of the aggregate size. The structure of the interpenetrated aggregate solution can thus be visualized as an ensemble of fractal 'blobs' with radius ξ_d and molar mass M_a, independent of the aggregate size. The peak in the structure factor at larger q-values that was found with SAXS (Pouzot et al., 2005) implies that the 'blobs' are regularly distributed in salt free solutions.

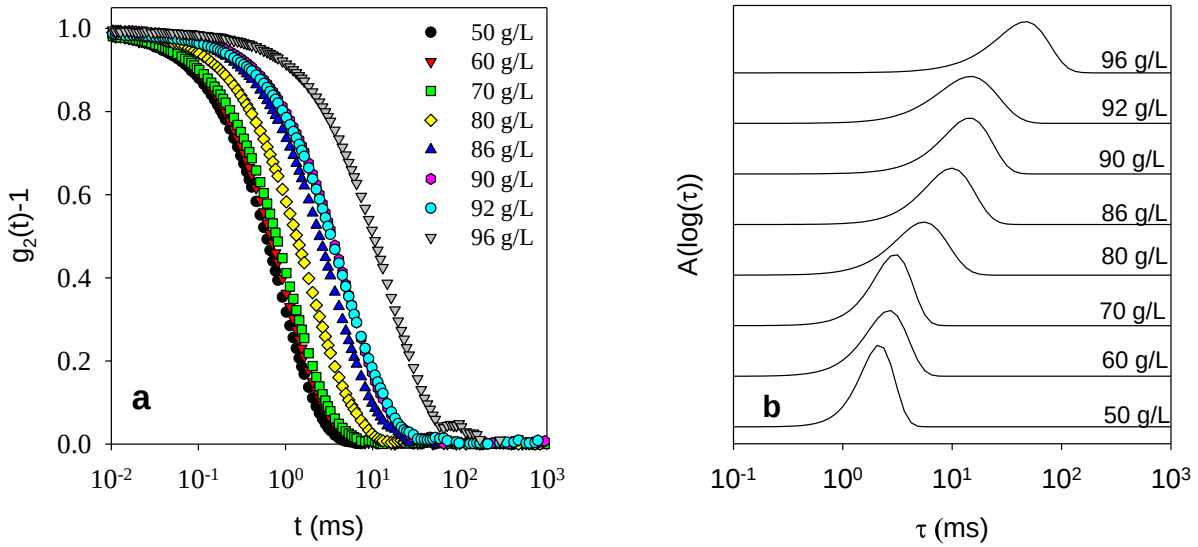

Figure 8. Examples of normalized correlograms (a) and the corresponding relaxation time distributions (b) of dilute solutions of aggregates formed by heating β-lg at different concentrations indicated in the figure. The scattering angle was 30°.

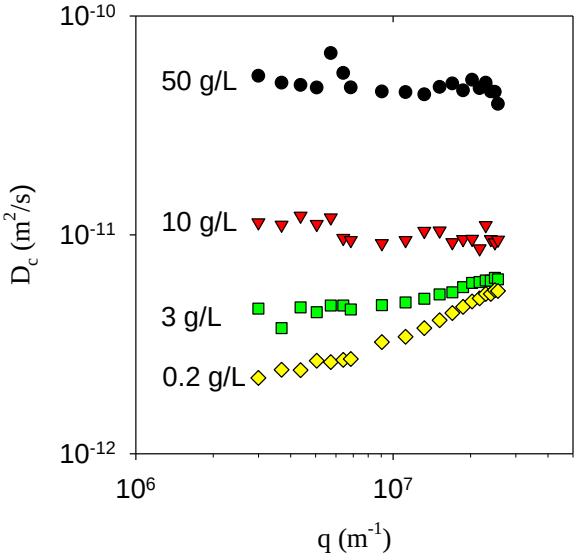

Figure 9. Dependence of the cooperative diffusion coefficient on q for solutions of aggregates formed by heating at C = 96 g/L that were subsequently diluted to different concentrations as indicated in the figure.

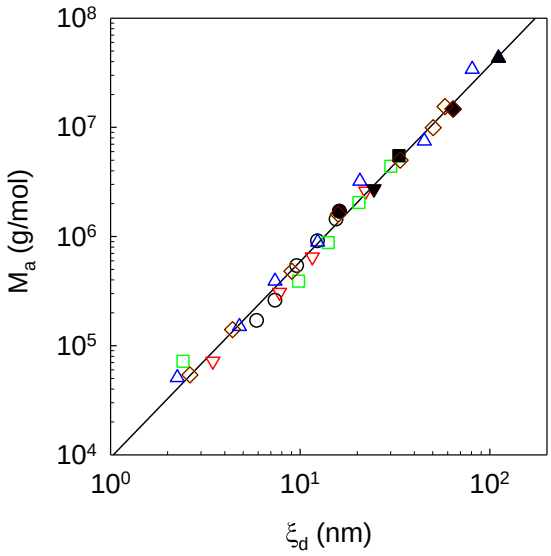

Figure 10. Dependence of the apparent molar mass on the dynamic correlation length for solutions of aggregates with different sizes measured at different protein concentrations. The filled symbols represent values at infinite dilutions where $M_a = M_w$ and $\xi_d = R_h$. The solid line has a slope of 1.7. The symbols are as in Fig. 6a.

3.3. Viscosity

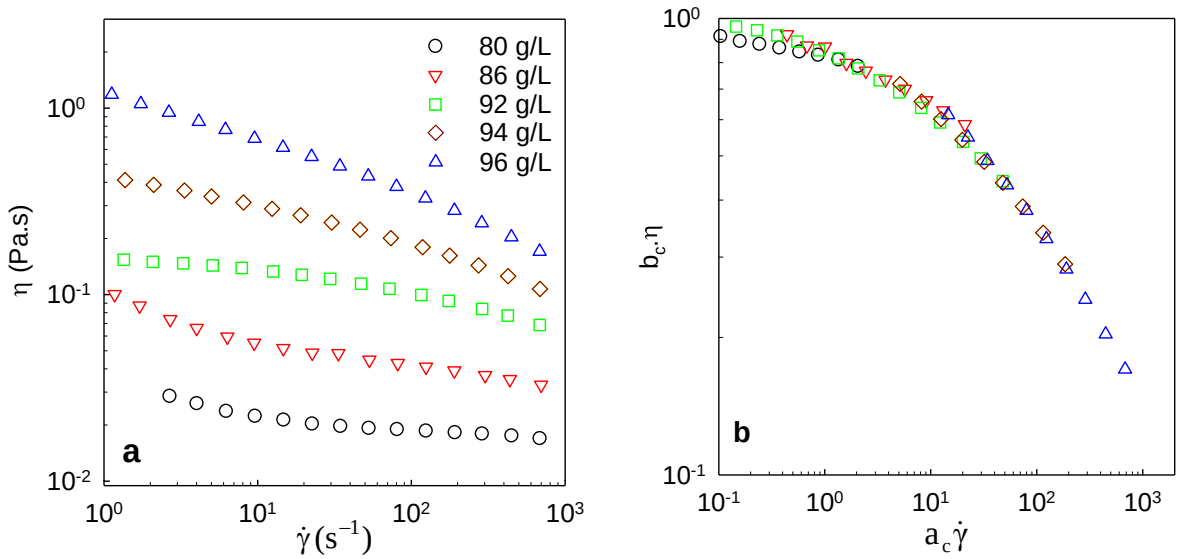

Figure 11. Shear rate dependence of the viscosity of heated β-lg solutions at different concentrations (a). Fig. 11b shows a master curve of the same data obtained by horizontal and vertical shifts with respect to the data at C = 96 g/L. The artificial upturns at low shear rates were removed from the master curve.

Solutions of β-lg at different concentrations were loaded onto the rheometer after heating and the viscosity (η) was determined as a function of the shear rate ($\dot{\gamma}$). For the more viscous solutions we observed shear thinning at larger shear rates, see Fig. 11a. We also observed an

increase of the viscosity with decreasing shear rate at low shear rates. However, as was mentioned in the Materials and Methods section, this increase is an artifact caused by the formation of a layer of proteins at the interface. If we ignore the artificial increase at low shear rates, the results obtained at different concentrations can be superimposed by horizontal and vertical shift factors, see Fig. 11b. This allowed us to obtain the limiting low shear viscosity (η_0) at all concentrations.

η_0 increased very sharply with increasing protein concentration for C > 70 g/L and diverged at the gel concentration, see Fig. 12a. The sharp increase of η_0 was caused by a combination of increasing protein concentration and increasing aggregate size. In order to distinguish these two effects, we measured the shear rate dependent viscosity as a function of the protein concentration keeping the aggregate size fixed. To this end, a solution of aggregates formed at C = 96 g/L with R_g = 320 nm was progressively diluted. Master curves could be obtained by superposition of the results obtained at different dilutions, see Fig. 1. The concentration dependence of η_0 for the aggregates with fixed size formed at C = 96 g/L and subsequently diluted is compared in Fig. 12a with that of aggregates with different sizes formed at different concentrations. Even though the concentration dependence of η_0 for solutions with the same large aggregates was steep, it was much more progressive than that of aggregates formed at different concentrations. This clearly demonstrates that the effect of increasing the aggregate size is more important than the effect of increasing the protein concentration. Similar results were obtained with a commercial WPI sample, see Fig. 12b, which is not surprising, because WPI forms similar fractal aggregates in heated aqueous solutions (Mahmoudi et al., 2007). The WPI solutions gelled at a slightly lower protein concentration (95 g/L) and therefore the steep increase of the viscosity occurred at slightly lower concentrations. In the following we focus on the results obtained with pure β-lg.

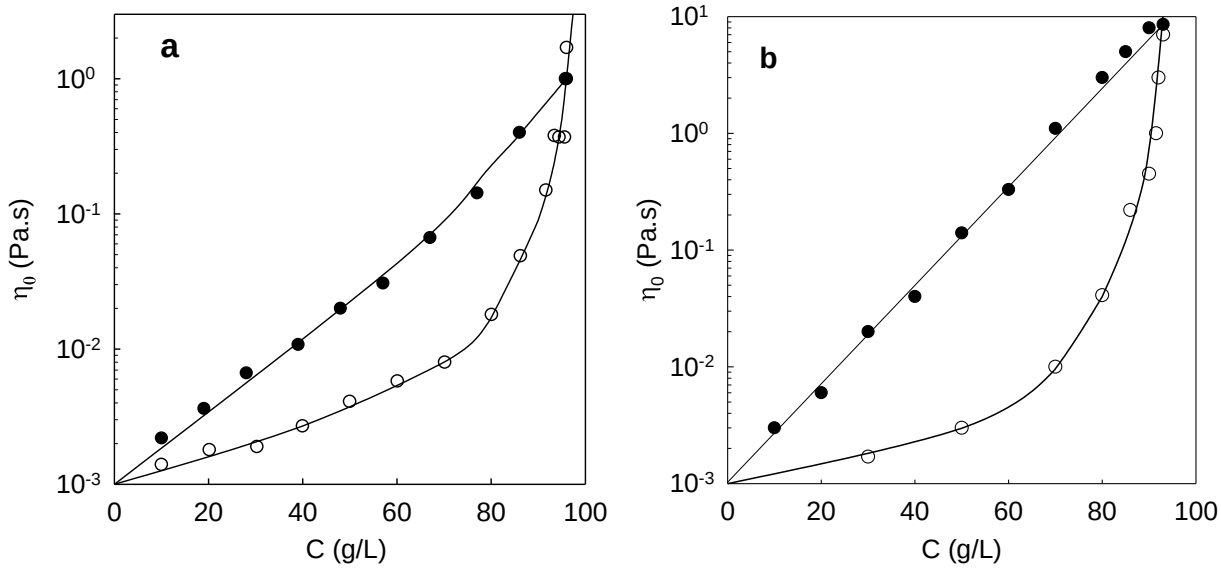

Figure 12. a). Zero shear rate of the viscosity for β-lg solutions that were heated at different concentrations (open symbols) or that were heated at C = 96 g/L and subsequently diluted (closed symbols). b). shows the results obtained for WPI heated at different concentrations (open symbols) or that were heated at C = 93 g/L and subsequently diluted (closed symbols).

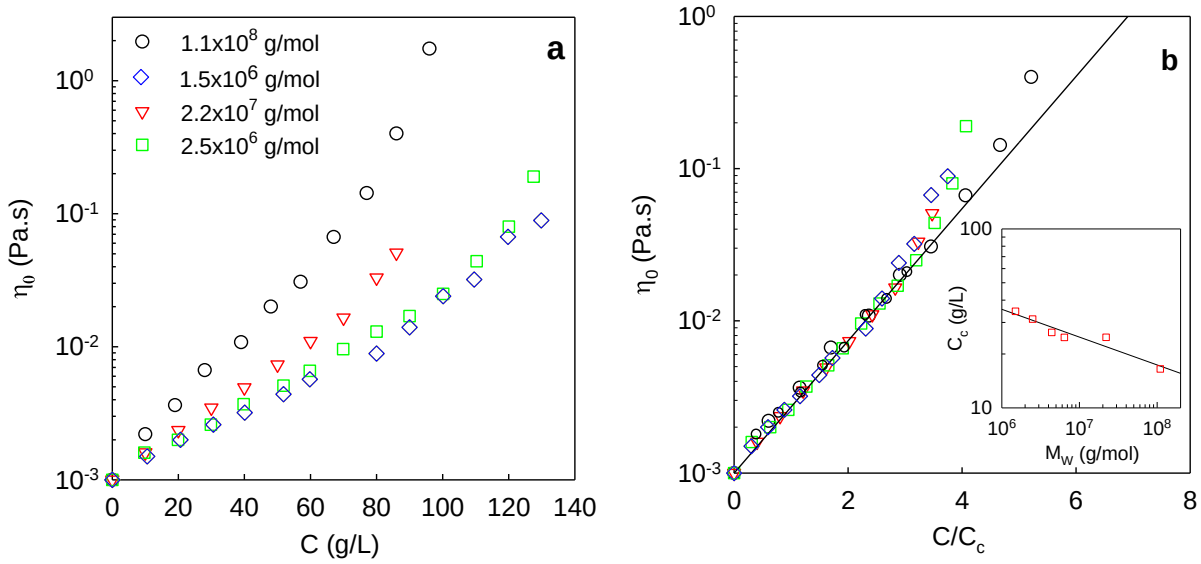

Figure 13. a). Concentration dependence of η_o for solutions of β-lg aggregates with different molar masses indicated in the figure. b). Master curve of the results shown in Fig. 13a obtained by dividing C with C_c. The solid line represents $\eta_0 = \eta_s.\exp(C/C_c)$. The dependence of C_c on M_w is shown in the inset, which also includes results obtained for 2 other aggregate sizes for which the concentration dependence was not shown for clarity.

In order to investigate the effect of the average aggregate size on the concentration dependence of η_0, solutions with different β-lg concentrations were heated. The viscosity of each system was subsequently measured as a function of the protein concentration by dilution. The smaller aggregates obtained by heating at C = 40 g/L and C = 70 g/L were first concentrated by ultrafiltration. Fig. 13a shows that in each case η_0 increased exponentially up to approximately 0.03 Pa.s: $\eta_0 = \eta_s \exp(C/C_c)$, with η_s being the solvent viscosity. The exponential increase obtained for the different aggregates superimposed when η_0 was plotted as a function of C/C_c, see Fig. 13b. C_c decreased weakly with increasing aggregate size from C_c = 35 g/L for $M_w = 1.5 \times 10^6$ g/mol to C_c = 16.5 g/L for $M_w = 1.1 \times 10^8$ g/mol, see inset of Fig. 13b.

At higher protein concentrations, η_0 increased more steeply until it diverged and a gel was formed. We also observed that at these higher concentrations the viscosity increased slowly with time and in some cases weak gels were formed with time. It appears that bonds formed slowly between aggregates in these dense protein aggregate suspensions causing a rise in the viscosity or gelation. This phenomenon of so-called cold gelation is well known to occur when electrostatic repulsion is reduced by adding salt or reducing the pH (Nicolai et al., 2011). The rate of gelation increased with increasing aggregate concentration, but for all systems studied here the effects on the viscosity was negligible during the first two days. Notice, however, that the scattering intensity and ξ_d were stable even if gels were formed, implying that formation of the bonds occurred without a significant change in the structure of the solutions.

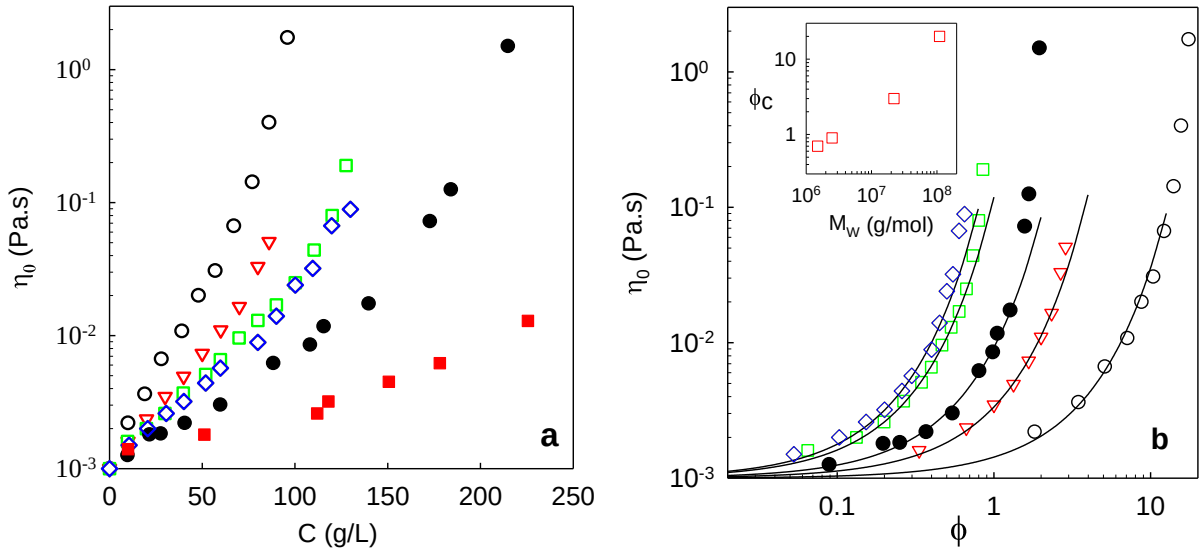

Figure 14. Dependence of the zero shear viscosity on the concentration (a) or the volume fraction (b) of solutions of fractal aggregates (open symbols) and microgels (filled symbols). For comparison the concentration dependence of the viscosity of native β-lg is shown in Fig. 14a (filled squares). Note that in Fig. 14b the horizontal axis is logarithmic. The solid lines in Fig. 14b represent exponential increases of η_o with ϕ. Different open symbols represent different molar masses as indicated in Fig 13. The inset of Fig. 14b shows the molar mass dependence of ϕ_c.

We have compared the behavior of large fractal aggregates with that of homogeneous microgels. As was discussed in Phan-Xuan et al. (2014), microgels can be formed by heating β-lg solutions in the presence of a small amount of $CaCl_2$. For the present investigation the microgels were formed by heating a β-lg solution at C = 40 g/L in the presence of 4.5 mM $CaCl_2$. With light scattering techniques the following characteristics were obtained: M_w = 1.1 × 10^9 g/mol, R_h = 160 nm, R_g = 200 nm. The structure of concentrated microgel suspensions could not be studied using light scattering, because they were highly turbid. In Fig. 14 the concentration dependence of η_0 of microgels is compared to that of the fractal aggregates. The viscosity of the fractal aggregate solutions increased more steeply with increasing protein concentration than for the microgel solutions, which was expected because the density of the latter is higher. However, the concentration dependence of the viscosity of the microgel solutions is still much larger than that of native proteins.

Alternatively, we may compare the viscosity as a function of the effective volume fraction calculated as $\phi_e = C/C^*$. In Fig. 14b, η_0 is plotted as a function of ϕ_e with C^* calculated using in eq. 10 the hydrodynamic radius. The values of C^* calculated in this way are shown in Fig. 7 for the fractal aggregates and for the microgels C^* = 110 g/L. In this representation, the viscosity of the microgel suspensions increased more steeply than for fractal aggregates with M_w = 1.1 × 10^8 g/mol and M_w = 2.2 × 10^7 g/mol, but less steeply than for the smaller aggregates. η_0 diverged at $\phi_c = C_c/C^* \approx 2$ for the microgels and $\phi_c \approx 20$, 3, 0.9 and 0.7 for the fractal aggregates with M_w = 1.1 × 10^8, 2.2 × 10^7, 2.5 × 10^6, and 1.5 × 10^6 g/mol, respectively, see inset of Fig. 14b. Except for the smallest aggregates, ϕ_c is larger than that of monodisperse hard spheres for which the viscosity diverges close to random close packing (ϕ_c = 0.63).

In part this can be explained by the polydispersity of the aggregates, which is large because they were formed by a random reaction limited aggregation process (Gimel et al., 1994). As was mentioned above, the values of R_g and R_h obtained from light scattering are strongly weighted by the largest aggregates so that the calculated value of C^* is too small and therefore φ_e is too large. The overestimation of ϕ_e would have been even worse if R_g or A_2 had been used to calculate C^*. The polydispersity of the fractal aggregates increases with increasing average size, which means that ϕ_e is increasingly overestimated. In fact, as was mentioned in the Introduction, the smallest aggregates are not fractal, but relatively monodisperse curved strands and are the building blocks of the larger fractal aggregates. The microgels are much less polydisperse than the larger fractal aggregates so that the overestimation ϕ_e is less important.

A second reason for the large values of φ_e is that the protein particles are soft so that they can be compressed to some extent. Much more importantly, polydisperse fractal aggregates interpenetrate in dense suspensions and the smaller aggregates are embedded within the larger ones. This effect is more important for larger fractal aggregates. As a consequence, the increase of the viscosity at a given concentration by using fractal aggregates instead of microgels or by using larger instead of smaller fractal aggregates is much less important than that might have been anticipated from the difference in C^* calculated from M_w and R_h or R_g.

4. Discussion

We have compared the behavior of dense suspensions of two types of protein aggregates. In pure water relatively monodisperse protein strands were formed for C < 50 g/L, which were the elementary units of the larger fractal aggregates formed at higher concentrations. The aggregation of the strands was reaction controlled and led to increasing polydispersity with increasing aggregate size. Solutions of the fractal aggregates were transparent, because smaller aggregates were embedded in the larger aggregates in a hierarchical manner. In addition, electrostatic repulsion between the proteins induced a weak local order. Interpenetration of the fractal aggregates explains why the structure of dense suspensions was independent of the aggregate size. The osmotic compressibility and the correlation length of dense suspensions were determined by the interactions between the elementary units of the fractal aggregates, i.e. small protein strands.

Spherical microgels of globular proteins were formed by addition of a small amount of $CaCl_2$ before heating. They probably consist of densely cross-linked network of small strands (Nicolai, 2016; Schmitt et al., 2010). The molar mass of microgels is much larger than that of fractal aggregates of the same size and therefore they scatter much more light. In addition, they are much less polydisperse and smaller microgels cannot penetrate larger ones. As a consequence, microgel suspensions were turbid at higher concentrations and the structure of dense suspensions could not be evaluated by light scattering techniques.

The viscosity of colloidal particles as a function of their concentration has been extensively studied in the past and the effects of their architecture and the interaction between the particles have been reviewed (Genovese, 2012; Quemada and Berli, 2002; Sciortino and Tartaglia, 2005; Vlassopoulos and Cloitre, 2014; Vlassopoulos and Fytas, 2009). The viscosity diverges at a critical volume fraction and the dependence on ϕ has often been described by the Krieger-Dougherty

equation (Krieger, 1972) or the Quemada model (Quemada, 1977): $\eta_0 = \eta_s.(1-\phi/\phi_c)^{-2}$. For monodisperse hard spheres ϕ_c is the concentration of close-packing, but in order to account for the effects of polydispersity, interaction or softness of the colloids ϕ_c has often been considered as an adjustable parameter. The same equation has been used to describe the concentration dependence for rigid clusters of randomly aggregated colloids (Aubry et al., 1998; Collins, 1996; Kovalchuk et al., 2010; Tsenoglou, 1990). The critical volume fraction of the colloids was found to decrease with increasing size of the fractal aggregates, because the density of the fractal aggregates decreased.

Here we find that the concentration dependence of the viscosity of the protein aggregates is much better described by an exponential increase except close to ϕ_c. An exponential increase of the viscosity was also reported for dendrimers (Rietveld and Bedeaux, 2001), polymeric micelles (Merlet-Lacroix et al., 2010) and randomly aggregated star polymers (Nzé et al., 2015). The latter study is particularly relevant here, because it is the only investigation of the viscosity of interpenetrated randomly aggregated particles with flexible bonds. Similar to the fractal protein aggregates, the osmotic compressibility of fractal aggregates of star polymers could be described by eq. 9 up to $\varphi \approx$ 0.4 and decreased more slowly at higher concentrations. Also for this system, the osmotic compressibility at high concentrations was found to be independent of the size of the aggregates and was determined by the interaction between the elementary units of the aggregates, i.e. the star polymers. The behavior of flexible fractal aggregates is very different from that of the rigid clusters, mainly because they can interpenetrate, but also because they are soft. This means that the viscosity of such systems cannot be interpreted in terms of the cumulated volume fraction of the aggregates.

If the size of the aggregates is increased at a fixed concentration, the effect on the viscosity will be different for fractal aggregates and microgels. For fractal aggregates the viscosity will increase with increasing aggregate size, because the density of the aggregates decreases. However, if larger microgels are formed at a fixed concentration the viscosity remains the same, assuming that the polydispersity and softness of the microgels do not depend on their size, because the volume fraction remains the same. If the size of the aggregates increases with increasing concentration, as was the case for the fractal aggregates formed at different concentrations, the viscosity increases very steeply due to the combined effects of increasing size and increasing concentration. Comparison of the two situations for globular protein aggregates showed that former effect was most important.

5. Conclusions

Fractal aggregates are formed by heating globular proteins in aqueous solutions at pH 7. The average aggregate size increases if the concentration at which the proteins are heated is increased and diverges at the critical gel concentration. For a given aggregate size the viscosity increases exponentially with the protein concentration. The increase is steeper if the aggregates are larger, because the density of the aggregates decreases with increasing size. However, the effect of the aggregate size is smaller than expected from the decrease of the density, because the aggregates are very polydisperse and smaller aggregates are embedded within the larger ones. The viscosity of protein solutions after heating at different concentrations increases very sharply over a small concentration range close to the critical gel concentration, because the average size of the aggregates increases sharply. The osmotic compressibility and the correlation length of the concentration fluctuations decrease with increasing concentration and are independent of the

aggregate size at high concentrations, where they are determined by the interaction between the elementary units of the aggregates. The behavior of aggregates formed by WPI is close to that for β-lg aggregates.

The behavior of microgels formed by heating globular proteins in the presence of a small amount of $CaCl_2$ is different from that of fractal aggregates, because they are denser and cannot interpenetrate. Therefore the increase of the viscosity of microgel solutions with increasing protein concentration is weaker and does not depend on the size of the microgels.

Acknowledgement

W.I. acknowledges financial support from the office of education affairs, the ministry of science and technology and the national institute of metrology of Thailand.

References

Aubry, T., Largenton, B., Moan, M., 1998. Study of Aggregate Density in Fumed Silica Suspensions. J. Colloid Interface Sci. 202, 551–553.

Baussay, K., Le Bon, C., Nicolai, T., Durand, D., Busnel, J.-P., 2004. Influence of the ionic strength on the heat-induced aggregation of the globular protein β-lactoglobulin at pH 7. Int. J. Biol. Macromol. 34, 21–28.

Berne, B.J., Pecora, R., 2000. Dynamic Light Scattering: With Applications to Chemistry, Biology, and Physics. Courier Corporation.

Boland, M., Singh, H., Thompson, A., 2014. Milk proteins: From expression to food. Academic Press.

Brown, W., 1996. Light scattering: principles and development. Oxford University Press.

Brown, W., 1993. Dynamic light scattering: the method and some applications. Oxford University Press, USA.

Carnahan, N.F., Starling, K.E., 1969. Equation of State for Nonattracting Rigid Spheres. J. Chem. Phys. 51, 635–636.

Collins, I.R., 1996. On the Viscosity of Concentrated Aggregated Suspensions. J. Colloid Interface Sci. 178, 361–363.

Donato, L., Garnier, C., Doublier, J.-L., Nicolai, T., 2005. Influence of the NaCl or CaCl2 Concentration on the Structure of Heat-Set Bovine Serum Albumin Gels at pH 7. Biomacromolecules 6, 2157–2163.

Genovese, D.B., 2012. Shear rheology of hard-sphere, dispersed, and aggregated suspensions, and filler-matrix composites. Adv. Colloid Interface Sci. 171, 1–16.

Gimel, J.C., Durand, D., Nicolai, T., 1994. Structure and distribution of aggregates formed after heat-induced denaturation of globular proteins. Macromolecules 27, 583–589.

Hagiwara, T., Kumagai, H., Nakamura, K., 1996. Fractal Analysis of Aggregates Formed by Heating Dilute BSA Solutions Using Light Scattering Methods. Biosci. Biotechnol. Biochem. 60, 1757–1763.

Higgins, J.S., Benoît, H., 1994. Polymers and neutron scattering. Clarendon press Oxford.

Kovalchuk, N.M., Kuchin, I., Starov, V., Uriev, N., 2010. Aggregation in colloidal suspensions and its influence on the suspension viscosity. Colloid J. 72, 379–388.

Krieger, I.M., 1972. Rheology of monodisperse latices. Adv. Colloid Interface Sci. 3, 111–136.

Mahmoudi, N., Mehalebi, S., Nicolai, T., Durand, D., Riaublanc, A., 2007. Light-scattering study of the structure of aggregates and gels formed by heat-denatured whey protein isolate and β-lactoglobulin at neutral pH. J. Agric. Food Chem. 55, 3104–3111.

Merlet-Lacroix, N., Cola, E.D., Cloitre, M., 2010. Swelling and rheology of thermoresponsive gradient copolymer micelles. Soft Matter 6, 984–993.

Mezzenga, R., Fischer, P., 2013. The self-assembly, aggregation and phase transitions of food protein systems in one, two and three dimensions. Rep. Prog. Phys. 76, 046601.

Micali, N., Villari, V., Castriciano, M.A., Romeo, A., Monsù Scolaro, L., 2006. From Fractal to Nanorod Porphyrin J-Aggregates. Concentration-Induced Tuning of the Aggregate Size. J. Phys. Chem. B 110, 8289–8295.

Nicolai, T., 2016. Formation and functionality of self-assembled whey protein microgels. Colloids Surf. B Biointerfaces 137, 32–38.

Nicolai, T., Britten, M., Schmitt, C., 2011. β-Lactoglobulin and WPI aggregates: Formation, structure and applications. Food Hydrocoll., 25 years of Advances in Food Hydrocolloid Research 25, 1945–1962.

Nzé, R.-P., Nicolai, T., Chassenieux, C., Nicol, E., Boye, S., Lederer, A., 2015. Effect of Connectivity on the Structure and the Liquid–Solid Transition of Dense Suspensions of Soft Colloids. Macromolecules 48, 7995–8002.

Phan-Xuan, T., Durand, D., Nicolai, T., Donato, L., Schmitt, C., Bovetto, L., 2014. Heat induced formation of beta-lactoglobulin microgels driven by addition of calcium ions. Food Hydrocoll. 34, 227–235.

Pouzot, M., Nicolai, T., Visschers, R.W., Weijers, M., 2005. X-ray and light scattering study of the structure of large protein aggregates at neutral pH. Food Hydrocoll. 19, 231–238.

Quemada, D., 1977. Rheology of concentrated disperse systems and minimum energy dissipation principle. Rheol. Acta 16, 82–94.

Quemada, D., Berli, C., 2002. Energy of interaction in colloids and its implications in rheological modeling. Adv. Colloid Interface Sci. 98, 51–85.

Rietveld, I.B., Bedeaux, D., 2001. The Viscosity of Solutions of Poly(propylene imine) Dendrimers in Methanol. J. Colloid Interface Sci. 235, 89–92.

Schmitt, C., Moitzi, C., Bovay, C., Rouvet, M., Bovetto, L., Donato, L., Leser, M.E., Schurtenberger, P., Stradner, A., 2010. Internal structure and colloidal behaviour of covalent whey protein microgels obtained by heat treatment. Soft Matter 6, 4876–4884.

Sciortino, F., Tartaglia, P., 2005. Glassy colloidal systems. Adv. Phys. 54, 471–524.

Sharma, V., Jaishankar, A., Wang, Y.-C., McKinley, G.H., 2011. Rheology of globular proteins: apparent yield stress, high shear rate viscosity and interfacial viscoelasticity of bovine serum albumin solutions. Soft Matter 7, 5150–5160.

Tsenoglou, C., 1990. Scaling concepts in suspension rheology. J. Rheol. 34, 15–24.

Vlassopoulos, D., Cloitre, M., 2014. Tunable rheology of dense soft deformable colloids. Curr. Opin. Colloid Interface Sci. 19, 561–574.

Vlassopoulos, D., Fytas, G., 2009. From Polymers to Colloids: Engineering the Dynamic Properties of Hairy Particles, in: High Solid Dispersions, Advances in Polymer Science. Springer, Berlin, Heidelberg, pp. 1–54.

Vreeker, R., Hoekstra, L.L., Den Boer, D.C., Agterof, W.G.M., 1992. Fractal aggregation of whey proteins. Food Hydrocoll. 6, 423–435.

Weijers, M., Visschers, R.W., Nicolai, T., 2002. Light Scattering Study of Heat-Induced Aggregation and Gelation of Ovalbumin. Macromolecules 35, 4753–4762.

Chapter 4. The effect of aggregation into fractals or microgels on the charge density and the isoionic point of globular proteins.

Published as

Kharlamova, A., Inthavong, W., Nicolai, T., Chassenieux, C., 2016. Food Hydrocolloids 60, 470-475.

Abstract

Potentiometric titration curves were obtained for aqueous solutions of native whey protein isolate (WPI) and β-lactoglobulin (β-lg) at different NaCl concentrations. The curves crossed at approximately the same pH, which is considered to be the isoionic point (IIP). Titration with NaCl confirmed that the pH was independent of the salt concentration up to 0.1 M at the IIP, which was 4.9 for WPI and 5.0 for β-lg. Fractal aggregates and microgels of different sizes were formed by heating protein solutions at different pH and different concentrations. The titration curves of the aggregates depended on the type of aggregates, but not on their size. The IIP increased by at most 0.2 pH units after aggregation. For a given pH larger than IIP, the charge density of the proteins (α) was reduced after denaturation and aggregation. The reduction was stronger for microgels than for fractal aggregates. Addition of NaCl or increasing the protein concentration mitigated the effect. Comparison between WPI and β-lg showed that the pH dependence of α was almost the same for pH > 5.0 both for native and aggregated proteins.

1. Introduction

Globular proteins have a dense well-defined structure in aqueous solutions. The net charge of proteins (α) is negative at high pH and positive at low pH, but over a wide pH range they contain both negatively and positively charged amino acids. The pH where α = 0 in the absence of adsorbed ions is called the isoionic point (IIP) and depends on the type of protein (Bryan, 1978; Cannan, 1942; Longsworth and Jacobsen, 1949; Salis et al., 2011). When globular proteins are heated their relatively rigid structure becomes more mobile, which allows the formation of bonds with other proteins causing aggregation (Amin et al., 2014; Mezzenga and Fischer, 2013). It was found that the morphology of the aggregates depends on the pH (Krebs et al., 2007; Langton and Hermansson, 1992; Nicolai and Durand, 2013). When the net charge of the proteins is high, relatively thin strands are formed, but when the pH is close to the IIP, spherical microgels are formed. At higher protein concentrations, the strands or the microgels will randomly crosslink into self-similar clusters that increase in size when the protein concentration is increased until at a critical concentration a system spanning network is formed (Clark et al., 2001; van der Linden and Foegeding, 2009).

Experimentally, the effect of α on the aggregation process is studied by varying the pH. However, it is long since known that the charge density of proteins at a given pH depends on the ionic strength, the type of ions, and the protein concentration. Therefore, when aggregation is compared at different concentrations or ionic strengths at a fixed pH value, α is not kept constant and, consequently, observed effects of the protein or salt concentration on aggregation for a given pH can be caused in part by a change of the charge density. In order to relate the aggregation process of proteins to their net charge density it is important to known how α relates to the pH at the conditions at which the aggregation occurred. In addition, aggregation of proteins may affect their buffer capacity and therefore the relationship between the pH and α. As far as we are aware, no systematic investigation of the effect of heat-induced aggregation on the relationship between the pH and the net charge density of globular proteins has been reported in the literature.

The effect of the pH and the ionic strength on heat-induced aggregation of globular proteins has probably been most intensively investigated for β-lactoglobulin (β-lg) and whey protein isolate (WPI) (Guyomarc'h et al., 2015; Kontopidis et al., 2004; Nicolai et al., 2011). The latter contains mainly β-lg (70 %), but also α-lactalbumin (α-lac) (20 %) and 10 % of other types of proteins (de Wit, 1998). Here we present a systematic investigation of the relationship between the pH and the charge density of native and aggregated β-lg and WPI as a function of the NaCl and the protein concentration using potentiometric titration. We will discuss the effect of the pH on aggregation of whey proteins reported in the literature in the light of the results that were obtained in the present study.

2. Experimental

The WPI powder was purchased from Lactalis (Laval, France). It contained 95 % protein on dry weight basis, of which 70 % β-lg and 20 % α-lactalbumin. The β-lg (Biopure, lot JE 001-8-415) used in this study was purchased from Davisco Foods International, Inc. (Le Sueur, MN, USA) and contained less than 2 wt% other whey proteins. The powders were dissolved in Milli-Q water while stirring overnight. The same results were obtained for dialysed and non-dialysed solutions, whereas significant differences were found when 10 mM NaCl was added. This means that the effect of the small amount of salt in the powder was negligible. The protein concentration was determined by UV absorption at 278 nm using extinction coefficients of 0.96 $Lg^{-1}cm^{-1}$ and 1.05 $Lg^{-1}cm^{-1}$ for β-lg and WPI, respectively.

Fractal whey protein aggregates were formed by heating salt-free WPI solutions at 80 °C and neutral pH until the reaction was finished. Stable suspensions of fractal aggregates of two different sizes were obtained by heating protein solutions at C = 62 g/L and C = 90 g/L, respectively. WPI microgels of two different sizes were obtained by heating WPI solutions at C = 40 g/L at pH 5.8 and at pH 6.1, respectively. In all cases the amount of HCl or NaOH needed to set the pH was carefully recorded and used to calculate the effect on the charge density. The average molar mass (M_w) and hydrodynamic radius (R_h) were determined with static and dynamic light scattering using the same methodology as described in Phan-Xuan et al. (2011).

Titration experiments were conducted at room temperature using an automatic titrator (TIM 856, Radiometer Analytical) equipped with a combined pH electrode and a temperature probe. The pH electrode was calibrated by a three-point calibration using standard buffers. When the pH of protein solutions was checked with a different pH-meter and a different probe it was found to be the same within 0.05 units. The pH of all samples was first set to 8.0 by titration with a standard solution of NaOH (0.1 M or 1 M, depending on the protein concentration) and then titrated to pH 4 with a standard solution of HCl (0.1 M or 1 M). A number of protein solutions at set pH values close to the IIP were titrated with a 2 M NaCl solution. Titrations were done at a rate of 0.1 mL per min, but no significant difference was observed when a lower rate was used.

The net charge density of the proteins as a function of the pH was deduced as follows. The number of H^+ bound or released per protein was calculated from the volume of the added NaOH and HCl solutions (V):

$$\Delta\alpha = \frac{V(HCl)\times[HCl]-V(NaOH)\times[NaOH]}{m/M_w}, \quad (1)$$

where m is the mass of titrated whey proteins, [HCl] and [NaOH] are the concentrations of the HCl and NaOH solutions and M_w is the average molar mass of the whey proteins ($M_w = 1.75 \times 10^4$ g/mol for WPI and 1.86×10^4 g/mol for β-lg). Notice that the amount of H^+ in the water is negligible in the pH range covered in the experiment. The dependence of the pH on α was subsequently calculated by taking $\alpha = 0$ at the IIP:

$$\alpha = \Delta\alpha - \Delta\alpha(\text{IIP}). \quad (2)$$

3. Results

3.1 Native proteins

β-lg solutions at C = 10 g/L with different NaCl concentrations ([NaCl]) were titrated as described in the Materials and Methods and were found to cross at approximately pH 5, see Fig. 1a. Crossing of the titration curves at a single value of the pH has earlier been reported for pure β-lg (Cannan et al., 1942), but also for egg ovalbumin (Cannan et al., 1941; Sørensen et al., 1927), lysozyme (Tanford and Wagner, 1954) and, very recently, for soy globulin (Chen et al., 2016). However, Salis et al. (2011) observed that titration curves of BSA at different NaCl concentrations did not cross at exactly the same pH, which they attributed to non-electrostatic interactions. The effect of salt on α can be understood in terms of the surface potential of the proteins, which at a fixed pH decreases with increasing ionic strength (Salis et al., 2011). Therefore, for a given pH the net charge density will be larger when the ionic strength is higher. As a consequence, for a fixed charge density the pH decreases with increasing [NaCl] when it is above the IIP, increases when it is below the IIP and is expected to be independent of [NaCl] at the IIP.

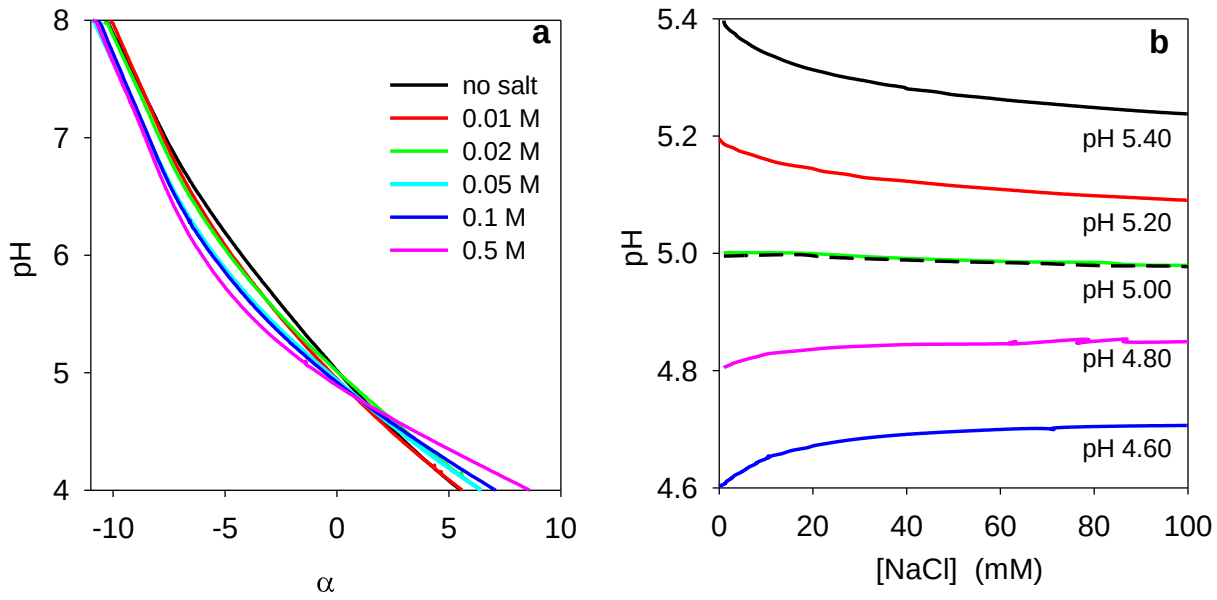

Figure 1. a). pH as a function of the net charge density for β-lg solutions at C = 10 g/L at different NaCl concentrations indicated in the figure. b). pH as a function of the NaCl concentration for β-lg solutions at C = 10 g/L set at different pH before titration. The dashed line represents result for C = 20 g/L.

In order to obtain a precise value of the IIP and to verify that the pH was truly independent of [NaCl] at the IIP, β-lg solutions at different pH close to pH 5 were titrated with 2 M NaCl, see Fig. 1b. For pH ≥ 5.2, the pH decreased with increasing [NaCl], whereas for pH ≤ 4.8 it increased. At pH 5.0, the pH was practically independent of [NaCl] up to 0.1 M and therefore we may conclude that IIP = 5.0 for native β-lg with an uncertainty of about ±0.1 pH units. We repeated the titration with NaCl at pH 5.0 for C = 20 g/L and again observed practically no effect on the pH, see the dashed line in Fig. 1b. We did, however, observed a decrease of the pH for [NaCl] > 0.1M for all pH tested, even at pH 4.6, at which the pH increased up to [NaCl] = 0.1M.

The value of the IIP found here is slightly smaller than that reported by Cannan et al. (1942) who found that titration curves of native β-lg at different KCl concentrations crossed at pH 5.2. Nozaki et al. (1959) determined the IIP by measuring the pH of a β-lg solution from which all ions other than H^+ or OH^- were removed and found in this way IIP = 5.4. They observed that the pH decreased when they added KCl at this pH, which they attributed to the adsorption of K^+. We also observed a decrease of the pH 5.4 when we added NaCl, but not at pH 5.0. Our results can be reconciled with those of Nozaki et al. if they had not succeeded in removing all ions other than H^+ or OH^-. It is interesting to compare the IIP with the isoelectric point (IEP) that is defined as the pH at which the ζ-potential is zero. The two are not necessarily the same, because ions adsorbed to the proteins may lead to a finite ζ-potential at the IIP. A relatively precise value of the IEP of β-lg was obtained by isoelectric focusing and was found to be 5.2 (Fredriksson, 1975), i.e. when the net charge of the proteins is almost –1, but it would not be prudent to draw firm conclusions from such a small difference.

WPI solutions at C = 10g/L were titrated with HCl and NaCl in a similar manner as for β-lg solutions. We found for WPI that IIP = 4.9, which is slightly lower than for pure β-lg. The dependence

of the pH on the charge density was very close for WPI and pure β-lg for pH > 5.0, but α was significantly smaller for WPI for a given pH at pH < 5.0, see Fig. 2. The WPI used for this study contained 20 % α-lac with an IIP ≈ 4.8 and 10 % of other whey proteins. The proximity of the IIP of β-lg and α-lac together with the small quantity of other proteins explains why the pH-dependence on α is almost the same for WPI and pure β-lg.

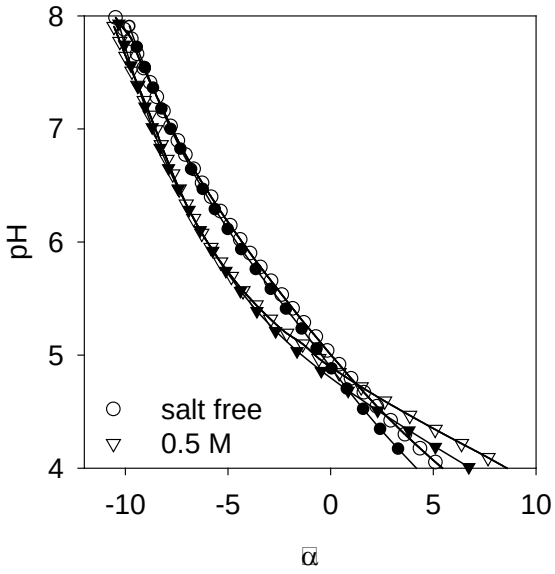

Figure. 2. Comparison of the pH as a function of the net charge density between native WPI (filled symbols) and β-lg (open symbols) without NaCl (circles) and with 0.5 M NaCl (triangles). The protein concentration was 10 g/L.

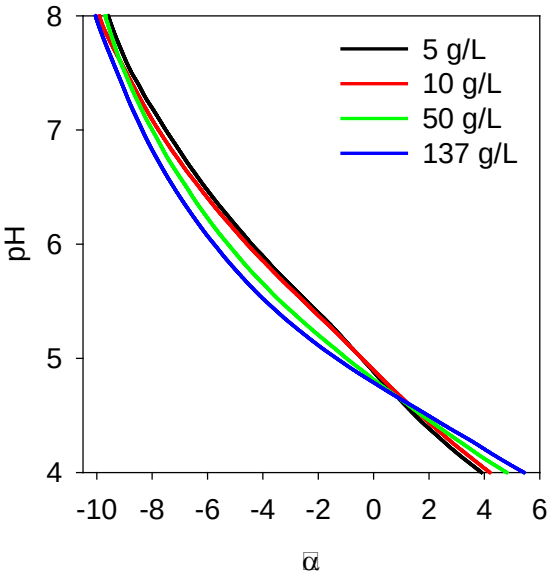

Figure 3. pH as a function of the net charge density for salt-free WPI solutions at different protein concentrations as indicated in the figure.

The effect of the protein concentration on the dependence of the pH on α was investigated for WPI up to 137 g/L, see Fig. 3. For $\alpha < 0$ increasing the protein concentration led to a decrease of the pH, whereas for $\alpha > 0$ it led to an increase. This is expected, because with increasing protein concentration the concentration of counterions is also increased, which has the same effect on the surface potential as adding NaCl. The effect of the protein concentration decreased when NaCl was added and disappeared altogether in the presence of 0.5 M NaCl (results not shown), because the increase of the ionic strength with increasing protein concentration becomes small compared to that of the added salt.

3.2 Aggregates

Fractal aggregates and microgels of WPI of two different sizes were formed by heating as described in the Material and Methods section. Fractal aggregates were formed at pH close 7; the pH before and after heating was found to be the same within the experimental error. Microgels were formed at pH 6.1 and pH 5.8. In this case, after heating, the pH increased to pH 6.4 and pH 6.1, respectively. An increase of the pH due to the formation of microgels has already been reported in the literature (Donato et al., 2009; Phan-Xuan et al., 2011). The hydrodynamic radii were 165 nm and 35 nm for the larger and smaller fractal aggregates and 370 nm and 100 nm for the larger and smaller microgels, respectively. The aggregate solutions were titrated with HCl at different NaCl concentrations and with NaCl at different pH values in the same manner as the native protein solutions.

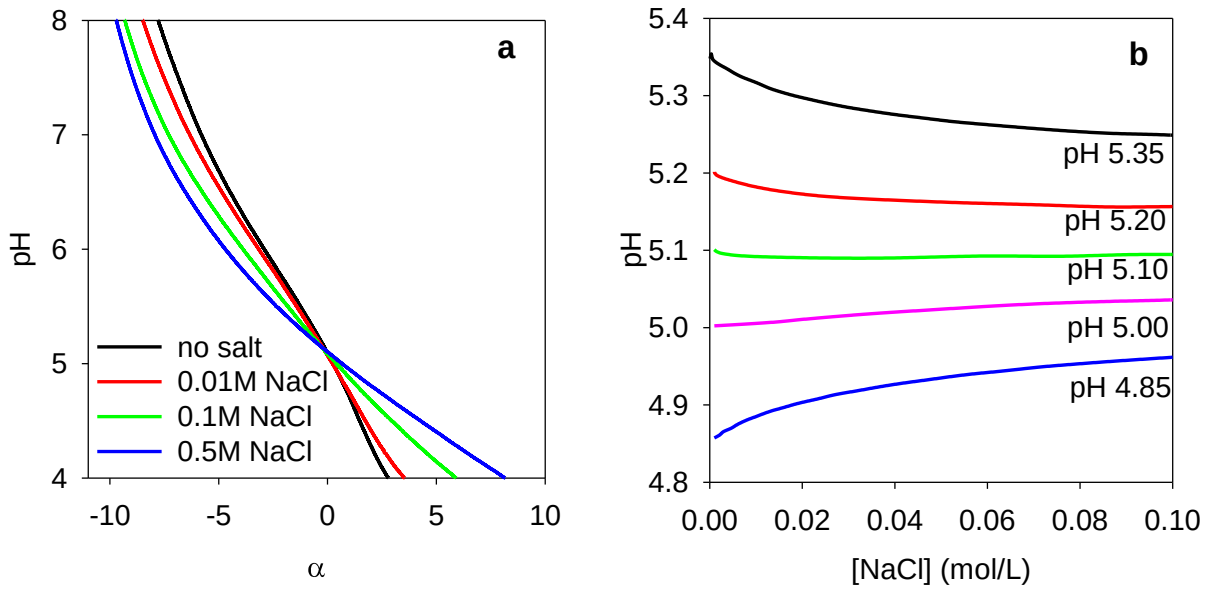

Figure 4. a). pH as a function of the net charge density for WPI microgels at C = 10 g/L at different NaCl concentrations indicated in the figure. b). pH as a function of the NaCl concentration for WPI microgels at C = 10 g/L set at different pH before titration.

The dependence of the pH on α for the smaller microgels is shown in Fig. 4a and the dependence of α on [NaCl] at different set pH values is shown in Fig. 4b. Again we find that the titration curves cross approximately at the same pH. Titration with NaCl showed that IIP = 5.1 (see

Fig. 4b), which is slightly larger than the value found for native WPI. The titration curves obtained for the larger microgels were the same within the experimental error as for the smaller microgels. Similar experiments for the fractal aggregates of WPI showed that IIP = 5.0. Again the titration curves were the same for the two aggregate sizes.

Fig. 5 compares the dependence of the pH on α for the two types of aggregates with that for the native proteins at C = 10 g/L in salt-free solutions (Fig. 5a) and in the presence of 0.5 M NaCl (Fig. 5b). The dependence of the pH on the net charge density of the proteins is significantly different after denaturation and aggregation. It depends on the aggregate structure, but not on the aggregate size, which is expected since protonation of amino acids is influenced by their local environment. Connecting proteins into aggregates leads to a closer proximity of the charged groups of protein molecules and therefore stronger electrostatic interaction, which decreases their total charge density. Microgels are much denser than fractal aggregates even locally, which may explain why the influence of aggregation was strongest for the microgels.

The implication of having a lower net charge density for a given pH after aggregation is that for a given charge density the pH is higher. An increase of the pH after heating was indeed observed in the narrow pH range where microgels are formed as was reported in more detail elsewhere (Donato et al., 2009). The effect is less important in the presence of salt, see Fig. 5b, because charge interaction is screened. For the same reason the effect is also weaker at higher protein concentrations. The effect of aggregation is smaller for fractal aggregates and in the presence of 0.5 M NaCl the difference with native proteins is very small for pH > 5.8. This explains why almost no change of the pH was observed when the proteins were heated at neutral pH and at relatively high protein concentrations.

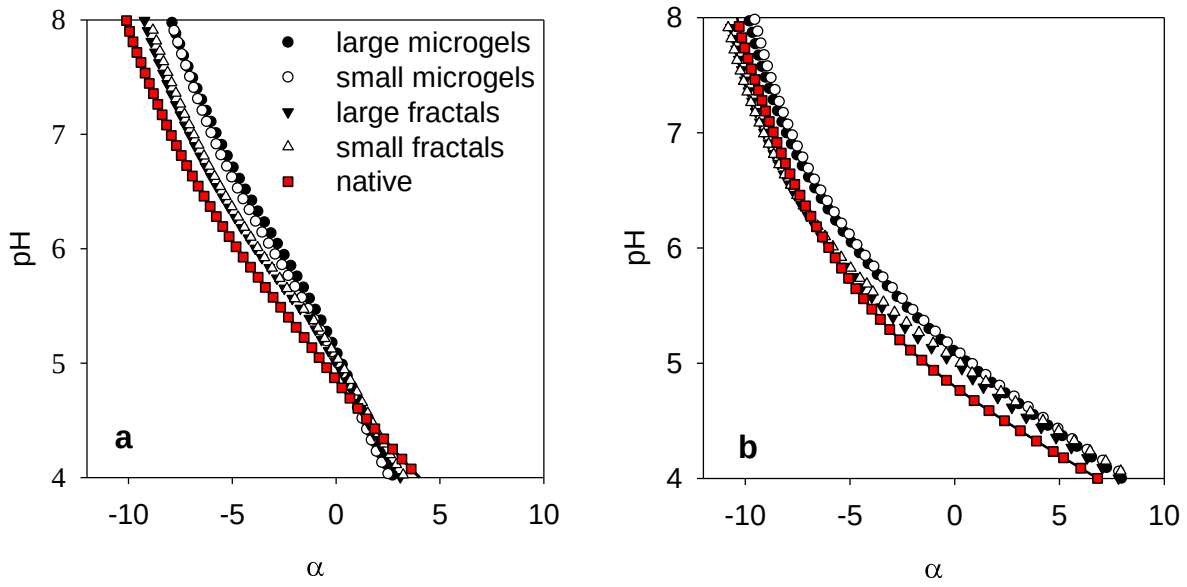

Figure 5. Comparison of the pH as a function of the net charge density for native WPI, fractals (R_h = 35 and 165 nm), and microgels (R_h = 100 and 370 nm) at C = 10 g/L in salt-free solutions (a) or at 0.5 M NaCl (b).

As mentioned in the introduction, similar aggregates are formed by pure β-lg and WPI. In order to check whether the dependence of the pH on α was different for the two protein powders, we compared the dependence for fractal aggregates formed by β-lg and WPI. For both we found that IIP = 5.0 and Fig. 6 shows that the dependence of the pH on α is almost the same both without NaCl and at 0.5 M NaCl.

Schmitt et al. (2009) studied the effect on the ζ-potential after formation of microgels by thermal aggregation of β-lg. They observed that the IEP shifted from 5.0 to 5.3 after aggregation. Morand et al. (2011) found that the IEP of fractal whey protein aggregates was 4.7 in 0.1 M NaCl. It appears as if the difference between the two aggregate morphologies is much larger for the IEP than for the IIP and that for microgels IEP > IIP and for fractal aggregates IEP < IIP. However, the IEP was determined in these studies by measuring the electrophoretic mobility at different pH and interpolation, which is not very accurate. It is quite possible that the differences between the IEP and the IIP are within the experimental error.

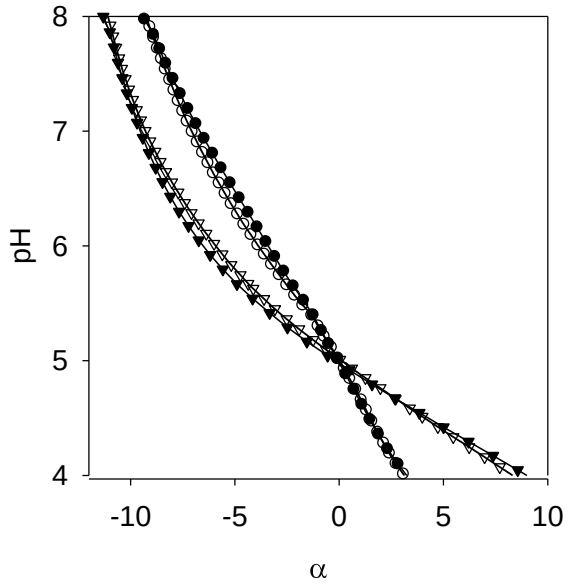

Figure 6. Comparison of the pH as a function of the net charge density for fractal aggregates formed by WPI (filled symbols) and β-lg (open symbols) without NaCl (circles) and with 0.5 M NaCl (triangles). The protein concentration was 10 g/L.

We have seen that α changes when the protein concentration is varied at fixed pH. This can have important implications for the interpretation of experimental results on pH-sensitive protein aggregation at different concentrations done at fixed pH and explains recently reported results on the aggregation of β-lg and of soy globulin. As was mentioned in the introduction, whether heat-denatured β-lg forms strands or microgels depends on the pH. However, in a detailed investigation of this phenomenon at different β-lg concentrations Phan-Xuan et al. (2011) observed that the critical pH at which the transition occurs shifted to higher pH with decreasing protein concentration. The critical pH below which microgels started to be formed shifted from pH 6.5 at C = 10 g/L to pH 6.3 at C = 40 g/L. In view of the results presented here, the shift can be explained by the fact that the transition is controlled not by a critical pH, but by a critical α and the pH at the critical value of α increases with decreasing protein concentration.

Very recently, self-assembly of native soy globulin into fractal aggregates was investigated as a function of the pH and the protein concentration (Chen et al., 2016). Erratic non monotonous concentration dependence was observed if the aggregate size was plotted as a function of the protein concentration at fixed pH. However, when the same results were plotted as a function of α determined in the same manner as was done here, the aggregate size increased in a coherent manner with increasing concentration.

4. Conclusions

At the isoionic points of native WPI (4.9) and native β-lactoglobulin (5.0), the pH is independent of the NaCl concentration up to 0.1 M, but decreases weakly at higher salt concentrations. The pH dependence of the net charge density of native WPI and native β-lg is very close for pH > 5.0. Heat-induced aggregation of WPI and pure β-lg leads to a small increase of the IIP by at most 0.2 pH units in comparison to the native proteins. For pH > IIP, the pH dependence on α is slightly stronger after aggregation so that for a given pH the net charge density of the proteins is smaller after aggregation. The effect of aggregation on the pH is less for fractal aggregates than for microgels, but does not depend on the aggregate size. The effect also decreases when salt is added or the protein concentration is increased. If aggregation processes are sensitive to small changes of α, the effect of the protein concentration and the ionic strength is easier to understand if α is kept constant instead of the pH.

References

Amin, S., Barnett, G.V., Pathak, J.A., Roberts, C.J., Sarangapani, P.S., 2014. Protein aggregation, particle formation, characterization & rheology. Curr. Opin. Colloid Interface Sci. 19, 438–449.

Bryan, W.P., 1978. The isoionic point of amino acids and proteins. Biochem. Educ. 6, 14–15.

Cannan, R.K., 1942. The Acid-Base Titration of Proteins. Chem. Rev. 30, 395–412.

Cannan, R.K., Kibrick, A., Palmer, A.H., 1941. The Amphoteric Properties of Egg Albumin. Ann. N. Y. Acad. Sci. 41, 243–266.

Cannan, R.K., Palmer, A.H., Kibrick, A.C., 1942. The hydrogen ion dissociation curve of β-lactoglobulin. J. Biol. Chem. 142, 803–822.

Chen, N., Zhao, M., Chassenieux, C., Nicolai, T., 2016. Structure of self-assembled native soy globulin in aqueous solution as a function of the concentration and the pH. Food Hydrocoll. 56, 417–424.

Clark, A.H., Kavanagh, G.M., Ross-Murphy, S.B., 2001. Globular protein gelation—theory and experiment. Food Hydrocoll., 5th International Hydrocolloids Conference 15, 383–400.

de Wit, J.N., 1998. Nutritional and Functional Characteristics of Whey Proteins in Food Products. J. Dairy Sci. 81, 597–608.

Donato, L., Schmitt, C., Bovetto, L., Rouvet, M., 2009. Mechanism of formation of stable heat-induced β-lactoglobulin microgels. Int. Dairy J. 19, 295–306.

Fredriksson, S., 1975. Scanning isoelectric focusing in small density-gradient columns: IV. The use of deuterium oxide for preparing the density gradient and its effects on isoelectric points of proteins. J. Chromatogr. A 108, 153–167.

Guyomarc'h, F., Famelart, M.-H., Henry, G., Gulzar, M., Leonil, J., Hamon, P., Bouhallab, S., Croguennec, T., 2015. Current ways to modify the structure of whey proteins for specific functionalities—a review. Dairy Sci. Technol. 95, 795–814.

Kontopidis, G., Holt, C., Sawyer, L., 2004. Invited Review: β-Lactoglobulin: Binding Properties, Structure, and Function. J. Dairy Sci. 87, 785–796.

Krebs, M.R.H., Devlin, G.L., Donald, A.M., 2007. Protein Particulates: Another Generic Form of Protein Aggregation? Biophys. J. 92, 1336–1342.

Langton, M., Hermansson, A.-M., 1992. Fine-stranded and particulate gels of β-lactoglobulin and whey protein at varying pH. Food Hydrocoll. 5, 523–539.

Longsworth, L.G., Jacobsen, C.F., 1949. An Electrophoretic Study of the Binding of Salt Ions by β-Lactoglobulin and Bovine Serum Albumin. J. Phys. Colloid Chem. 53, 126–134.

Mezzenga, R., Fischer, P., 2013. The self-assembly, aggregation and phase transitions of food protein systems in one, two and three dimensions. Rep. Prog. Phys. 76, 046601.

Morand, M., Guyomarc'h, F., Pezennec, S., Famelart, M.-H., 2011. On how κ-casein affects the interactions between the heat-induced whey protein/κ-casein complexes and the casein micelles during the acid gelation of skim milk. Int. Dairy J., IDF Symposium on Science and Technology of Fermented Milk 21, 670–678.

Nicolai, T., Britten, M., Schmitt, C., 2011. β-Lactoglobulin and WPI aggregates: Formation, structure and applications. Food Hydrocoll., 25 years of Advances in Food Hydrocolloid Research 25, 1945–1962.

Nicolai, T., Durand, D., 2013. Controlled food protein aggregation for new functionality. Curr. Opin. Colloid Interface Sci. 18, 249–256.

Nozaki, Y., Bunville, L.G., Tanford, C., 1959. Hydrogen Ion Titration Curves of β-Lactoglobulin1. J. Am. Chem. Soc. 81, 5523–5529.

Phan-Xuan, T., Durand, D., Nicolai, T., Donato, L., Schmitt, C., Bovetto, L., 2011. On the Crucial Importance of the pH for the Formation and Self-Stabilization of Protein Microgels and Strands. Langmuir 27, 15092–15101.

Salis, A., Boström, M., Medda, L., Cugia, F., Barse, B., Parsons, D.F., Ninham, B.W., Monduzzi, M., 2011. Measurements and Theoretical Interpretation of Points of Zero Charge/Potential of BSA Protein. Langmuir 27, 11597–11604.

Schmitt, C., Bovay, C., Vuilliomenet, A.-M., Rouvet, M., Bovetto, L., Barbar, R., Sanchez, C., 2009. Multiscale characterization of individualized β-lactoglobulin microgels formed upon heat treatment under narrow pH range conditions. Langmuir 25, 7899–7909.

Sørensen, S.P.L., Linderstrøm-Lang, K., Lund, E., 1927. The Influence of Salts Upon the Ionisation of Egg Albumin. J. Gen. Physiol. 8, 543–599.

Tanford, C., Wagner, M.L., 1954. Hydrogen Ion Equilibria of Lysozyme1,2. J. Am. Chem. Soc. 76, 3331–3336.

van der Linden, E., Foegeding, E.A., 2009. Gelation: principles, models and applications to proteins, in: Modern Biopolymer Science. Elsevier Burlington, MA, pp. 29–91.

Chapter 5. Calcium-induced gelation of whey protein aggregates: kinetics, structure and rheological properties.

Published as

Kharlamova, A., Nicolai, T. and Chassenieux, C., 2018. Food Hydrocolloids 79, 145-475.

Abstract

Cold gelation of preformed whey protein aggregates was induced by adding $CaCl_2$. The gels were investigated using rheology and confocal laser scanning microscopy in order to study the evolution with time of the elasticity and the microstructure as a function of the protein and calcium concentrations, the size and shape of the aggregates and the temperature. The net charge density of the proteins was fixed, but the effect of adding $CaCl_2$ on the pH was investigated and was related to specific binding of Ca^{2+} to the proteins. The gelation process was correlated with the effective charge density of the proteins that was reduced by specific binding of Ca^{2+} to the proteins. Increasing the temperature or the $CaCl_2$ concentration ($[CaCl_2]$) strongly increased the rate of gelation, but did not influence the stiffness or the structure of the gels. The temperature dependence of the gelation time was characterized by an activation energy of 210 kJ/mol independent of the $CaCl_2$ ($[CaCl_2]$ = 2 – 50 mM) and protein concentrations (C = 5 – 60 g/L). Increasing the protein concentration not only sped up gelation, but also increased the gel stiffness and rendered the gels more homogeneous. The size of fractal aggregates did not influence the gel structure, the gel stiffness and very little the gelation rate. Gelation of fractal aggregates was compared with that of microgels, which formed weaker and more heterogeneous gels at the same protein concentration. It is shown how syneresis can be avoided by a proper choice of $[CaCl_2]$, temperature and aggregate size.

1. Introduction

Globular proteins in aqueous solutions have a compact configuration with the non-polar amino-acids shielded from water within the tertiary structure (Clark & Lee-Tuffnell, 1998). Upon heating, the peptide chains become mobile rendering hydrophobic groups and cysteines accessible. As a result, strong bonds including covalent disulfide bonds can be formed between different protein molecules leading to formation of aggregates of different sizes and morphologies depending on the pH, ionic strength, type of salt and protein concentration (Amin, Barnett, Pathak, Roberts, & Sarangapani, 2014; Cory M. Bryant & McClements, 1998; Chi, Krishnan, Randolph, & Carpenter, 2003; Mezzenga & Fischer, 2013; Nicolai, Britten, & Schmitt, 2011).

Aggregates formed by globular proteins are of particular interest for applications in food products due to their exceptional functional properties, such as formation of gels, thickening properties, stabilization of emulsions and foams, formation of films and encapsulation (Foegeding & Davis, 2011; Nicolai et al., 2011; Nicolai & Durand, 2013; Purwanti, van der Goot, Boom, & Vereijken,

2010). Gelation of globular protein aggregates in aqueous solutions can be induced by reducing the electrostatic repulsion between the aggregates. This process is known as “cold gelation”, because it can occur at room temperature contrary to heat-induced gelation of native globular proteins. Cold gelation is a two-step process, in which a stable solution of protein aggregates is first obtained by heating solutions of native globular proteins at neutral pH and at a low ionic strength. In the second step gelation is induced either by addition of salt (Ako, Nicolai, & Durand, 2010; S. Barbut, 1997; S. Barbut & Foegeding, 1993; Shai Barbut, 1995; Chinchalikar, Kumar, Aswal, Kohlbrecher, & Wagh, 2014; Clare, Lillard, Ramsey, Amato, & Daubert, 2007; Glibowski, Mleko, & Wesolowska-Trojanowska, 2006; B. Hongsprabhas & Barbut, 1997a, 1997b; P. Hongsprabhas & Barbut, 1997; P. Hongsprabhas, Barbut, & Marangoni, 1999; Parichat Hongsprabhas & Barbut, 1996, 1997; Kuhn, Cavallieri, & Da Cunha, 2010; Kundu, Chinchalikar, Das, Aswal, & Kohlbrecher, 2014; Marangoni, Barbut, McGauley, Marcone, & Narine, 2000; Navarra et al., 2009; Wu, Arosio, Podolskaya, Wei, & Morbidelli, 2012; Wu, Xie, & Morbidelli, 2005) or by decreasing the pH (Alting et al., 2004; Alting, de Jongh, Visschers, & Simons, 2002; Alting, Hamer, de Kruif, Paques, & Visschers, 2003; Alting, Hamer, de Kruif, & Visschers, 2000; Britten & Giroux, 2001; Cavallieri, Costa-Netto, Menossi, & Da Cunha, 2007; Cavallieri & Da Cunha, 2008; Donato, Kolodziejcyk, & Rouvet, 2011; Ju & Kilara, 1998b, 1998a; Mleko & Foegeding, 2000; Rabiey & Britten, 2009; Sadeghi, Madadlou, & Yarmand, 2014). The globular protein gels formed by cold gelation have a more homogeneous structure and are more transparent compared to heat-set gels formed by native proteins at the same conditions (Ako et al., 2010; Doi, 1993; Vardhanabhuti, Foegeding, McGuffey, Daubert, & Swaisgood, 2001).

Cold gelation has been reported for different types of globular proteins: β-lg (Ako et al., 2010), BSA (Kundu et al., 2014; Navarra et al., 2009; Wu et al., 2012), ovalbumin (Alting et al., 2004; Doi, 1993), whey protein isolate (C. M. Bryant & McClements, 2000; Glibowski et al., 2006; B. Hongsprabhas & Barbut, 1997a; Parichat Hongsprabhas & Barbut, 1997; Kuhn et al., 2010; Wu et al., 2005), soy protein isolate (Chen, Chassenieux, & Nicolai, 2017; Lu, Lu, Yin, Cheng, & Li, 2010; Maltais, Remondetto, Gonzalez, & Subirade, 2005; Murekatete, Hua, Chamba, Djakpo, & Zhang, 2014). Salt-induced gelation has been studied most often using $CaCl_2$, but the effect of the type of salt has also been investigated (Ako et al., 2010; S. Barbut & Drake, 1997; C. M. Bryant & McClements, 2000; Chinchalikar et al., 2014; Ju & Kilara, 1998b; Kuhn et al., 2010; Kundu et al., 2014; Marangoni et al., 2000; Navarra et al., 2009; G. E. Remondetto, Paquin, & Subirade, 2002; Gabriel E. Remondetto & Subirade, 2003). From these studies it is clear that divalent cations are much more efficient to induce gelation than monovalent cations, because they can bind specifically to the proteins.

It was well-established that using a higher protein concentration or applying more intense preheating leads to faster gelation after addition of salt and to stiffer gels. It was also generally found that faster gelation and stiffer gels can be obtained by adding more salt at least at lower salt concentrations. At higher salt concentrations the reverse has been observed. However, quantitative systematic investigations of how the gelation rate and gel stiffness depend on the size and structure of the aggregates, the salt and protein concentrations, and the temperature for the same type of protein and salt are rare.

Here we report on a systematic investigation of cold gelation induced by addition of $CaCl_2$ to solutions of aggregates formed by preheating whey protein isolate (WPI). WPI consists predominantly of β-lactoglobulin and α-lactalbumin. During heating in dilute aqueous solutions, whey proteins form aggregates with three distinct morphologies depending on the conditions (Jung,

Savin, Pouzot, Schmitt, & Mezzenga, 2008; Nicolai & Durand, 2013). Long rigid fibrillar aggregates are formed between pH 1.5 and pH 2.5 (Adamcik & Mezzenga, 2011; Lara, Gourdin-Bertin, Adamcik, Bolisetty, & Mezzenga, 2012; van der Linden & Venema, 2007), whereas dense spherical particles with radii between 50 nm and 500 nm, called microgels, are formed close to the isoelectric point (Schmitt, Bovay, Rouvet, Shojaei-Rami, & Kolodziejczyk, 2007). At pH > 6.1 small curved strands are formed (Phan-Xuan et al., 2014). At higher protein concentrations strands and microgels further associate into larger aggregates with a self-similar (fractal) structure (Mahmoudi, Mehalebi, Nicolai, Durand, & Riaublanc, 2007; Phan-Xuan et al., 2011). The size of the fractal aggregates obtained at steady state increases with increasing protein concentration and gels are formed above a critical concentration.

The objective of the present study was to investigate in a systematic manner the influence of the size and concentration of the aggregates, the $CaCl_2$ concentration ($[CaCl_2]$) and the temperature on the gelation rate, the structure of the gels and their mechanical properties. The properties of the gels formed by fractal aggregates and microgels were compared. In order to understand the effect of divalent salt it is important to distinguish specific binding that reduces the effective charge density of the aggregates from non-specific screening of electrostatic interactions by ions in solution. The first effect depends on the molar ratio of Ca^{2+} to protein, whereas the second depends on the total free Ca^{2+} concentration. Therefore the effect of adding $CaCl_2$ will be discussed both in terms of $[CaCl_2]$ and the number of Ca^{2+} ions per protein (R). The Ca^{2+} activity was measured in order to determine the fraction of bound and free Ca^{2+} in the aggregate solutions.

2. Materials and Methods

2.1 Materials

2.1.1. Preparation of WPI aggregates

The WPI powder used for this study was purchased from Lactalis (Laval, France). It contained 89 wt% protein, 6 wt% moisture, < 0.4 wt% fat, < 4 wt% lactose, and 2.0 wt% ash, including 0.25 wt% calcium. Size exclusion chromatography showed that the proteins consisted of 70 % β-lg and 20 % α-lac, the remaining being other whey proteins and caseins. The powder was dissolved by stirring during 4–6 hours in Milli-Q water containing 200 ppm of sodium azide as an antimicrobial preservative. The solution was filtered two times through 0.45 µm and 0.2 µm syringe filters (Acrodisc®). The protein concentration of stock solutions obtained this way (C ≈ 13.5 wt%) was determined by UV absorption at 278 nm using extinction coefficient of 1.05 L g^{-1} cm^{-1}. The net charge density of the protein molecules (α) in the stock solution before pH adjustment was –6.7 as determined by potentiometric titration (see Chapter 4).

For preparation of stable solutions of WPI aggregates the pH of the stock solution was adjusted from 6.3 to 7.0 by addition of 2 mol NaOH per mol WPI, which means that the net negative charge density was increased from α = –6.7 to α = –8.7. Subsequently, the stock solution was diluted to the required protein concentration, hermetically closed in glass bottles and heated for 24 hours at 80 °C. It has been shown before that these heating conditions ensure denaturation and aggregation of practically all native proteins of WPI even at low protein and salt concentrations (Mahmoudi et al.,

2007). We note that these long heating times are only necessary to complete the reaction at low protein concentrations and in the absence of salt. Once all native proteins have reacted the growth of aggregates is arrested and no further changes in the aggregate size or structure were observed for the duration of the heating process. The z-average hydrodynamic radius (R_h) of the aggregates was determined using dynamic light scattering as described in Mahmoudi et al. (2007). Aggregates of different sizes were prepared by heating solutions at different protein concentrations: R_h = 35, 77, 115 or 170, and > 500 nm at C = 62, 80, 90 and 93 g/L, respectively. The difference in size of the two batches of aggregates formed at 90 and 93 g/L is explained by the steep dependency of the aggregate size on protein concentration close to the gel concentration (C_g = 100 g/L) (Inthavong, Kharlamova, Chassenieux, & Nicolai, 2016). R_h of the largest aggregates could not be determined as the measured value depended on scattering wave vector over the whole accessible range implying that the radius was larger than 500 nm. After heating, the pH had not changed significantly, but titration of the aggregates showed that formation of aggregates at these conditions led to a small reduction of the net charge density to α = –8.0 (see Chapter 4). Aggregate solutions were stored in the fridge before use.

Microgels with R_h = 140 nm and 370 nm were prepared by heating WPI solutions at C = 40 g/L at pH 6.1 and at pH 5.8, respectively. From the amount of HCl added to the WPI solution we calculated that after pH adjustment α = –6.3 and –5.2, respectively. During heating the pH increased to 6.4 and 6.1, respectively. Titration showed that after heating the negative net charge density had decreased to α = –4.9 and –3.8, respectively (see Chapter 4). The rate of conversion to microgels was determined by centrifugation as described in Phan-Xuan et al. (2011) and was found to be approximately 85 %. In order to compare the behavior of microgels with that of fractal aggregates, NaOH was added to the microgel suspensions so that α was the same, without considering, however, the effect of aggregation on α. The effect on α caused by aggregation was slightly stronger for microgels than for fractals resulting in α = –7.3 and –6.9 for small and large microgels, respectively, to be compared with α = –8 for the fractal aggregates.

2.1.2. Preparation of gels

Solutions of $CaCl_2$ ([$CaCl_2$] = 0.1 M or 1 M) were prepared from $CaCl_2$ powder purchased from Sigma. The required amount of a $CaCl_2$ solution diluted in Millipore water was added to an aggregate solution under constant agitation keeping the temperature of the solution below 10 °C. Subsequently the solutions were heated inducing gelation.

2.2. Titration with calcium chloride

The change of pH with addition of $CaCl_2$ was measured at 20 °C using an automatic titrator (TIM 856, Radiometer Analytical) equipped with a combined pH electrode and a thermoprobe. The electrode was calibrated by three-point calibration in the pH range between 4 and 10. A freshly prepared solution of $CaCl_2$ at a molar concentration [$CaCl_2$] = 1 M was slowly added to 30 mL of aggregate solutions at different protein concentrations under constant agitation. The speed of addition was varied between 0.01 and 0.08 mL/min depending on the protein concentration. The pH was automatically recorded during the addition. The measurements were conducted at room temperature.

2.3. Calcium activity measurements

The calcium activity measurements were performed at 20 °C using ELIT solid state ion selective electrode (Nico2000 Ltd.) complemented with a conventional reference electrode. The calibration curve was obtained by measuring the potential (in mV) of four standard solutions of $CaCl_2$ in the concentration range 10^{-4} – 10^{-1} M. The Ca^{2+} activity of WPI aggregate solutions at C = 20 g/L with different $CaCl_2$ concentrations was measured immediately after the calibration. The measurement of the series of samples was repeated three times. A stable value of the potential was obtained after placing the electrodes in the studied solution for 5 minutes. The free calcium concentration ($[Ca^{2+}]_f$) in the solution was deduced from the calibration curve. The number of bound calcium ions per protein (R_b) was calculated by subtracting $[Ca^{2+}]_f$ from the total calcium concentration in the system and dividing by the molar concentration of protein molecules in the solution considering an average molar mass of 1.75×10^4 g/mol for WPI. In the calculation of R_b we took into consideration the calcium present in the protein powder that contained 7 mM of Ca^{2+} per 100 g of protein, i.e. 1.2 Ca^{2+} per protein molecule.

2.4. Rheological measurement

Oscillatory shear measurements were performed with two stress imposed rheometers (AR2000 and ARG2, TA Instruments) using a cone-plate geometry (d = 40 mm) with a Peltier system used for the temperature control. The aggregate solutions were placed on the geometry immediately after addition of $CaCl_2$ and covered with mineral oil. All the measurements were conducted in the linear response regime at 0.1 Hz, except for the oscillatory strain sweep measurements performed at 1 Hz up to fracture.

2.5. Confocal laser scanning microscopy (CLSM)

WPI aggregates were labeled by adding a small amount of rhodamine B (5 ppm) and the solutions were hermetically sealed in cavity slides. The slides were heated on a rack in a water bath after which the microstructure was inspected at 20 °C with a Leica TCS-SP2 microscope (Leica Microsystems Heidelberg, Germany) using two water immersion objectives; HC × PL APO 63 × NA = 1.2 and HC × PL APO 20 × NA = 0.7.

3. Results

In the following we show results obtained for $CaCl_2$ induced gelation of fractal aggregates formed by heating native WPI at pH 7. A brief comparison with $CaCl_2$ induced gelation of microgels will be presented in section 3.8.

3.1 Specific binding of Ca^{2+} and the effect on the pH

We studied binding of Ca^{2+} to native and aggregated WPI in aqueous solution by measuring the calcium ion activity in solutions at C = 20 g/L as a function of $[CaCl_2]$ up to 10 mM as described in the Materials and Methods. Fig. 1 compares the number of bound Ca^{2+} per protein (R_b) as a function of $[Ca^{2+}]_f$ between native WPI and aggregates. Aggregated WPI binds approximately 3 Ca^{2+} per

protein in excess $CaCl_2$, while native protein binds about 2 Ca^{2+} per protein, implying that denatured protein has more Ca^{2+} binding sites. Notice that the WPI powder already contained 1.2 Ca^{2+} per protein which we considered in the calculation of R_b. Saturation was reached when $[Ca^{2+}]_f$ is larger than about 3 mM.

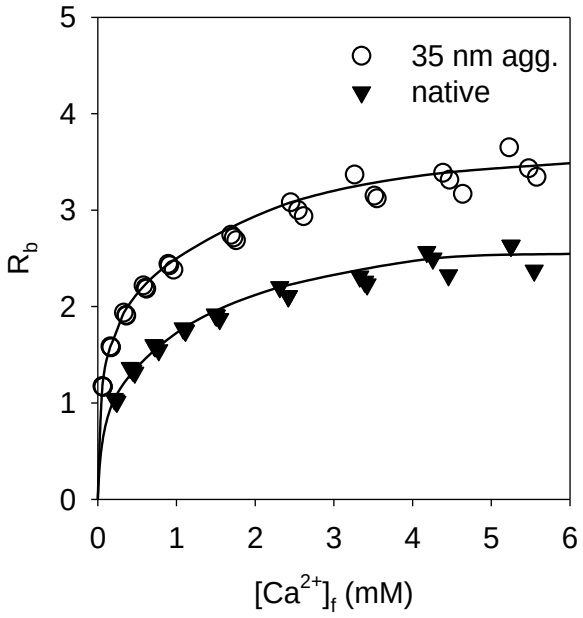

Figure 1. Number of bound calcium ions per protein (R_b) as a function of the free Ca^{2+} concentration for solutions of native WPI and WPI aggregates (R_h = 35 nm) at C = 20 g/L. The lines are guides to the eye.

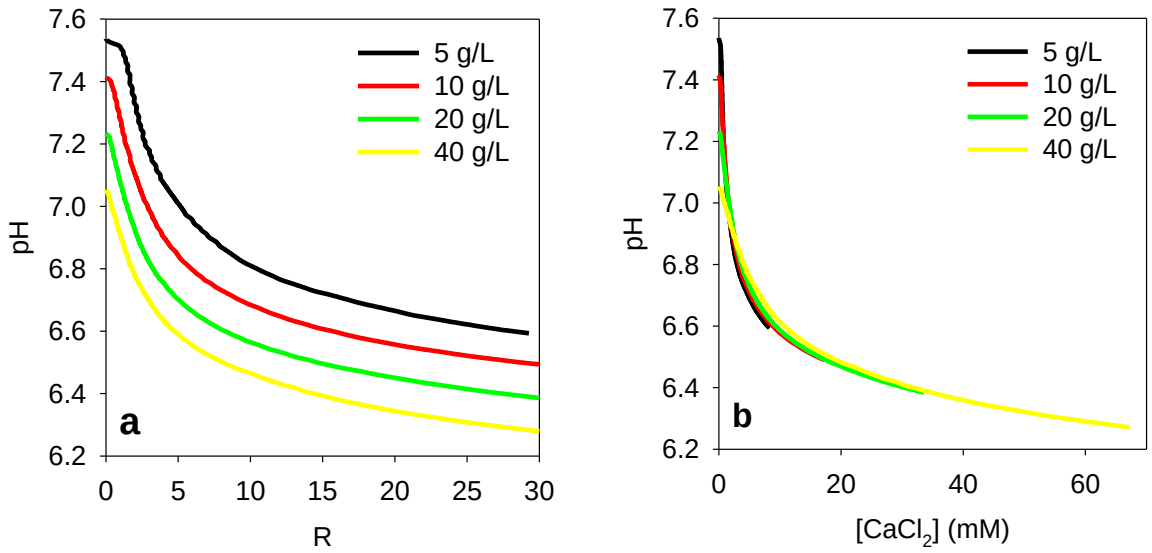

Figure 2. Change of the pH of solutions of aggregates (R_h = 35 nm) as a function of R (a) or [$CaCl_2$] (b). The protein concentrations are indicated in the figure.

Addition of $CaCl_2$ (and salts in general) to solutions of proteins leads to a decrease of the pH caused by the interaction of proteins with ions (Tanford & Nozaki, 1959). The change of the pH with $CaCl_2$ addition to solutions of WPI aggregates was investigated by titration measurements as explained in the Materials and Methods. Solutions of aggregates with R_h = 35 nm at different concentrations between 5 and 40 g/L were titrated with 1 M $CaCl_2$. The change of the pH of solutions as a function of [$CaCl_2$] is presented in Fig. 2.

Fig. 2a shows the pH as a function of R. The pH of the solutions before salt addition decreased with increasing aggregate concentration, which is caused by the increase of concentration of counterions that screen electrostatic interactions between charged groups on the protein (Kharlamova et al., 2016; Salis et al., 2011). The initial steep decrease of the pH with increasing R is caused by binding of calcium ions to specific sites of the proteins driving release of protons to the solution. The more gradual decrease at higher R, when all Ca^{2+} binding sites are saturated, is caused by screening of the electrostatic interactions and depends on the concentration of free ions independent of the protein concentration. At larger [$CaCl_2$] the fraction of bound Ca^{2+} is negligible and the pH depends on [$CaCl_2$] independently of the protein concentration, see Fig. 2b. We verified that the pH change with addition of $CaCl_2$ was the same for aggregates with R_h = 35, 77 and 170 nm (see Fig. 3).

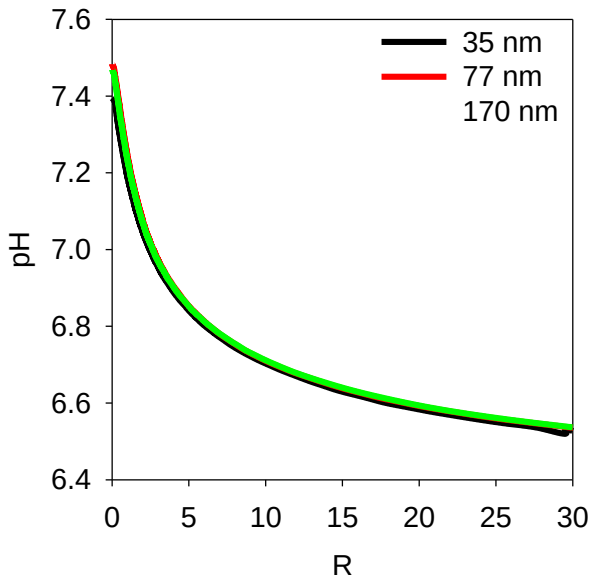

Figure 3. Change of the pH of 10 g/L solutions of aggregates of three sizes indicated in the figure with addition of calcium. The concentration of calcium is presented in terms of added R - the molar ratio between Ca^{2+} ions and protein molecules.

It is important to realize that even though the pH decrease was significant, the amount of H^+ released per protein molecule was negligible and therefore that addition of $CaCl_2$ did not lead to a significant change of the degree of protonation of the proteins. It is a common practice in studies to readjust the pH of protein solutions to a fixed value after addition of salt or to use a buffer, which modifies α. For the current investigation we did not do this and kept α constant so that the effect of adding $CaCl_2$ on aggregation was not confounded with the effect of varying α. As mentioned above, α = –8.7 and –8.0 for the native WPI and the fractal aggregates, respectively. At saturation binding of

calcium ions leads to the reduction of the effective net charge density to –4.7 for native WPI (after binding 2 Ca^{2+}) and to –2.0 for WPI aggregates (after binding 3 Ca^{2+}). We stress that the effective charge density depends on R and should not be confused with α that is practically independent of R. Figure 4 shows a schematic representation of protein aggregates with positively and negatively charged groups in water and after addition of a small amount of $CaCl_2$, an excess of $CaCl_2$ or HCl.

	water	+ $CaCl_2$ (R = 1)	+ $CaCl_2$ (R = 7)	+ HCl
Na^+ Cl^- Ca^{2+} H^+	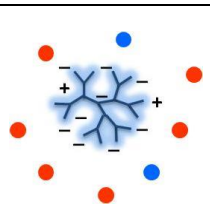	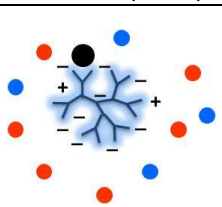	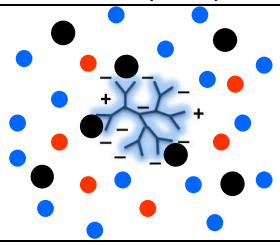	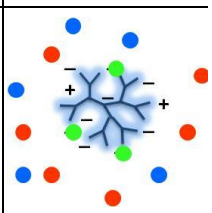
net charge density	**–8**	**–8**	**–8**	**–5**
effective charge density	**–8**	**–6**	**–2**	**–5**
screening	**+**	**+**	**+++**	**+**

Figure 4. Schematic representation of fractal aggregates in water and after addition of a small amount of $CaCl_2$, an excess of $CaCl_2$ or HCl. In water only counterions contribute to screening of electrostatic interactions. In little $CaCl_2$ all Ca^{2+} is bound to the proteins and reduces the effective charge density without influencing significantly the net charge density nor the screening. In excess $CaCl_2$ the proteins are saturated with bound Ca^{2+} that does not change the net charge density, but excess salt increases screening. After addition of HCl the net charge density and therefore the effective charge density are reduced by protonation without influencing the effect of screening significantly.

3.2 Sol-gel state diagrams

In first instance, gelation of WPI aggregates with R_h = 77 nm was studied by heating solutions at different protein concentrations (5 – 60 g/L) and R (0 – 24) for 15 min at 80 °C. Before heating, the solutions stayed liquid at C = 10 g/L at least up to R = 24 ([$CaCl_2$] = 14 mM), whereas at C = 20 g/L there was a steep increase of the viscosity at approximately R = 12 and flocculation of proteins was visible at R ≥ 18 ([$CaCl_2$] ≥ 20 mM). At C = 40 g/L the viscosity of the solution increased at R = 10 and the system gelled within a few hours at room temperature at R ≥ 13 ([$CaCl_2$] ≥ 30 mM). Finally, at C = 60 g/L the viscosity increased already at R = 2 and the system gelled within a few hours at room temperature at R ≥ 7 ([$CaCl_2$] ≥ 24 mM). At all concentrations, the samples were transparent at low calcium concentrations, but became turbid at higher R.

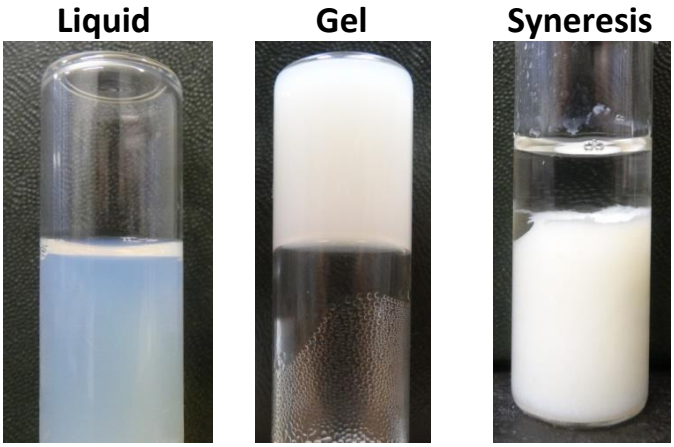

Figure 5. Pictures of liquid, gelled and syneresed systems of aggregates with calcium formed after heating for 15 minutes at 80 °C.

After heating, three different states were distinguished: a liquid that flowed when tilted, a homogeneous gel that did not flow when tilted to 45° or a gel undergoing syneresis. Some samples at low protein concentrations (5 – 10 g/L) formed very weak gels that broke on turning the vials by 90°. Photos of the heated systems illustrating the three different states are shown in Fig. 5. The extent of syneresis was measured by carefully removing the expelled water with a paper towel and dividing the mass of removed water by the initial mass of the sample. If the amount of expelled water exceeded 5 wt%, the system was considered undergoing syneresis. The liquid-gel state diagram obtained for aggregates with R_h = 77 nm is shown in Fig. 6a in terms of R and in terms of [$CaCl_2$] in Fig. 6b.

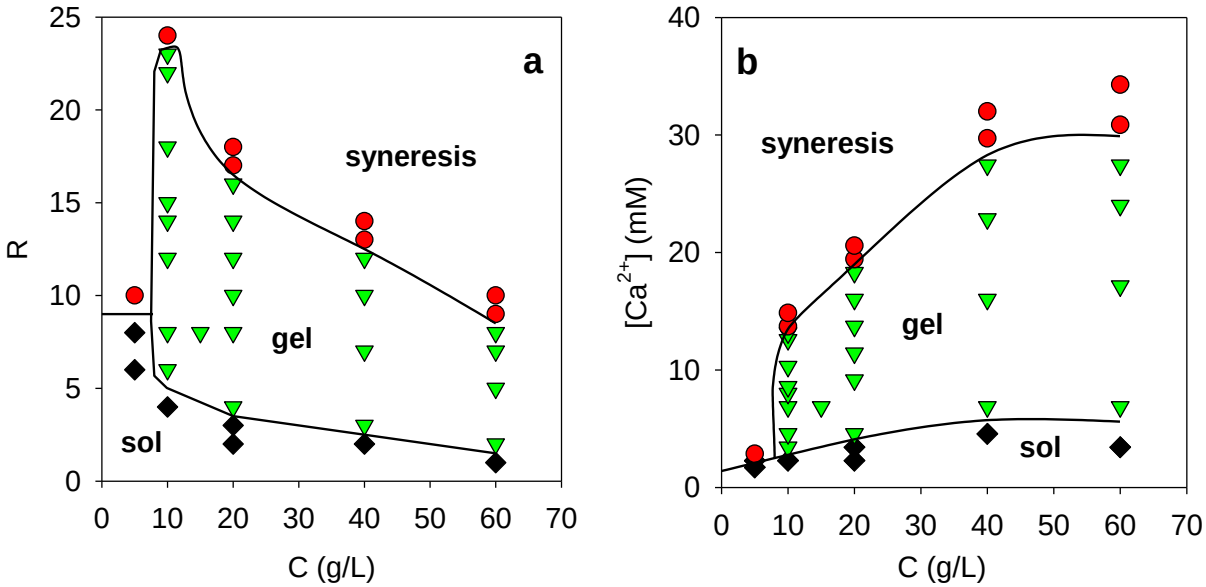

Figure 6. Sol-gel state diagram as function of the concentration of aggregates (R_h = 77 nm) and R (a) or [$CaCl_2$] (b) for solutions heated for 15 minutes at 80 °C. Black diamonds indicate systems that stayed liquid, green triangles indicate homogeneous gels and red circles indicate systems undergoing syneresis.

The sol-gel transition occurred at relatively small values of R that decreased with increasing protein concentration. The gelation was mainly induced by a decrease of the effective negative charge density of the proteins due to specific binding of Ca^{2+}. This explains why more $CaCl_2$ was needed to induce gelation at these conditions at larger protein concentrations. Syneresis occurred at relatively large values of R where the Ca^{2+} binding sites were saturated and was therefore caused by screening of electrostatic interactions. Syneresis occurred at larger [$CaCl_2$] for more densely crosslinked gels formed at larger protein concentrations. At very low aggregate concentrations (C < 10 g/L) it was not possible to form a self-supporting gel at these heating conditions. The solutions at larger R either formed very weak gels with strong syneresis or macroscopically flocculated suspensions.

It is important to realize that the solutions had not reached steady state after heating for 15 min at 80 °C, but continued to evolve. The state diagram, therefore, strongly depends on the heating time and temperature. An increase of the heating time resulted in a downward shift of both sol-gel and gel-syneresis borders (results not shown).

We studied the influence of the aggregate size on the state diagram by repeating the measurements with smaller aggregates (R_h = 35 nm) and much larger aggregates (R_h > 500 nm). The comparison of the state diagrams for aggregates of three sizes is presented in Fig. 7 in terms of R (Fig. 7a) and [$CaCl_2$] (Fig. 7b). The sol-gel transition was at the same R for aggregates with R_h = 35nm and R_h = 77 nm, but at slightly smaller R for the largest aggregates. The effect of aggregate size on the appearance of syneresis was much more important as it shifted to significantly higher [$CaCl_2$] for smaller aggregates. As a consequence, it was possible to form gels at lower protein concentrations with smaller aggregates.

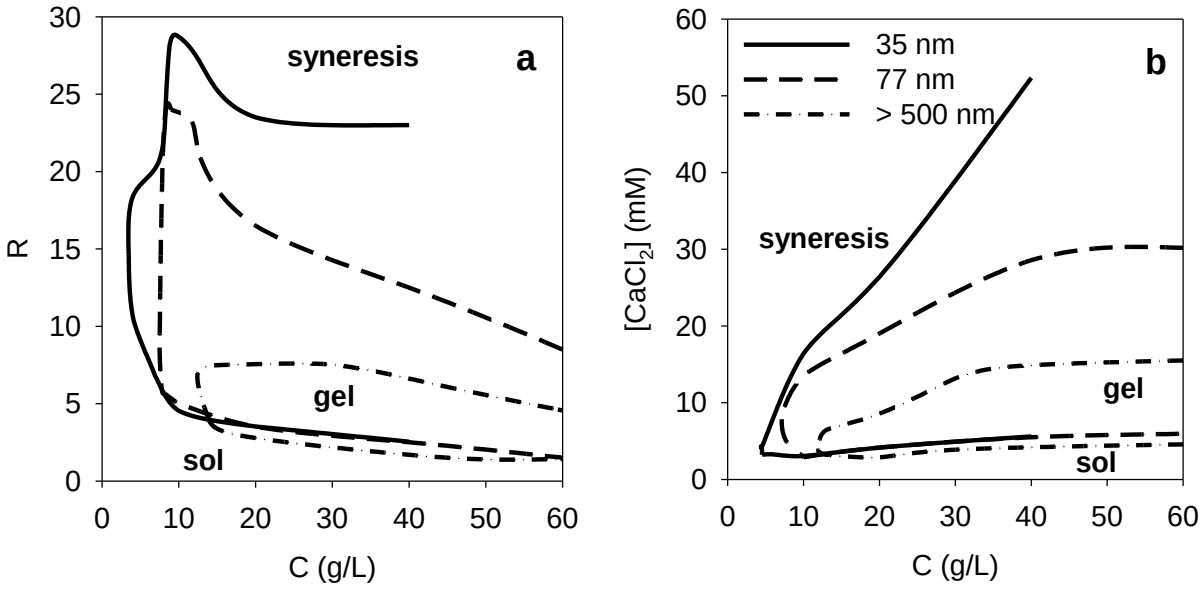

Figure 7. State diagrams obtained for solutions of WPI aggregates with three different R_h indicated in the figure as function of C and R (a) or [$CaCl_2$] (b) after heating for 15 minutes at 80 °C.

3.3 Influence of heating temperature and duration

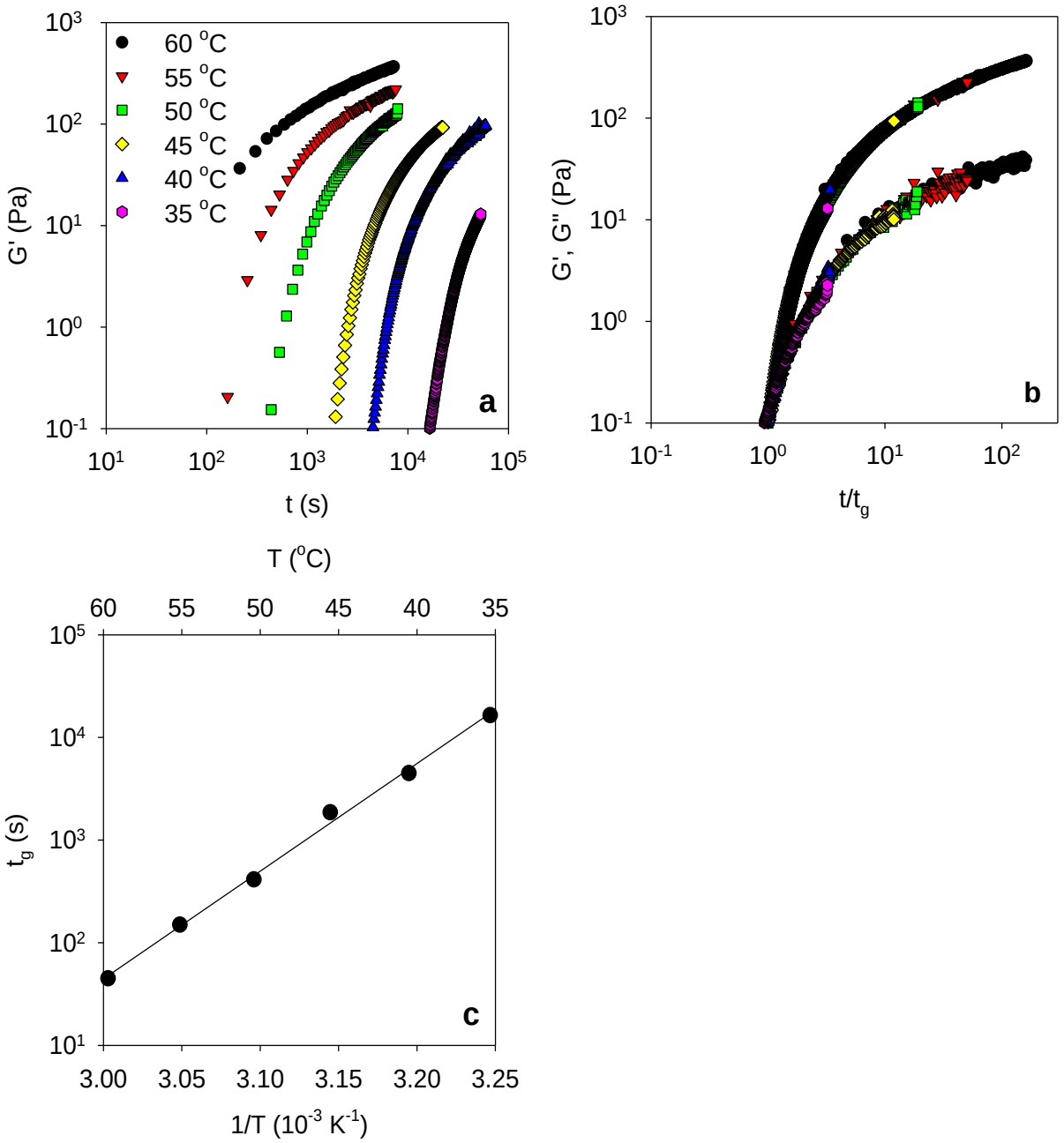

Figure 8. (a) Evolution with heating time of G' at 0.1 Hz at different temperatures for solution of WPI aggregates (R_h = 35 nm) at C = 40 g/L and R = 4 ([$CaCl_2$] = 9 mM). (b) The same data as in Fig. 8a normalized by the gel time. (c) Arrhenius representation of the temperature dependence of the gel time.

The influence of the heating time and temperature on the gelation process was studied by measuring the shear moduli of aggregate solutions after addition of $CaCl_2$ during heating at different temperatures. The temperature was raised from 20 °C to the required value within one minute. Fig. 8a shows the evolution of the storage modulus (G') with time at different temperatures for solutions of aggregates with R_h = 35 nm at C = 40 g/L and R = 4 ([$CaCl_2$] = 9 mM).

Decreasing the temperature slowed down the gelation process. However, it was possible to superimpose the curves obtained at different temperatures by normalizing the time of heating by the gel time (t_g) defined here as the time required to reach G' = 0.1 Pa, see Fig. 8b. The implication is that temperature influences only the gelation rate, but not the gel stiffness. Notice that G' rises very steeply close to t_g, which means that t_g is not sensitive to the choice of G' at which we consider that a gel is formed. The loss moduli also superimposed when the time of heating was normalized by t_g and became much smaller than G' at prolonged heating, see Fig. 8b. The frequency dependence of G' and G" was weak for the gels (not shown). The temperature dependence of t_g is linear in the Arrhenius representation and from the slope we found E_a = 200 kJ/mol, see Fig. 8c.

3.4 Influence of the Ca^{2+} concentration

The measurements were repeated at C = 40 g/L for different [$CaCl_2$] between 5.7 and 18 mM corresponding to R between 2.5 and 8. The range of R that could be explored was limited at low R by too slow gelation at 80 °C and at large R by too fast gelation at room temperature. In each case master curves at reference temperature T_{ref} = 40 °C could be obtained by time-temperature superposition using only horizontal shift factors (a_T), see Fig. 9a. Shift factors at different [$CaCl_2$] were close, see Fig. 10, implying that the activation energy did not depend on the salt concentration. Combining the results at all [$CaCl_2$] we found E_a = 210 ± 10 kJ/mol. Gelation at R = 2.5 and R = 3 was very slow and could not be determined experimentally at 40 °C. Therefore the results obtained at higher temperatures for these samples were shifted to T_{ref} = 40 °C using shift factors found at larger R. Interestingly, master curves obtained at different R were close when plotted as a function of t/t_g, see Fig. 9b, implying that though [$CaCl_2$] strongly influenced the speed of gelation it did not influence much the stiffness of the gels.

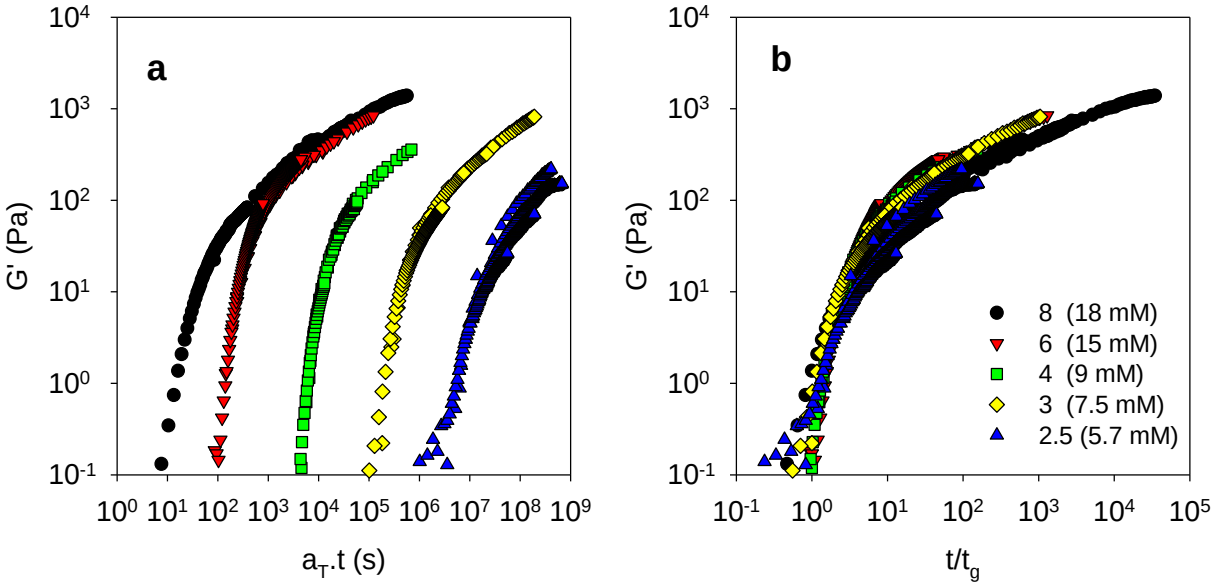

Figure 9. (a). Master curves G' at 0.1 Hz vs time for solutions of WPI aggregates (R_h = 35 nm, C = 40 g/L) at different R ([$CaCl_2$]) obtained by time-temperature superposition at T_{ref} = 40 °C. (b). The same data as in Fig. 9a as a function of t/t_g.

In Fig. 11 the temperature dependence of t_g at different R is shown in the Arrhenius representation demonstrating the strong increase of the gelation time with decreasing R. The strong dependence of the kinetics on [$CaCl_2$] rendered it impossible to determine t_g experimentally over a broad range of R. However, the fact that the activation energy does not depend on [$CaCl_2$] allows one to predict t_g for aggregate solutions at low R or low temperatures that evolve extremely slowly by utilizing the results obtained at higher temperatures. Fig. 12 shows predicted values of t_g as a function of R and [$CaCl_2$] at different temperatures for solutions of aggregates with R_h = 35 nm at C = 40 g/L. The increase of t_g with decreasing R was approximately exponential between R = 8 and 4, but became stronger for R < 3. The latter may indicate that there is a critical value of R below 2 that is needed to induce gelation. Indeed no gelation was observed for R = 1 when heating overnight at 80 °C.

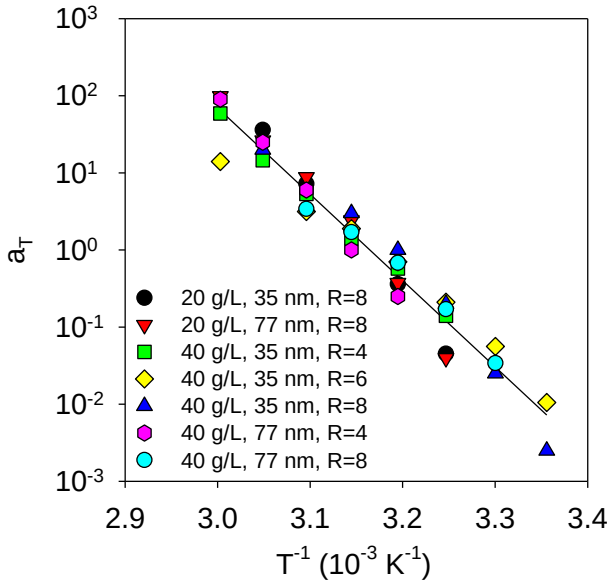

Figure 10. Arrhenius representation of the characteristic shift factors of gelation curves obtained for systems indicated in the figure (protein content, aggregate size, calcium ratio). The solid line represents a linear least-squares fit to the data.

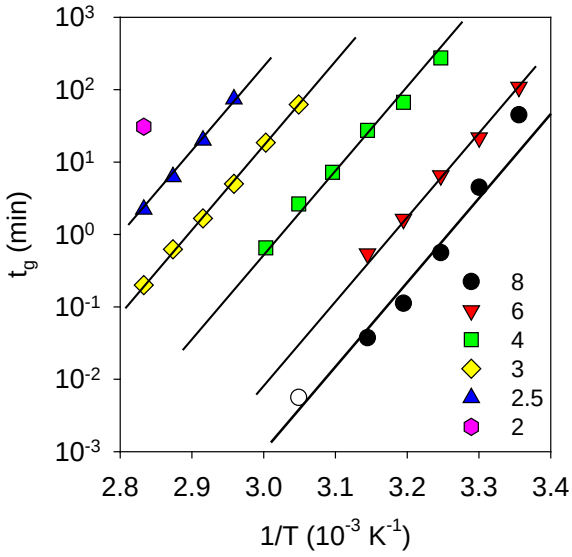

Figure 11. Arrhenius representation of the temperature dependence of the gel time for WPI aggregate solutions (C = 40 g/L, R_h = 35 nm) at different R. The straight lines correspond to E_a = 210 kJ/mol.

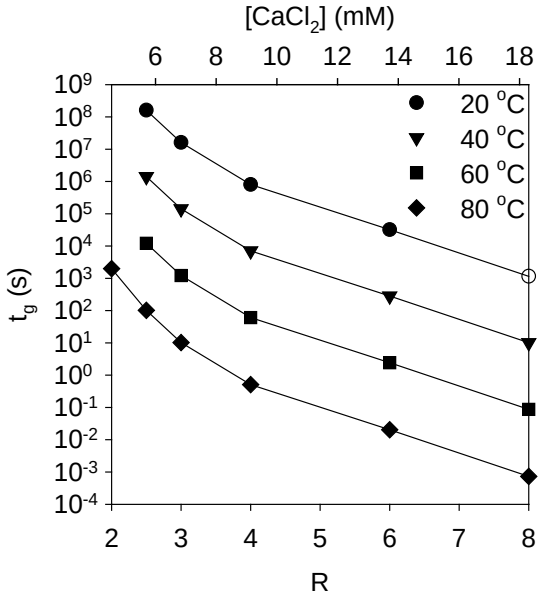

Figure 12. Predicted dependence of the gelation time on R and $[CaCl]_2$ at different temperatures for solutions of WPI aggregates with R_h = 35 nm at C = 40 g/L.

3.5 Influence of the protein concentration

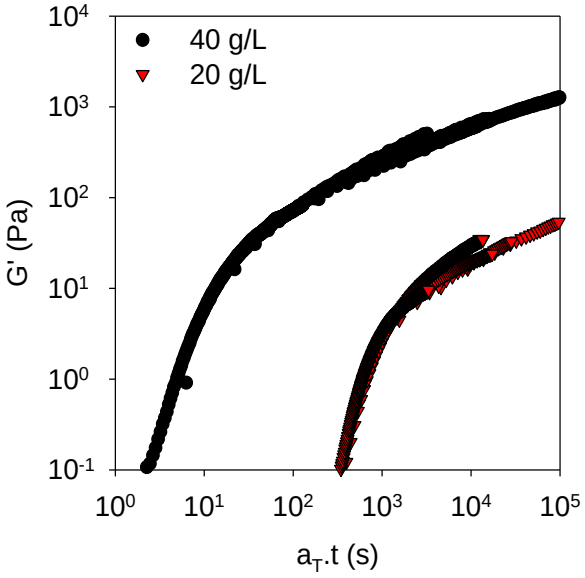

Figure 13. Master curves of G' at 0.1 Hz vs time for solutions of WPI aggregates (R_h = 35 nm) at R = 8 and two protein concentrations indicated in the figure obtained by time-temperature superposition at T_{ref} = 45 °C.

Fig. 13 shows master curves of the heating time dependence of G' for solutions of aggregates with R_h = 35 nm at R = 8 for two protein concentrations: C = 20 g/L and 40 g/L. The temperature dependence of the shift factors was found to be the same (see Fig. 10) implying that the activation energy does not depend on the protein concentration. The comparison shows that there is a strong influence of C on both the gelation rate and the stiffness of the gels as an increase of C from 20 to 40 g/L led to an increase of G' by more than one order of magnitude. The difference is not caused by different [$CaCl_2$] (9 mM at C = 20 g/L and 18 mM at C = 40 g/L), because we showed above that G' did not depend on [$CaCl_2$].

To quantify the influence of the protein concentration on the stiffness of the gels in more detail, solutions with aggregate concentrations between 7 and 60 g/L at R = 6 were heated at 80 °C, see Fig. 14a. The gelation rate increased with increasing protein concentration and at higher concentrations gelation occurred during the increase of the temperature. The steep initial increase of G' with time caused by the formation of the network was followed by a weak increase due to slow reinforcement of the bonds.

After heating for 1 hour the systems were cooled to 20 °C and the frequency dependency was measured between 10 and 0.01 Hz. The elastic modulus increased after cooling by about a factor 3, probably caused by strengthening of hydrogen bonds. The values of G’ at 0.1 Hz as a function of the protein concentration are plotted in Fig. 14b. The strong increase of G' with increasing protein concentration can be approximated by a power law dependence for C ≥ 20 g/L: $G' \propto C^3$. At lower concentrations G' decreased more steeply with decreasing C and below 7 g/L the gels collapsed under their own weight. Here we fixed R = 6, which means that [$CaCl_2$] increased with increasing C from 3.5 to 21 mM between 10 and 60 g/L. However, considering that G' was found to be

independent of [$CaCl_2$] in this explored range it is not important if R or [$CaCl_2$] is fixed. The value or R = 6 was chosen to ensure fast gelation without syneresis.

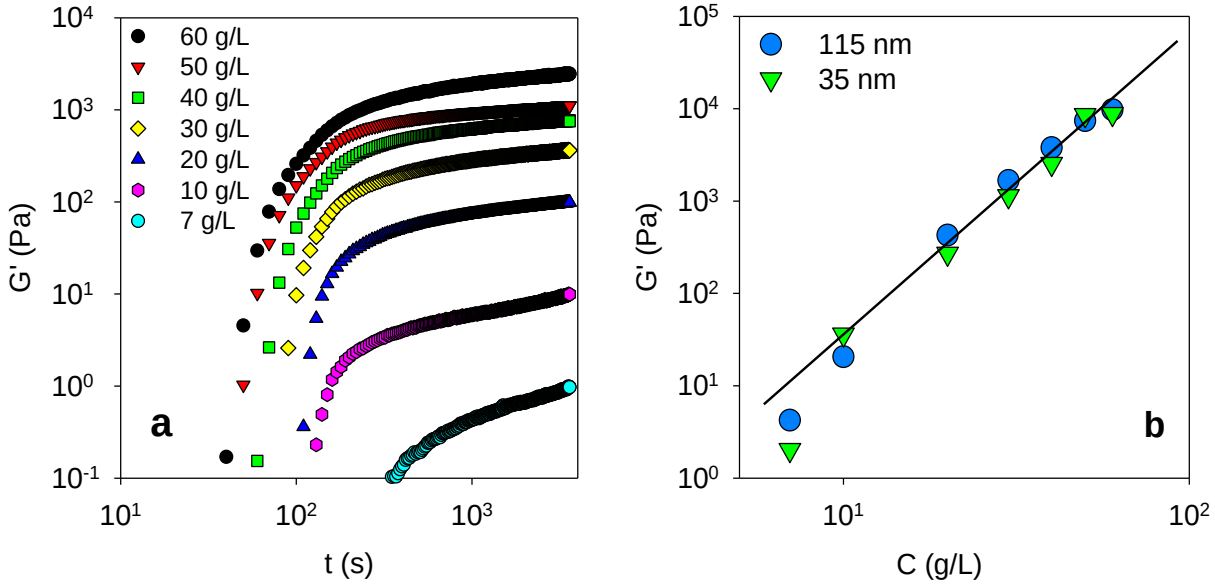

Figure 14. (a) Evolution of the storage shear modulus with heating time at 80 °C for solutions of WPI aggregates (R_h = 35 nm, R = 6) at different protein concentrations indicated in the figure. (b) Dependence of the elastic modulus at 0.1 Hz of gels formed after heating for 1 h at 80 °C and cooling to 20 °C. The straight line has slope 3.

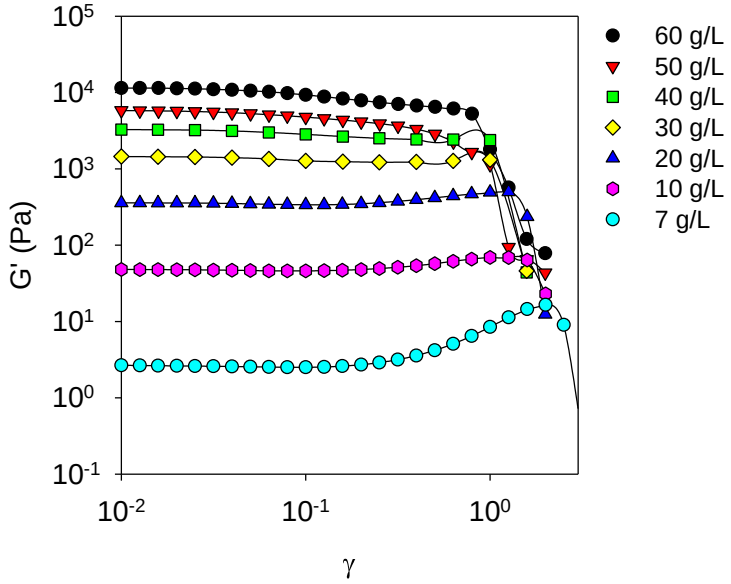

Figure 15. Strain dependence of the storage shear moduli at 1 Hz for gels formed by heating solutions of 35 nm aggregates at concentrations indicated in the figure and R = 6 for 1 hour at 80 °C and cooling them to 20 °C.

We also measured G' as a function of the applied strain, see Fig. 15. It shows that the gels break at a critical strain (γ_b) that decreased weakly with increasing concentration between 2 at C = 7 g/L and 1 at C = 60 g/L. As a consequence the stress at breakage (σ_b) increased strongly since $\sigma_b = \gamma_b$

× G'. For weak gels (G' < 10^3 Pa) shear hardening was observed before breakage. These results were very similar to those reported for gels formed by heating native β-lg solutions with 0.1 M NaCl (Pouzot, Nicolai, Benyahia, & Durand, 2006), which is another indication that the elementary structure of heat-set gels of native globular proteins is the same as that of salt induced gels of protein aggregates. We refer to Pouzot et al. (2006) for an in depth discussion of the non-linear properties of these gels.

3.6 Effect of the size of the aggregates

The effect of the aggregate size on the state diagram of the heated solutions has been discussed above. The effect of the aggregate size on the mechanical properties of the gels was studied by comparing gelation of aggregates with R_h = 115 nm at concentrations between 7 and 60 g/L at R = 6 with results described in section 3.5 for smaller aggregates. The evolution of G' at 80 °C for solutions of the aggregates is compared in Fig. 16. It shows that the gelation rate is only slightly faster for the larger aggregates. The concentration dependence of G' for gels obtained after heating for 1 h and cooling to 20 °C is compared with that of gels formed by smaller aggregates in Fig. 14b. It shows that the size of the aggregates did not significantly influence the gel stiffness.

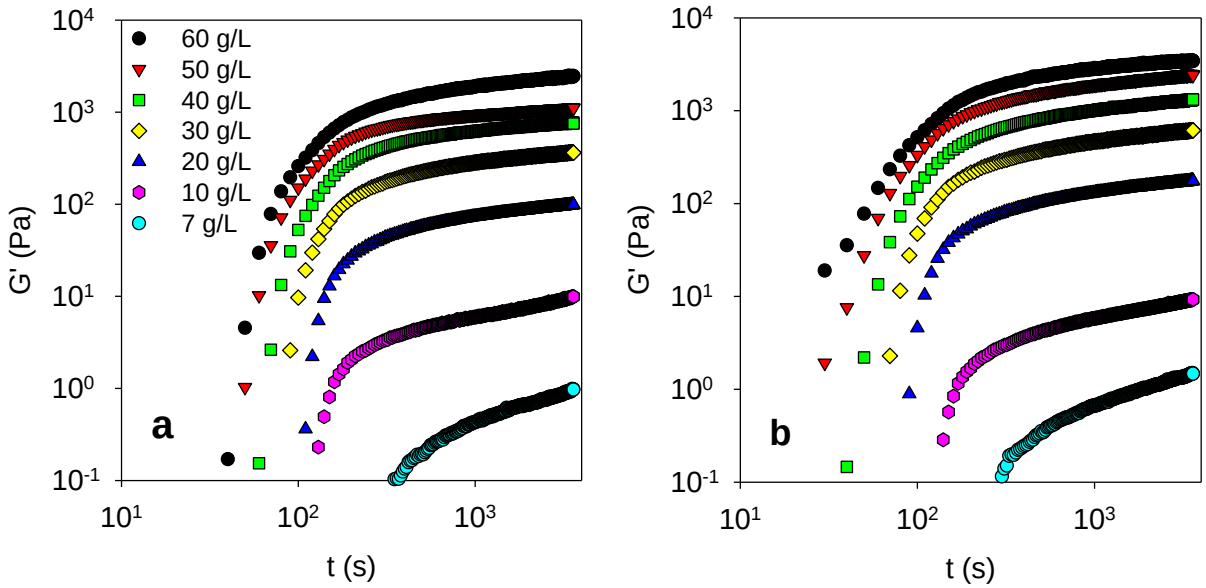

Figure 16. Evolution of the storage shear modulus with heating time at 80 °C for systems with calcium at molar ratio R = 6 and different concentrations of 35 nm (a) and 115 nm (b) aggregates. The aggregate concentrations are indicated in the figure.

3.7 Structure of the gels

The evolution of the microstructure during gelation was probed using CLSM. Before heating solutions of aggregates with calcium appeared homogeneous on length scales accessible to CLSM, i.e. larger than about 0.1 µm, but the systems became microscopically heterogeneous at a critical R that decreased with increasing aggregate concentration and increasing aggregate size. For instance,

systems with aggregates with R_h = 35 nm became microscopically heterogeneous before heating at R = 16 (18.3 mM) at C = 20 g/L and at R = 13 (30 mM) at C = 40 g/L, see Fig. 17.

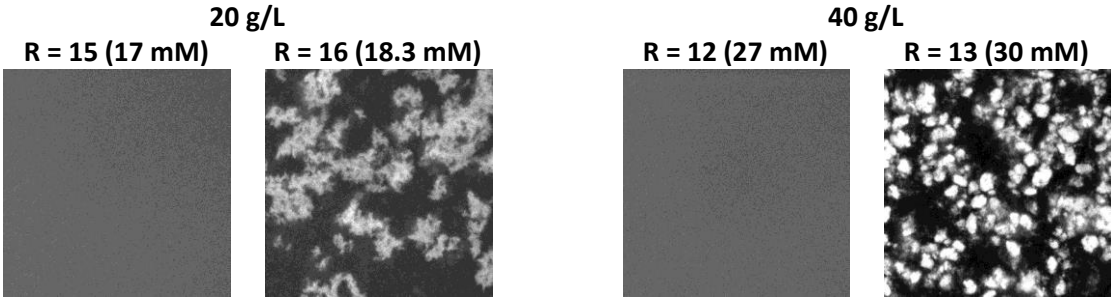

Figure 17. CLSM images (160 µm × 160 µm) of solutions of 35 nm aggregates at 20 and 40 g/L and indicated calcium ratios (concentrations) obtained shortly after preparation at room temperature.

Fig. 18 shows CLSM images of solutions of aggregates with R_h = 35 nm at C = 10 g/L and R = 5 ([$CaCl_2$] = 3 mM) before heating and after heating at 80 °C for different times. At these conditions gelation was slow. Before heating, the solution was homogeneous on length scales accessible to CLSM. After approximately 5 hours of heating the solution gelled and the images became heterogeneous. The heterogeneity increased as the gel strengthened, but after approximately 7 hours the structure no longer changed even though G' kept increasing slowly.

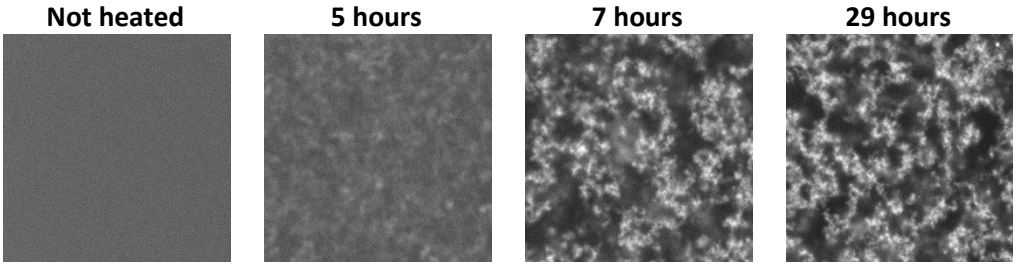

Figure 18. CLSM images (40 × 40 µm) of heated solutions of WPI aggregates (R_h = 35 nm, C = 10 g/L) at R = 5 ([$CaCl_2$] = 3 mM) at 80 °C for different times.

Fig. 19 shows the structure of solutions of aggregates with R_h = 35 nm at C = 10 g/L at different R between 5 and 15 after heating for 15 minutes at 80 °C. At R = 5 the solutions gelled slowly (as shown in Fig. 18), therefore one does not observe formation of a gel after 15 minutes of heating. However, at R > 10 the solutions gelled rapidly and therefore the steady state structure was reached after already 15 minutes at 80 °C. We found that the steady state structure of the gels did not depend on the calcium concentration, which corroborates our earlier observations that calcium influences only the gelation kinetics and not the gelation process. Heating solutions at R = 5 for longer times eventually led to the formation of the same structure that was obtained after 15 min at large R. This explains why the structure of the gel at R = 5 heated for 29 hours shown in Fig. 18 is similar to the structure of gels at larger R in Fig. 19.

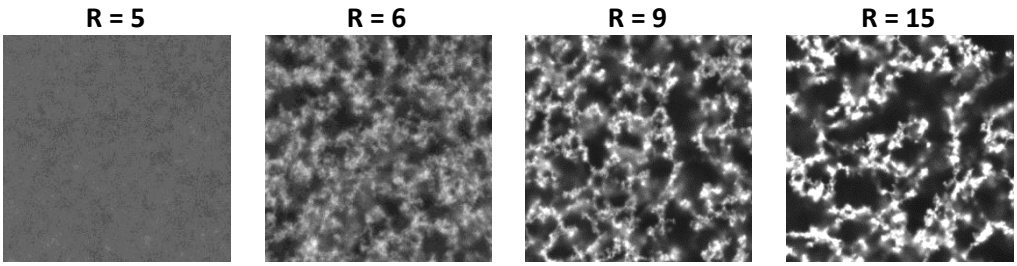

Figure 19. CLSM images (40 µm × 40 µm) of heated solutions of WPI aggregate (R_h = 35 nm, C = 10 g/L) at different R at 80 °C for 15 minutes. The corresponding values of [$CaCl_2$] vary between 3 and 9 mM.

In Fig. 20 the structure of the gels at steady state with the same composition formed by aggregates of two different sizes is shown. The structure of the two gels is similar, which supports the results obtained by the rheological measurements, therefore aggregates of different sizes form gels with identical structure and mechanical properties.

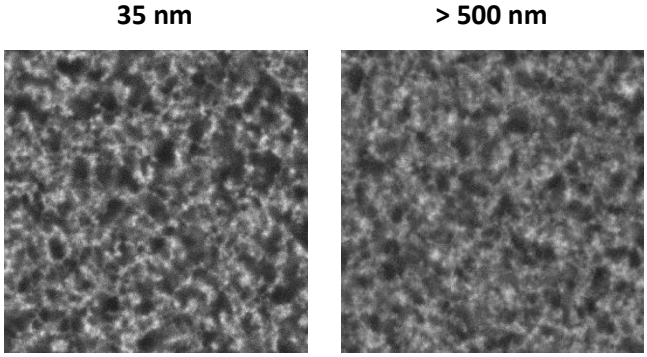

Figure 20. CLSM images (40 µm × 40 µm) of gels formed by WPI aggregate solutions (C = 20 g/L, R = 6, [$CaCl_2$] = 6.9 mM) with R_h = 35 nm (left) and R > 500 nm (right) after heating at 80 °C for 15 minutes.

Fig. 21 shows CLSM images of gels formed by heating solutions of aggregates with R_h = 35 nm for 15 min at 80 °C at different protein concentrations in the range between 10 and 40 g/L. R was fixed at 7, which means that [$CaCl_2$] increased between 4 mM at C = 10 g/L and 16 mM at C = 40 g/L. It is clear that the proteins were more homogeneously distributed in the gels at higher protein concentrations even though [$CaCl_2$] increased.

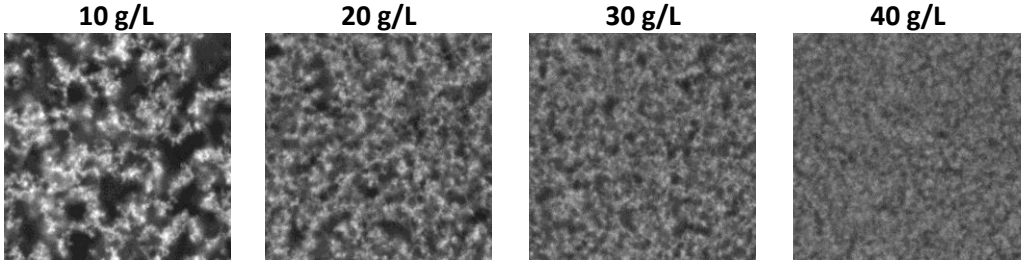

Figure 21. CLSM images (40 µm × 40 µm) of gels formed by solutions of WPI aggregates (R_h = 35 nm, R = 7, [$CaCl_2$] = 4 - 16 mM) with different protein concentrations after heating at 80 °C for 15 minutes.

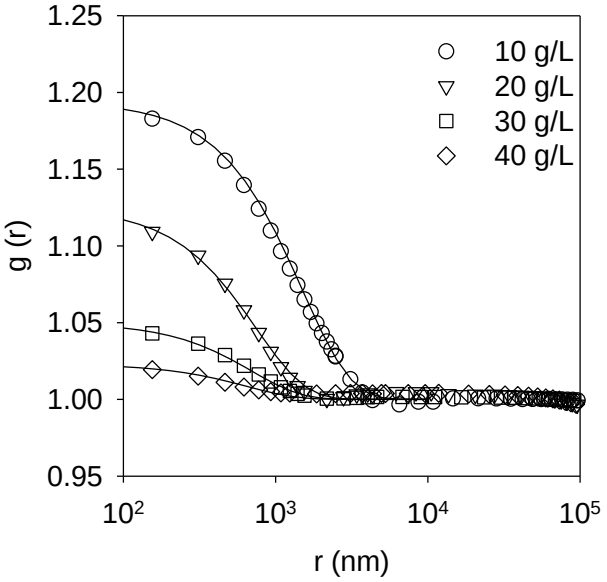

Figure 22. Semi-logarithmic representation of the pair correlation functions for gels formed by solutions of WPI aggregates (R_h = 35 nm, R = 7, [$CaCl_2$] = 4 - 16 mM) with different protein concentrations after heating at 80 °C for 15 minutes. The solid lines represent fits to eq. 1.

The structural differences were quantified by calculating the pair correlation functions of the fluorescence intensity fluctuations as described in detail in Ako, Durand, Nicolai & Becu (2009), see Fig. 22. The fluorescence intensity fluctuations correspond to the protein concentration fluctuations that were frozen in by gelation. The decrease of g(r) could be described by a stretched exponential decay:

$$g(r) = Bexp\left[-(r/\xi)^{\beta}\right] + 1 \quad (1)$$

where *B* characterizes the amplitude of the concentration fluctuations and ξ is the correlation length of the concentration fluctuations. The same equation was used to describe g(r) of gels formed by heating native β-lactoglobulin in the presence of salt (Ako, Durand, et al., 2009). We found that eq. 1 with β ≈ 1.35 described the decay at all 4 protein concentrations. *B* decreased from 0.19 at 10 g/L to 0.023 at 40 g/L and ξ = 1.5, 0.75, 0.7 and 0.65 μm for C = 10, 20, 30 and 40 g/L, respectively. Increasing the protein concentration strongly decreased the amplitude of the concentration fluctuations of gels confirming the visual impression that the gels became more homogeneous with increasing protein concentration. However, the characteristic length scale of the concentration fluctuations decreased only weakly with increasing protein concentration for C ≥ 20 g/L. We believe that the local gel structure on length scales not accessible to CLSM is the same as the fractal structure of the aggregates and that the microscopic structure that is seen in the images is caused by concentration fluctuations of the growing aggregates before they were frozen-in by gelation.

3.8 Effect of the aggregate structure

So far we have discussed cold gelation of fractal aggregates formed at pH 7. As was mentioned in the introduction, when native WPI is heated closer to the isoionic point homogeneous microgels are formed. It is of interest to compare properties of the gels formed by adding $CaCl_2$ to microgels with those formed by fractal aggregates discussed above. Fractal aggregates at C = 20 g/L

formed gels after 15 minutes at 80 °C at R ≥ 4 ([$CaCl_2$] ≥ 4.6 mM), while for microgels with R_h = 140 nm gels were formed at the same conditions only for R ≥ 6 ([$CaCl_2$] ≥ 6.9 mM). For microgels at C = 20 g/L, syneresis was observed at R ≥ 14 ([$CaCl_2$] ≥ 16 mM), which is higher than for very large fractal aggregates, but much lower than for small aggregates, see Fig. 7. At C = 40 g/L the sol-gel transition occurred at R = 4 ([$CaCl_2$] = 9.1 mM) for microgels compared to R = 3 ([$CaCl_2$] = 6.9 mM) for the fractal aggregates.

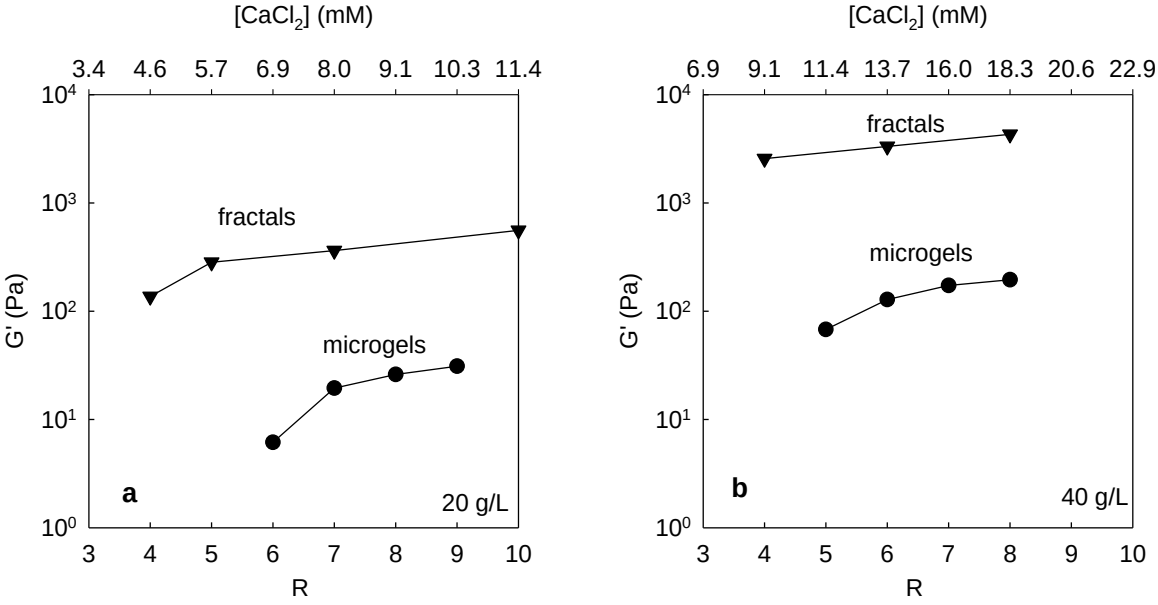

Figure 23. Storage shear modulus at 0.1 Hz for gels formed by solutions of fractal aggregates (R_h = 77 nm), and microgels (R_h = 140 nm) at different R after heating for 1 hour at 80 °C and cooling to 20 °C. Results at C = 20 g/L (a) and at C = 40 g/L (b) are shown.

The stiffness of gels formed by solutions of microgels at different R after heating for 1 h at 80 °C and cooling to 20 °C is compared to that of gels formed by fractal aggregates with R_h = 35 nm in Fig. 23 for C = 20 g/L and C = 40 g/L. For both systems, G' was independent of R if gelation was sufficiently fast so that fully formed networks were formed after 1 h at 80 °C. However, the elastic modulus of gels formed by the microgels was an order of magnitude smaller than that formed by fractals at the same protein concentration. In addition, more $CaCl_2$ was needed for microgels to form gels at these conditions. We showed above that the gel stiffness did not depend on the size of fractal aggregates. This was not the case for microgels, because trials with larger microgels (R_h = 370 nm) showed that the elastic modulus was even smaller and most gels simply collapsed under gravity.

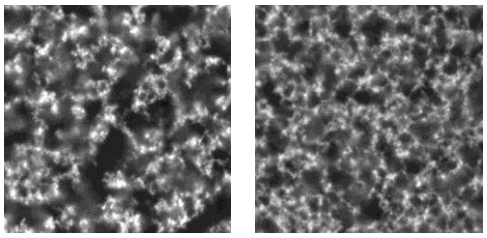

Figure 24. CLSM images (40 µm × 40 µm) of gels formed by microgels (R_h = 140 nm) (left) or strands (R_h = 35 nm) (right) after heating at 80 °C for 15 minutes (C = 20 g/L, R = 14, [$CaCl_2$] = 16 mM).

Similarly to gels formed by fractals, the structure of gels formed by microgels at steady state was independent of R. However, gels formed by microgels were more heterogeneous at the same protein concentration, see Fig. 24.

4. Discussion

The growth and gelation of protein aggregates is determined by the electrostatic interaction between proteins. The latter depends on the pH, which therefore is commonly considered to be an important control parameter. However, the pH is only indirectly related to the net charge density of the proteins, because the pH changes when the protein concentration is varied or when salt is added, whereas α remains practically the same. For instance, a decrease from pH 7 to pH 6 due to addition of salt corresponds to an increase of the H_3O^+ concentration by 10^{-6} M, i.e. less than one H^+ per 200 proteins of WPI at C = 5 g/L. On the other hand, due to the buffering capacity of proteins about 3 H^+ per protein are needed to readjust the pH back to 7. Therefore if the pH is kept constant either by readjustment or by adding a buffer, α varies significantly. Keeping α constant allows one to decouple the effect of interactions with ions from changes of the intrinsic net charge density.

When $CaCl_2$ is added to a WPI aggregate solution a fraction of the Ca^{2+} ions binds to the proteins, which reduces the effective charge density of the proteins, while maintaining the same α. The rest of the added Ca^{2+} is free in solution and screens together with the Cl^- the electrostatic interactions. Fig. 1 shows that for $[Ca^{2+}]_f < 0.5$ mM most added Ca^{2+} is bound to the proteins and that for $[Ca^{2+}]_f > 3$ mM most added Ca^{2+} remains in solution. The total $CaCl_2$ needed to obtain a certain value of $[Ca^{2+}]_f$ depends on the protein concentration, see Supplementary Information: for C = 10 - 60 g/L, $[CaCl_2]$ = 1.1 - 3.9 mM at $[Ca^{2+}]_f$ = 0.5 mM and 4.1 - 9.9 mM at $[Ca^{2+}]_f$ = 3 mM. The corresponding values of R are: R = 1.9 - 1.1 at $[Ca^{2+}]_f$ = 0.5 mM and R = 7.3 - 2.9 at $[Ca^{2+}]_f$ = 3 mM for C = 10 - 60 g/L, respectively. When $[Ca^{2+}]_f < 0.5$ mM the principal effect of adding $CaCl_2$ is reduction of the effective charge density of the proteins which is best understood by considering R. When $[Ca^{2+}]_f > 3$ mM the effect of adding more $CaCl_2$ is mostly screening and it is more useful to consider $[CaCl_2]$. At intermediate values, addition of $CaCl_2$ both reduces the effective charge density and screens interactions.

The sol-gel transition occurred at small R and was driven predominantly by the decrease of the effective charge density due to binding of Ca^{2+}. However, syneresis that appeared at larger R when all Ca^{2+} binding sites were saturated was mostly driven by screening of electrostatic interactions. The $CaCl_2$ concentration above which syneresis became apparent increased with increasing protein concentration, because gels formed at higher protein concentrations contract less easily as they are more homogeneous and more densely crosslinked.

The strong increase of the growth rate of the aggregates with increasing $[CaCl_2]$ has been reported before in the literature (Bryant & McClements, 2000; P. Hongsprabhas et al., 1999; Marangoni et al., 2000; Wu et al., 2005) and was explained by the increased possibility to form Ca^{2+}-bridges between proteins. However, a decrease of the growth rate was found at $CaCl_2$ concentrations larger than those explored here that was interpreted in terms of screening of electrostatic interaction causing Ca^{2+}-bridges to be formed with more difficulty. The present results show that the $CaCl_2$ concentration has only a kinetic effect on the mechanical and structural properties of gels at

least at the relatively low concentrations explored here ([$CaCl_2$] < 25 mM). In the literature a small increase of the gel stiffness with increasing [$CaCl_2$] was reported at low salt concentrations followed by independence at higher [$CaCl_2$] (Bryant & McClements, 2000; B. Hongsprabhas & Barbut, 1997b; Marangoni et al., 2000). However, these measurements were done at a fixed time. Here we find that G' continues to increase with time and therefore it is likely that the origin of the decreasing gel stiffness at low [$CaCl_2$] after a fixed time was caused by the decrease of the gelation rate. When the comparison is made at the same reduced time with respect to the gel time (t/t_g), as was done here, there is no longer an effect of [$CaCl_2$] either on the gel stiffness or on the micro structure.

However, it has been reported that at higher ionic strengths the gel stiffness decreased with increasing salt concentration (Navarra et al., 2009; G. E. Remondetto et al., 2002). We have also observed a decrease of G' with time at higher [$CaCl_2$] (results not shown) in systems that eventually showed syneresis. We believe that the decrease is caused by local densification of the network that was facilitated by screening of electrostatic repulsions. The same phenomenon explains why coarse microstructures have been observed at higher ionic strengths, whereas in the [$CaCl_2$] range investigated here the structure did not depend on [$CaCl_2$] for fully formed gels.

As might be expected, the gel stiffness increased with increasing protein concentration. Over a limited range the concentration dependence of G' can be described by a power law. Power law dependence over a limited concentration range was reported earlier for the $CaCl_2$-induced gelation of WPI aggregates by Hongsprabhas et al. (1999). The power law exponent was found to be about 2.5 independent of [$CaCl_2$] for [$CaCl_2$] > 10 mM, i.e. slightly smaller than found here. The lower observed value may be related to the fact that it was determined between 60 and 100 g/L whereas here it was determined between 20 and 60 g/L. The dependence of G' on C is in reality not a single power law, but curves so that the apparent exponent decreases with increasing concentration. Hongsprabhas et al. (1999) used the so-called fractal gel model to deduce a fractal dimension of about 2.6 for the flocs that build the network. Approximately the same fractal dimension was deduced from analyses of microscopy images using the so-called box counting methods. However, we don't think that the fractal gel model is applicable here. Wu et al. (2005) showed that in very dilute solutions the growing aggregates have indeed a fractal structure although with a smaller fractal dimension (1.85), but at C > 20 g/L such fractal aggregates will fill up the space before they are very big and the resulting network would be homogeneous at length scales exceeding a few tens of nm. The fact that structure is nevertheless observed on microscopic length scales implies reorganization on larger length scales. Elsewhere we suggested in the context of heat-induced globular protein gelation that when electrostatic repulsion between the fractal aggregates is weak, microphase separation occurs leading to the coarser gel structure (Ako, Nicolai, Durand, & Brotons, 2009). Pair correlation functions of these systems did not show a power law dependence over a significant range of length scales. In fact, the correlation length of gels studied here was less than 1 µm for C > 10 g/L. The box counting method may nevertheless give an apparent fractal dimension, but it was shown that this is an artefact that depends on the chosen threshold value (Ako, Durand, et al., 2009).

Here we found that the aggregate size did not influence the elastic modulus and the structure of the gels. This is in apparent contradiction with some of the older literature in which it was generally found that a more intensive heat treatment led to stiffer gels. The reason for this discrepancy is most likely that more intensive heat treatment increases conversion of native proteins into aggregates. The observed increase of the gel stiffness was therefore caused by an increase of the

aggregate concentration rather than an increase of the aggregate size. Ako, Nicolai and Durand (2010) found that large aggregates formed by association of smaller ones after addition of NaCl had the same self-similar structure as those formed by heating native proteins at pH 7. The same conclusion can be drawn for the growth of WPI aggregates in dilute solutions after addition of $CaCl_2$ that was studied by Wu et al. (2005). It explains why starting with small or large aggregates does not have a significant effect on the gel properties, but an effect on the kinetics is expected, because more time is needed for smaller aggregates to grow and percolate to form the network. However, the relatively small increase of the gelation rate with increasing aggregate size cannot explain the strong effect of aggregate size on syneresis that was observed in the present study. Currently, we do not have a satisfactory explanation for this effect, but it may reflect subtle differences in the spatial organization or bond elasticity of the network formed by aggregates of different sizes.

Even though the size of preheated fractal aggregates did not have much influence on the structure and the elastic modulus, the morphology of the aggregates made a big difference. When microgels were used instead of fractals, much weaker gels were formed at the same protein concentration and they had a more heterogeneous microstructure. Similar findings were reported by Donato et al. (2011) who compared acid-induced gelation of WPI microgels with that of fractal aggregates. The difference can be explained by the fact that microgels have a much higher density than fractals of the same size and therefore require higher protein concentrations to form a space filling network. Large microgels form weaker gels than small microgels, because they need even more protein to form a space filling network. There is no difference between starting with large and small fractal aggregates, because the elementary unit of the final network is in this case independent of the aggregate size.

It has been noted in the literature that increasing temperature leads to faster gelation (Ako et al., 2010; McClements & Keogh, 1995), but the temperature dependence has been little investigated in detail. Ako et al. (2010) found that for NaCl-induced gelation the temperature dependence of the growth rate was characterized by an activation energy of E_a = 70 kJ/mol, but the aggregation process was the same. Here we also find that for $CaCl_2$-induced gelation temperature only affected the kinetics and not the gelation process as the evolution of the shear moduli and the structure was the same after normalization of time with the gel time. The temperature dependence of the $CaCl_2$-induced gelation process was characterized by $E_a \approx 210$ kJ/mol independently of [$CaCl_2$], the protein concentration and the aggregate size. The larger activation energy compared to NaCl-induced gelation is perhaps related to the fact that $CaCl_2$-induced gelation occurs at much lower ionic strengths and involves formation of calcium bridges. In any case, the activation energy for salt-induced gelation by either NaCl or $CaCl_2$ is smaller than for gelation of native whey protein, which is controlled by the rate of denaturation (Dannenberg & Kessler, 1988; Le Bon, Nicolai, & Durand, 1999).

Very recently, a systematic investigation was reported on gelation of fractal aggregates of soy protein isolate (SPI) induced by NaCl and compared with a more limited investigation of gelation induced by $CaCl_2$ (Chen et al., 2017). It was observed that the gelation kinetics was controlled by an activation energy independent of the aggregate size, the protein concentration and the salt concentration. The activation energy in the presence of NaCl (E_a = 72 kJ/mol) was close to that of whey protein aggregates. The activation energy was larger in the presence of $CaCl_2$ (E_a = 120 kJ/mol)

than in the presence of NaCl as was observed here for WPI aggregates, but the difference was less important for SPI aggregates.

Interestingly, the strong temperature dependence of $CaCl_2$-induced gelation can be exploited to form gels at lower [$CaCl_2$] relatively quickly by heating. Further evolution of the gels can then be stopped, or at least hugely slowed down, by cooling. In this manner syneresis during storage can be avoided, which would inevitably occur if $CaCl_2$-induced gelation was done with more $CaCl_2$ at room temperature. Of course, this procedure is only applicable in practice if all ingredients are resistant to heating.

5. Conclusions

WPI aggregate solutions form gels after addition of $CaCl_2$. Increasing the protein concentration sped up gelation, increased the stiffness of the gels and rendered the microstructure more homogeneous. Increasing the $CaCl_2$ concentration only increased the gelation rate, but did not influence gel structure nor the elastic modulus. The size of fractal aggregates formed by preheating native proteins at pH 7 did not have a significant influence on the gel properties probably because larger aggregates formed by smaller aggregates after addition of salt have the same structure as larger aggregates formed during preheating. However, it appears that gels formed by larger aggregates are more prone to syneresis, the reasons for which remain speculative. $CaCl_2$-induced gelation of WPI microgels was much less efficient, because more protein is needed to form a space filling network with microgels compared to fractals. The gelation rate of a given solution can be controlled by the temperature as the process is characterized by an activation energy of 210 kJ/mol independent of the aggregate size, [$CaCl_2$] and protein concentration. This strong temperature dependence can be exploited to form gels at lower [$CaCl_2$] at higher temperature and quench the evolution of the gels that eventually leads to syneresis by cooling.

Acknowledgements

Bba association, Le Mans University and the Regional councils of Brittany and Pays de la Loire who funded this work through the interregional PROFIL project, carried out by the association "Pole Agronomique Ouest", are thanked. We also thank Dr. J. Léonil of the INRA for the scientific coordination.

References

Adamcik, J., & Mezzenga, R. (2011). Proteins fibrils from a polymer physics perspective. Macromolecules, 45(3), 1137‑1150.

Ako, K., Durand, D., Nicolai, T., & Becu, L. (2009). Quantitative analysis of confocal laser scanning microscopy images of heat-set globular protein gels. Food Hydrocolloids, 23(4), 1111‑1119.

Ako, K., Nicolai, T., & Durand, D. (2010). Salt-induced gelation of globular protein aggregates: structure and kinetics. Biomacromolecules, 11(4), 864‑871.

Ako, K., Nicolai, T., Durand, D., & Brotons, G. (2009). Micro-phase separation explains the abrupt structural change of denatured globular protein gels on varying the ionic strength or the pH. Soft Matter, 5(20), 4033‑4041.

Alting, A. C., de Jongh, H. H., Visschers, R. W., & Simons, J.-W. F. (2002). Physical and chemical interactions in cold gelation of food proteins. Journal of Agricultural and Food Chemistry, 50(16), 4682‑4689.

Alting, A. C., Hamer, R. J., de Kruif, C. G., Paques, M., & Visschers, R. W. (2003). Number of thiol groups rather than the size of the aggregates determines the hardness of cold set whey protein gels. Food Hydrocolloids, 17(4), 469‑479.

Alting, A. C., Hamer, R. J., de Kruif, C. G., & Visschers, R. W. (2000). Formation of disulfide bonds in acid-induced gels of preheated whey protein isolate. Journal of Agricultural and Food Chemistry, 48(10), 5001‑5007.

Alting, A. C., Weijers, M., de Hoog, E. H., van de Pijpekamp, A. M., Cohen Stuart, M. A., Hamer, R. J., … Visschers, R. W. (2004). Acid-induced cold gelation of globular proteins: effects of protein aggregate characteristics and disulfide bonding on rheological properties. Journal of Agricultural and Food Chemistry, 52(3), 623‑631.

Amin, S., Barnett, G. V., Pathak, J. A., Roberts, C. J., & Sarangapani, P. S. (2014). Protein aggregation, particle formation, characterization & rheology. Current Opinion in Colloid & Interface Science, 19(5), 438‑449.

Barbut, S. (1995). Effects of calcium level on the structure of pre-heated whey protein isolate gels. LWT-Food Science and Technology, 28(6), 598‑603.

Barbut, S. (1997). Relationships between optical and textural properties of cold-set whey protein gels. LWT-Food Science and Technology, 30(6), 590‑593.

Barbut, S., & Drake, D. (1997). Effect of reheating on sodium-induced cold gelation of whey proteins. Food research international, 30(2), 153‑157.

Barbut, S., & Foegeding, E. A. (1993). Ca2+-induced gelation of pre-heated whey protein isolate. Journal of Food Science, 58(4), 867‑871.

Britten, M., & Giroux, H. J. (2001). Acid-induced gelation of whey protein polymers: effects of pH and calcium concentration during polymerization. Food Hydrocolloids, 15(4), 609‑617.

Bryant, C. M., & McClements, D. J. (1998). Molecular basis of protein functionality with special consideration of cold-set gels derived from heat-denatured whey. Trends in Food Science & Technology, 9(4), 143‑151.

Bryant, C. M., & McClements, D. J. (2000). Influence of NaCl and CaCl2 on Cold-Set Gelation of Heat-denatured Whey Protein. Journal of Food Science, 65(5), 801‑804.

Cavallieri, A. L. F., Costa-Netto, A. P., Menossi, M., & Da Cunha, R. L. (2007). Whey protein interactions in acidic cold-set gels at different pH values. Le Lait, 87(6), 535‑554.

Cavallieri, A. L. F., & Da Cunha, R. L. (2008). The effects of acidification rate, pH and ageing time on the acidic cold set gelation of whey proteins. Food Hydrocolloids, 22(3), 439‑448.

Chen, N., Chassenieux, C., & Nicolai, T. (2017). Kinetics of NaCl induced gelation of soy protein aggregates: Effects of temperature, aggregate size, and protein concentration. Food Hydrocolloids.

Chi, E. Y., Krishnan, S., Randolph, T. W., & Carpenter, J. F. (2003). Physical stability of proteins in aqueous solution: mechanism and driving forces in nonnative protein aggregation. Pharmaceutical research, 20(9), 1325‑1336.

Chinchalikar, A. J., Kumar, S., Aswal, V. K., Kohlbrecher, J., & Wagh, A. G. (2014). SANS study of understanding mechanism of cold gelation of globular proteins. In AIP Conference Proceedings (Vol. 1591, p. 186‑188). AIP.

Clare, D. A., Lillard, S. J., Ramsey, S. R., Amato, P. M., & Daubert, C. R. (2007). Calcium effects on the functionality of a modified whey protein ingredient. Journal of agricultural and food chemistry, 55(26), 10932‑10940.

Clark, A. H., & Lee-Tuffnell, C. D. (1998). Gelation of globular proteins. Functional properties of food macromolecules, 2, 77‑142.

Dannenberg, F., & Kessler, H.-G. (1988). Reaction kinetics of the denaturation of whey proteins in milk. Journal of Food Science, 53(1), 258‑263.

Doi, E. (1993). Gels and gelling of globular proteins. Trends in Food Science & Technology, 4(1), 1‑5.

Donato, L., Kolodziejcyk, E., & Rouvet, M. (2011). Mixtures of whey protein microgels and soluble aggregates as building blocks to control rheology and structure of acid induced cold-set gels. Food Hydrocolloids, 25(4), 734‑742.

Foegeding, E. A., & Davis, J. P. (2011). Food protein functionality: A comprehensive approach. Food Hydrocolloids, 25(8), 1853‑1864.

Glibowski, P., Mleko, S., & Wesolowska-Trojanowska, M. (2006). Gelation of single heated vs. double heated whey protein isolate. International dairy journal, 16(9), 1113‑1118.

Hongsprabhas, B., & Barbut, S. (1997a). Ca 2+-induced cold gelation of whey protein isolate: effect of two-stage gelation. Food Research International, 30(7), 523‑527.

Hongsprabhas, B., & Barbut, S. (1997b). Protein and Salt Effects on Ca2+-Induced Cold Gelation of Whey Protein Isolate. Journal of Food Science, 62(2), 382‑385.

Hongsprabhas, P., & Barbut, S. (1996). Ca2+-induced gelation of whey protein isolate: effects of pre-heating. Food Research International, 29(2), 135‑139.

Hongsprabhas, P., & Barbut, S. (1997). Effect of gelation temperature on Ca2+-induced gelation of whey protein isolate. LWT-Food Science and Technology, 30(1), 45-49.

Hongsprabhas, P., & Barbut, S. (1997). Structure-forming processes in Ca 2+-induced whey protein isolate cold gelation. International Dairy Journal, 7(12), 827-834.

Hongsprabhas, P., Barbut, S., & Marangoni, A. G. (1999). The structure of cold-set whey protein isolate gels prepared with Ca++. LWT-Food Science and Technology, 32(4), 196-202.

Inthavong, W., Kharlamova, A., Chassenieux, C., & Nicolai, T. (2016). Structure and flow of dense suspensions of protein fractal aggregates in comparison with microgels. Soft matter, 12(10), 2785-2793.

Ju, Z. Y., & Kilara, A. (1998a). Effects of preheating on properties of aggregates and of cold-set gels of whey protein isolate. Journal of Agricultural and Food Chemistry, 46(9), 3604-3608.

Ju, Z. Y., & Kilara, A. (1998b). Textural Properties of Cold-set Gels Induced from Heat-denatured Whey Protein Isolates. Journal of Food Science, 63(2), 288-292.

Jung, J.-M., Savin, G., Pouzot, M., Schmitt, C., & Mezzenga, R. (2008). Structure of heat-induced β-lactoglobulin aggregates and their complexes with sodium-dodecyl sulfate. Biomacromolecules, 9(9), 2477-2486.

Kharlamova, A., Inthavong, W., Nicolai, T., & Chassenieux, C. (2016). The effect of aggregation into fractals or microgels on the charge density and the isoionic point of globular proteins. Food Hydrocolloids, 60, 470-475.

Kuhn, K. R., Cavallieri, Â. L. F., & Da Cunha, R. L. (2010). Cold-set whey protein gels induced by calcium or sodium salt addition. International journal of food science & technology, 45(2), 348-357.

Kundu, S., Chinchalikar, A. J., Das, K., Aswal, V. K., & Kohlbrecher, J. (2014). Mono-, di-and tri-valent ion induced protein gelation: Small-angle neutron scattering study. Chemical Physics Letters, 593, 140-144.

Lara, C., Gourdin-Bertin, S., Adamcik, J., Bolisetty, S., & Mezzenga, R. (2012). Self-assembly of ovalbumin into amyloid and non-amyloid fibrils. Biomacromolecules, 13(12), 4213-4221.

Le Bon, C., Nicolai, T., & Durand, D. (1999). Kinetics of aggregation and gelation of globular proteins after heat-induced denaturation. Macromolecules, 32(19), 6120-6127.

Lu, X., Lu, Z., Yin, L., Cheng, Y., & Li, L. (2010). Effect of preheating temperature and calcium ions on the properties of cold-set soybean protein gel. Food research international, 43(6), 1673-1683.

Mahmoudi, N., Mehalebi, S., Nicolai, T., Durand, D., & Riaublanc, A. (2007). Light-scattering study of the structure of aggregates and gels formed by heat-denatured whey protein isolate and β-lactoglobulin at neutral pH. Journal of Agricultural and Food Chemistry, 55(8), 3104-3111.

Maltais, A., Remondetto, G. E., Gonzalez, R., & Subirade, M. (2005). Formation of soy protein isolate cold-set gels: protein and salt effects. Journal of Food Science, 70(1).

Marangoni, A. G., Barbut, S., McGauley, S. E., Marcone, M., & Narine, S. S. (2000). On the structure of particulate gels—the case of salt-induced cold gelation of heat-denatured whey protein isolate. Food hydrocolloids, 14(1), 61-74.

McClements, D. J., & Keogh, M. K. (1995). Physical properties of cold-setting gels formed from heat-denatured whey protein isolate. Journal of the Science of Food and Agriculture, 69(1), 7-14.

Mezzenga, R., & Fischer, P. (2013). The self-assembly, aggregation and phase transitions of food protein systems in one, two and three dimensions. Reports on Progress in Physics, 76(4), 046601.

Mleko, S., & Foegeding, E. A. (2000). pH induced aggregation and weak gel formation of whey protein polymers. Journal of food science, 65(1), 139-143.

Murekatete, N., Hua, Y., Chamba, M. V. M., Djakpo, O., & Zhang, C. (2014). Gelation Behavior and Rheological Properties of Salt-or Acid-Induced Soy Proteins Soft Tofu-Type Gels. Journal of texture studies, 45(1), 62-73.

Navarra, G., Giacomazza, D., Leone, M., Librizzi, F., Militello, V., & San Biagio, P. L. (2009). Thermal aggregation and ion-induced cold-gelation of bovine serum albumin. European Biophysics Journal, 38(4), 437-446.

Nicolai, T., Britten, M., & Schmitt, C. (2011). β-Lactoglobulin and WPI aggregates: Formation, structure and applications. Food Hydrocolloids, 25(8), 1945-1962.

Nicolai, T., & Durand, D. (2013). Controlled food protein aggregation for new functionality. Current Opinion in Colloid & Interface Science, 18(4), 249-256.

Phan-Xuan, T., Durand, D., Nicolai, T., Donato, L., Schmitt, C., & Bovetto, L. (2011). On the Crucial Importance of the pH for the Formation and Self-Stabilization of Protein Microgels and Strands. Langmuir, 27(24), 15092-15101.

Phan-Xuan, T., Durand, D., Nicolai, T., Donato, L., Schmitt, C., & Bovetto, L. (2014). Heat induced formation of beta-lactoglobulin microgels driven by addition of calcium ions. Food Hydrocolloids, 34, 227-235.

Pouzot, M., Nicolai, T., Benyahia, L., & Durand, D. (2006). Strain hardening and fracture of heat-set fractal globular protein gels. Journal of colloid and interface science, 293(2), 376-383.

Purwanti, N., van der Goot, A. J., Boom, R., & Vereijken, J. (2010). New directions towards structure formation and stability of protein-rich foods from globular proteins. Trends in food science & technology, 21(2), 85-94.

Rabiey, L., & Britten, M. (2009). Effect of protein composition on the rheological properties of acid-induced whey protein gels. Food Hydrocolloids, 23(3), 973-979.

Remondetto, G. E., Paquin, P., & Subirade, M. (2002). Cold Gelation of β-lactoglobulin in the Presence of Iron. Journal of Food Science, 67(2), 586-595.

Remondetto, G. E., & Subirade, M. (2003). Molecular mechanisms of Fe2+-induced β-lactoglobulin cold gelation. Biopolymers, 69(4), 461‐469.

Sadeghi, S., Madadlou, A., & Yarmand, M. (2014). Microemulsification–cold gelation of whey proteins for nanoencapsulation of date palm pit extract. Food Hydrocolloids, 35, 590‐596.

Salis, A., Boström, M., Medda, L., Cugia, F., Barse, B., Parsons, D. F., … Monduzzi, M. (2011). Measurements and Theoretical Interpretation of Points of Zero Charge/Potential of BSA Protein. Langmuir, 27(18), 11597‐11604.

Schmitt, C., Bovay, C., Rouvet, M., Shojaei-Rami, S., & Kolodziejczyk, E. (2007). Whey protein soluble aggregates from heating with NaCl: physicochemical, interfacial, and foaming properties. Langmuir, 23(8), 4155‐4166.

Tanford, C., & Nozaki, Y. (1959). Physico-chemical comparison of β-lactoglobulins A and B. Journal of Biological Chemistry, 234(11), 2874‐2877.

van der Linden, E., & Venema, P. (2007). Self-assembly and aggregation of proteins. Current Opinion in Colloid & Interface Science, 12(4), 158‐165.

Vardhanabhuti, B., Foegeding, E. A., McGuffey, M. K., Daubert, C. R., & Swaisgood, H. E. (2001). Gelation properties of dispersions containing polymerized and native whey protein isolate. Food hydrocolloids, 15(2), 165‐175.

Wu, H., Arosio, P., Podolskaya, O. G., Wei, D., & Morbidelli, M. (2012). Stability and gelation behavior of bovine serum albumin pre-aggregates in the presence of calcium chloride. Physical Chemistry Chemical Physics, 14(14), 4906‐4916.

Wu, H., Xie, J., & Morbidelli, M. (2005). Kinetics of cold-set diffusion-limited aggregations of denatured whey protein isolate colloids. Biomacromolecules, 6(6), 3189‐3197.

Annex

Relation between $[CaCl_2]$ or R and $[Ca^{2+}]_f$ at different protein concentrations

The $CaCl_2$ concentration ($[CaCl_2]$, in mM) that is required to obtain a certain value of $[Ca^{2+}]_f$ depends on the protein concentration as follows:

$$[CaCl_2] = [Ca^{2+}]_f + [Ca^{2+}]_b - R_{wpi} \times [WPI],$$

where R_{wpi} is the molar ratio of Ca^{2+} per protein present in the WPI powder (R_{wpi} = 1.2, i.e. 1.2 Ca^{2+} ions are bound per protein in the powder). Here [WPI] is the molar concentration of WPI in the solution, ($[WPI] = C / (1.75 \times 10^4)$) and $[Ca^{2+}]_b = R_b \times [WPI]$ is the concentration of Ca^{2+} bound to protein. The corresponding value of R (the number of added Ca^{2+} ions per protein required to obtain a certain value of $[Ca^{2+}]_f$) is calculated as $R = [CaCl_2] / [WPI]$.

We are interested here to find $[CaCl_2]$ and R at $[Ca^{2+}]_f$ = 0.5 mM and $[Ca^{2+}]_f$ = 3 mM. From Fig. 1 we find that for WPI aggregates R_b = 2.2 at $[Ca^{2+}]_f$ = 0.5 mM and R_b = 3.2 at $[Ca^{2+}]_f$ = 3 mM. The values of R and $[CaCl_2]$ for $[Ca^{2+}]_f$ = 0.5 mM and 3 mM at different protein concentrations are summarized in the following table.

C (g/L)	**for $[Ca^{2+}]_f$ = 0.5 mM**		**for $[Ca^{2+}]_f$ = 3 mM**	
	$[CaCl_2]$ (mM)	**R**	**$[CaCl_2]$ (mM)**	**R**
10	1.1 mM	1.9	4.1 mM	7.3
20	1.6 mM	1.4	5.3 mM	4.6
30	2.2 mM	1.3	6.4 mM	3.8
40	2.8 mM	1.2	7.6 mM	3.3
60	3.9 mM	1.1	9.9 mM	2.9

Chapter 6. Acid-induced gelation of whey protein aggregates: kinetics, gel structure and rheological properties.

Anna Kharlamova, Taco Nicolai*, Christophe Chassenieux

Abstract

Acid-induced gelation of fractal aggregates with different sizes formed by preheating whey protein isolate solutions has been investigated in the protein concentration range 10-60 g/L as a function of the net protein charge density (α). Homogeneous gels could be formed in a range of α that depended on the heating time and temperature. Decrease of the negative charge density of the proteins increased the rate of gelation, but lowering α to less negative values than approximately –2.5 (lowering the pH) by adding HCl increased turbidity of the solutions and led to syneresis. Strong syneresis also occurred at more negative net charge densities (higher pH) if the heat treatment was too severe. The elastic modulus of homogeneous gels increased with increasing protein concentration. The heterogeneity of the gels decreased with increasing protein concentration. The temperature dependence of the gelation rate was characterized by an activation energy of 155 kJ/mol independent of the charge density, protein concentration and aggregate size. Increase of the temperature increased the gelation rate, but did not influence the elastic modulus of the gels. The present findings on acid-induced gelation are compared with gelation of the same WPI aggregates induced by adding $CaCl_2$ reported recently.

1. Introduction

Globular proteins of milk whey are compact approximately spherical particles with a well-defined structure (Fox et al., 2015). Upon heating, the proteins denature allowing formation of bonds resulting in aggregation, which leads to gelation if the protein concentration is above a critical gel concentration (C_g) (Amin et al., 2014; Nicolai et al., 2011; Nicolai and Durand, 2013). If the solution is heated at $C < C_g$ a suspension of stable aggregates is produced. At pH > 6.1 small curved strands are formed at low protein concentrations that further aggregate into self-similar fractal aggregates at higher concentrations (Jung et al., 2008; Nicolai et al., 2011). Aggregates of other morphologies (microgels and fibrils) are formed at lower pH or in presence of calcium (Donato et al., 2009; Mezzenga and Fischer, 2013; Schmitt et al., 2009). Another mechanism to form globular protein gels is known as “cold gelation” and involves two steps (Bryant and McClements, 1998; Nicolai et al., 2011; van Vliet et al., 2004). In the first step, a solution of aggregates is formed by heating the globular proteins at $C < C_g$. In the second step, the electrostatic repulsions between aggregates are reduced either by addition of salt (salt-induced gelation) (Bryant and McClements, 1998; Nicolai et al., 2011; Nicolai and Durand, 2013) or decrease of the pH towards the isoionic point (pI = 5.0, see Chapter 4) (acid-induced gelation) (Alting et al., 2000, 2003a, 2003b, 2004; Bryant and McClements, 1998; Donato et al., 2011). This results in gelation of the suspension and can happen even at ambient temperatures and is therefore advantageous for food products susceptible to high temperatures. Cold gelation has been studied intensively in the literature, in particular gelation induced by addition of calcium ions, and we have recently investigated Ca^{2+}-induced gelation of WPI aggregates in

considerable detail (see Chapter 5). In comparison, acid-induced gelation has been investigated much less.

In the studies of acid-induced gelation reported so far the pH was lowered by addition of glucono-δ-lactone (GDL) (Alting et al., 2000, 2003a, 2003b; Britten and Giroux, 2001; Cavallieri et al., 2007; Cavallieri and Da Cunha, 2008; Donato et al., 2011; Ju and Kilara, 1998a, 1998b; Rabiey and Britten, 2009). GDL hydrolyzes progressively in water releasing one proton per molecule. The advantage of using GDL is that it allows progressive in-situ acidification of the suspensions (De Kruif, 1997). With increasing GDL concentration the rate of acidification increases and a lower final pH is reached (De Kruif, 1997). With GDL the pH can be reduced without stirring and homogeneous gels can be formed at lower pH values that cannot be reached with HCl, because in the latter case gels are formed during addition of the acid. Another reason for using GDL is that it simulates progressive acidification of milk during yoghurt formation.

Ju and Kilara (1998a, 1998b) studied the influence of preheating WPI at different concentrations and for different heating times. They observed that the hardness of acid-induced gels increased with increasing protein concentration and heating time, which was explained by a higher conversion rate of native protein. A power-law increase of the gel hardness in the protein concentration range between 1 and 8 % was found. Alting et al. (2003b) prepared gels from WPI aggregates of the same size with fixed final pH 5.0 and obtained a power-law dependency of the storage shear modulus (G') at concentrations between 0.5 % and 9 %.

The influence of the aggregate morphology on acid-induced gelation was studied by Britten and Giroux (2001) and Donato et al. (2011). Britten and Giroux produced different aggregates by varying pH and calcium content of WPI solutions and found that the shape of the aggregates affects crosslinking during acidification, with smaller particles produced without calcium forming firmer gels than larger spherical particles formed in presence of calcium. Donato et al. (2011) studied gels formed by acidification of fractal aggregates with R_h = 100 nm and microgels with R_h = 270 nm as well as their mixtures. They found that microgels produced weaker gels requiring lower pH for the onset of gelation. Gel stiffness decreased below pH 4.3. The microstructure of the gels was found to vary dramatically with composition. Rabiey and Britten (2009) investigated the effect of the ratio of β-lg and α-lac in the aggregates on acid-induced gelation. They observed that the onset of gelation occurred at approximately the same pH, but that stiffer gels were formed if the aggregates contained more β-lg, possibly due to the absence of free cysteine in α-lac.

Alting et al. (2000, 2003a, 2003b) studied in detail the effect of formation of disulfide bridges during acid-induced gelation of WPI aggregates by comparing systems with and without thiol-blocking agents. The gelation kinetics and the structure of the gels were found to be the same. However, the hardness of the gels formed with thiol-blocking agents was 5 to 10 fold less implying that initial formation of the network by non-covalent interactions is followed by the reinforcement through formation of disulfide bonds without changing the gel structure. They also observed that if the net negative charge density of the aggregates was increased by succinylation, a lower pH was required to induce gelation, clearly demonstrating the effect of the electrostatic interactions (Alting et al., 2003a).

Cavallieri and Da Cunha (2008) studied gelation of WPI aggregates at C = 7 % after addition of different amounts of GDL. Acidification was faster at higher GDL contents and led to a lower final pH.

They observed that the pH at which WPI aggregates started to gel depended on the rate of pH decrease: pH 5.8 at the slowest rate and pH 5.6 at the highest rate. The elastic modulus increased with decreasing pH, but was systematically lower at a given pH when acidification was faster. It was concluded that the acidification rate influenced the stiffness of the gels at a given pH with slower acidification allowing more time for the gels to develop so that they are stiffer at a given pH.

The disadvantage of using GDL is that the final pH is reached slowly and therefore the kinetics of acidification is confounded with the kinetics of gelation. For this reason the kinetics of acid-induced gelation at constant pH has not yet been investigated. In addition, steady state properties have only been investigated at relatively low pH values. Here we report on an investigation of acid-induced gelation of WPI fractal aggregates as a function of the net charge density of the proteins (α). In Chapter 4 we showed how α depends on the pH for WPI aggregates at different concentrations. The properties of the gels were studied as a function of the gelation temperature, aggregate concentration (10-60 g/L) and aggregate size (35-500 nm). Acidification was done by addition of HCl in order to reach the desired value of α rapidly, which allows investigation of the kinetics of the gelation process at constant pH. Addition of HCl meant that acid-induced gelation could only be investigated at pH values where it was sufficiently slow at low temperatures so that gelation did not occur during mixing. As was mentioned above, very recently we reported on an extensive investigation of calcium-induced gelation of WPI aggregates close to neutral pH (see Chapter 5). For that study α was fixed, but the effective charge density was reduced by specific binding of Ca^{2+}. The main objective for the present investigation was to compare acid-induced gelation with calcium-induced gelation.

2. Experimental

2.1 Preparation of WPI aggregates

Whey protein isolate powder was purchased from Lactalis (Laval, France). It contained 89.3 wt% protein, 6 wt% moisture, < 0.4 wt% fat, < 4 wt% lactose, and 2.0 wt% ash, including 0.25 wt% calcium. The proteins included 70 % β-lg and 20 % α-lac, according to the size exclusion chromatography analysis. The WPI powder was mixed with Milli-Q water containing 200 ppm of sodium azide as an antimicrobial preservative and stirred for 4-6 hours. Prepared solution was filtered twice through 0.45 and 0.2 µm syringe filters (Acrodisc®). The pH of the concentrated WPI solution (WPI concentration ~13.5 wt%) was adjusted from pH ≈ 6.25 to 7.00 by addition of a recorded amount of a standard 1 M NaOH solution (Fisher Scientific UK). The protein content of the obtained stock solution was measured on samples diluted to concentrations below 1 g/L by UV absorption at 278 nm using an extinction coefficient of 1.05 L g^{-1} cm^{-1}. The stock solution was then diluted to the required protein concentration, hermetically sealed in glass bottles and heated at 80 °C for 24 hours. After heating, solutions of aggregates were stored in a fridge at 4 °C.

The size of the aggregates was determined using dynamic light scattering as described elsewhere (Phan-Xuan et al., 2011). Aggregates with R_h = 35, 77, 200 and > 500 nm were obtained by heating solutions at 62, 80, 91, and 93 g/L, respectively. The charge density of the protein aggregates was determined by potentiometric titration (see Chapter 4) and found to be α = –8.0 expressed in number of charges per protein considering an average molar mass M = 1.75 × 10^3 g/mol for WPI.

2.2 Preparation of gels

For preparation of gels, aggregates were placed in 40 mL plastic cups with a magnetic bar. Standard HCl solutions with molar concentration [HCl] = 0.1 or 1 M (Fisher Scientific UK) were diluted in Milli-Q water to ensure the required final concentration of aggregates (C) and added dropwise to the aggregate suspension under constant agitation. The amount of acid was calculated to obtain the desired change in the net charge density of the proteins ($\Delta\alpha$):

$$\Delta\alpha = \frac{m(HCl)\times [HCl] \times M}{m(agg) \times C}, \quad (1)$$

where m(HCl) and m(agg) are the weights of the HCl and aggregate solutions. The value of α was calculated from $\Delta\alpha$ and the initial charge density of the aggregates ($\alpha_{.}$ = –8.0). As we will show below, gelation can be slowed down by cooling. Therefore HCl was added to the aggregate suspensions cooled to a few degrees on ice. The pH of the prepared solutions was measured with an accuracy of $\pm$0.05 using an automatic titrator (TIM 856, Radiometer Analytical) equipped with a combined pH electrode and a thermoprobe. The electrode was calibrated by a three-point calibration in the pH range between 4.0 and 10.0.

In order to construct sol-gel state diagrams, aggregate suspensions were placed in 7 mL glass bottles with a diameter of 1 cm, hermetically sealed and heated in a water bath. To compare gelation induced by addition of HCl with gelation by addition of glucono-δ-lactone (GDL) the aggregates were mixed in a similar manner with a freshly prepared solution of GDL powder purchased from Sigma. The GDL solution was used within 1 hour after preparation. We considered that one proton was released per GDL molecule at steady state.

2.3 Titration with NaCl

Titration experiments were conducted at room temperature using an automatic titrator (TIM 856, Radiometer Analytical). The charge density of the aggregate solutions was adjusted before the experiment by addition of a recorded amount of standard HCl solution at constant stirring. Solutions were subsequently titrated with 2 M NaCl added at the speed of 0.2 mL/min. The pH was recorded automatically during the experiment.

2.4 Rheological measurements

The rheological measurements were performed with two stress-imposed rheometers (AR2000 and ARG2, TA Instruments) using a cone-plate geometry with diameter 40 mm. The temperature was controlled within 0.1 °C by a Peltier system. The samples were placed on the rheometer immediately after preparation and covered with mineral oil to prevent evaporation. All measurements were conducted in the linear response regime and at oscillation frequency 0.1 Hz.

2.5 Confocal laser scanning microscopy

Prepared samples of aggregates with adjusted net charge density were labeled by adding a small amount of rhodamine B (5 ppm) and hermetically sealed on cavity slides. The slides were heated on a rack placed in a water bath and observed using Leica TCS-SP2 microscope (Leica Microsystems Heidelberg, Germany) with a water immersion objective lens HC × PL APO 63 × NA = 1.2.

3. Results and discussion

3.1 Relationship between alpha and pH

The process of acid-induced gelation of protein aggregates is determined by the net protein charge density and is commonly studied in the literature by varying the pH. However, the pH is related to the charge density only indirectly and α does not change with pH in the same way at different protein and salt concentrations, which can be demonstrated by potentiometric titration (Kharlamova et al., 2016; Salis et al., 2011). The net charge density of the proteins is zero at the isoionic point (IIP), which is equal to the isoelectric point where the surface potential is zero if no ions bind to the proteins. At the IIP the pH is independent of the salt concentration and the protein concentration as there is no specific binding of ions. Elsewhere we showed that the IIP of WPI fractal aggregates is at pH 5.0 independent of the aggregate size by comparing titration curves at different NaCl concentrations (see Chapter 4). Titration of aggregate suspensions with NaCl at different α confirms that the pH doesn't change significantly with addition of NaCl close to pH = 5.0 where $\alpha = 0$, see Fig. 1. The pH decreases with increasing NaCl concentration when $\alpha < 0$ and increases when $\alpha > 0$.

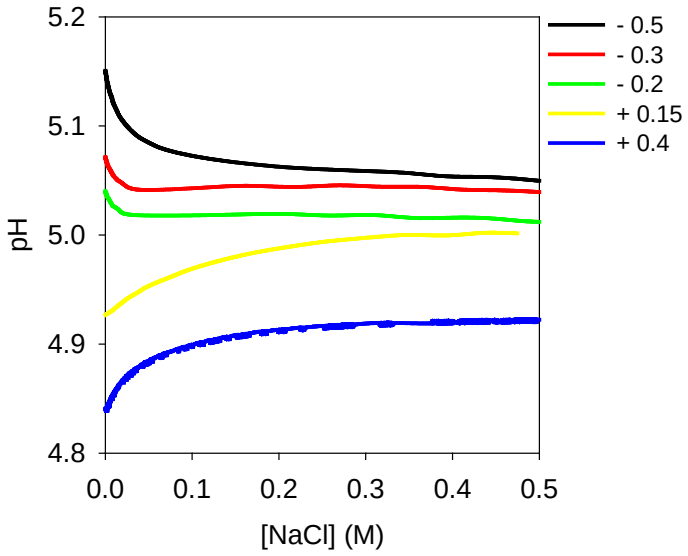

Figure 1. pH as a function of the NaCl concentration for solutions of WPI aggregates with R_h = 35 nm at C = 10 g/L at different α indicated in the figure.

Gelation of WPI aggregates was investigated at protein concentrations between C = 10 and 60 g/L and between $\alpha = -6$ and 0. The corresponding pH values are shown in Fig. 2. The pH of aggregate solutions at a given α increases with decreasing protein concentration. On the other hand, when the pH is fixed, the negative charge density is smaller at lower protein concentrations. We verified that the dependence of pH on the charge density was the same for aggregates of different sizes.

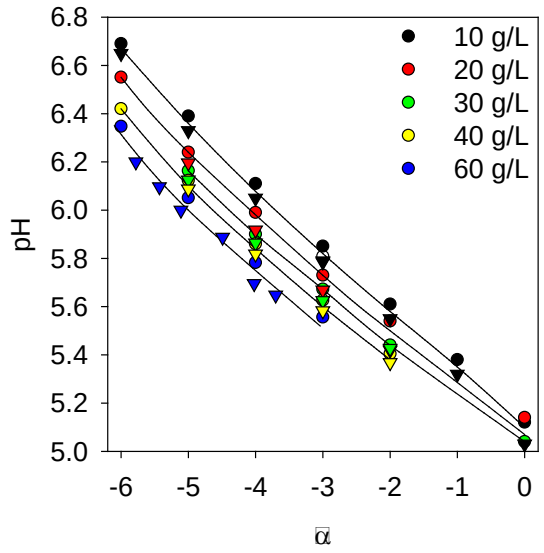

Figure 2. Dependency of the pH on the charge density of WPI aggregates with R_h = 35 nm (triangles) and R_h = 77 nm (circles) at different aggregate concentrations indicated in the figure. The lines are guides to the eye.

3.2 Sol-gel state diagram at 20 °C and 80 °C

When α of the aggregates was decreased in suspensions at concentrations between 10 and 60 g/L that were kept on ice, all samples stayed liquid and transparent down to α = –3 where they became translucent. By a decrease of α in this work we mean the decrease of the initial net negative charge density to values closer to zero. Samples at C = 50-60 g/L gelled quickly (within 15 min) at room temperature at α = –3.0. At α = –2.5 it was not possible to form homogeneous systems at C = 50-60 g/L as the suspensions gelled during mixing even when kept on ice and formed highly heterogeneous gels. The systems remained visually homogeneous liquids down to α = –2.0 at C ≤ 30 g/L but became very turbid. Fig. 3 shows confocal laser scanning microscopy (CLSM) images of aggregate (R_h = 35 nm) suspensions at C = 20 g/L at different α taken at room temperature. Decrease of the net negative charge density to α = –2.5 led to formation of microscopic structures visible with CLSM and at α = –2.0 large scale flocculations were observed.

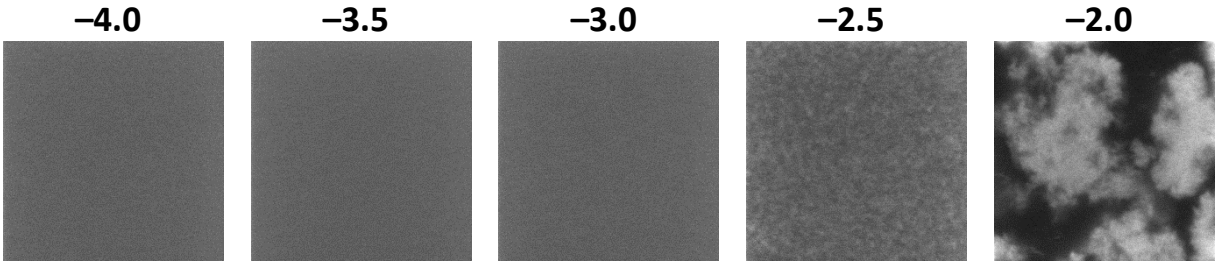

Figure 3. CLSM images (25 µm × 25 µm) of solutions of aggregates with R_h = 35 nm at C = 20 g/L with different net charge densities indicated in the figure. The images were taken at 20 °C shortly after preparation.

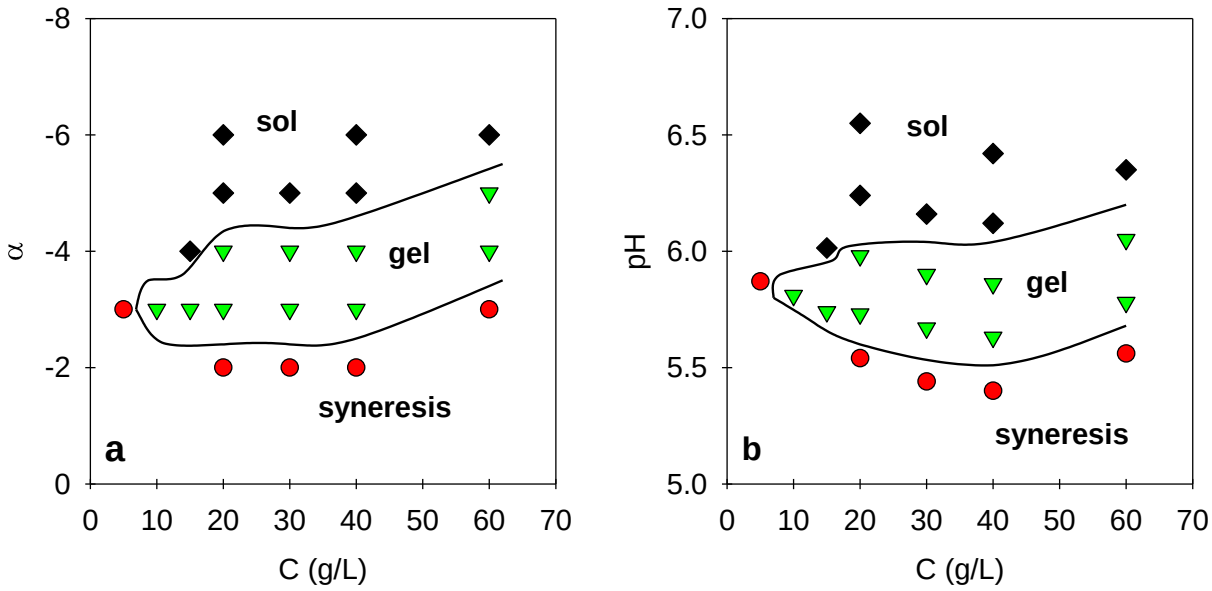

Figure 4. State diagram as function of the concentration of aggregates (R_h = 77 nm) and the net charge density (a) or the pH (b) for aggregate suspensions that were heated for 15 minutes at 80 °C. The black diamonds indicate systems that stayed liquid, green triangles indicate gels and red circles indicate systems undergoing syneresis.

State diagrams were obtained by decreasing α in steps of Δα = 1. Freshly prepared samples were heated in a water bath at 80 °C for 15 minutes. The samples were then quickly cooled with tap water and investigated visually. Three states were distinguished: liquid samples, gels (self-supporting gels without syneresis that resisted flow when tilted) and gels undergoing syneresis. The state diagram for aggregates with R_h = 77 nm is presented as a function of α in Fig. 4a and as a function of the pH in Fig. 4b. Homogeneous gels were formed in a narrow range of α between –4 and –3 at C = 20 to 40 g/L. At C = 10 g/L a gel was formed only at α = –3 and at C = 60 g/L gels were formed at α = –4 and –5. These charge densities correspond to a narrow pH range between approximately 5.6 and 6.1, see Fig. 4b. At C < 10 g/L the solutions either stayed liquid or large protein flocks were formed. Some liquid samples close to the sol-gel transition became turbid during heating. The transition between homogeneous gels and systems showing syneresis was very sharp at these heating conditions as at C = 20 to 40 g/L homogeneous gels were formed at α = –3, whereas a lot of water was expelled at α = –2.

The same experiment was done with smaller (R_h = 35 nm) and bigger (R_h > 500 nm) aggregates. In Fig. 5 the state diagrams for aggregates of different sizes are compared. The diagrams for aggregates with R_h = 35 and R_h = 77 nm are similar, whereas very large aggregates (R_h > 500 nm) were more prone to syneresis and expelled water at lower protein concentrations (C < 30 g/L). However, at higher protein concentrations the state of the systems was the same for aggregates of different sizes.

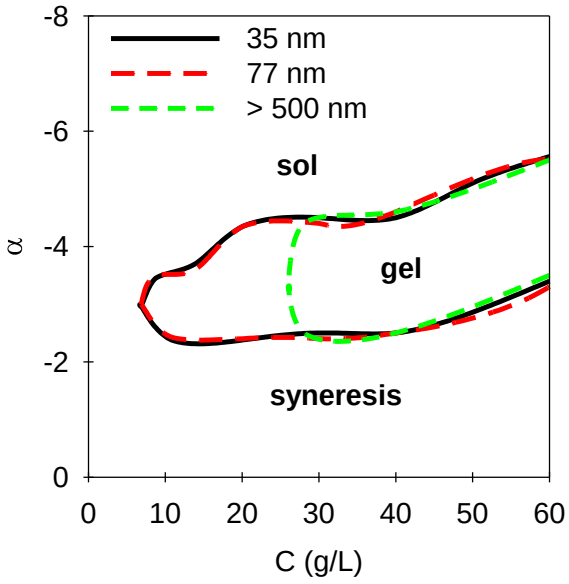

Figure 5. State diagram as function of the concentration of aggregates and their charge density for aggregates with three different sizes indicated in the figure heated for 15 minutes at 80 °C.

The effect of the heating time and temperature on the state diagram is shown in Fig. 6 for aggregates with R_h = 35 nm. At 80 °C the largest area where homogeneous gels are formed is obtained after 1 min of heating. With increasing heating time both sol-gel and gel-syneresis transitions shift to more negative net charge densities corresponding to higher pH. After 16 hours of heating homogeneous gels were obtained only in a very narrow range of C and α. At 20 °C the gels were formed in a narrower range of C and α compared to systems heated at 80 °C. At this temperature the shift of the sol-gel transition with time was much weaker.

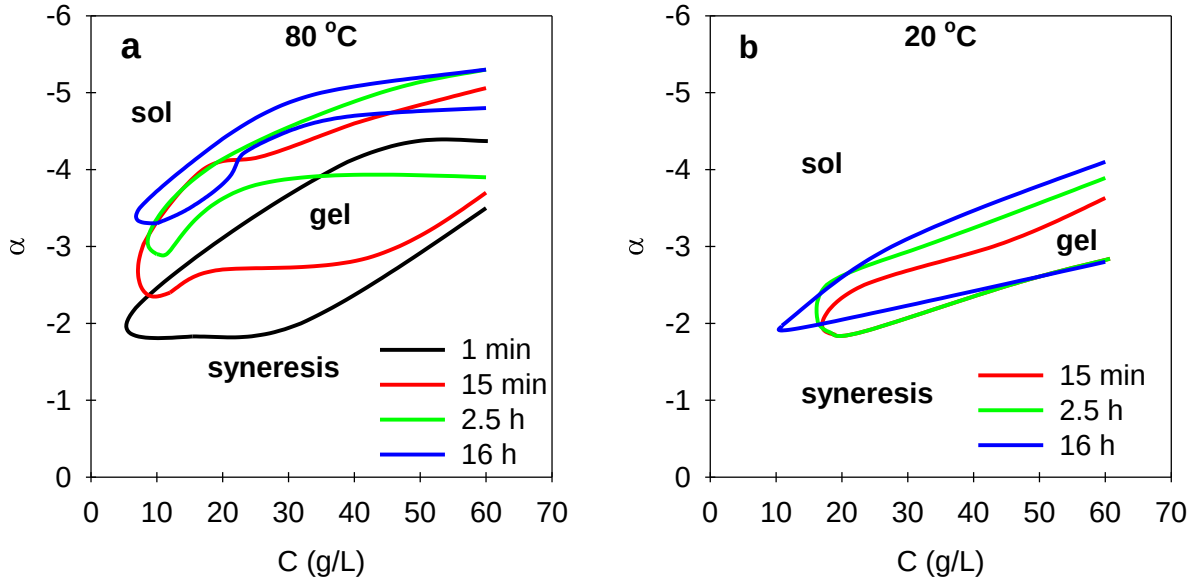

Figure 6. State diagrams at 80 °C (a) and 20 °C (b) at different times indicated in the figure for aggregates with R_h = 35 nm as a function of the net protein charge density and the aggregate concentration.

The results show that at higher protein concentrations gelation is faster at a given charge density and can be induced at more negative charge densities corresponding to higher pH. Here we found that self-supporting gels could not be formed below C = 10 g/L, whereas Alting et al. (2000) and Je and Kilara (1998a) reported formation of gels with WPI aggregates at concentrations as low as 5 g/L at lower pH induced by adding GDL. The difference is perhaps due to the fact that the pH was set here by addition of HCl, which led to flocculation during acidification at lower pH. To compare gelation induced by GDL and HCl we repeated the experiments at 80 °C with solutions prepared with a freshly diluted GDL powder instead of HCl. We obtained the same results after prolonged heating ($t \geq 2.5$ hours), i.e. when all GDL was degraded and the same pH was reached. This means that as long as flocculation can be avoided during acidification it does not matter if the pH is reduced with GDL or with HCl.

3.3 Influence of temperature

The influence of temperature on acid-induced gelation of WPI aggregates was investigated quantitatively by heating solutions of aggregates at different temperatures after setting α. In Fig. 7a a solution of aggregates with R_h = 35 nm at C = 60 g/L and α = –4.5 (corresponding to pH 5.9) was heated at temperatures between 45 and 70 °C. The temperature was increased to the required value within one minute. The elastic modulus (G') increased steeply when gels were formed and leveled off after prolonged heating. The gelation time (t_g) defined here as the time required to reach G’ = 0.1 Pa decreased strongly with increasing temperature. The evolution with time of the storage and the loss moduli superimposed when time was normalized by t_g, see Fig. 7b. This implies that temperature had only a kinetic effect on the gelation process and did not influence much the gel stiffness. We note, however, that when gels formed at 80 °C were subsequently cooled to 20 °C, G' increased by a factor of 2-3.

The values of t_g obtained at different temperatures are plotted in an Arrhenius representation in Fig. 7c showing a linear dependency in the temperature range between T = 45 °C and 75 °C. From the slope we deduced an activation energy: E_a = 150 kJ/mol.

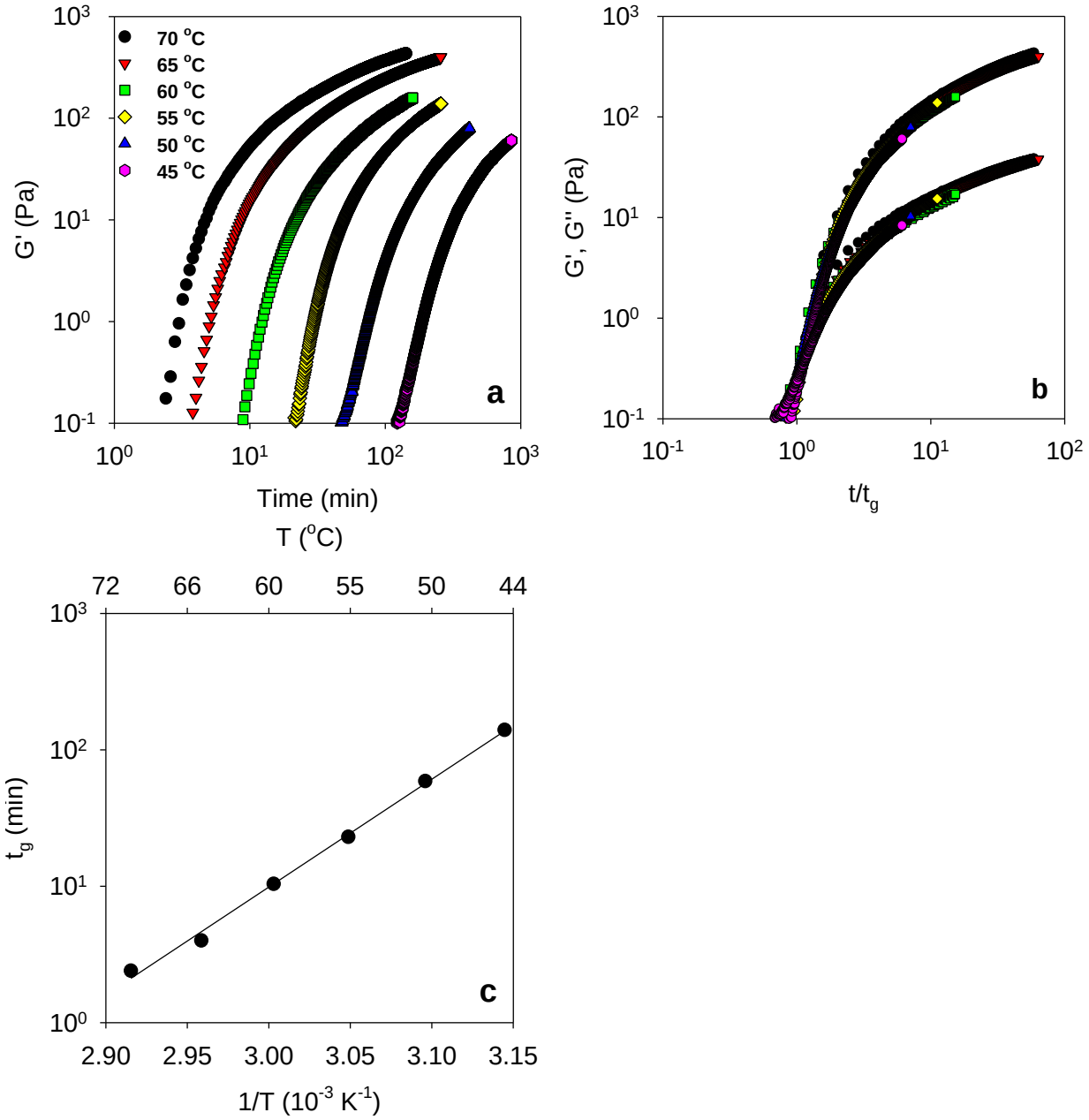

Figure 7. a). Evolution of the storage shear modulus at 0.1 Hz with heating time for solutions of WPI aggregates with R_h = 35 nm at C = 60 g/L and α = –4.5 (pH 5.9) at different temperatures.
b). Evolution of the storage and loss moduli at different temperatures as a function of heating time normalized by the gel time.
c). Arrhenius representation of temperature dependence of the gel time.

3.4 Influence of the charge density

Measurements were repeated with the same aggregate solutions after adjusting α to different values. Fig. 8a shows master curves obtained from time-dependent measurements of G' at different temperatures. The decrease of the net negative charge from α = –4.8 to α = –3.7 (corresponding to pH decrease from 5.95 to 5.65) resulted in an increase of the gelation rate by more

than three orders of magnitude. At α = –5.8 (pH 6.2) aggregates did not gel even after overnight heating at 90 °C, whereas at α = –3.7 (pH 5.65) gelation happened within 15 min at room temperature. When master curves are normalized by t_g, they approximately superimpose, see Fig. 8b, implying that the elastic modulus does not depend on the protein charge density in the studied range.

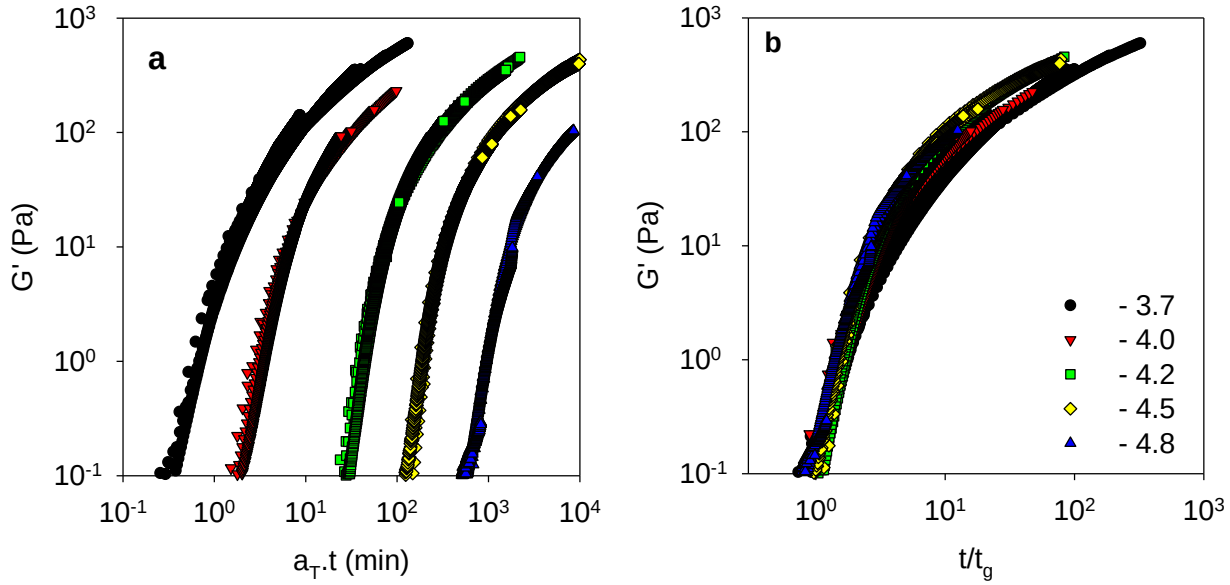

Figure 8. a). Master curves for solutions of WPI aggregates with R_h = 35 nm at C = 60 g/L at different charge densities indicated in the figure obtained by temperature-time superposition with T_{ref} = 45 °C. The range of α between –4.8 and –3.7 corresponds to a pH range between 5.95 and 5.65.

b). Same data as in Fig. 8a normalized by the gel time.

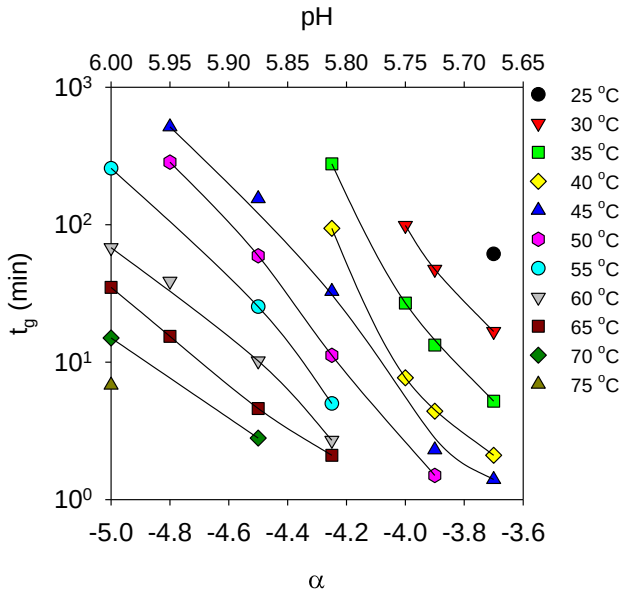

Figure 9. Gel time as a function of α at different temperatures indicated in the figure for solutions of aggregates with R_h = 35 nm at C = 60 g/L. Lines are guides to the eye.

In Fig. 9 t_g is plotted as a function of α and the pH at different temperatures. The gel time decreased steeply with decreasing net negative charge density and corresponding pH. The activation energy was found to be independent of α within the experimental error at least in the narrow range where it could be determined, see Fig. 11.

3.5 Influence of the protein concentration

Fig. 10 shows master curves obtained at different protein concentrations at α = –4.2 (pH 5.8-5.9) at T_{ref} = 65 °C. The gelation rate increased strongly with increasing protein concentration between 30 and 50 g/L, but increasing C further to 60 g/L did not have a significant effect on gelation rate, because gelation happened fast at high concentrations. At longer heating times G' no longer increased and even showed a tendency to decrease. We attribute this phenomenon to syneresis leading to partial detachment of the gels from the geometry. The maximum values of G' increased with increasing protein concentration.

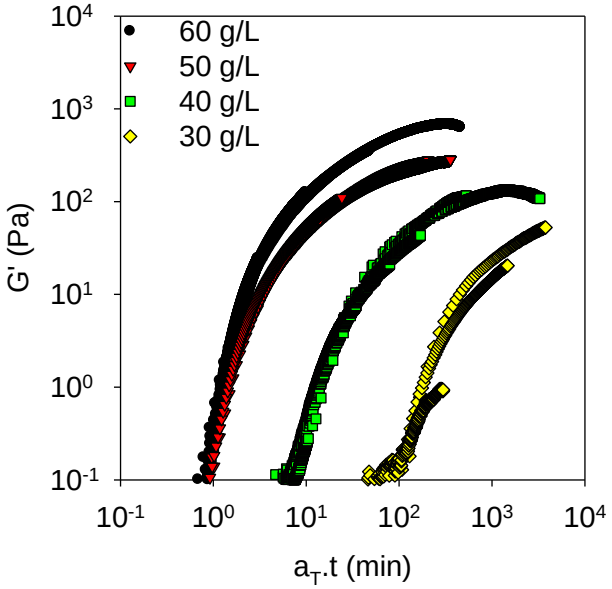

Figure 10. Master curves of G' vs time at T_{ref} = 65 °C for solutions of aggregates with R_h = 35 nm at α = –4.2 (pH = 5.8-5.9) at different protein concentrations obtained by superposition of measurements of G' at different temperatures.

Fig. 11 shows that the shift factors a_T used to superimpose measurements at different temperatures were the same within the experimental error at different concentrations, which means that the activation energy was independent of the protein concentration. From the slope we found an average activation energy E_a = 155 kJ/mol.

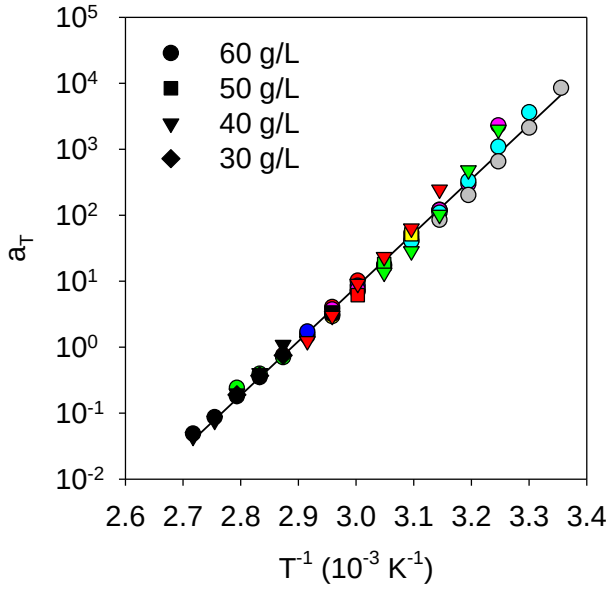

Figure 11. Arrhenius representation of the shift factors used to superimpose time-dependent measurements of G' at different temperatures for solutions of aggregates with R_h = 35 nm at different concentrations. Different colors correspond to different charge densities.

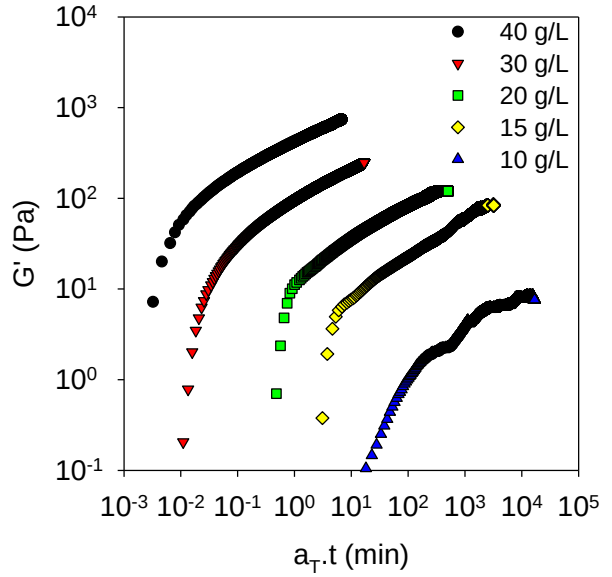

Figure 12. Evolution of G' with time for solutions of aggregates with R_h = 35 nm at α = –3 and different protein concentrations indicated in the figure. The measurements were done at different temperatures and shifted to T_{ref} = 65 °C considering E_a = 155 kJ/mol.

The influence of the protein concentration on the elastic modulus was investigated at lower protein concentrations (C = 10-40 g/L) for α = –3 corresponding to pH 5.6-5.9. The results were similar to those obtained at α = –4.2 and confirmed that gels were formed faster at higher protein concentrations. In each case G' continued to increase progressively after a fast initial increase until it started to decrease due to syneresis, see Fig. 12. The temperature was reduced to 20 °C when G' started to decrease. Fig. 13 shows G' at 20 °C and 0.1 Hz as a function of the aggregate concentration. A systematic increase of G' with increasing concentration was observed, but repeated

measurements at the same concentrations showed significant scatter, which we believe is caused by non-reproducibility of the effect of syneresis. Results obtained for gels formed by addition of $CaCl_2$ at $\alpha = -8$ are also shown in Fig. 13. We will compare the two types of gelation below and mention here only that the effects of syneresis appeared later during gelation induced by Ca^{2+}.

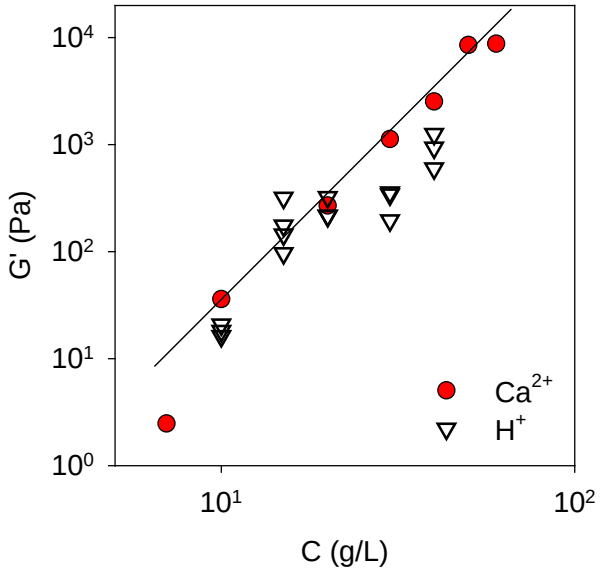

Figure 13. Elastic moduli of gels at 20 °C and 0.1 Hz obtained with WPI aggregate (R_h = 35 nm) solutions as a function of the aggregate concentration. Results for aggregates at $\alpha = -3$ in the absence of added salt (triangles) are compared with results for the same aggregates at $\alpha = -8$ containing 6 Ca^{2+} per protein (R = 6) taken from Chapter 5 (circles). The line is a guide to the eye.

Donato et al. (2011) obtained G' = 5 × 10^2 Pa at C = 40 g/L and pH 4.2 for gels of fractal WPI aggregates formed by adding GDL, which is close to the value obtained in this study. However, Alting et al. (2003b) obtained significantly larger values of G' at pH 5.0 between 10^2 Pa and 4 × 10^3 Pa with increasing protein concentration between 10 and 40 g/L.

3.6 Influence of the aggregate size

To study the influence of the aggregate size we conducted measurements with larger aggregates (Rh = 200 nm) at C = 60 g/L and $\alpha = -4$ (pH 5.7). Gelation of aggregates was measured at different temperatures and master curves were obtained. In Fig. 14 the master curve of G' vs time at T_{ref} = 35 °C for aggregates with R_h = 200 nm is compared with the one obtained for aggregates with R_h = 35 nm. Gelation was faster for the larger aggregates, but the final elastic modulus was not affected by the aggregate size. The activation energy was within the experimental error the same for the two aggregate sizes.

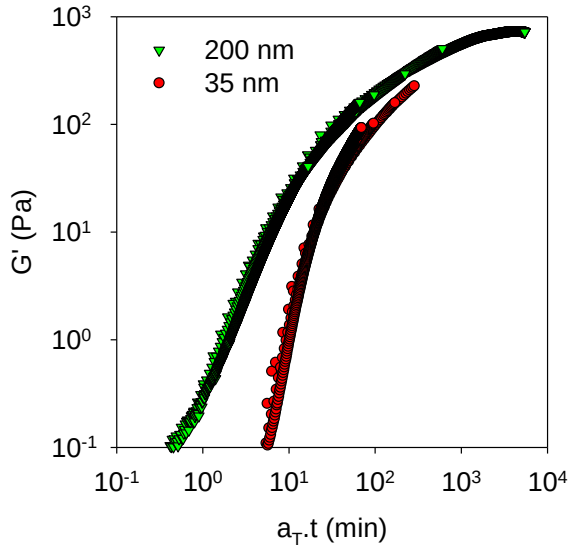

Figure 14. Comparison of master curves at T_{ref} = 35 °C obtained for aggregates of two different sizes indicated in the figure at C = 60 g/L and α = –4.0 (pH 5.7).

3.7 Microstructure of the gels

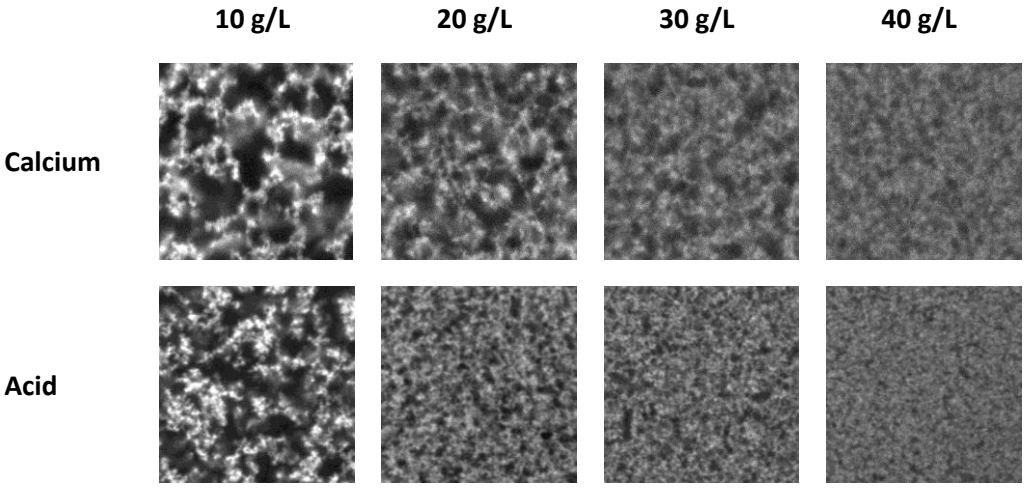

Figure 15. CLSM images (25 µm × 25 µm) of fully developed gels obtained by heating solutions of aggregates with R_h = 35 nm at α = –8 with 9 calcium ions added per protein (R = 9) (top) and at α = –3 without salt (bottom) and at aggregate concentrations shown in the figure.

The microstructure of the gels was studied with CLSM. The structure developed during the initial stage of gelation, but remained the same at longer times while the elastic modulus continued to increase slowly. No significant differences in the structure of fully developed gels were observed for gels formed at different temperatures, α and aggregate size. However, the microstructure appeared more homogeneous when the protein concentration was higher, see Fig. 15. The microstructures at different protein concentrations were similar to those of gels formed by adding $CaCl_2$ to suspensions of WPI aggregates at α = –8 (approximately neutral pH). The latter images were analyzed in terms of the pair correlation function of the fluorescence intensity fluctuations which correspond to the protein concentration fluctuations (see Chapter 5). It was found that both the

amplitude and the correlation length of the concentration fluctuations decreased with increasing concentration, though the effect on the latter was relatively small. We note that Ju and Kilara (1998a) also found similar microstructures for gels formed from WPI aggregates (8 %) by adding GDL (final pH 5.0) or $CaCl_2$ (20 mM, R = 4.4) using transmission electron microscopy.

3.8 Comparison of acid-induced and calcium-induced cold-set gels of WPI aggregates

As was mentioned in the Introduction, gelation of aggregates of globular proteins can be induced by addition of salt or decrease of the pH, which causes in both cases a decrease of the electrostatic repulsion between the aggregates. We may compare the present results for acid-induced gelation with our recent detailed investigation of calcium-induced gelation of the same WPI aggregates at $\alpha = -8$ (see Chapter 5). Though addition of $CaCl_2$ led to a decrease of the pH from close to neutral to about pH 6 the effect on the degree of protonation and thus α was negligible. The effect of adding $CaCl_2$ is that up to 3 Ca^{2+} ions per protein molecule bind specifically to the aggregates, which causes a decrease of their effective charge density. In addition, added ions that remain free contribute to screening of the electrostatic repulsion.

Qualitatively, acid-induced gelation of WPI aggregates resembles Ca^{2+}-induced gelation. Gels can be formed when the electrostatic repulsion is reduced beyond a certain extent. However, extensive flocculation occurs already during mixing if too much acid is added. The latter occurred for acid-induced gelation studied here at $\alpha > -2.5$ corresponding approximately to pH < 5.5. Both acid- and calcium-induced gelation are activated processes and the gelation rate can be increased by heating. The activation energy was found to be independent of the protein concentration, the aggregate size and the strength of the electrostatic interactions, but E_a was larger for Ca^{2+}-induced gelation (E_a = 210 kJ/mol) than for acid-induced gelation (E_a = 155 kJ/mol). We note that Ako et al. (2010) reported a much smaller activation energy (E_a = 70 kJ/mol) for gelation of β-lg aggregates induced by adding NaCl. An important difference between $CaCl_2$ and NaCl is that Na^+ does not bind to the proteins and therefore does not reduce the effective charge density. As a consequence much more NaCl than $CaCl_2$ is needed to induce gelation.

The gelation rate was found to decrease very strongly with increasing electrostatic repulsion, i.e. increasing the net negative charge density or decreasing the Ca^{2+} concentration. Acid-induced gelation took more than a day even at 80 °C when the net negative charge was larger than –4 or –5 depending on the protein concentration corresponding to pH larger than about 6. For Ca^{2+}-induced gelation at $\alpha = -8$ we found that this was the case when less than 2 Ca^{2+} per protein were added. It is important to stress that the gels continued to evolve with time leading eventually to contraction of the protein network and consequently expulsion of water. We found that syneresis occurred sooner during acid-induced gelation than Ca^{2+}-induced gelation. As we mentioned in the Introduction, Alting et al. (2000, 2003a, 2003b) found that disulfide bridging was important for the strengthening of the gel, but not its initial formation. It is possible that formation of disulfide bridges was slower at lower pH, which may have caused the different evolution of the gels. In order to avoid syneresis, gels should be formed at higher temperatures and at conditions where electrostatic repulsion is stronger. In that case the evolution of the gels will be very slow after cooling and therefore syneresis can be hugely delayed.

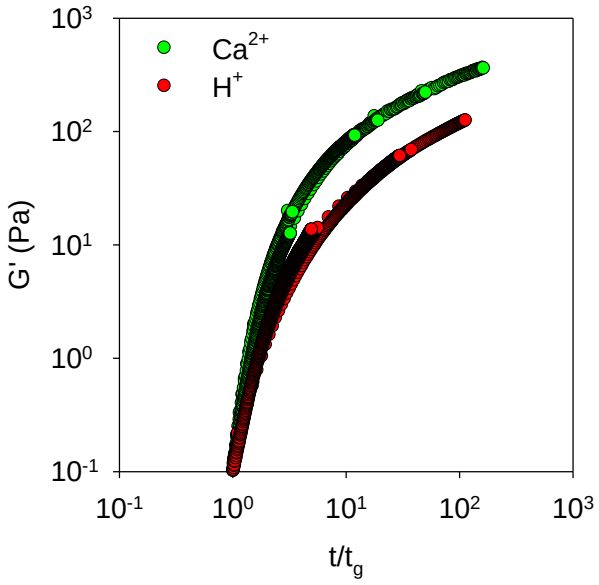

Figure 16. Master curves for solutions of WPI aggregates with R_h = 35 nm at C = 40 g/L normalized by t_g. Gelation was induced by addition of HCl to achieve the charge density α = –3.7 (pH 5.7) or addition of 4 Ca^{2+} ions per protein (R = 4) at α =–8.

Although the gelation rate depended strongly on temperature and electrostatic interactions, the gel stiffness for a given t/t_g only depended on the protein concentration for both acid- and calcium-induced gelation. However, we found that at a given protein concentration somewhat stiffer gels were formed by Ca^{2+}-induced gelation, see Fig.13, even though the microstructure of the two types of gel was close, see Fig. 15, and the evolution of G' with time was similar, see Fig. 16. We believe that the reason for the different stiffness is that, as mentioned above, acid-induced gels showed syneresis sooner and therefore could not be allowed to evolve as long as the Ca^{2+}-induced gels. We note that Ju and Kilara (1998a) found higher hardness for gels formed by adding GDL to WPI aggregates compared to Ca^{2+}-induced gels However, the kinetics of the gelation process was not taken into consideration in that study.

The comparison between acid- and Ca^{2+}-induced gelation of suspensions of WPI fractal aggregates is summarized in Table 1. Gels with comparable stiffness and structure can be formed by acid-induced gelation or Ca^{2+}-induced gelation. For both methods the elastic modulus is not influenced by the size of the aggregates, but gelation is somewhat faster if larger aggregates are used. For both methods the temperature dependence of the gelation rate is controlled by an activation energy that is independent of the aggregate size, the protein concentration and the interaction strength, but E_a is larger for Ca^{2+}-induced gelation. Both methods require balancing the rate of gelation with the rate at which syneresis appears, but this can be done more easily for Ca^{2+}-induced gelation of aggregates with a relatively high net charge density. Obviously, cold gelation can also be induced by combining a decrease of the negative value of α with addition of $CaCl_2$. However, it is clear from the present study that in order to form homogeneous gels fine-tuning of the $CaCl_2$ concentration is required for each chosen α and vice versa.

Table 1. Comparison of acid- and Ca^{2+}-induced gelation of fractals.

	Ca^{2+}	H^+
The mechanism of reduction of the negative charge	Binding of Ca^{2+} ions (change of the **effective charge density**) + screening of electrostatic interactions by excess salt.	Binding of protons to proteins (change of the **net charge density**).
E_a	210 kJ/mol	155 kJ/mol
	E_a is independent of the protein concentration, the aggregate size, $[Ca^{2+}]$, $[H^+]$.	
G'	Elastic moduli of the same order of magnitude.	
Microstructure	Similar at a given protein concentration and independent of the aggregate size, $[Ca^{2+}]$, $[H^+]$, heating time. More homogeneous gels at higher aggregate concentrations.	
Syneresis	Syneresis occurs sooner for acid- than calcium-induced gelation.	

4. Conclusions

Reducing the net negative charge density by acidification towards the isoionic point where α = 0 strongly increases the rate of gelation of solutions of fractal WPI aggregates, but doesn't influence the elastic modulus of the gels. Visually homogeneous gels can be formed in a narrow range of α (pH) that depends on the heat treatment. After prolonged heat treatment water is expelled from the gels, but syneresis can be avoided by cooling the systems after gels are formed and before water is expelled. The temperature dependence of acid-induced gelation is characterized by an activation energy of 155 kJ/mol. The increase of the temperature leads to an increase of the gelation rate, but does not influence the elastic modulus. Increase of the protein concentration increases the gelation rate and the elastic modulus and renders gels microscopically more homogeneous. Using larger aggregates leads to somewhat faster gelation, but does not influence the elastic modulus. Gelation of WPI aggregates induced by adding acid is similar to that induced by adding $CaCl_2$, leading to gels with similar microstructure. However, the activation energy of the gels formed with Ca^{2+} is larger, they are more resistant to syneresis and somewhat stiffer than gels produced by acidification.

Acknowledgements

Bba association, Le Mans University and the Regional councils of Brittany and Pays de la Loire who funded this work through the interregional PROFIL project, carried out by the association "Pole Agronomique Ouest", are thanked. We also thank Dr. J. Léonil of the INRA for the scientific coordination.

References

Ako, K., Nicolai, T., Durand, D., 2010. Salt-induced gelation of globular protein aggregates: structure and kinetics. Biomacromolecules 11, 864–871.

Alting, A.C., Hamer, R.J., de Kruif, C.G., Paques, M., Visschers, R.W., 2003a. Number of thiol groups rather than the size of the aggregates determines the hardness of cold set whey protein gels. Food Hydrocoll. 17, 469–479.

Alting, A.C., Hamer, R.J., de Kruif, C.G., Visschers, R.W., 2003b. Cold-set globular protein gels: interactions, structure and rheology as a function of protein concentration. J. Agric. Food Chem. 51, 3150–3156.

Alting, A.C., Hamer, R.J., de Kruif, C.G., Visschers, R.W., 2000. Formation of disulfide bonds in acid-induced gels of preheated whey protein isolate. J. Agric. Food Chem. 48, 5001–5007.

Alting, A.C., Weijers, M., de Hoog, E.H., van de Pijpekamp, A.M., Cohen Stuart, M.A., Hamer, R.J., de Kruif, C.G., Visschers, R.W., 2004. Acid-induced cold gelation of globular proteins: effects of protein aggregate characteristics and disulfide bonding on rheological properties. J. Agric. Food Chem. 52, 623–631.

Amin, S., Barnett, G.V., Pathak, J.A., Roberts, C.J., Sarangapani, P.S., 2014. Protein aggregation, particle formation, characterization & rheology. Curr. Opin. Colloid Interface Sci. 19, 438–449.

Britten, M., Giroux, H.J., 2001. Acid-induced gelation of whey protein polymers: effects of pH and calcium concentration during polymerization. Food Hydrocoll. 15, 609–617.

Bryant, C.M., McClements, D.J., 1998. Molecular basis of protein functionality with special consideration of cold-set gels derived from heat-denatured whey. Trends Food Sci. Technol. 9, 143–151.

Cavallieri, A.L.F., Costa-Netto, A.P., Menossi, M., Da Cunha, R.L., 2007. Whey protein interactions in acidic cold-set gels at different pH values. Le Lait 87, 535–554.

Cavallieri, A.L.F., Da Cunha, R.L., 2008. The effects of acidification rate, pH and ageing time on the acidic cold set gelation of whey proteins. Food Hydrocoll. 22, 439–448.

De Kruif, C.G., 1997. Skim milk acidification. J. Colloid Interface Sci. 185, 19–25.

Donato, L., Kolodziejcyk, E., Rouvet, M., 2011. Mixtures of whey protein microgels and soluble aggregates as building blocks to control rheology and structure of acid induced cold-set gels. Food Hydrocoll., Food Colloids 2010: On the Road from Interfaces to Consumers 25, 734–742.

Donato, L., Schmitt, C., Bovetto, L., Rouvet, M., 2009. Mechanism of formation of stable heat-induced β-lactoglobulin microgels. Int. Dairy J. 19, 295–306.

Fox, P.F., Uniacke-Lowe, T., McSweeney, P.L.H., O'Mahony, J.A., 2015. Milk Proteins, in: Dairy Chemistry and Biochemistry. Springer, Cham, pp. 145–239.

Ju, Z.Y., Kilara, A., 1998a. Effects of preheating on properties of aggregates and of cold-set gels of whey protein isolate. J. Agric. Food Chem. 46, 3604–3608.

Ju, Z.Y., Kilara, A., 1998b. Textural Properties of Cold-set Gels Induced from Heat-denatured Whey Protein Isolates. J. Food Sci. 63, 288–292.

Jung, J.-M., Savin, G., Pouzot, M., Schmitt, C., Mezzenga, R., 2008. Structure of heat-induced β-lactoglobulin aggregates and their complexes with sodium-dodecyl sulfate. Biomacromolecules 9, 2477–2486.

Kharlamova, A., Inthavong, W., Nicolai, T., Chassenieux, C., 2016. The effect of aggregation into fractals or microgels on the charge density and the isoionic point of globular proteins. Food Hydrocoll. 60, 470–475.

Mezzenga, R., Fischer, P., 2013. The self-assembly, aggregation and phase transitions of food protein systems in one, two and three dimensions. Rep. Prog. Phys. 76, 046601.

Nicolai, T., Britten, M., Schmitt, C., 2011. β-Lactoglobulin and WPI aggregates: Formation, structure and applications. Food Hydrocoll., 25 years of Advances in Food Hydrocolloid Research 25, 1945–1962.

Nicolai, T., Durand, D., 2013. Controlled food protein aggregation for new functionality. Curr. Opin. Colloid Interface Sci. 18, 249–256.

Phan-Xuan, T., Durand, D., Nicolai, T., Donato, L., Schmitt, C., Bovetto, L., 2011. On the Crucial Importance of the pH for the Formation and Self-Stabilization of Protein Microgels and Strands. Langmuir 27, 15092–15101.

Rabiey, L., Britten, M., 2009. Effect of protein composition on the rheological properties of acid-induced whey protein gels. Food Hydrocoll. 23, 973–979.

Salis, A., Boström, M., Medda, L., Cugia, F., Barse, B., Parsons, D.F., Ninham, B.W., Monduzzi, M., 2011. Measurements and Theoretical Interpretation of Points of Zero Charge/Potential of BSA Protein. Langmuir 27, 11597–11604.

Schmitt, C., Bovay, C., Vuilliomenet, A.-M., Rouvet, M., Bovetto, L., Barbar, R., Sanchez, C., 2009. Multiscale characterization of individualized β-lactoglobulin microgels formed upon heat treatment under narrow pH range conditions. Langmuir 25, 7899–7909.

van Vliet, T., Lakemond, C.M., Visschers, R.W., 2004. Rheology and structure of milk protein gels. Curr. Opin. Colloid Interface Sci. 9, 298–304.

Chapter 7. Heat-induced gelation of mixtures of casein micelles with whey protein aggregates.

Anna Kharlamova, Taco Nicolai, Christophe Chassenieux

Abstract

Gelation of aqueous solutions of casein micelles in mixtures with fractal aggregates of whey protein isolate (WPI) has been studied by addition of different amounts of aggregates at a fixed concentration of micelles and by substitution of micelles with aggregates at a fixed total protein concentration. Addition of small amounts of aggregates (1 – 5 g/L) to suspensions of micelles (20 – 60 g/L) at a fixed pH led to a strong decrease of the gelation temperature (T_g) and to an increase of the elastic modulus of the mixed gels. A minimum in T_g and a maximum in G' as a function of the WPI fraction was obtained in mixtures with fixed total protein concentration and explained by the opposing influence of increasing WPI aggregate concentration and decreasing concentration of micelles. The influence of the protein concentration, pH, addition of $CaCl_2$ and aggregate size has been studied. Potentiometric titration curves showed that protonation of the micelles and the WPI aggregates in the mixtures was independent. Possible mechanisms of gelation in mixtures of micelles with fractal aggregates have been considered.

1. Introduction

The proteins of milk can be divided into two fractions: whey proteins (mainly α-lactalbumin and β-lactoglobulin) and caseins (O'Mahony and Fox, 2014). The caseins (α_{s1}-, α_{s2}-, β- and κ- caseins) make up 80 % of the protein content in bovine milk (Dalgleish, 2011). In milk they are organized in "dynamic association colloids" (De Kruif, 2014) called casein micelles with an average hydrodynamic radius $R_h \approx 100$ nm. At the pH of milk (pH 6.7) small particles of calcium phosphate, so-called colloidal calcium phosphate (CCP), play a crucial role in maintaining the micellar structure (Broyard and Gaucheron, 2015; Fox, 2003; Horne, 2009).

The properties of micellar casein (MC) have been widely studied mainly in skim milk and the influence of heat treatment, decrease of the pH, addition of calcium chelatants, and salt have been investigated. Micelles are stable in milk during heating below 100 °C, but above 70 °C when whey proteins denature they interact with intact micelles, which increases the hardness of acidified gels and the pH of the onset of gelation (Dalgleish and Corredig, 2012; Kethireddipalli et al., 2010; Lucey et al., 2001; Raikos, 2010). With decreasing pH, the CCP progressively dissolves until it is completely solubilized below pH 5.2 (Broyard and Gaucheron, 2015; Gaucheron, 2005; Ingham et al., 2016; Lucey and Horne, 2009). Nevertheless, the structure of micelles remains intact down to this pH, because other types of attractive interactions are sufficient to keep the casein together at lower pH (Marchin et al., 2007). Below pH 5.2 the micelles aggregate and may form a network, because the net charge density of caseins becomes small (Broyard and Gaucheron, 2015; Ingham et al., 2016). Even when all CCP is released from the micelles a significant fraction of Ca^{2+} remains bound to the proteins down to pH 3.5 (Gaucheron, 2005; Le Graet and Brulé, 1993). Addition of calcium chelatants (EDTA, citrate,

phosphate, sodium caseinate) also causes release of CCP (Broyard and Gaucheron, 2015; Panouillé et al., 2004; Thomar and Nicolai, 2015; Udabage et al., 2000).

Koutina et al. (Koutina et al., 2014; Koutina and Skibsted, 2015) demonstrated that gelation of skim milk starts at higher pH values when acidification was done at higher temperatures and related this to the release of calcium phosphate to the soluble phase. Vasbinder et al. (2003) found that when the pH is reduced at room temperature, gelation can be induced by heating above a critical temperature which decreases with decreasing pH. Thomar and Nicolai (2016) studied in more detail heat-induced gelation of aqueous MC suspensions over a range of concentrations (25 – 160 g/L) as a function of the pH (5.2 – 6.7). Gelation of micelles occurred at and above a critical temperature (T_C) and did not occur at $T \leq T_C - 5$ °C. T_C was found to decrease with increasing MC concentration and decreasing pH. The elastic modulus of the gels depended on the MC concentration, but was independent of the pH. Balakrishnan et al. (2018) have recently demonstrated that T_C decreased strongly after addition of $CaCl_2$ and increased steeply when a calcium chelatant (EDTA) was added. The role of calcium could not be explained simply by reduction of electrostatic repulsions as addition of NaCl increased T_C, and it was speculated that calcium bridge formation was involved in the association between the micelles. Silva et al. (2018) have shown that addition of native whey protein to MC suspensions increased T_C.

The gels formed by aqueous MC suspensions are weaker and more prone to syneresis than gels obtained from skim milk (Auty et al., 2005; Famelart et al., 1996; Thomar and Nicolai, 2016). The presence of whey proteins has been shown to reinforce the network formed by casein micelles. Nguyen et al. (2017) and Balakrishnan et al. (2017) have recently studied heat-induced gelation of MC in mixtures with native whey protein isolate (WPI). It has been shown that MC gels formed at temperature above T_C were reinforced by co-aggregation with denatured whey proteins above 70 °C. The obtained gels had higher elastic moduli and showed less syneresis compared to gels obtained with pure MC.

Globular whey proteins have different functional properties compared to caseins. In aqueous solutions they are present as particles with radii of a few nm with a compact well-defined structure (O'Mahony and Fox, 2013). During heating, they denature, which leads to irreversible aggregation and gelation at a critical concentration C_g. If concentration is kept below C_g, suspensions of soluble aggregates are formed (Bryant and McClements, 1998; Nicolai et al., 2011; Nicolai and Durand, 2013). Aggregates of different morphologies have been reported in the literature depending on heating conditions. At neutral pH and at low protein concentrations small elongated strands are formed that further aggregate at higher concentrations into larger clusters with a self-similar (fractal) structure. Stable suspensions of homogeneous WPI microgels are formed when native WPI solutions are heated in a narrow pH range around pH 6.0 (Nicolai, 2016; Schmitt et al., 2007, 2010, 2011). When electrostatic repulsions between these aggregates in suspensions are reduced by addition of salt or decrease of the pH (Bryant and McClements, 1998; Nicolai et al., 2011), gelation may occur even at ambient temperature – a process known as cold gelation. We recently revisited the process of cold gelation induced by acidification or addition of $CaCl_2$ (see Chapters 5 and 6).

The effect of WPI aggregates on acid-induced gelation of casein micelles has been studied by Schorsch et al. (2001), Guyomarc'h et al. (2003), Vasbinder et al. (2004) and more recently Andoyo et al. (2014). It was found that the mixtures started to gel at higher pH values and formed stiffer gels

than equivalent mixtures of MC with native whey protein. Here we present an investigation of heat-induced gelation of mixtures of micelles with fractal aggregates of WPI in water as a function of the pH. The protein composition of the mixtures was varied either by fixing the MC concentration and varying the WPI concentration or by fixing the total protein concentration (C_{tot}) and varying the fraction of WPI in the mixture. We will address the influence of protein concentration, pH, aggregate size, addition of $CaCl_2$, and aging of the mixtures before heating on the gelation temperature T_g and the gel stiffness. The effect of adding microgels of WPI will be compared with that of adding fractal aggregates.

2. Experimental

2.1 Materials

2.1.1 WPI aggregates

The commercial WPI powder used for this study contained 89.3 wt% protein, 6 wt% moisture, < 0.4 wt% fat, < 0.4 wt% lactose, and 2.0 wt% ash, including 0.25 wt% calcium. Proteins consisted of 70 % β-lg and 20 % α-lac. The powder was mixed with Milli-Q water containing 200 ppm of sodium azide as an antibacterial preservative and stirred for 4-6 hours. The solution was filtered through 0.45 µm and 0.2 µm syringe filters (Acrodisc®). The pH of the obtained concentrated solution (13.5-13.7 wt%) was adjusted to 7.0 by addition of 1 M NaOH (purchased from Fisher Scientific UK). The net negative charge of WPI proteins after pH adjustment was determined by potentiometric titrations (see Chapter 4): $\alpha = -8.7$. The weight-average molar mass of WPI was considered to be 1.75×10^4 g/mol. The protein concentration of the obtained stock solution was determined by UV absorption at 280 nm using extinction coefficient $\varepsilon = 1.05$ L g^{-1} cm^{-1}.

WPI aggregates were prepared by diluting prepared stock solutions to the required concentration and heating in hermetically closed glass bottles for 24 hours at 80 °C. It has been demonstrated elsewhere that these heating conditions ensure denaturation of practically all native protein (Mahmoudi et al., 2007). The hydrodynamic radius of the aggregates (R_h) was determined by dynamic light scattering as described in Mahmoudi et al. (2007). Aggregates with R_h = 35 nm were prepared by heating stock solutions at C_{WPI} = 62 g/L, with R_h = 170 nm – at 90 g/L and R_h = 200 nm – at 91 g/L. Microgels with R_h = 110 nm were prepared by heating solutions at C_{WPI} = 40 g/L at pH 6.1.

2.1.2 Micellar casein

The micellar casein powder (Promilk 852B, batch 13610656) was purchased from Cremo SA (Fribourg, Switzerland) and contained 82 wt% protein of which 92 % caseins and 8 % whey proteins (determined by RP-HPLC analysis). The mineral composition of the powder was (g/100 g): 2.6 Ca, 0.10 Mg, 0.07 Na, 0.29 K, 1.6 P and 0.05 Cl. The powder was mixed with Milli-Q water containing 200 ppm NaN_3 and constantly stirred with a magnetic bar in a water bath at 50 °C for 16 hours. We verified that the turbidity of the MC suspensions obtained this way was the same as the suspension prepared by homogenization in a microfluidizer.

2.1.3 Preparation of mixtures

Cooled stock solutions of micelles and aggregates were mixed in plastic cups and diluted to slightly above the required final concentration. The pH of the mixtures was adjusted to the required value by addition of 0.1 M HCl (Fischer Scientific UK) while stirring. Small amounts of Milli-Q water were finally added if necessary to adjust the concentration. The mixtures were characterized within a few minutes after preparation unless specified.

2.2 Titration experiments

Protonation of MC and WPI was studied using an automatic titrator (TIM 856, Radiometer Analytical) equipped with a combined pH electrode and a thermoprobe. The electrode was calibrated by a three-point calibration in the pH range between 4 and 10. The pH of solutions of MC was first adjusted to 8.1 by addition of NaOH and then titrated back to pH 3.9 with HCl. Depending on titrated protein concentration, 0.1 and 1 M standard solutions of titrants were used (Fisher Scientific UK).

The number of added protons per casein (N) was calculated as following:

$$N = \frac{V(HCl)\times[HCl]-V(NaOH)\times[NaOH]}{m/M_w}, \quad (1)$$

where V(HCl) and V(NaOH) are the volumes of added standard solutions with concentrations [HCl] and [NaOH], m is the total mass of the titrated protein and M_w is average molar mass of casein (2.3×10^4 g/mol).

2.3 Rheological measurements

The oscillatory shear moduli were determined using two stress imposed rheometers (AR2000 and ARG2, TA instruments) equipped with cone-plate geometries (40 mm radius) and a Peltier system for the temperature control. Samples were loaded on the rheometer immediately after preparation at 20 °C. The measurements were conducted at 0.1 Hz within the linear response regime. Temperature ramps were done at a rate of 5 °C per minute. For iso-thermal measurements the temperature was raised from 20 °C to the required value within one minute.

2.4 CLSM

The structure of the gels was studied with Zeiss LSM800 microscope (Carl Zeiss Microscopy GmbH, Germany) equipped with a water immersion objective lens LCI plnN 63 × / NA = 1.3 DICIII. The proteins were labeled by addition of 5 ppm of rhodamine B, placed on cavity slides, hermetically sealed with a cover slip and heated on a rack placed in a water bath.

2.5 Turbidity measurements

Turbidity measurements were carried out using a UV-Visible spectrometer Varian Cary-50 Bio (Les Ulis, France), the temperature was regulated with a water bath. Studied solutions were placed in air tight quartz cuvettes with a pathway of 5 mm. Turbidity of the solutions was deduced from the measured absorbance at λ = 500 nm. To slow down the dissociation of the micelles, dilutions were made with saturated calcium phosphate at pH 6.0 prepared by adding 15 mM $CaCl_2$ to 10 mM Na_2HPO_4 (purchased from Sigma). The excess of calcium phosphate precipitated under gravity within

1-2 hours and the supernatant was used for dilutions. The turbidity of micelles diluted with prepared calcium phosphate remained constant for approximately 100 min after dilution.

3. Results

3.1 Effect of adding HCl on the critical gelation temperature

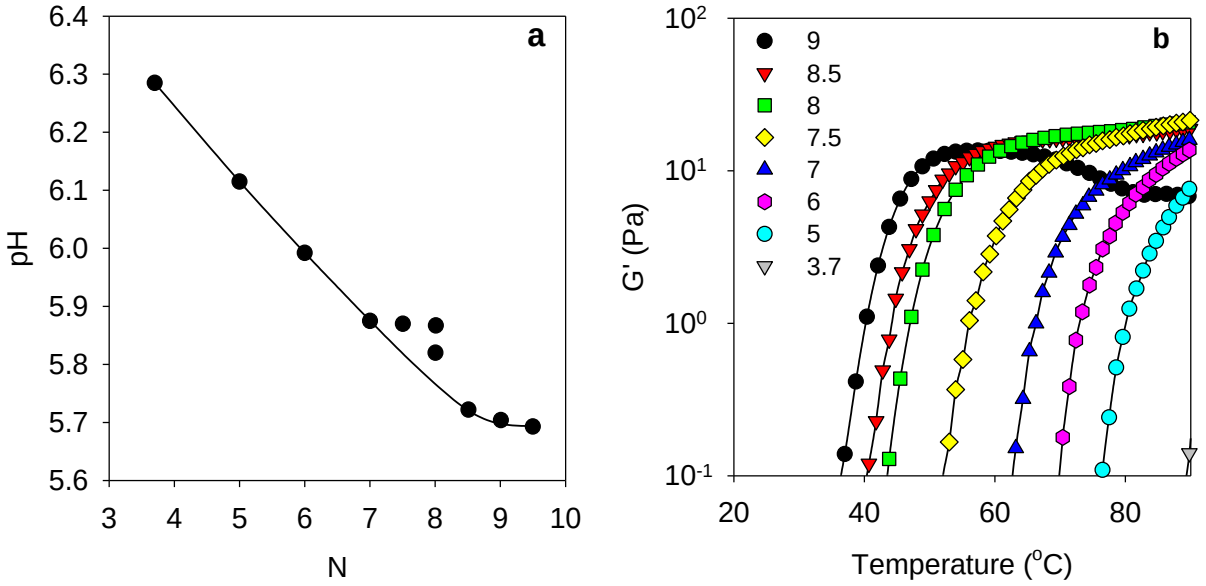

Figure 1. a). pH of MC suspensions at C_{MC} = 40 g/L as a function of the number of protons added per casein. b) Evolution of G' with increasing temperature for MC suspensions C_{MC} = 40 g/L at different N indicated in the figure.

Heat-induced gelation of MC suspensions was studied as a function of the number of protons per casein (N) added to the suspension in the form of HCl. Fig. 1a shows the corresponding pH as function of N for freshly prepared samples at C_{MC} = 40 g/L. At N > 9 addition of acid led to macroscopic flocculation of MC. Freshly prepared samples were loaded on the rheometer at room temperature and the temperature was subsequently increased to 90 °C at a rate of 5 °C/min. The evolution of G' with increasing temperature at different N is presented in Fig. 1b. The elastic modulus is low in the beginning and increases steeply at the temperature of gelation (T_g) as was already reported for a different MC powder by Thomar and Nicolai (2016). At N = 3.7 (pH 6.3) T_g > 90 °C, but T_g decreased steeply with increasing N down to 35 °C at N = 9 (pH 5.7). We note that at N = 9 the elastic modulus decreased during heating, which we attribute to syneresis caused by detachment of a fraction of the gel from the geometry.

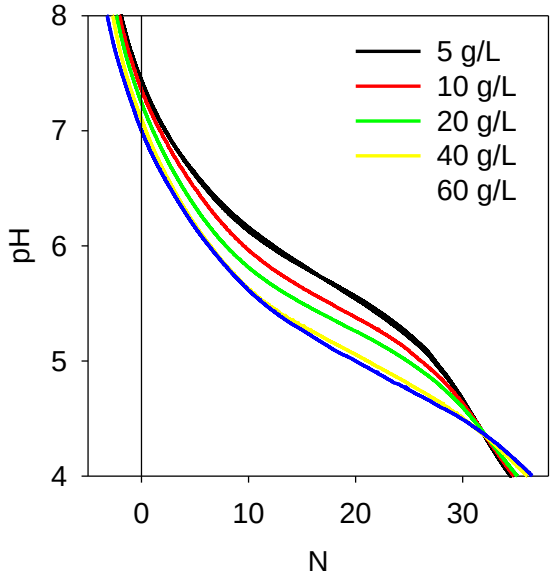

Figure 2. Dependence of the pH on the number of protons added per protein for suspensions of micellar casein at protein concentrations indicated in the figure.

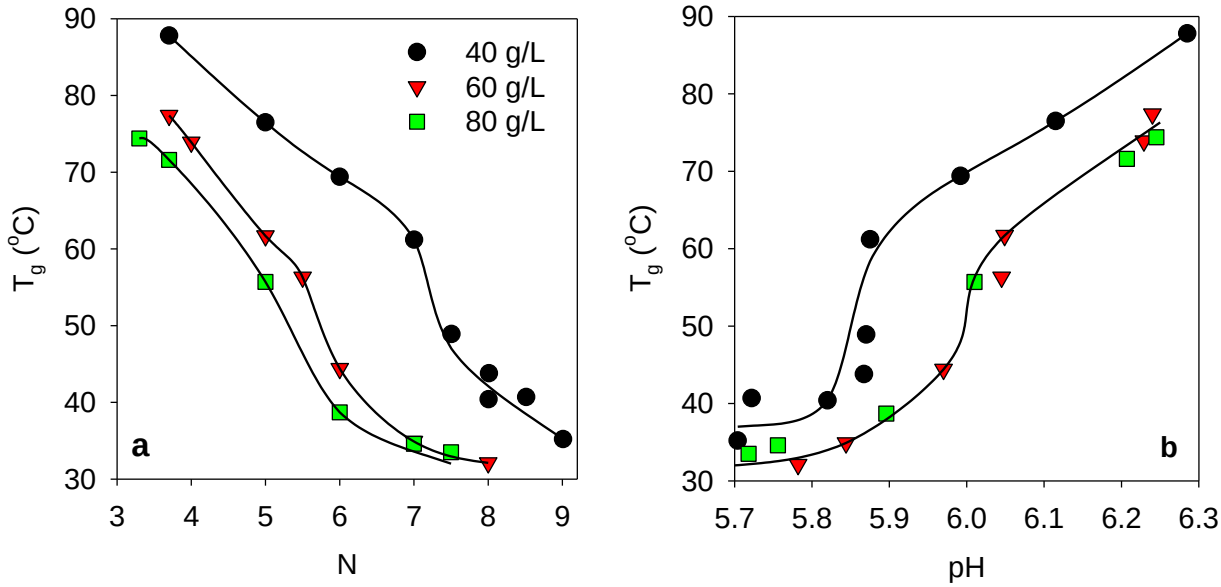

Figure 3. Temperature of gelation as a function of N (a) and pH (b) obtained for MC suspensions at concentrations indicated in the figure. The lines are guides to the eye.

Titration curves of MC suspensions at different C_{MC} showed that the pH is systematically smaller for higher MC concentrations at a given value of N for pH > 4.4, see Fig. 2. The implication is that the pH range where CCP is released is lower when the MC concentration is higher. At pH 4.4 all CCP is released from the micelles and the cross point indicates that at this pH there is no influence of the amount of minerals on the protonation of the caseins, because they have a net zero charge density (Kharlamova et al., 2016; Salis et al., 2011). Figure 3 shows T_g as a function of N (Fig. 3a) and pH (Fig. 3b) for MC suspensions at three different concentrations. Addition of HCl led to a decrease

of T_g at all concentrations, but T_g was systematically significantly lower at C_{MC} = 60 g/L than at C_{MC} = 40 g/L. Further increase to C_{MC} = 80 g/L had a relatively small influence on T_g.

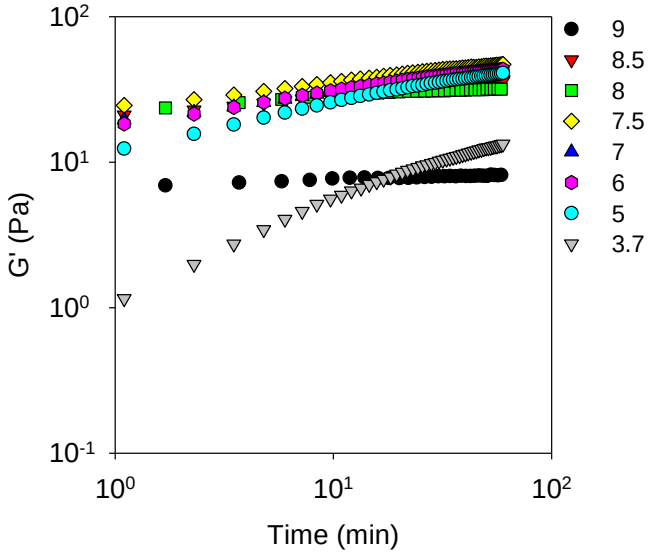

Figure 4. Evolution of G' during one hour heating at 90 °C for 40 g/L suspensions of micelles at different N indicated in the figure. The temperature was first increased from 20 to 90 °C at the rate of 5 °C/min.

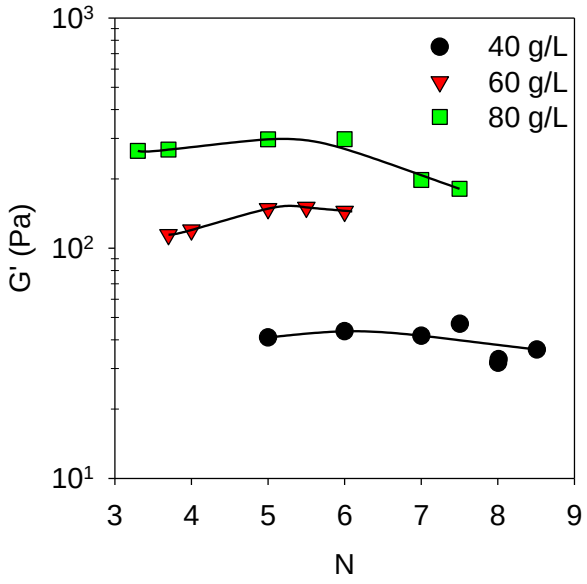

Figure 5. The elastic moduli (G') at 90 °C, obtained after heating for one hour, as a function of N for MC suspensions at different concentrations indicated in the figure. The lines are guides to the eye.

After the temperature ramp the samples were kept at 90 °C for one hour, while measuring the shear moduli. The values of G' and G" increased very weakly with heating time once the gel was formed, see Fig. 4. The values of G' of fully formed gels increased with increasing MC concentration, but did not depend significantly on N, in agreement with results reported by Thomar and Nicolai

(2016), see Fig. 5. G' increased with cooling to 20 °C due to strengthening of hydrogen bonds (results not shown).

The values of T_g at C_{MC} = 60 g/L as a function of the pH obtained here were close to those reported at C_{MC} = 55 g/L by Thomar and Nicolai (2016). However, they found lower values for G': 1 Pa, 10 Pa and 80 Pa compared to 40, 150 and 300 Pa for C_{MC} = 40, 60, 80 g/L, respectively, found here. In addition, self-supporting gels could be formed at lower C_{MC} with the MC powder used in this study. We speculate that the difference is caused by the presence of 8 % of whey proteins in the powder used in this study. It was shown that addition of whey proteins reinforces MC gels when heated above 70 °C (Nguyen et al., 2017).

3.2 Effect of adding WPI aggregates at fixed MC concentrations

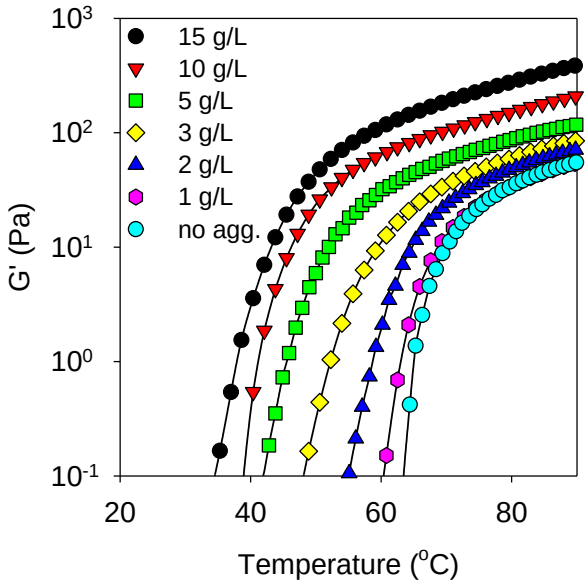

Figure. 6. Evolution of G' with increasing temperature for mixtures at C_{MC} = 60 g/L at pH 6.0 with different concentrations of WPI aggregates with R_h = 35 nm indicated in the figure.

In first instance we studied the effect of adding fractal WPI aggregates with R_h = 35 nm at a constant MC concentration of 60 g/L. The pH was fixed at 6.0. Fig. 6 shows the evolution of G' during temperature ramps for mixtures with C_{WPI} = 0 – 15 g/L. T_g gradually decreased with increasing concentration of aggregates, from 61 °C without aggregates down to 35 °C with C_{WPI} = 15 g/L. Remarkably, a decrease of T_g was observed already after addition of only 1 g/L of aggregates. Fig. 6 also shows that the elastic modulus increased with increasing concentration of aggregates. Continued heating of the samples at 90 °C led to a weak further increase of the moduli with heating time, see Fig. 7.

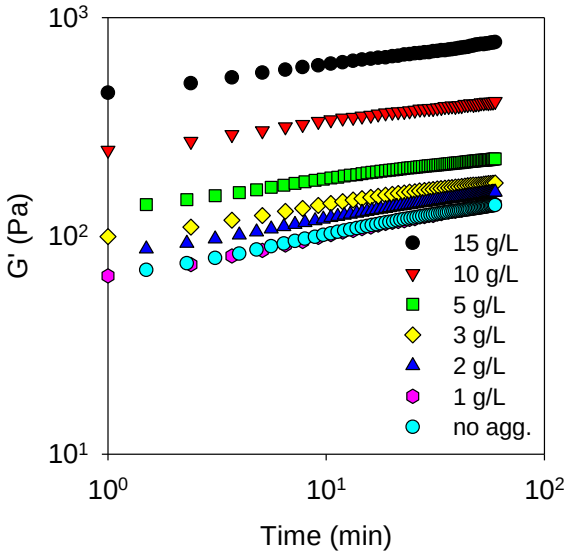

Figure 7. Evolution of G' during heating at 90 °C for 1 hour for mixtures of 60 g/L micelles with 35 nm aggregates at different concentrations indicated in the figure at pH 6.0. The temperature was first increased from 20 to 90 °C at the rate of 5 °C/min.

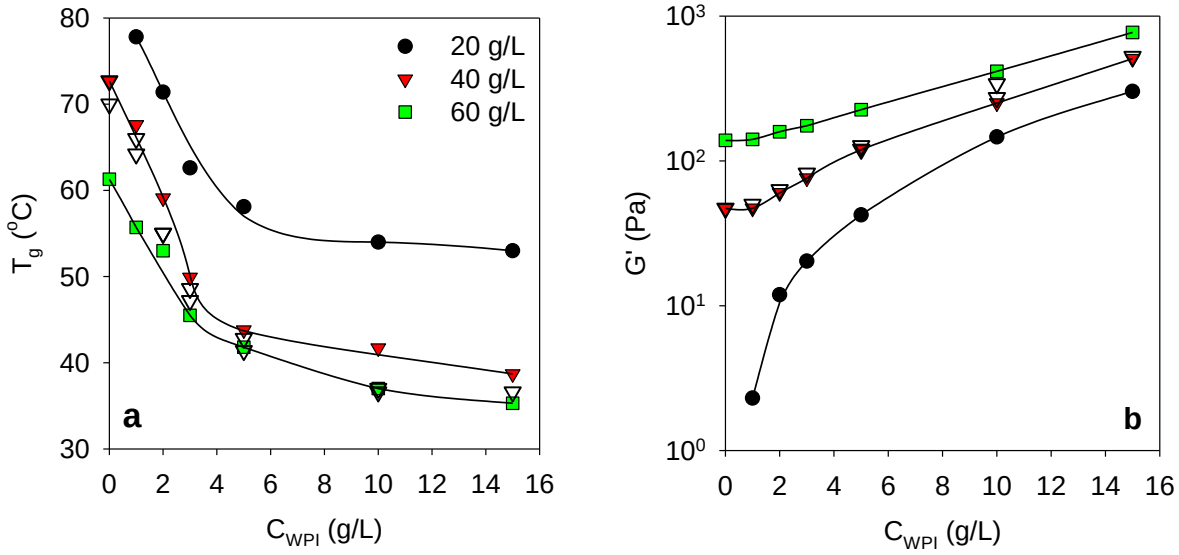

Figure 8. Temperature of gelation (a) and elastic moduli (b) obtained for mixtures of micelles at C_{MC} indicated in the legend and as function of the concentration of 35 nm (filled symbols) or 210 nm (open symbol) aggregates at pH 6.0. The value of the elastic modulus is obtained at 90 °C after heating for 1 h. The lines are guides to the eye.

Similar measurements were done at two lower MC concentrations: C_{MC} = 20 and 40 g/L. The values of T_g and G' as a function of C_{WPI} are shown in Fig. 8. With increasing C_{WPI}, T_g first decreased sharply followed by a weak decrease for C_{WPI} > 5 g/L (see Fig. 8a). Notice that at C_{MC} = 20 g/L solutions without WPI did not gel below 90 °C. The elastic modulus of the gels increased strongly with increasing concentration of aggregates, see Fig. 8b. The effect was particularly strong at C_{MC} = 20 g/L, because pure MC solutions did not gel. The effect of the size of the WPI aggregates was

tested by adding aggregates with R_h = 210 nm to MC solutions at C_{MC} = 40 g/L. Fig. 8 shows that the decrease of T_g and increase of G' were to approximately the same values as for smaller aggregates.

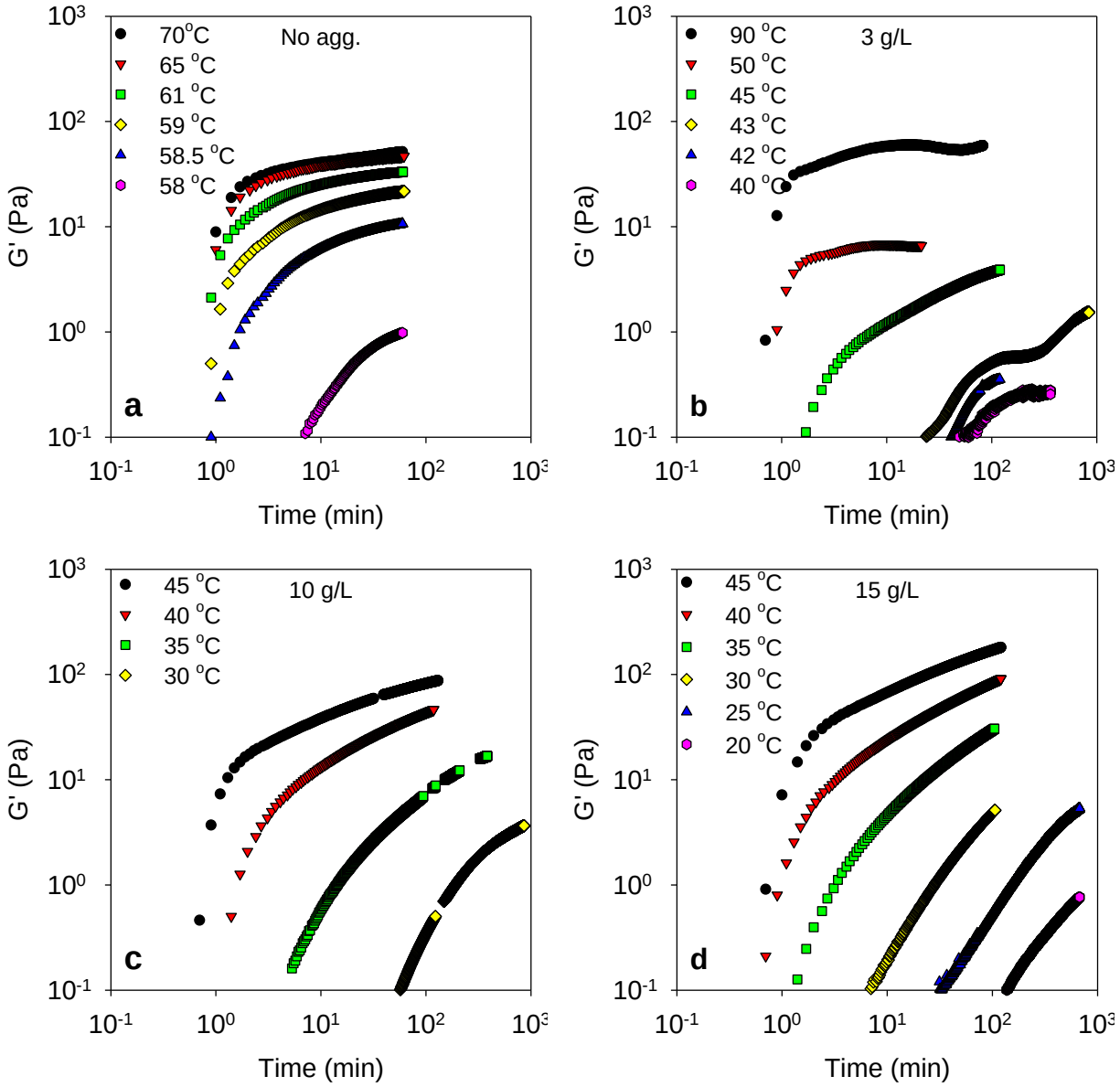

Figure 9. Evolution of the storage modulus G' with time at different temperatures indicated in the figure for MC suspensions at C_{MC} = 60 g/L at pH 6.0 without WPI aggregates and with different concentrations of aggregates with R_h = 35 nm as indicated in the figures.

Thomar and Nicolai (2016) showed that the elastic modulus of pure MC drops sharply in a narrow temperature range below a critical gelation temperature T_C. At temperatures more than 5 °C below T_C MC suspensions remained liquid after overnight heating. However, it was recently shown that the temperature dependence of gelation of WPI aggregates induced by addition of Ca^{2+} or reduction of the pH is characterized by an activation energy (see Chapters 5 and 6). The rate of gelation of pure WPI aggregate suspensions increased rapidly with increasing temperature, but the results superimposed if G' was plotted as a function of time normalized by the gel time (t_g). Fig. 9 shows G' as a function of time at different temperatures for MC suspension at C_{MC} = 60 g/L without WPI aggregates and mixed with 3, 10 or 15 g/L of WPI aggregates with R_h = 35 nm. In the absence of

WPI aggregates we observed a sharp decrease of the gel stiffness with decreasing temperature close to $T_g \approx 60$ °C as was already reported by Thomar and Nicolai (2016). No gelation was observed after overnight heating below 57 °C. In the presence of 3 g/L WPI aggregates the gelation behavior still appears critical, but the drop in the gel stiffness occurred at lower temperatures. However, in the presence of 10 or 15 g/L WPI aggregates we observed progressive slow down of gelation with decreasing temperature.

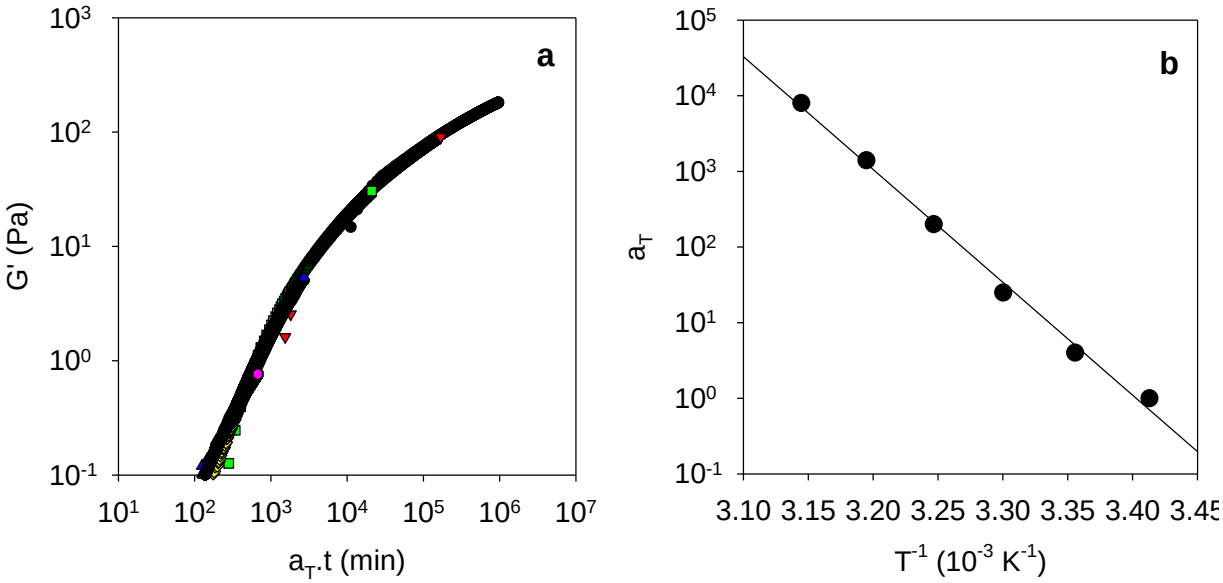

Figure 10. a). Master curve of the data shown in Fig. 9d for a mixture with C_{MC} = 60 g/L and C_{WPI} = 15 g/L at pH 6.0 obtained by time-temperature superposition. b). Arrhenius representation of the shift factors used to obtain the master curve shown in Fig. 10a.

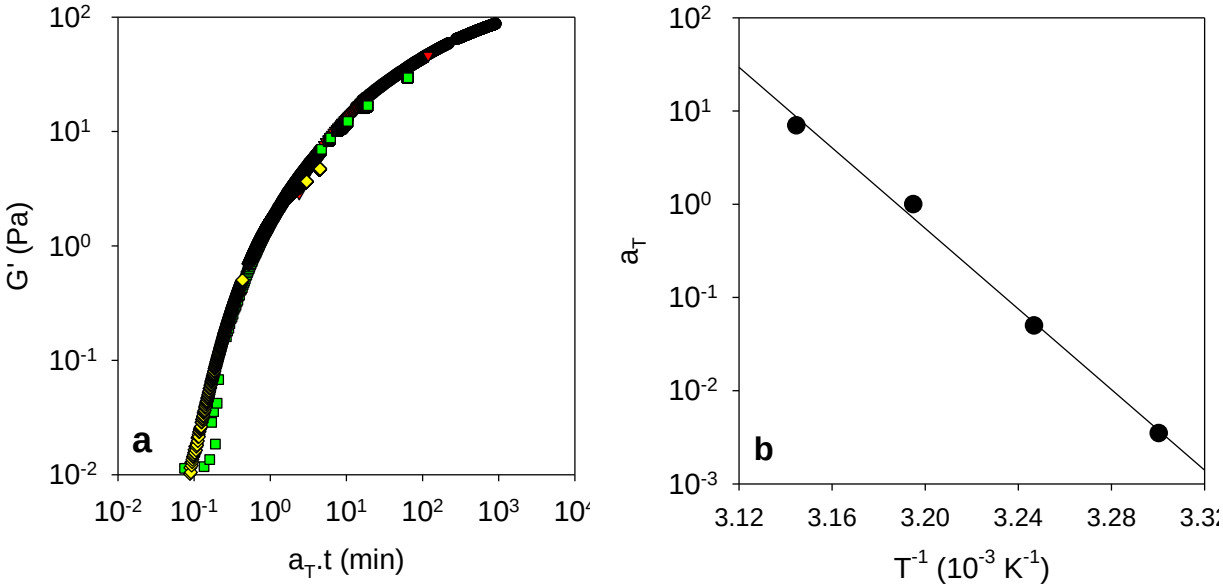

Figure 11. a) Master curve of the results shown in Fig. 9c for a mixture with C_{MC} = 60 g/L and C_{WPI} = 10 g/L at pH 6.0 obtained by time-temperature superposition. b). Arrhenius representation of the shift factors.

At C_{WPI} = 15 g/L the curves obtained at different temperatures superimposed using horizontal shift factors implying that the elastic modulus was independent of the temperature for these systems, see Fig. 10a. In an Arrhenius representation the shift factors had a linear dependency, from which we deduced an activation energy $E_a \approx 285$ kJ/mol, see Fig. 10b. Master curves were also obtained in this manner at C_{WPI} = 10 g/L with $E_a \approx 414$ kJ/mol, see Fig. 11. These values may be compared with the activation energy for Ca^{2+}-induced cold gelation of pure fractal aggregates that we reported elsewhere: $E_a \approx 210$ kJ/mol (see Chapter 5). There appears to be a transition between a critical temperature dependence when no or very little WPI is present and an Arrhenius temperature dependence similar to that of pure WPI aggregates when C_{WPI} is larger. The implication is that for mixtures at higher concentrations of WPI, T_g depends on the rate at which the temperature is increased.

To study the effect of aggregate morphology on thermal gelation of micelles, mixtures of MC with microgels were investigated at pH 6.0. In Fig. 12 T_g and G' obtained for mixtures at C_{MC} = 40 g/L with microgels with R_h = 110 nm are compared with the results for mixtures with fractals with R_h = 35 nm. It is clear that the effect of adding microgels is much smaller. We stress that the difference cannot be attributed to the difference in size, because as we showed in Fig. 8, there was little effect of the size of the fractal aggregates. The difference is most likely related to the fact that microgels are much denser and therefore occupy a much smaller volume fraction than fractals at the same protein concentration.

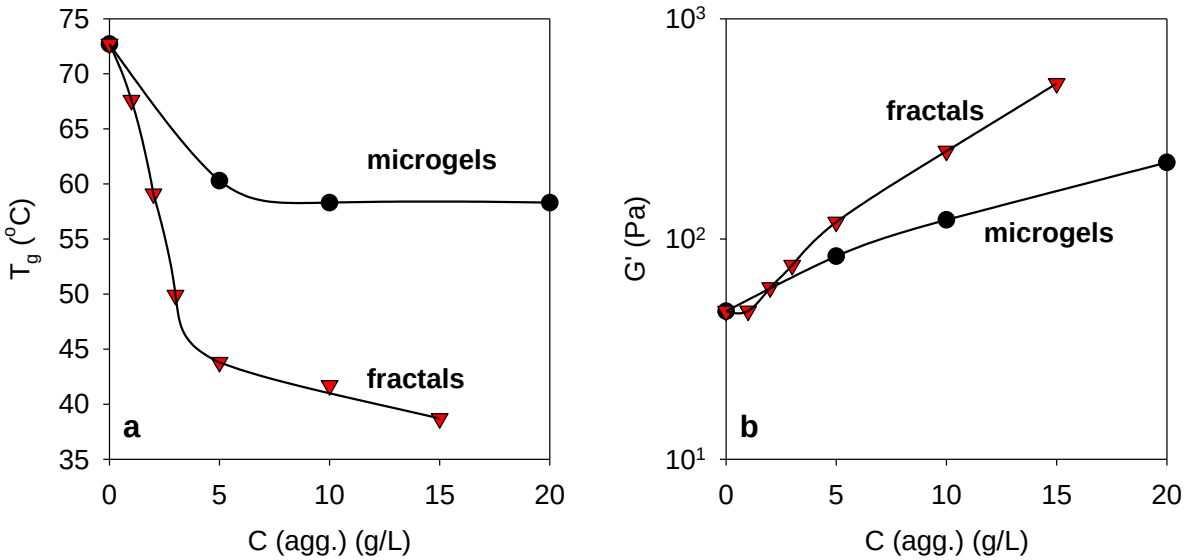

Figure 12. Gelation temperature (a) and elastic modulus (b) as a function of the WPI aggregate concentration obtained for mixtures of micelles at C_{MC} = 40 g/L with WPI microgels with R_h = 110 nm and fractal aggregates with R_h = 35 nm at pH 6.0. The lines are guides to the eye.

Fig. 13 shows the structure of gels formed by MC suspensions at C_{MC} = 40 g/L with different concentrations of WPI fractals with R_h = 35 nm or microgels with R_h = 110 nm. The increase of the concentration of fractals or microgels renders the gel structure more homogeneous, but the effect on the microstructure is obtained at lower C_{WPI} for fractals than for microgels.

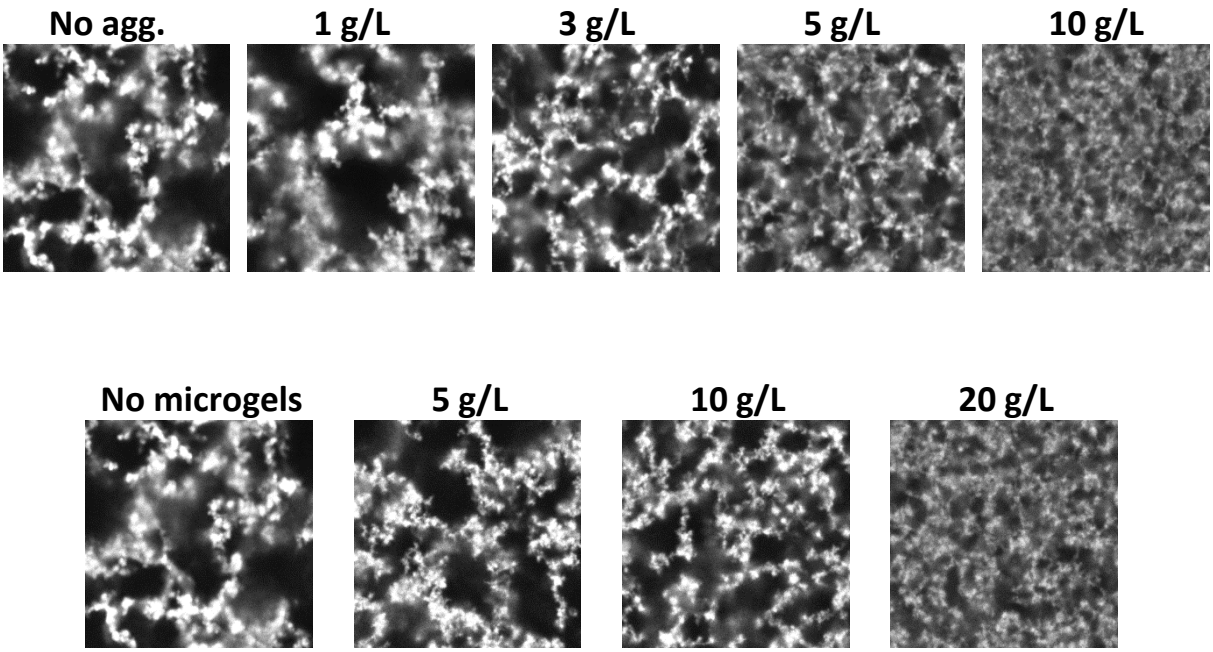

Figure 13. CLSM images (25 × 25 µm) of gels formed by mixtures of MC at C_{MC} = 40 g/L with different concentrations of fractal aggregates with R_h = 35 nm (top) or microgels with R_h = 110 nm at pH 6.0 after heating for 10 min at 80 °C.

3.3 Effect of replacing MC with WPI aggregates at a fixed total protein concentration

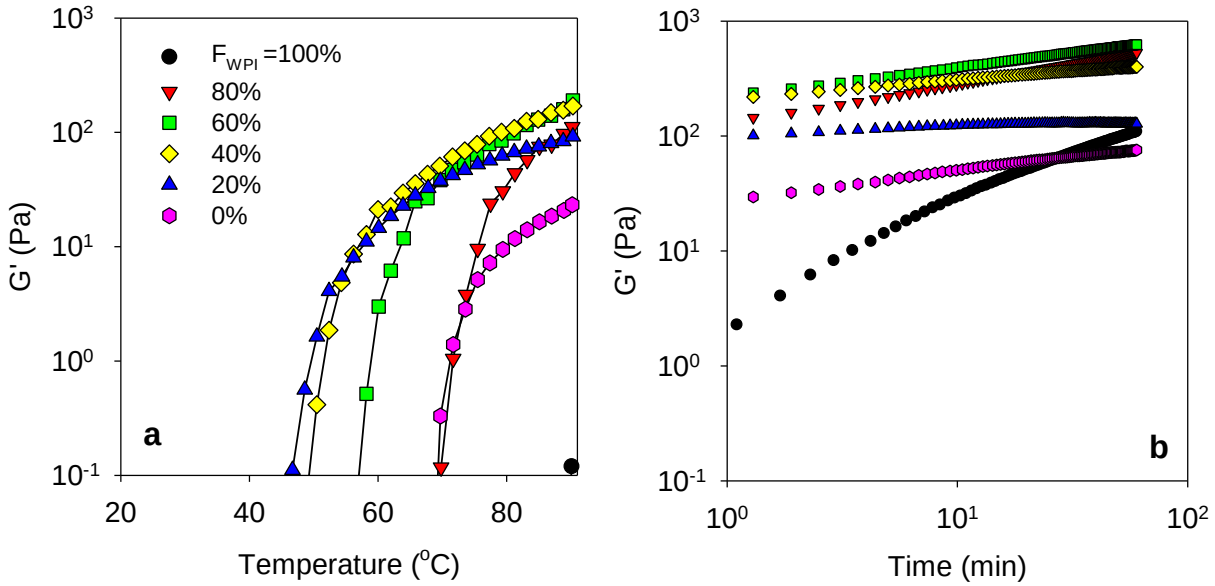

Figure 14. Evolution of G' with increasing temperature (a) and during 1 hour heating at 90 °C (b) for mixtures of micelles with 35 nm fractals with total protein concentration 40 g/L at pH 6.0 with different fractions of aggregates indicated in the figure.

The effect of substitution of micelles with fractal aggregates with R_h = 35 nm was studied at fixed total protein concentrations (C_{tot}). The weight fraction of WPI (F_{WPI}) was varied between 0 and 100 %. The measurements of T_g and G' for mixtures with C_{tot} = 40 g/L at pH 6.0 with different protein composition is shown in Fig. 14.

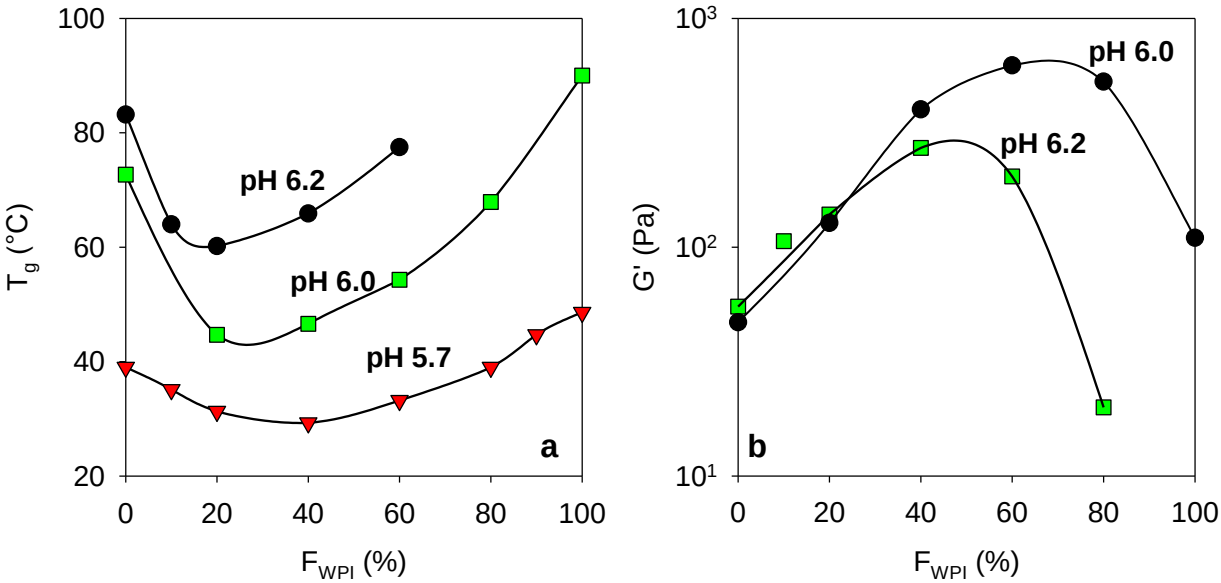

Figure 15. Gelation temperature (a) and elastic moduli obtained at 90 °C after 1 h heating (b) for mixtures of micelles and fractal aggregates with R_h = 35 nm at C_{tot} = 40 g/L as function of the weight fraction of aggregates . The lines are guides to the eye.

Fig. 15a shows the dependence of T_g on the weight fraction of WPI at C_{tot} = 40 g/L for mixtures at different pH. With increasing the fraction of WPI T_g initially decreased reaching a minimum before increasing again at larger F_{WPI}. The same qualitative behavior was observed at different pH, but the values of T_g were systematically higher and the minimum was reached at lower F_{WPI} when the pH was higher.

The elastic modulus obtained after heating for 1 h at 90 °C increased with increasing F_{WPI} reaching a maximum and decreased at higher F_{WPI}, see Fig. 15b. Much stiffer gels were obtained by mixtures than by either pure MC or pure WPI aggregates showing the important synergy between the two components. We note that mixtures at pH 5.7 showed significant effects of syneresis and were therefore not included in Fig. 15b.

The influence of total protein concentration between 20 and 60 g/L has been studied at pH 6.0. Fig. 16 shows that qualitatively the same behavior was observed at all total protein concentrations, but T_g was systematically lower at higher protein concentrations and G' was systematically higher. Elsewhere we already showed that for pure WPI aggregate suspensions the gelation rate and the gel stiffness increased with increasing protein concentration (see Chapters 5 and 6).

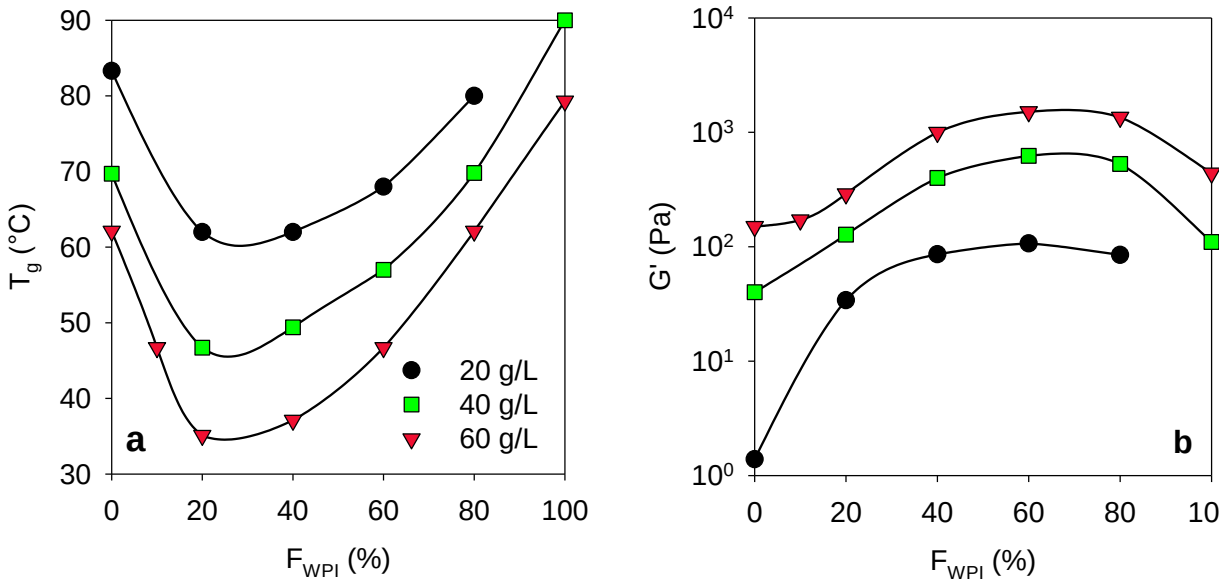

Figure 16. Gelation temperature (a) and elastic moduli at 90 °C after 1 h heating (b) obtained for mixtures of micelles with 35 nm fractals at pH 6.0 and different total protein concentrations indicated in the figure. The lines are guides to the eye.

Finally, the influence of the aggregate size has been studied by comparing mixtures of MC with WPI fractal aggregates with R_h = 35 and 170 nm at C_{tot} = 40 g/L and pH 6.0, see Fig. 17. Slightly lower values of T_g were obtained with larger WPI aggregates, but the elastic moduli were the same. Similar results were already reported elsewhere that for pure WPI aggregates the size did not influence the gel stiffness (see Chapters 5 and 6).

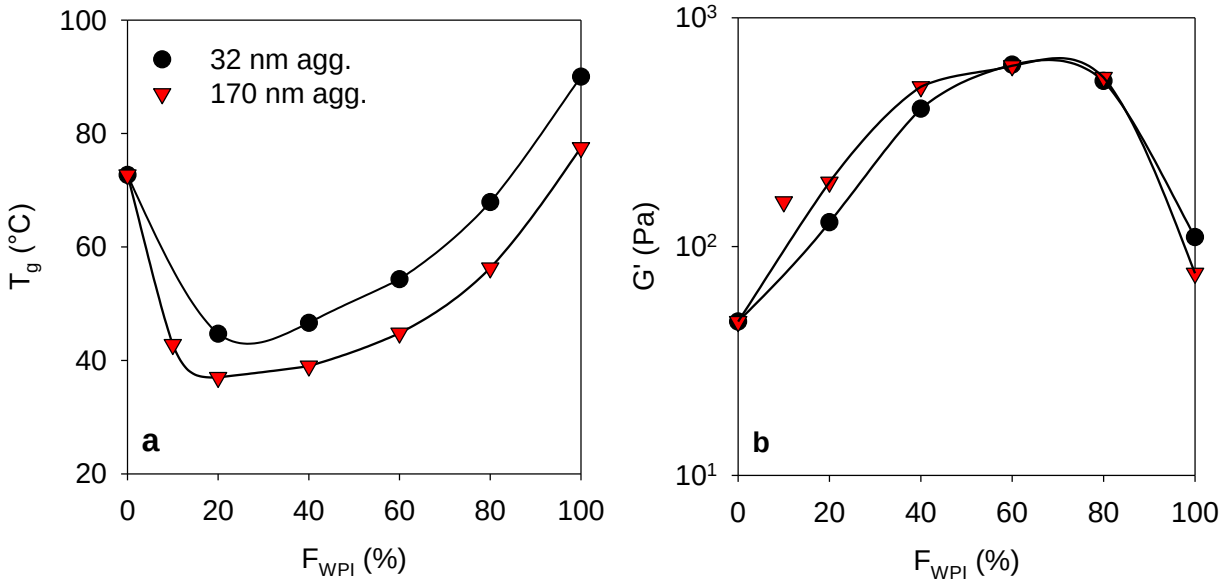

Figure 17. Gelation temperature (a) and the elastic moduli at 90 °C after 1 h heating (b) obtained for mixtures of micelles with aggregates of two sizes indicated in the figure at total protein concentration 40 g/L and pH 6.0. The lines are guides to the eye.

3.4 Influence of calcium

As was mentioned in the Introduction, Balakrishnan et al (2018) demonstrated that addition of $CaCl_2$ to aqueous suspensions of micelles decreases strongly the critical gelation temperature and weakly increases the elastic modulus of MC gels. We have recently shown that with increasing $CaCl_2$ concentration the rate of gelation of pure WPI aggregate suspensions increases strongly, without influencing the elastic modulus of gels (see Chapter 5). Here we studied the effect of calcium on mixtures of MC at C_{MC} = 60 g/L with WPI aggregates at C_{WPI} = 5 and 10 g/L by adding $CaCl_2$ (0 – 0.2 M). No HCl was added to the protein suspensions (N = 0) and the pH was 6.9 for a sample without added salt. However, addition of $CaCl_2$ caused a decrease of the pH of solutions independent of the WPI concentration down to 6.2 at $[CaCl_2]$ = 0.2 M, see Fig. 18.

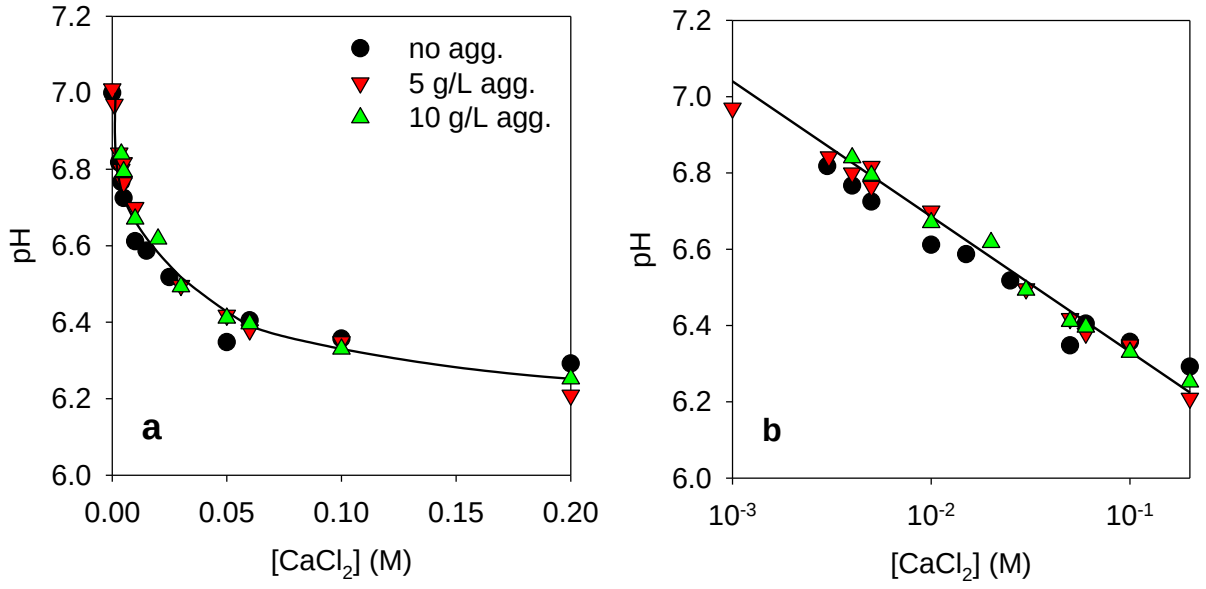

Figure 18. Dependence of the pH on $[CaCl_2]$ for mixtures of MC at C_{MC} = 60 g/L with WPI aggregates with R_h = 35 nm at different concentrations indicated in the figure.

In the absence of $CaCl_2$, gels were not formed below 90 °C, but in all cases T_g decreased sharply with addition of $CaCl_2$ up to 20 mM and increased progressively at higher $[CaCl_2]$, see Fig. 19a. T_g was systematically lower when more aggregates were present. The elastic modulus of the gels obtained after heating for 1 h at 90 °C increased sharply when a small amount of $CaCl_2$ was added, but did not depend significantly on the calcium concentration for $[CaCl_2]$ > 10 mM, see Fig. 19b.

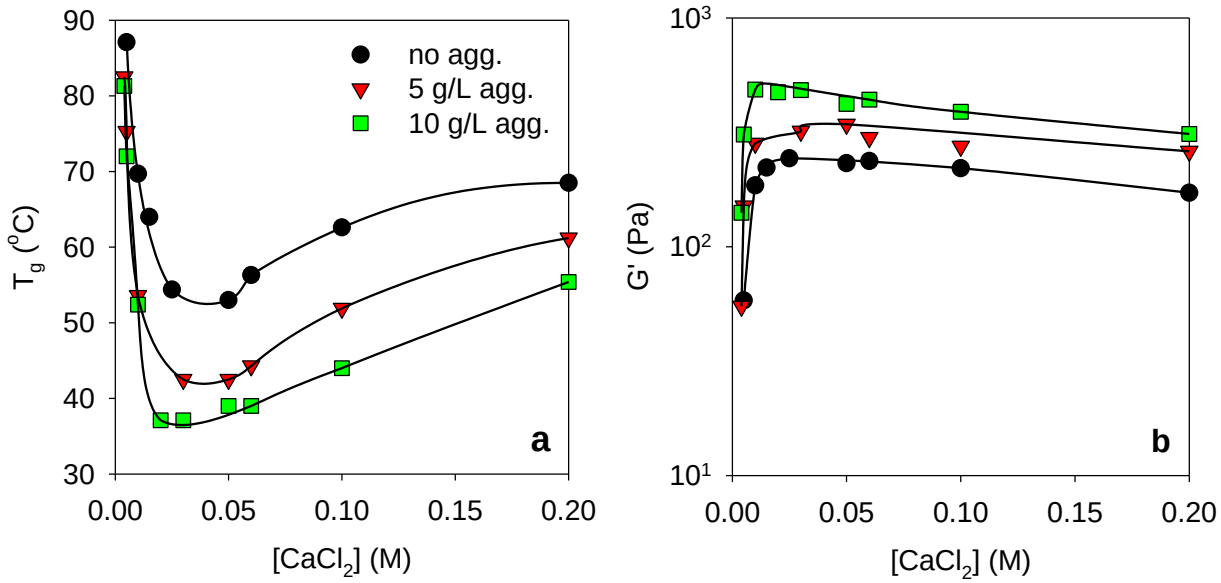

Figure 19. Gelation temperature (a) and the elastic moduli at 90 °C after heating for 1 hour (b) obtained for a pure 60 g/L suspension of micelles and 60 g/L mixtures of MC with 5 and 10 g/L of 35 nm aggregates as function of added calcium chloride concentration.

Similar measurements were done with mixtures at 2 and 4 protons added per casein (pH 6.5 and 6.2, respectively). In all cases addition of $CaCl_2$ led to a decrease of the pH, see Fig. 20, but the relative decrease was smaller when the initial pH was lower. The decrease of T_g with increasing $CaCl_2$ concentration was much less important in solutions at lower initial pH, see Fig. 21a. Nevertheless, in all cases T_g decreased with addition of $CaCl_2$ up to 20 mM reaching lower T_g values when the starting pH was lower. Approximately the same values of the elastic modulus were obtained for all systems as long as T_g was significantly lower than the heating temperature (90 °C) implying that G' depended only on the protein concentration, see Fig. 21b.

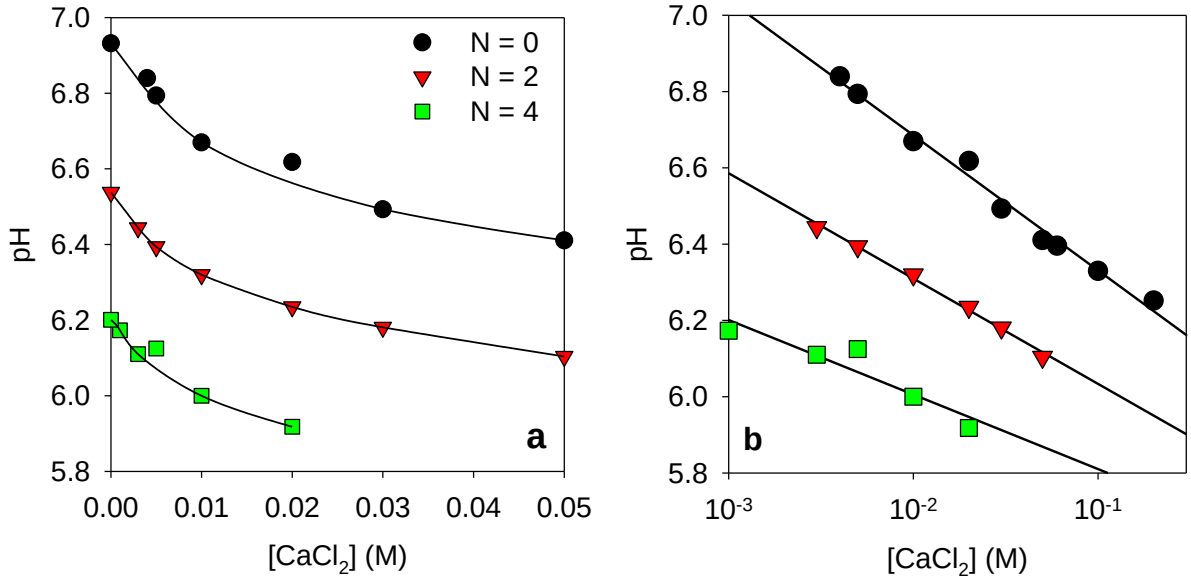

Figure 20. Dependence of the pH on [$CaCl_2$] for mixtures of MC at C_{MC} = 60 g/L with WPI aggregates with R_h = 35 nm at C_{WPI} = 10 g/L with N protons added per casein.

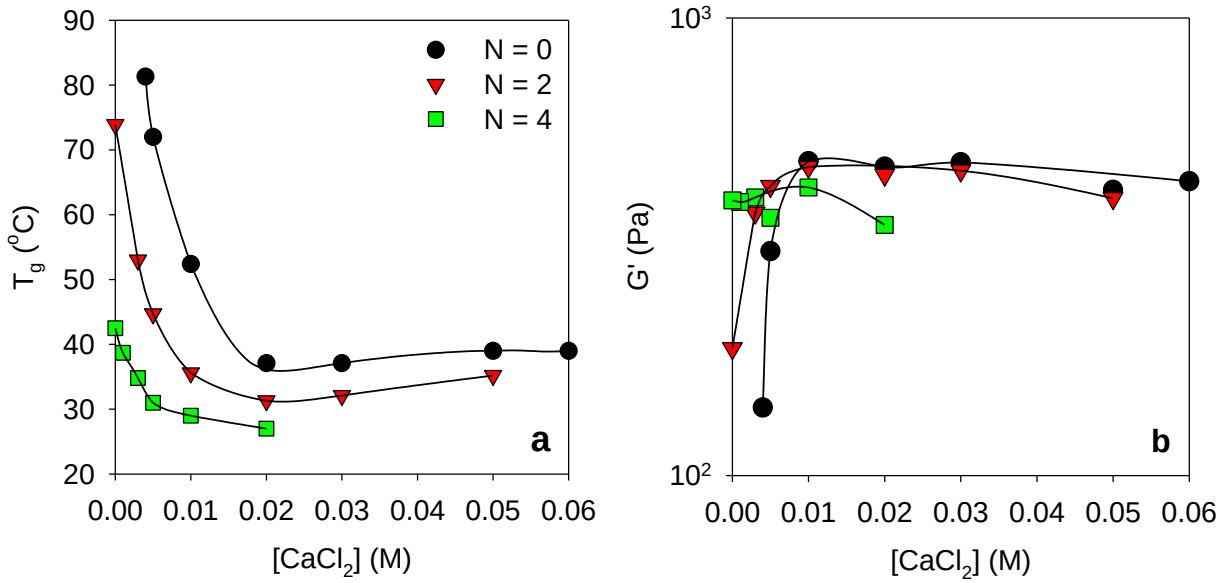

Figure 21. Gelation temperature (a) and the elastic moduli at 90 °C after heating for 1 h (b) for mixtures of 60 g/L micelles with 10 g/L 35 nm strands at different initial pH values as a function of added calcium.

3.5 Effect of ageing before heating.

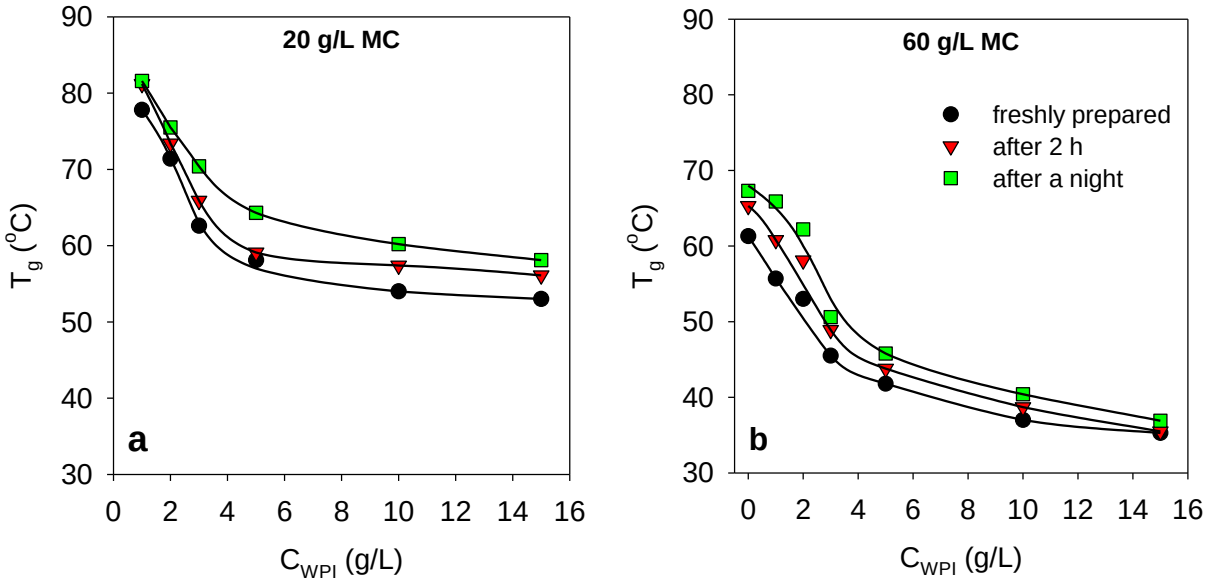

Figure 22. Dependence of the gelation temperature on C_{WPI} at different times after sample preparation for mixtures at C_{MC} = 20 g/L (a) and 60 g/L (b) with WPI aggregates with R_h = 35 nm at different concentrations at pH 6.0. The lines are guides to the eye.

The results shown so far were obtained on freshly prepared samples that were heated within a few minutes after addition of HCl. In order to test the effect of ageing before heating, measurements were done after standing for 2 hours or overnight after addition of HCl to the suspensions. Fig. 22 shows for mixtures at C_{MC} = 20 or 60 g/L at pH 6.0 mixed with different amounts of WPI aggregates with R_h = 35 nm that ageing caused a small systematic increase of T_g. The pH of the

samples increased weakly with time to 6.3 or 6.2 after standing overnight at C_{MC} = 20 g/L or 60 g/L, respectively. The pH increase was independent of the WPI concentration in the range investigated. The elastic modulus of the gels was not influenced by ageing (results not shown).

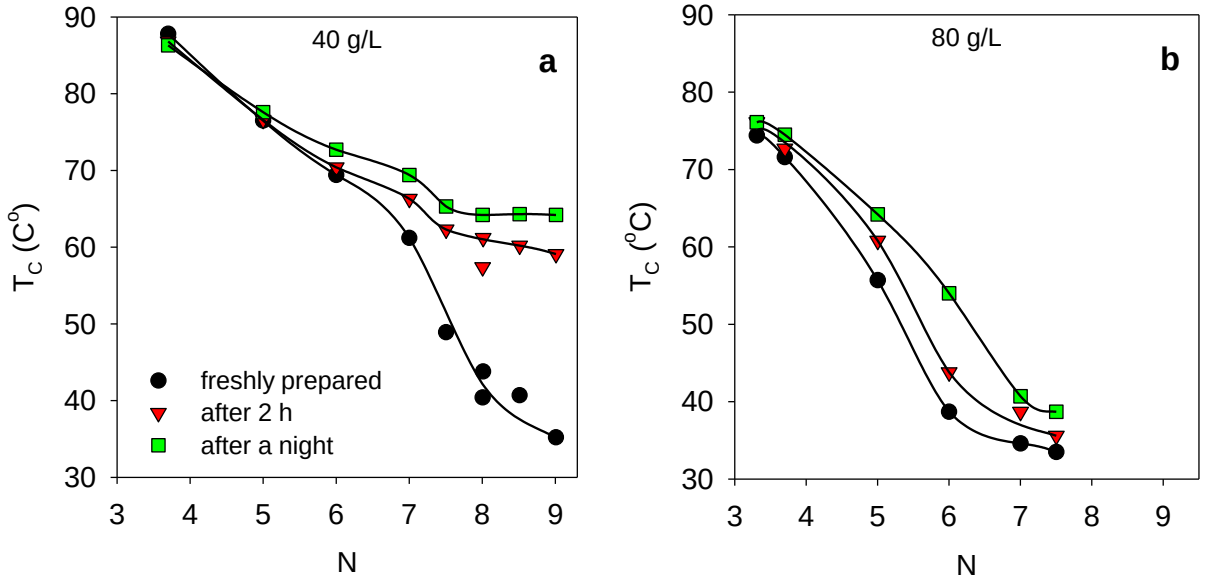

Figure 23. Dependence of T_g on N at different times after addition of HCl for pure MC suspensions at C_{MC} = 40 g/L (a) and 80 g/L (b).

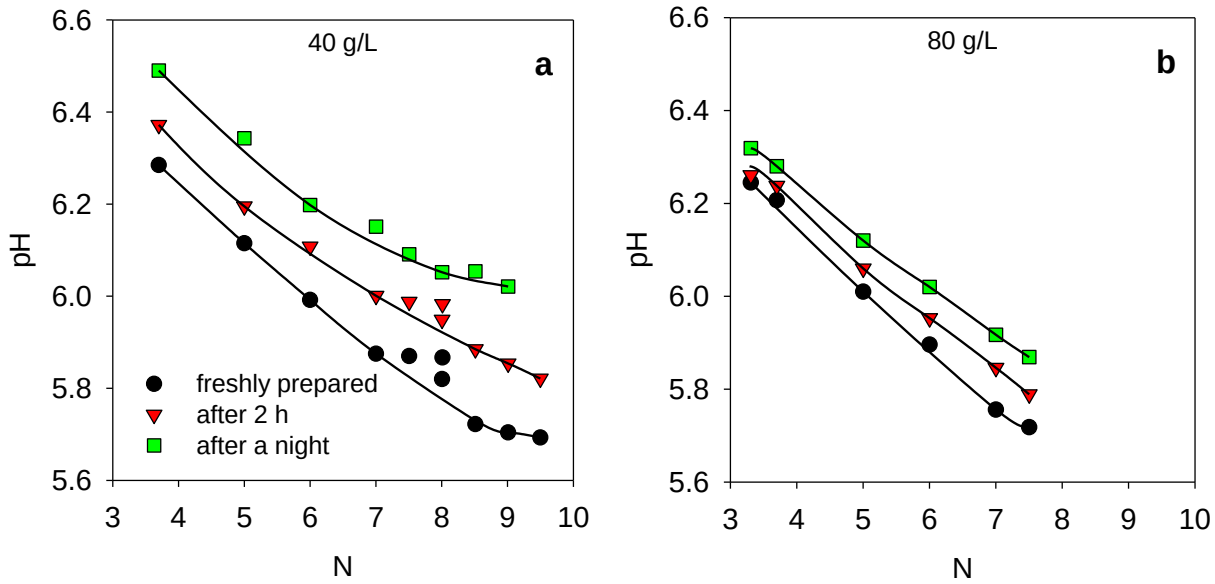

Figure 24. Increase of pH with time after addition of HCl for suspensions of micelles at 40 g/L (a) and 80 g/L (b).

The effect of ageing was studied at different amounts of added HCl for pure MC suspensions at C_{MC} = 40 g/L and C_{MC} = 80 g/L , see Fig. 23. We found in all cases an increase of T_g and pH after ageing. The effect on T_g was small (< 10 °C) except at C_{MC} = 40 g/L when N > 7 (pH ≤ 5.9) and at C_{MC} = 80 g/L at N = 6 (pH = 5.9). The increase of the pH during ageing was more important for larger N and lower MC concentration (see Fig. 24). It appears that, relatively slow internal reorganization of the micelles occurred which modified the effective interaction between micelles leading to a weak increase of the pH and to an increased heat stability.

4. Discussion

Gelation of aqueous solutions of WPI aggregates is fundamentally different from that of casein micelles. Gelation of WPI fractal aggregates is characterized by an activation energy of 210 kJ/mol when it is induced by addition of $CaCl_2$ and 155 kJ/mol when it is induced by adding HCl (see Chapters 5 and 6). Decrease of the temperature reduces the gelation rate, but doesn't change the properties of the gels. The gelation is favored by the increase of the salt concentration or decrease of the pH due to reduction of the electrostatic repulsion between the aggregates. Although the rate of gelation increases strongly with increasing $CaCl_2$ or HCl concentration, the activation energy remains approximately the same.

On the other hand, gelation of aqueous suspensions of micelles occurs at a critical temperature that decreases with decreasing pH and increasing MC concentration. It also depends weakly on ageing of the MC suspension after setting the pH. Association of the casein micelles at a critical temperature is expected if they behave as colloidal spheres with a short attraction range that increases with temperature (De Kruif, 1997; De Kruif and Roefs, 1996). This process leads eventually to macroscopic phase separation if the associated particles can reorganize and densify. In the case of MC suspensions, associated micelles form relatively strong bonds that become even stronger after cooling. For this reason a network is formed instead of a dense phase of MC.

We have demonstrated in the present study that addition of even a small amount of fractal aggregates to MC suspensions reduces the gelation temperature. This is in sharp contrast with the observation that addition of native WPI causes an increase of T_g (Silva et al, 2018). It is well-known that WPI aggregates formed in the absence of salt at neutral pH have a tendency to associate with each other when Ca^{2+} is added or when the pH is reduced (Bryant and McClements, 1998; Kharlamova et al., 2018; Nicolai et al., 2011). The rate of gelation of WPI aggregates was shown to be strongly temperature dependent and controlled by an activation energy (see Chapters 5 and 6). E_a was found to be independent of the protein concentration, aggregate size, pH and $CaCl_2$ concentration, but it was higher for Ca^{2+}-induced gelation at neutral pH (210 kJ/mol) than for acid-induced gelation in the absence of Ca^{2+} (155 kJ/mol). These two effects are combined in the present study for mixtures of WPI aggregates, because we have reduced the pH and Ca^{2+} was released from the added micelles. It is likely that association of WPI aggregates occurred in the mixtures. However, association of WPI aggregates does not by itself lead to self-supporting gels at $C_{WPI} < 10$ g/L (see Chapter 5), whereas the effect on gelation of mixtures was already important at much lower C_{WPI}. Therefore we suggest that the effect of WPI aggregates is caused by temperature dependent co-aggregation with the micelles (see Fig. 25).

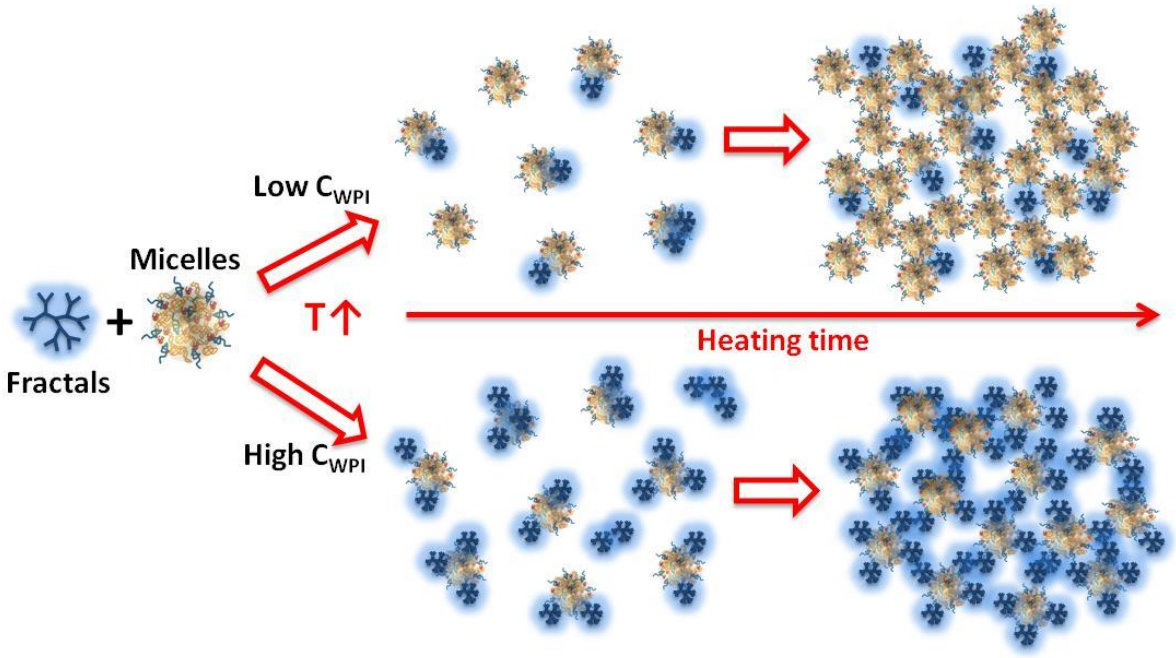

Figure 25. Mechanism of gelation in mixtures of micelles with low (above) and high (below) concentration of fractal aggregates.

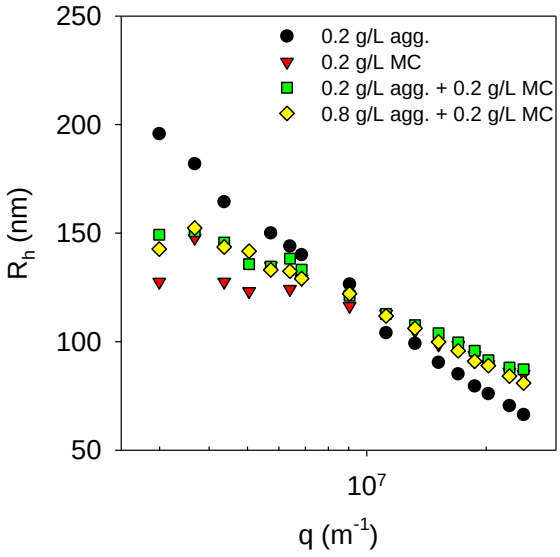

Figure 26. q-Dependence of the apparent average hydrodynamic radii for pure suspensions and mixtures of MC at C_{MC} = 0.2 g/L and WPI aggregates with R_h = 200 nm at C_{WPI} = 0.2 g/L and their mixtures in saturated calcium phosphate at pH 6.0.

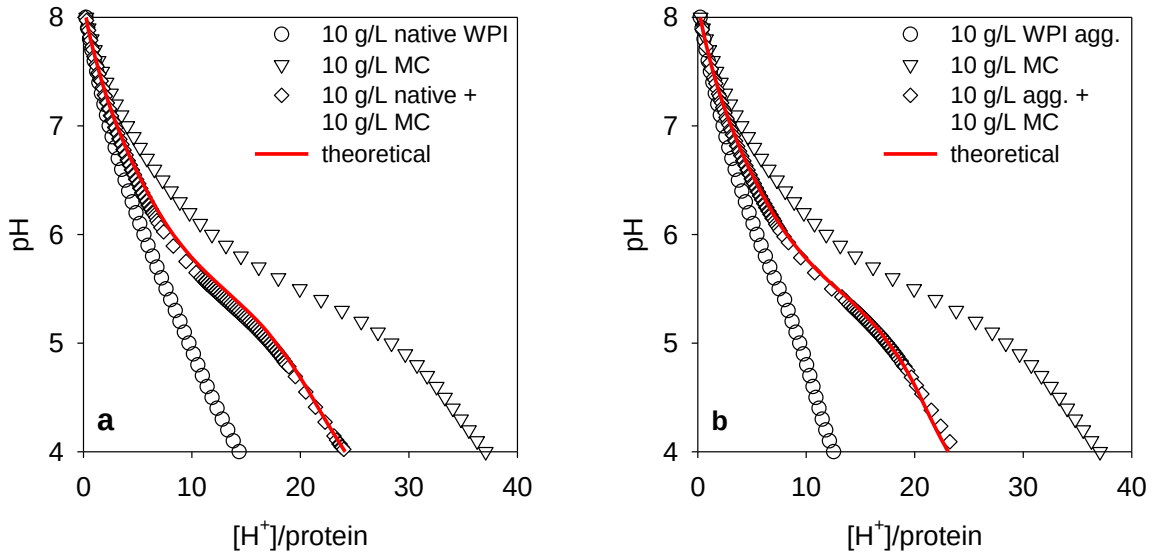

Figure 27. Dependence of the pH with addition of HCl to pure solutions of MC and native WPI (a) or WPI aggregates with R_h = 35 nm (b) and their mixtures. The red line shows the expected results for the mixtures if protonation of WPI and MC is independent.

We have verified with light scattering that there is no association between micelles and WPI aggregates at conditions far below T_g, see Fig. 26, which is in agreement with the results obtained by Vasbinder et al. (2004) with capillary electrophoresis analysis. Furthermore, titration measurements showed that protonation of WPI aggregates and MC in the mixtures is not significantly influenced by the presence of the other type of protein, see Fig. 27, which also suggests that no complexes are formed at $T << T_g$. However, the association rate increased rapidly with increasing temperature and was controlled by an activation energy that increased with decreasing WPI concentration (E_a = 414 kJ/mol at C_{WPI} = 10 g/L and E_a = 280 kJ/mol at C_{WPI} = 15 g/L). At C_{WPI} = 3 g/L, the temperature dependence of T_g was very strong and can still be considered as critical. However, it is not possible to distinguish between a critical gelation temperature and a very large activation energy. Nevertheless, even at C_{WPI} = 3 g/L the gelation temperature was significantly lower than for pure MC suspensions. It means that even if the WPI aggregates do not fully cover the micelles their presence reduces the repulsive interaction between the micelles. A schematic representation of the situation at $C_{WPI} << C_{MC}$ and $C_{WPI} \lesssim C_{MC}$ is shown in Fig. 25.

The initiation of the association process by WPI aggregates can be clearly seen with turbidity measurements at low protein concentrations. In Fig. 28 the evolution of the turbidity is compared during heating for suspensions of pure MC at C_{MC} = 0.5 g/L, pure WPI aggregates with R_h = 200 nm at C_{WPI} = 0.5 g/L and mixtures containing both MC and WPI aggregates at the same concentrations. At these conditions, pure MC associated only close to 90 °C, whereas pure WPI aggregates started to associate at about 50 °C. The association of the mixtures started at the same temperature as the pure WPI aggregates demonstrating that the latter drive the process. However, the increase of turbidity for the mixtures was much stronger than the sum of the turbidities of the pure MC and pure aggregate solutions showing that co-aggregation occurred as soon as the WPI aggregates started to associate.

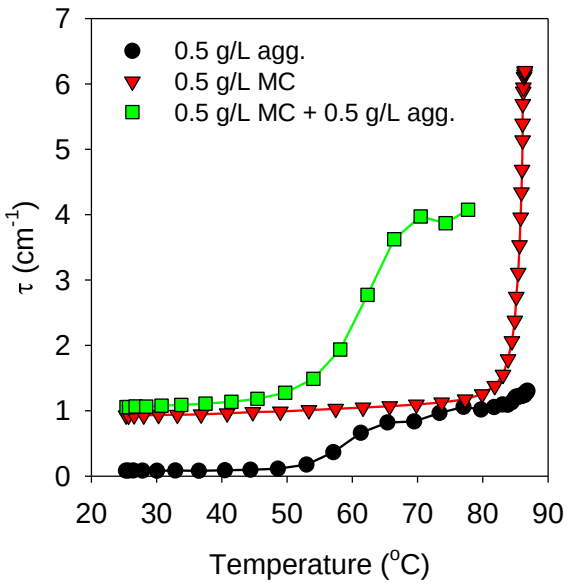

Figure 28. Turbidity at λ = 500 nm as function of temperature for suspensions of pure WPI aggregates with R_h = 200 nm at C_{WPI} = 0.5 g/L, pure MC at C_{MC} = 0.5 g/L and their mixtures at the same concentrations in saturated calcium phosphate at pH 6.0.

We believe that in mixtures of MC with whey protein aggregates gelation is initiated by association of the aggregates with each other and with the micelles that is induced by the presence of Ca^{2+} and lowering the pH.

The reinforcement of the MC gel by co-aggregation with denatured WPI shown here is similar in mixtures with native WPI that are heated above the denaturation temperature of the whey proteins (Nguyen et al., 2017; Schorsch et al., 2001; Silva et al. 2018). However, in mixtures of MC with native WPI, the micelles first form a network at T_c without interacting with the whey proteins. The MC network is subsequently reinforced only upon further heating above the denaturation temperature by co-aggregation with denatured whey proteins. In mixtures with WPI aggregates there is no need to strongly heat in order to denature the whey proteins and strong MC/WPI hybrid gels can be formed even at room temperature. The size of the WPI fractal aggregates did not influence the elastic modulus of the hybrid gels. The same was also observed for calcium or acid induced gels of pure WPI aggregate suspensions. The reason is most likely that smaller WPI aggregates associate with each other to form larger fractal aggregates with the same structure (Ako et al., 2010). However, a small decrease of T_g was observed for mixtures with larger aggregates. Faster gelation was already reported for pure suspensions of fractal WPI aggregates induced by adding HCl (see Chapter 6) and is expected as smaller aggregates need some time to reach the same size as the larger aggregates.

5. Conclusions

Addition of fractal WPI aggregates to aqueous suspensions of MC at a fixed MC concentration decreases the temperature of gelation and increases the elastic modulus of the gels. Decrease of the pH, increase of the protein concentration and addition of $CaCl_2$ cause a decrease of

T_g. The aggregates do not interact with micelles at T << T_g, but co-aggregation of MC and WPI aggregates occurs at an increasing rate when the temperature is increased leading to formation of a hybrid MC/ WPI network. The temperature dependence of the gelation is controlled by an activation energy that decreases with increasing amount of added WPI aggregates. When the total protein content is kept constant, the gel stiffness has a maximum for mixtures containing between 40 % and 80 % WPI and the gelation temperature has a minimum between 20 % and 40 % WPI. Addition of WPI microgels also decreases T_g and increases G' but the effect is much weaker than for fractal aggregates.

Acknowledgements

Bba association, Le Mans University and the Regional councils of Brittany and Pays de la Loire who funded this work through the interregional PROFIL project, carried out by the association "Pole Agronomique Ouest", are thanked. We also thank Dr. J. Léonil of the INRA for the scientific coordination.

References

Ako, K., Nicolai, T., Durand, D., 2010. Salt-induced gelation of globular protein aggregates: structure and kinetics. Biomacromolecules 11, 864–871.

Andoyo, R., Guyomarc'h, F., Cauty, C., Famelart, M.-H., 2014. Model mixtures evidence the respective roles of whey protein particles and casein micelles during acid gelation. Food Hydrocoll. 37, 203–212.

Auty, M.A.E., O'Kennedy, B.T., Allan-Wojtas, P., Mulvihill, D.M., 2005. The application of microscopy and rheology to study the effect of milk salt concentration on the structure of acidified micellar casein systems. Food Hydrocoll. 19, 101–109.

Balakrishnan, G., Nguyen, B.T., Schmitt, C., Nicolai, T., Chassenieux, C., 2017. Heat-set emulsion gels of casein micelles in mixtures with whey protein isolate. Food Hydrocoll.

Balakrishnan, G., Silva, J.V.C., Nicolai, T., Chassenieux, C., Bovay, C., Buczkowski, J., Schmitt, C., 2018. Specific effect of calcium ions on thermal gelation of aqueous micellar casein suspensions. Colloids Surf. B Biointerfaces 163, 218–224.

Broyard, C., Gaucheron, F., 2015. Modifications of structures and functions of caseins: a scientific and technological challenge. Dairy Sci. Technol. 95, 831–862.

Bryant, C.M., McClements, D.J., 1998. Molecular basis of protein functionality with special consideration of cold-set gels derived from heat-denatured whey. Trends Food Sci. Technol. 9, 143–151.

Dalgleish, D.G., 2011. On the structural models of bovine casein micelles—review and possible improvements. Soft Matter 7, 2265–2272.

Dalgleish, D.G., Corredig, M., 2012. The structure of the casein micelle of milk and its changes during processing. Annu. Rev. Food Sci. Technol. 3, 449–467.

De Kruif, C.G., 2014. The structure of casein micelles: a review of small-angle scattering data. J. Appl. Crystallogr. 47, 1479–1489.

De Kruif, C.G., 1997. Skim milk acidification. J. Colloid Interface Sci. 185, 19–25.

De Kruif, C.G., Roefs, S., 1996. Skim milk acidification at low temperatures: A model for the stability of casein micelles. Ned. Melk En Zuiveltijdschr. 50, 113–120.

Famelart, M.H., Lepesant, F., Gaucheron, F., Le Graet, Y., Schuck, P., 1996. pH-Induced physicochemical modifications of native phosphocaseinate suspensions: Influence of aqueous phase. Le lait 76, 445–460.

Fox, P.F., 2003. Milk proteins: general and historical aspects, in: Advanced Dairy Chemistry—1 Proteins. Springer, pp. 1–48.

Gaucheron, F., 2005. The minerals of milk. Reprod. Nutr. Dev. 45, 473–483.

Guyomarc'h, F., Queguiner, C., Law, A.J.R., Horne, D.S., Dalgleish, D.G., 2003. Role of the Soluble and Micelle-Bound Heat-Induced Protein Aggregates on Network Formation in Acid Skim Milk Gels. J. Agric. Food Chem. 51, 7743–7750.

Horne, D.S., 2009. Casein micelle structure and stability. Milk Proteins Expr. Food 133–162.

Ingham, B., Smialowska, A., Erlangga, G.D., Matia-Merino, L., Kirby, N.M., Wang, C., Haverkamp, R.G., Carr, A.J., 2016. Revisiting the interpretation of casein micelle SAXS data. Soft Matter 12, 6937–6953.

Kethireddipalli, P., Hill, A.R., Dalgleish, D.G., 2010. Protein interactions in heat-treated milk and effect on rennet coagulation. Int. Dairy J. 20, 838–843.

Kharlamova, A., Inthavong, W., Nicolai, T., Chassenieux, C., 2016. The effect of aggregation into fractals or microgels on the charge density and the isoionic point of globular proteins. Food Hydrocoll. 60, 470–475.

Kharlamova, A., Nicolai, T., Chassenieux, C., 2018. Calcium-induced gelation of whey protein aggregates: Kinetics, structure and rheological properties. Food Hydrocoll. 79, 145–157.

Koutina, G., Knudsen, J.C., Andersen, U., Skibsted, L.H., 2014. Temperature effect on calcium and phosphorus equilibria in relation to gel formation during acidification of skim milk. Int. Dairy J. 36, 65–73.

Koutina, G., Skibsted, L.H., 2015. Calcium and phosphorus equilibria during acidification of skim milk at elevated temperature. Int. Dairy J. 45, 1–7.

Le Graet, Y., Brulé, G., 1993. Les équilibres minéraux du lait: influence du pH et de la force ionique. Le Lait 73, 51–60.

Lucey, J.A., Horne, D.S., 2009. Milk salts: technological significance, in: Advanced Dairy Chemistry. Springer, pp. 351–389.

Lucey, J.A., Tamehana, M., Singh, H., Munro, P.A., 2001. Effect of heat treatment on the physical properties of milk gels made with both rennet and acid. Int. Dairy J. 11, 559–565.

Mahmoudi, N., Mehalebi, S., Nicolai, T., Durand, D., Riaublanc, A., 2007. Light-scattering study of the structure of aggregates and gels formed by heat-denatured whey protein isolate and β-lactoglobulin at neutral pH. J. Agric. Food Chem. 55, 3104–3111.

Marchin, S., Putaux, J.-L., Pignon, F., Léonil, J., 2007. Effects of the environmental factors on the casein micelle structure studied by cryo transmission electron microscopy and small-angle x-ray scattering/ultrasmall-angle x-ray scattering. J. Chem. Phys. 126, 01B617.

Nguyen, B.T., Chassenieux, C., Nicolai, T., Schmitt, C., 2017. Effect of the pH and NaCl on the microstructure and rheology of mixtures of whey protein isolate and casein micelles upon heating. Food Hydrocoll. 70, 114–122.

Nicolai, T., 2016. Formation and functionality of self-assembled whey protein microgels. Colloids Surf. B Biointerfaces 137, 32–38.

Nicolai, T., Britten, M., Schmitt, C., 2011. β-Lactoglobulin and WPI aggregates: Formation, structure and applications. Food Hydrocoll., 25 years of Advances in Food Hydrocolloid Research 25, 1945–1962.

Nicolai, T., Durand, D., 2013. Controlled food protein aggregation for new functionality. Curr. Opin. Colloid Interface Sci. 18, 249–256.

O'Mahony, J.A., Fox, P.F., 2014. Milk: an overview. Milk Proteins Expr. Food 19–73.

O'mahony, J.A., Fox, P.F., 2013. Milk proteins: Introduction and historical aspects, in: Advanced Dairy Chemistry. Springer, pp. 43–85.

Panouillé, M., Nicolai, T., Durand, D., 2004. Heat induced aggregation and gelation of casein submicelles. Int. Dairy J. 14, 297–303.

Raikos, V., 2010. Effect of heat treatment on milk protein functionality at emulsion interfaces. A review. Food Hydrocoll. 24, 259–265.

Salis, A., Boström, M., Medda, L., Cugia, F., Barse, B., Parsons, D.F., Ninham, B.W., Monduzzi, M., 2011. Measurements and Theoretical Interpretation of Points of Zero Charge/Potential of BSA Protein. Langmuir 27, 11597–11604.

Schmitt, C., Bovay, C., Rouvet, M., Shojaei-Rami, S., Kolodziejczyk, E., 2007. Whey protein soluble aggregates from heating with NaCl: physicochemical, interfacial, and foaming properties. Langmuir 23, 4155–4166.

Schmitt, C., Bovay, C., Vuilliomenet, A.-M., Rouvet, M., Bovetto, L., 2011. Influence of protein and mineral composition on the formation of whey protein heat-induced microgels. Food Hydrocoll., Food Colloids 2010: On the Road from Interfaces to Consumers 25, 558–567.

Schmitt, C., Moitzi, C., Bovay, C., Rouvet, M., Bovetto, L., Donato, L., Leser, M.E., Schurtenberger, P., Stradner, A., 2010. Internal structure and colloidal behaviour of covalent whey protein microgels obtained by heat treatment. Soft Matter 6, 4876–4884.

Schorsch, C., Wilkins, D.K., Jones, M.G., Norton, I.T., 2001. Gelation of casein-whey mixtures: effects of heating whey proteins alone or in the presence of casein micelles. J. Dairy Res. 68, 471–481.

Silva, J. V. C., Balakrishnan, G., Schmitt, C., Chassenieux, C., & Nicolai, T. (submitted). Heat-induced gelation of aqueous micellar casein systems as affected by globular protein addition. Food Hydrocoll.

Thomar, P., Nicolai, T., 2016. Heat-induced gelation of casein micelles in aqueous suspensions at different pH. Colloids Surf. B Biointerfaces 146, 801–807.

Thomar, P., Nicolai, T., 2015. Dissociation of native casein micelles induced by sodium caseinate. Food Hydrocoll. 49, 224–231.

Udabage, P., McKinnon, I.R., Augustin, M.-A., 2000. Mineral and casein equilibria in milk: effects of added salts and calcium-chelating agents. J. Dairy Res. 67, 361–370.

Vasbinder, A.J., Rollema, H.S., Bot, A., de Kruif, C.G., 2003. Gelation Mechanism of Milk as Influenced by Temperature and pH; Studied by the Use of Transglutaminase Cross-Linked Casein Micelles. J. Dairy Sci. 86, 1556–1563.

Vasbinder, A.J., van de Velde, F., de Kruif, C.G., 2004. Gelation of Casein-Whey Protein Mixtures. J. Dairy Sci. 87, 1167–1176.

General conclusions and perspectives

The objective of this work was to study the functionality of two types of aggregates produced by heat treatment of whey protein: fractal aggregates and microgels. Thermal aggregation of globular proteins of milk whey has been studied extensively in the literature and the mechanism of aggregation and aggregate structure have been described well. This work is an investigation on the behavior of the aggregates in different systems: in pure solutions and in mixtures with other dairy proteins (caseins) in varied conditions. The knowledge of the functional properties of the aggregates opens the possibility of their application as innovative, efficient and versatile 'clean label' texturizing ingredients in food products. The popular term 'clean label' doesn't have a legal definition but it implies using simple ingredients that consumers are familiar with instead of complex 'chemical' ingredients. Dairy proteins are ideal for this purpose as they are generally perceived as healthy, nutritional 'dietary' components.

We firstly studied the behavior of the aggregates in the simplest systems, i.e. in water solutions. It has been demonstrated that fractal aggregates and microgels have very different properties in solutions. Fractal aggregates efficiently fill up the space increasing the viscosity of the solutions. It was shown that larger fractal aggregates have lower density and fill up more space than smaller aggregates at the same protein concentration. Therefore larger fractal aggregates might be used to modify the viscosity of dairy products. The viscosity of a product might be fine-tuned by varying the aggregate size and concentration in a product. By contrast, microgels are dense aggregates that have low viscosity in solutions. Therefore, they might be used in liquid products in order to increase their protein content without increasing the viscosity, for example in drinking products for older people, people experiencing difficulty in swallowing or in sports drinks. An advantage of using aggregates in this context is that, contrary to native whey proteins, they can be heat stable.

Another important functional property of the aggregates is their ability to form gels by adding salt or reducing the pH. We therefore studied gelation of water suspensions of aggregates upon addition of calcium chloride or HCl. Gelation of aggregates of globular proteins upon salt addition or acidification is known as cold gelation because it can happen at ambient temperatures. We extended the understanding of the process and established that it is thermally activated and characterized by an activation energy of 210 kJ/mol in case of Ca-induced gelation and 155 kJ/mol in case of acid-induced gelation. The protein concentration is the most important parameter determining the gel stiffness and structure, while the increase of temperature and calcium concentration or decrease of the pH only influence the speed of gelation. The understanding of the role of different parameters allows prediction of the evolution of the gels with time, and therefore the change of a dairy product quality during storage. For instance the undesirable syneresis might be avoided by heating a solution of aggregates with low salt content and at higher pH until the gel is formed and then decreasing the temperature. Smaller fractal aggregates are better for the application as a gelling agent as we showed that gels with them have higher water holding capacity than the ones prepared with larger aggregates. Microgels, on the other hand, are not efficient for gelation as they require higher protein and calcium concentrations to form a network.

Fractal aggregates have been shown to improve the quality of gels formed by casein micelles dispersed in water. Water suspensions of pure micelles form gels that are prone to syneresis, while addition of aggregates allows formation of gels with higher water holding capacity and elastic modulus and at lower temperatures. Therefore aggregates might be applied for manufacturing of dairy products of consistent quality from isolated dairy components.

In conclusion, the aggregates formed from whey protein demonstrate important properties for applications as texturizing ingredients. They might be successfully used to control product viscosity, to form gels and for protein enrichment.

An attempt has been made to understand functionality of dairy proteins more fundamentally, i.e. as function of their charge density. This approach is not common in food research and pH is routinely used as a control parameter. We demonstrated how the charge density of dairy proteins might be determined and that it is a useful parameter for the explanation of observed phenomena.

Concerning further development, there remain plenty of questions that require further investigation. We studied the influence of the pH and calcium on gelation of aggregates separately, but it would be interesting to look at how the two parameters work in combination. The binding of calcium to aggregates as function of the pH needs to be studied in order to understand gelation influenced by the two parameters.

We have seen the synergetic effect during gelation in mixtures of micelles and aggregates and suggested that it is caused by co-aggregation between the two components. However, the exact mechanism of gelation resulting in the decrease of the gelation temperature and improvement of the gel quality was not established. The understanding of the gelation mechanism of water suspensions of micelles is helpful for the understanding of the processes happening in more complex systems such as skim milk. In terms of more applied research the investigation of gelation of whey protein aggregates and casein micelles in water needs to be extended to more complex systems that approach the composition of real food products.

In terms of more fundamental research, the study of proton and calcium binding in mixtures of proteins appears a fascinating area of investigation. We demonstrated how gelation might be correlated to the charge density of proteins. In mixtures a competition for ions might take place and the principles of ion binding in mixtures are interesting to look at.

The study of the functionality of milk ingredients is important for innovation in the dairy industry that is crucial for the development of such a large manufacturer of milk as regions of Pays de la Loire and Brittany in France.

UNIVERSITE BRETAGNE LOIRE

Le Mans Université

Thèse de Doctorat

Anna KHARLAMOVA

Texturer des matrices laitières avec des agrégats de protéines laitières.

Texturization of dairy protein systems with whey protein isolate aggregates.

Résumé

Dans le lait on peut distinguer deux classes de protéines : les protéines sériques et les caséines. Les protéines sériques sont des protéines globulaires qui se trouvent dans le sérum du lait et elles sont connues pour leurs propriétés fonctionnelles exceptionnelles. Quand une solution de protéines sériques est chauffée, elles perdent leur structure native et peuvent s'agréger. Elles forment des agrégats de différentes formes, tailles et densités en fonction des conditions appliquées lors du chauffage : des cylindres, des agrégats fractals, des microgels et des agrégats fibrillaires. De l'autre côté, les caséines sont organisées dans des unités appelées micelles de caséine d'un rayon environ 100-200 nm stabilisées par du phosphate de calcium colloïdal (CCP).

Au cours de ce travail, nous avons cherché à comprendre comment les agrégats de protéines sériques pouvaient être utilisés en mélange avec les micelles de caséine pour obtenir et contrôler la texture de produits laitiers. Dans un premier temps, nous avons étudié le processus de « cold gelation » induit par ajout de calcium et/ou acidification d'agrégats et de microgels de protéines sériques seuls. Dans une deuxième partie, nous nous sommes intéressés à la fonctionnalité des agrégats dans les mélanges plus complexes avec les autres protéines laitières et en présence de minéraux. L'addition de petites quantités d'agrégats fractals dans des suspensions de micelles diminuait leur température critique de gélification, augmentait le module élastique et diminuait la synérèse des gels.

Les agrégats et les microgels de protéines sériques peuvent être utilisés pour modifier la viscosité des mélanges respectivement comme gélifiant ou pour enrichir la teneur en protéine du milieu sans en augmenter la viscosité. Les propriétés des agrégats fractals et des microgels ont été étudiées et comparées. Les agrégats de protéines sériques peuvent être considérés comme des ingrédients texturants « clean label » bien perçus par les consommateurs et qui n'exigent pas d'évaluation par l'autorité européenne de sécurité des aliments (AESA) compte tenu de leur origine.

Mots clés

Agrégats de protéines sériques, micelles de caséines, microgels, cold gelation, viscosité, texture, clean label

Abstract

The proteins of milk might be divided into two categories: the whey proteins and caseins. Whey proteins are compact globular proteins that are found in the aqueous phase of milk. They are well-known for their exceptional functional properties. Upon heating, individual whey proteins denature and aggregate, forming aggregates of different morphologies and sizes, such as strands, fractal aggregates, microgels and fibrillar aggregates, depending on the heating conditions. On the other hand, the caseins in milk are organized in complex protein units with a diameter of 100-200 nm called casein micelles stabilized by colloidal calcium phosphate (CCP).

The current work is an endeavor to understand how whey protein aggregates might be used in mixtures with other dairy proteins, such as casein micelles, in order to get a particular texture in a dairy product. We first extended the knowledge of the process of so-called "cold gelation" of pure WPI aggregates induced by calcium and acidification and then studied how the aggregates work in more complex mixtures of proteins and minerals. Interestingly, addition of small amounts of fractal aggregates to suspensions of casein micelles has been demonstrated to decrease the critical gelation temperature, increase the elastic modulus and decrease the syneresis of the gels.

The aggregates are to be used to modify the viscosity of a product, as a gelling agent and for protein enrichment. The properties of strands, fractal aggregates and microgels have been studied and compared. WPI aggregates might be considered as "clean label" texturizing ingredients that are perceived as healthy by consumers and do not require approval from the European Food Safety Authority (EFSA).

Key words

WPI aggregates, casein micelles, microgels, cold gelation, viscosity, texture, clean label